Micro-engineered substrates as bone extracellular matrix mimics

Ibrahim Bilem

THÈSE EN COTUTELLE PRÉSENTÉE
POUR OBTENIR LE GRADE DE

DOCTEUR DE
L'UNIVERSITÉ DE BORDEAUX
ET DE L'UNIVERSITÉ LAVAL

ÉCOLE DOCTORALE DES SCIENCES CHIMIQUES

ÉCOLE DOCTORALE DU PARTENAIRE

SPÉCIALITÉ: PHYSICO-CHIMIE DE LA MATIÈRE CONDENSÉE

Par Ibrahim BILEM

Micro-structuration de la surface des matériaux avec ligands bioactifs pour mimer la matrice extra-cellulaire osseuse

Sous la direction de Dr. Marie-Christine DURRIEU
et Pr. Gaétan LAROCHE

Soutenue le: **31 Août 2016**

Membres du jury:

M. René Therrien	Vice-doyen de FSG de l'université Laval, Canada	Président
M. Eli SONE	Professeur de l'université de Toronto, Canada	Co-directeur
M. Emmanuel PAUTHE	Professeur de l'université de Cergy-Pontoise, France	Rapporteur
Mme. Nathalie FAUCHEUX	Professeure de l'université de Sherbrooke, Canada,	Rapporteur
M. Jean-Christophe FRICAIN	Professeur de l'université de Bordeaux (PU-PH), France	Examinateur

Micro-structuration de la surface des matériaux avec ligands bioactifs pour mimer la matrice extracellulaire osseuse

Résumé

Il est de plus en plus évident que la matrice extracellulaire (MEC), au-delà de sa fonction d'échafaudage cellulaire, génère des signaux de nature biochimique et biophysique jouant un rôle primordial au cours du processus de différenciation des cellules souches. A l'heure actuelle, plus de 15 différents facteurs extrinsèques (environnementaux), incluant l'organisation spatiale de la MEC, sa topographie, rigidité, porosité, biodégradabilité et chimie ont été identifiés comme modulateurs potentiels de la différenciation des cellules souches en lignées cellulaires spécialisées. Ainsi, il est plausible que l'intégration d'un biomatériau au sein de l'organisme dépendra largement de sa capacité à mimer les propriétés de la MEC du tissu à remplacer.

Récemment, les techniques de micro-ingénierie ont émergé comme outil innovant pour découpler les différentes propriétés de la MEC et étudier l'impact individuel ou combiné de ces facteurs sur le comportement des cellules souches. De plus, ces techniques de microfabrication ont un intérêt particulier dans une perspective de reconstruction de la MEC dans tous ses aspects, *in vitro*.

Dans ce projet de thèse, le concept de déconstruction/reconstruction de la complexité de la MEC a été appliqué pour récapituler, *in vitro*, plusieurs aspects inhérents à la MEC osseuse et explorer leurs effets individuels ou combinés sur la différenciation ostéoblastique des cellules souches mésenchymateuses (CSMs) humaines.

Trois principales composantes ont été utilisées tout au long du projet : un matériau modèle (verre borosilicate), des séquences peptidiques mimétiques dérivées de la MEC naturelle, favorisant à la fois l'adhérence cellulaire (peptide RGD) et la différenciation ostéoblastique (peptide BMP-2) des CSMs prélevées de la moelle osseuse des patients.

La première étude du projet consiste à greffer, d'une manière aléatoire, les peptides RGD et/ou BMP-2 sur la surface du matériau. Brièvement, nous avons développé trois types de matériaux bioactifs : matériaux fonctionnalisés avec le peptide RGD, matériaux fonctionnalisés avec le peptide BMP-2 et matériaux bi-fonctionnalisés avec les peptides RGD/BMP-2. La caractérisation physicochimique de ces matériaux a été réalisée en utilisant la spectrométrie photoélectrique à rayons X (XPS) pour évaluer la composition chimique de la surface, la microscopie à force atomique (AFM) pour évaluer la topographie de la surface et la microscopie à fluorescence pour confirmer la présence des peptides sur la surface et évaluer

leur densité. L'objectif de cette étude est d'évaluer le potentiel individuel et synergétique de ces peptides à induire et contrôler la différentiation ostéoblastique des CSMs. Dans un premier temps, la caractérisation physicochimique nous a permis de confirmer l'immobilisation covalente des peptides sur la surface et de mesurer leur densité. En effet, la densité des peptides, mesurée sur les surfaces greffées uniquement avec le peptide RGD ou BMP-2, était de 1.8 ± 0.2 pmol/mm² et 2.2 ± 0.3 pmol/mm², respectivement. Cependant, sur les surfaces bi-fonctionnalisées, la densité de chaque peptide a diminué de presque la moitié, atteignant 0.7 ± 0.1 pmol/mm² pour le peptide RGD et 1 ± 0.1 pmol/mm² pour le peptide BMP-2. Ensuite, l'évaluation biologique des différents matériaux fonctionnalisés a clairement révélé que contrairement au peptide RGD, le peptide BMP-2 induit la différenciation ostéoblastique des CSMs. Cependant, le greffage simultané des peptides RGD/BMP-2 améliore significativement la différenciation des CSMs en ostéoblastes et cela malgré la diminution significative de la densité de chaque peptide sur les surfaces bi-fonctionnalisées, comparativement aux surfaces contenant qu'un seul peptide. Ces résultats montrent que les peptides RGD et BMP-2 peuvent engendrer un effet synergétique pour améliorer la différenciation ostéoblastique des CSMs.

Le second chapitre de thèse vise à déterminer si la microstructuration de la surface des matériaux avec des ligands bioactifs améliore la différenciation ostéoblastique des CSMs. En effet, les peptides RGD et BMP-2 ont été greffés séparément sur la surface du matériau sous forme de micro-motifs de différentes formes mais de taille similaire. En se basant sur des précédents travaux de littérature – discutés dans le chapitre II – nous avons sélectionné trois différentes formes de motifs peptidiques (triangle, carré et rectangle) dont la surface est de 50 µm². Ces micromotifs ont été créées grâce à une technique assez répondue et facile à utiliser qui est la photolithographie. Les surfaces microstructurées ont été caractérisées avec l'interférométrie optique et la microscopie à fluorescence. Les résultats montrent que les micromotifs peptidiques ont à la fois la forme et les dimensions prédéfinies. *In vitro*, les résultats de différenciation cellulaire ont révélé que la distribution spatiale des ligands à l'échelle micrométrique joue un rôle très important dans l'engagement et la différenciation des CSMs en ostéoblastes. En effet, contrairement aux micromotifs peptidiques en forme de rectangles, les micromotifs triangulaires et carrés améliorent significativement l'expression des marqueurs ostéogéniques (Runx-2 et Ostéopontine) comparativement à la distribution aléatoire des peptides. Il est important de noter que ce profile d'expression des marqueurs biologiques a été observé que sur les matériaux fonctionnalisés avec le peptide BMP-2, tant dis que les matériaux fonctionnalisés avec le peptide RGD n'ont induit aucun effet spécifique

sur la différenciation des CSMs et cela peu importe la forme des micromotifs peptidiques. En conclusion, cette étude a permis d'identifier un nouveau facteur extracellulaire capable de contrôler la différenciation des CSMs. De plus, nous avons démontré que la distribution spatiale des ligands à l'échelle micrométrique affecte le devenir des CSMs, dépendamment de la nature du principe actif.

Finalement, la troisième étude de ce projet de thèse est une suite logique de l'étude 1 et 2, puisqu'elle consiste à greffer simultanément les peptides RGD et BMP-2 sous forme de micromotifs. En effet, ces surfaces ont été développées afin de bénéficier à la fois de l'effet synergétique des peptides RGD/BMP-2, observé dans l'étude 1 (facteur 1), et de l'effet de la distribution spatiale contrôlée des ligands, observé dans l'étude 2 (facteur 2). Les différents types de matériaux ont été caractérisés avec les mêmes techniques de caractérisation de surface mentionnées dans l'étude 2. Les résultats montrent clairement que les surfaces microstructurées sont très bien définies et correspondent à un damier de micromotifs RGD, intercalé par un damier de micromotifs BMP-2. L'évaluation de la différenciation des CSMs sur ces matériaux a révélé que la combinaison des facteurs 1 et 2 améliore significativement la différenciation des CSMs vers le lignage ostéoblastique, comparativement à l'exposition des CSMs à un seul facteur extracellulaire (1 ou 2). De plus, cette étude confirme les résultats obtenus dans l'étude 2, puisque les micromotifs triangulaires et carrés ont permis une meilleure différenciation cellulaire, comparativement aux micromotifs rectangulaires.

Il est important de noter également que l'évaluation biologique des différentes surfaces biomimétiques a été réalisée dans un milieu de culture basal qui ne contient pas de facteurs ostéogéniques solubles, afin d'étudier d'une manière assez précise et fiable les interactions des CSMs avec les différents microenvironnements *in vitro* développés dans ce projet.

En conclusion générale, les travaux effectués jusqu'à présent ont permis d'identifier deux aspects de la MEC qui influencent considérablement la différenciation ostéoblastique des CSMs. De plus, nous avons démontré que ces deux facteurs peuvent coopérer pour induire une meilleure différenciation cellulaire. Cela révèle clairement l'intérêt des techniques de micro-ingénierie pour une meilleure et plus profonde compréhension des mécanismes d'interactions des cellules souches avec leurs niches, ce qui permettra éventuellement de concevoir des produits d'ingénierie tissulaire sur-mesure.

Mots clés : Micro-structuration de la surface des matériaux, matrice extracellulaire biomimétique, peptides mimétiques, BMP-2, cellules souches, ostéogenèse.

Micro-engineered substrates as bone extracellular matrix mimics

Abstract

It is becoming increasingly appreciated that the role of extracellular matrix (ECM) extends beyond acting as scaffolds to providing biochemical and biophysical cues, which are critically important in regulating stem cell self-renewal and differentiation. To date, more than 15 different extrinsic (environmental) factors, including the matrix spatial organization, topography, stiffness, porosity, biodegradability and chemistry have been identified as potent regulators of stem cells specification into lineage-specific progenies. Thus, it is plausible that the behavior of biomaterials inside the human body will depend to a large extent on their ability to mimic ECM properties of the tissue to be replaced. Recently, nano- and microengineering methods have emerged as an innovative tool to dissect the individual role of ECM features and understand how each element regulates stem cell fate. In addition, such tools are believed to be useful in reconstructing complex tissue-like structures resembling the native ECM to better predict and control cellular functions.

In the thesis project presented here, the concept of deconstructing and reconstructing the ECM complexity was applied to reproduce several aspects inherent to the bone ECM and harness their individual or combinatorial effect on directing human mesenchymal stem cells (hMSCs) differentiation towards the osteoblastic lineage.

Three main components were used throughout this project: a model material (borosilicate glass), ECM derived peptides (adhesive RGD and osteoinductive BMP-2 mimetic peptides) and bone marrow derived hMSCs. All cell differentiation experiments were performed in the absence of soluble osteogenic factors in the medium in order to precisely assess the interplay between hMSCs and the different artificial matrices developed in the current study.

First, RGD and/or BMP-2 peptides were covalently immobilized and randomly distributed on glass surfaces. The objective here was to investigate the effect of each peptide as well as their combination on regulating hMSCs osteogenic differentiation. The most important funding was that RGD and BMP-2 peptides can act synergistically to enhance hMSCs osteogenesis.

Then, micropatterning technique (photolithography) was introduced to control the spatial distribution of RGD and BMP-2 at the micrometer scale. The peptides were grafted individually onto glass substrates, as specific micropatterns of varied shapes (triangular, square and

rectangle geometries) but constant size (50 µm² *per* pattern). In this second part of the project, the focus was made on investigating the role of ligands presentation in a spatially controlled manner in directing hMSCs differentiation into osteoblasts. Herein, we demonstrated that the effect of microscale geometric cues on stem cell differentiation is peptide dependent.

Finally, glass surfaces modified with combined and spatially distributed peptides were used as *in vitro* cell culture models to evaluate the interplay between RGD/BMP-2 crosstalk and microscale geometric cues in regulating stem cell fate. In this study, we revealed that the combination of several ECM cues (ligand crosstalk and geometric cues), instead of the action of individual cues further enhances hMSCs osteogenesis.

Overall, our findings provide new insights into the role of single ECM features as well their cooperation in regulating hMSCs fate. Such studies would allow the reconstruction of stem cell microenvironment in all the aspects *ex vivo*, which may pave the way towards the development of clinically relevant tissue-engineered constructs.

Keywords: Chemical micropatterning, bioactive surfaces, mimetic peptides, BMP-2, mesenchymal stem cells, stem-cell commitment & differentiation, stem-cell niche, osteogenesis.

Unité de recherche

3 BIO's TEAM: BIOactive surfaces, BIOmaterials and BIOmimetic tissue-engineered products, Institute of Chemistry & Biology of Membranes & Nanoobjects (UMR5248 CBMN), 2 Rue Escarpit, 33607 Pessac, France.

Table of contents

List of tables

List of figures

Abbreviations

ADSCs	Adipose Derived Stem Cells
AFM	Atomic Force Microscopy
ALP	Alkaline Phosphatase
Al_2O_3	Alumina
AR	Aspect Ratio
BCP	Biphasic Calcium Phosphate
BMPCs	Blood Mesenchymal Precursor Cells
BMPR	Bone Morphogenetic Protein Receptor
BMSCs	Bone Marrow Mesenchymal Stem Cells
BSP	Bone Sialoprotein
CAGR	Compound Annual Growth Rate
CaP	Calcium Phosphate
Co-Cr	Cobalt/Chromium
Cr	Chromium
ECM	Extracellular Matrix
ERK	Extracellular Signal Regulated Kinase
FAK	Focal Adhesion Kinase
FDA	Food and Drug Administration
FGF	Fibroblast Growth Factor
GVHD	Graft Versus Host Disease
HA	Hydroxyapatite
HA	Hyaluronic Acid
hESCs	human Embryonic Stem Cells
hMSCs	Human Mesenchymal Stem Cells
HSC	Hematopoietic Stem Cells
HUVEC	Human Umbilical Vein Endothelial Cells
IGF	Insulin-like Growth Factor
iPS	Induced Pluripotent Stem Cells
JNK	c-Jun N terminal kinase
MAPCs	Multipotent Adult Progenitor Cells
MAPK	Mitogen Activated Protein Kinase
Ni	Nickel
Nb	Niobium
OCN	Osteocalcin
ON	Osteonectin
OPG	Osteoprotegerin
OPN	Osteopontin
PAA	polyacrylic Acid
PCL	Polycaprolactone
PDGF	Platelet Derived Growth Factor
PDMS	Poldimethylsiloxane
PEEK	Polyetheretherketone
PEG	Polyethylene Glycol
PEO	Polyethylene Oxide
PET	Polyethylene Terephthalate
PGA	Polyglycol Acid
PLGA	Polyglycol Lactic Acid
PLA	Poly Lactic Acid

PMMA	Polymethyl Methacylate
Poly-HEMA	Poly-hydroxyethylmethacrylate
PPAR-γ	Peroxisome Proliferator Activated Receptor gamma
(P(PF-co-EG))	Poly(propylene furmarate-co-ethylene glycol)
PS	Polystyrene
PVA	Polyvinyl Alcohol
PTFE	Polytetrafluoroethylene
PTH	Parathyroïd Hormone
RANK	Receptor Activator of Nuclear factor Kappa-B
rhBMP	Bone Morphogenetic Protein
RhoA	Ras homolog gene family, member A
ROCK	Rho-Associated Protein Kinase
Runx-2	Runt Related Transcription Factor 2
SAMs	Self-assembled Monolayers
α-SMA	Alpha-Smooth Muscle Actin
SS	Stainless Steel
TCP	Tricalcium Phosphate
TGF-β	Transforming Growth Factor-beta
Ti	Titanium
TiO_2	Titanium Oxide
THR	Total Hip Replacement
TKA	Total Knee Arthroplasty
TRAP	Tartrate Resistant Acid Phosphatase
UHMWPE	Ultra High Molecular Weight Polyethylene
VEGF	Vascular Endothelial Growth Factor
WHO	World Health Organization
XPS	X-ray photoelectron spectroscopy
ZrO_2	Zirconia

« L'esprit d'équipe ? C'est des mecs
qui sont une équipe, ils ont un esprit !
Alors, ils partagent ! »
Michel Colucci "Coluche"

«*Mice predict the effect on humans with*
about 43 % efficiency, so sometimes
it would seem that tossing a coin would
***give a better result* ! »** Dr. Thomas Hartung.

«*The more you know, the more you realize*
how much you don't know- The less you
***know, the more you think you know*»**
David T. Freeman

A ma famille,
A mes amis…

Acknowledgement

Je tiens tout d'abord à remercier les membres du jury, Madame Nathalie Faucheux, Monsieur Emmanuel Pauthe et Monsieur Jean-Christophe Fricain d'avoir accepté d'évaluer ce travail à titre de rapporteurs et d'examinateurs et Monsieur Diego Mantovani qui a gentiment accepté d'effectuer la prélecture de ce document. Je vous remercie pour vos appréciations et vos commentaires pertinents, particulièrement Madame Nathalie Faucheux pour vos questions et remarques très instructives sur ce manuscrit de thèse, lors de mon examen predoctoral et également au congrès mondial WBC 2016. Je remercie également Monsieur René Therrien pour avoir eu la gentillesse de présider cette soutenance.

Je remercie très sincèrement mon directeur de thèse Gaétan Laroche pour m'avoir accueilli si chaleureusement au sein de son laboratoire et m'avoir accordé une très grande liberté quant à l'organisation et l'amélioration du projet au fil des années. Merci pour m'avoir confié la responsabilité sur ce projet à la fois original et passionnant, pour m'avoir laissé proposer des idées et de les appliquer, tout en gardant un œil attentif sur l'avancement des travaux. Je te remercie également pour m'avoir donné l'opportunité de faire des activités très enrichissantes en parallèle à mon projet de thèse, y compris l'enseignement, la participation à la rédaction d'un chapitre de livre et l'organisation et la participation à des congrès nationaux et internationaux.

Je remercie également ma directrice de thèse Marie-Christine Durrieu pour son accueil au sein de son laboratoire, pour m'avoir donné la chance de travailler sur un projet innovant et d'avoir dirigé de près ce travail. Je te remercie aussi pour ta disponibilité et tout ce que tu m'avais appris.

Thanks Eli Sone for your contribution to the project as a co-supervisor. I really appreciated your very insightful comments and recommendations throughout my thesis. I hope working with you on further challenging projects.

Je remercie les co-auteurs qui ont contribué à la réalisation de ce projet ; Pascale Chevallier et Laurent Plawinski. Je remercie également Andrée-Anne Guay-Begin, Christian Sarra-Bournet et Cedric Ayela pour leurs précieux conseils et pour m'avoir aidé à me familiariser avec des techniques que je n'avais pas utilisées auparavant, XPS, AFM, photolithographie. Je remercie particulièrement et du fond du cœur Pascale Chevallier d'avoir cru en moi de début à la fin, pour son grand soutien et sa grande générosité. Je te remercie énormément

pour tout ce que tu m'as apporté durant ces années de thèse, professionnellement et personnellement parlant. T'avais toujours les bons mots et les bons gestes pour me remonter le moral et me redonner le sourire quand ça n'allait pas. Tu fais partie des plus belles rencontres que j'ai faites au Canada et je révérais travailler avec toi dans le future ou du moins travailler avec des personnes avec autant de qualités que toi !!!

Je remercie les organismes subventionnaires, les programmes CRSNG et NCPRM qui ont assumé généreusement les couts de ce projet. Merci également à Karine Fortin, Ginette Cadieux, Andrée Lord, Martine Demers et Geneviève Bruneau pour leur travail irréprochable, leur accueil très chaleureux et pour m'avoir beaucoup facilité les démarches administratives et l'établissement de mon statut au Canada.

Je remercie tous mes collègues du coté Canadien qui étaient une deuxième famille pour moi et qui m'ont accueilli les bras grands ouverts. Je m'estime très chanceux d'avoir eu l'opportunité de travailler durant toutes ces années dans un environnement multiculturel où j'ai pu rencontrer des personnes aussi chaleureuses que généreuses de tous les coins du monde. Je dois dire que c'était une expérience humaine extraordinaire qui m'a fait beaucoup gagner en humanité, maturité et ouverture d'esprit. Je remercie Stéphane, Morgane, Marie, Gad, Corinne, Michael (encore une fois Pascale et Andrée-Anne; elles méritent !), Farid, Ivan, Audrey, Stéphanie, Jessie, Max, Sébastien, Carlo, Lucie, Vanessa, Eléonore, Nina, Livia, Caroline, Essowè, Ranna, Juliana, Mahrokh, Dimitria, Clayton, Maxime, Olexandr, Francesco et tous les autres sans exception.

Un merci aussi sincère à mes collègues de France ; Laurence, Caroline, Guillaume, Gregor, Marie-Christine, L'équipe de Madame Reiko Oda, Emilie, Sylvain et Marion.

Un merci particulier à Mathieu (le mentor !), Laurence (Roomie), Morgane et Marie (collègues de bureau) et Ludivine (et ses histoires super drôles !) avec qui j'ai partagé des moments inoubliables au travail et en dehors du travail.

Je remercie chaleureusement mes amis en France et au Canada et tous ceux qui ont contribué d'une manière ou d'une autre à cet étape de ma vie ; Manal, Akli, Nesrine, Marie-Hélène, Kamal, Enora, Wiame, Sid Ali, Alexandra, Basma, Victoria, Yamanda, Tanu et tous ceux que j'oublie.

Milles merci à Nesrine….. Sans toi j'aurais eu beaucoup plus de difficultés à surmonter les périodes difficiles de ma thèse. T'es tout simplement une personne en or et même si j'écris autant de pages que ce que j'ai écrit dans mon manuscrit de thèse je manquerai certaines de

tes qualités. T'es la plus belle rencontre que j'ai faite depuis que je suis à l'étranger et j'espère que notre amitié durera pour la vie (Je croise les doigts pour que brahman ne croise plus le chemin de Babi !!).

J'adresse mes remerciements à mes meilleurs amis d'enfance qui sont toujours restés dans mon cœur et mes pensées malgré les milliers de kilomètres qui nous séparent ; Amine, Abdou, Aminou, Mhamed, Nour eddine et Ala. Merci pour votre fidélité, disponibilité, générosité et d'être là dans le meilleur et le pire. Pour rien au monde je vous oublierai.

A ma famille…. Ma mère Djamila et mon père Abdelmajid… Je vous dédie ce travail en témoignage de ma profonde reconnaissance, mon grand amour et ma gratitude pour vos sacrifices. Vous êtes ma fierté, mon exemple dans la vie et ma source d'inspiration et de motivation. Je suis tellement reconnaissant envers vous que j'ai pris la décision en étant encore très jeune de quitter la maison en ayant un seul objectif ; c'est de revenir vous revoir un jour avec un stent qui stabilisera à vie la maladie de mon père…. J'ai travaillé dur et je travaillerai encore plus dur pour y arriver... Je vous aime plus que tout, que dieu vous vous accorde une longue vie. Merci de m'avoir, en plus, donné 3 formidables frère et sœurs; Amel, Ayoub et la petite merveille Ines. Mon amour pour vous est inconditionnel et je serai toujours là pour vous. Merci ma petite princesse Ines pour le beau gâteau que tu as fait à cette occasion que je n'ai pas eu la chance de le gouter ; tu me manques tellement…

FOREWORD

The use of orthopaedic biomaterials has expanded dramatically during the past decades owing to increased life-expectancy and musculoskeletal diseases, changes in lifestyle and progress in implantology. Several facts reflect the rapid growing of orthopaedic biomaterials prevalence. Babies born today will live almost 3 decades longer than those born in 1900 [1] and almost 7 years than those born in 1960 [2], which reflects an increase in life-expectancy and worldwide population. It was estimated that 90 % of the population over the age of 40 years suffers from a degenerative joint disease [3]. Chronic disability among the elderly has decreased by almost one-third, showing that medical devices have improved both the quality and the length of person's life [4]. The Bone and Joint Decade organization has been launched in 2000, remandated in 2010 and endorsed by the United Nations and the World Health Organization (OMS) [5]. Last decade's estimates showed that orthopaedic implants are the bulk of all implanted devices worldwide and will remain the largest segment in biomaterials market [6] [7].

Although these facts and statistical data highlight the upsurge in the demand of orthopedic biomaterials as well as their substantial contribution in improving the life and comfort of patients, the acceptance of these implants by the human body is far from being trivial. In addition, the consequences of implant rejection are sometimes more dramatic than what untreated damaged bone do.

Currently, there are several clinical needs that are not satisfactory filled in orthopaedic, spinal, dental, cranial and maxillofacial surgery. The work presented here, although being in its infancy, addresses two main issues. The reader will be introduced to the thesis project challenges by means of a set of questions that span from the current clinical needs in orthopaedics to the approach proposed in this research project as a promising way toward the resolution of the addressed clinical issues.

❖ **What are the main unmet clinical needs in orthopaedic surgery?**

Clinical need 1: The long term performance of orthopaedic biomaterials, especially used in load bearing parts, given that their lifespan is still limited to 10-15 years after implantation [8].

Clinical need 2: The reconstruction of large bone defects caused by diseases, non-union fractures or tumor resection.

❖ **Why is the long term performance of commercially available orthopaedic biomaterials limited** (*Clinical need 1*)**?**

One key raison for their limited performance is the lack of a robust integration of implanted biomaterial with the host bone tissue, often due to the formation of a fibrous layer at the interface bone/implant.

❖ **Why large bone defects reconstruction is still a challenging task** (*Clinical need 2*)**?**

This is due to the low potential of currently used biomaterials in clinics to induce mesenchymal stem cells (MSCs) and progenitor cells migration to the defect site and ensure their differentiation into mature bone cells. Consequently, the implant is poorly colonized by bone cells, resulting in a weak host bone-to-implant contact.

One promising approach to enhance the biological compatibility of biomaterials is to combine them with the patient's MSCs, differentiated *ex-vivo*, prior to implantation. Nevertheless, this strategy has limited impact nowadays because MSCs can be harvested from the human body only in few amounts [9]. In addition, e*x-vivo* expansion and differentiation of stem cells are not only time-consuming protocols but also fail to produce clinically relevant amounts of osteogenic cells.

❖ **How the underlying clinical needs could be met?**

From a rational point of view, the most effective and reliable approach to circumvent the underlying concerns is to mask the bio-inertness of biomaterials used as cell culture platforms or orthopaedic implants by creating on their surfaces an artificial extracellular matrix (ECM). This ECM should mimic the *in vivo* microenvironment features that mediate the switch of MSCs from their stemness state into an osteoblast lineage.

While creating a biomimetic microenvironment on biomaterial surfaces seems to be a good idea to overcome the above-mentioned issues, translating this idea to bone tissue-engineered product is extremely complex, owing to the complexity of the native ECM. Just 40 years ago, the ECM was considered as an inert scaffold, providing only a supportive environment on which cells can attach [10]. To date, thanks to increased investments, funding and grants in biomaterials and stem cell research [4], the ECM is recognized to do more than just support the cells, as over 15 different factors have been shown to influence MSC fate. Among these ECM features, physical properties, including stiffness, topography and porosity, and biochemical cues, including ligands density, spatial distribution and combinatorial effects have been extensively studied during the last decade [11] [12] [10]. All these ECM aspects are interlinked and can act independently or in concert to control MSCs fate decision *in vivo*, hence the difficulty of mimicking ECM features *in vitro*. Therefore, deconstructing the complexity of the native ECM and harnessing the interplay between MSCs and individual ECM cues will undoubtedly pave the way towards the reconstruction of finely-tuned artificial MSC microenvironments for bone tissue engineering applications.

In this regard, the studies illustrated in this manuscript provide new insights into the potential role of the native ECM features, especially biochemical cues, in directing human MSCs (hMSCs) osteogenesis. Two aspects innate to the natural microenvironment and expected to drive hMSCs osteogenic differentiation *in vivo* will be addressed: *(1)* the cooperation between integrin ligands and growth factors and *(2)* the spatial distribution of ECM adhesive ligands and growth factors at the micrometer scale. A schema providing an overview of the general methodology of the thesis project is depicted in **Figure 1**.

In the first stage, cell adhesive RGD and osteoinductive BMP-2 mimetic peptides were covalently immobilized onto a model material (glass substrates). Three different conditions were prepared; glass surfaces homogeneously functionalized with RGD, BMP-2 or combined RGD/BMP-2 peptides (Paper I). The objective here was to investigate the effect of each peptide on hMSCs fate and whether or not these peptides can act synergistically to enhance osteogenesis, when combined. Also, the stimulatory effect of BMP-2 was correlated to its surface density. The peptide grafting was ascertained using complementary physical-chemical techniques, X-ray photoelectron spectroscopy (XPS), atomic force microscopy (AFM) and fluorescence microscopy. Cell differentiation analyses revealed that BMP-2 peptide induced hMSCs osteogenic differentiation and the presence of RGD peptide improved

its osteoinductive capacity, even in the absence of soluble osteogenic factors in the cell culture medium. Thereby, the study described in the paper 1 highlighted the existence of a certain crosstalk between ECM derived adhesive ligands and growth factors in regulating stem cell fate.

Subsequently, by seeking to harness the potential presentation of ECM derived ligands in a spatially controlled manner, which somewhat mimics the *in vivo* situation, RGD and BMP-2 peptides were finely distributed over glass surfaces at the micrometer scale, using micropatterning strategy (photolithography) (Paper II). To this end, the peptides were grafted as specific micropatterns of varied shapes (triangle, rectangle and square) but constant overall area (50 μm^2) in order to evaluate the effect of geometric cues on hMSC fate decision. Peptide micropatterns were assessed for their shape, size and reproducibility by optical microscopy, interferometry and fluorescence microscopy. hMSCs cultured on the different micropatterned surfaces exhibited different cell behaviors in relationship with the pattern shape and the type of patterned ligand. In fact, on RGD micropatterned surfaces, geometric cues did not affect hMSCs osteogenic differentiation as the expression of osteogenic markers was very low and similar between homogenous and micropatterned surfaces functionalized with RGD peptide. In contrast, the effect of geometric cues was clearly visible on BMP-2 surfaces containing BMP-2 peptide. That is, osteogenesis was significantly enhanced on triangular and square BMP-2 micropatterns as compared to the rectangular ones. Thus, we evidenced throughout this set of experiments (Paper II) that micro-scale geometric cues, when carefully selected, can effectively dictate hMSCs specification towards the osteoblastic lineage.

The third challenge in this thesis has raised by considering the insightful knowledge gained from the studies 1 and 2. By seeking to partially recapitulate ECM cues that dictate the switch in lineage differentiation from MSCs into osteoblasts *in vivo*, we created artificial ECMs where both peptides crosstalk and geometric cues signaling could be triggered to regulate MSCs osteogenesis. Therefore, this biomimetic microenvironment consisted of a checkerboard of juxtaposed RGD and BMP-2 micropatterns (Paper III). The patterns were similar in shape and size to those used in the study II and characterized using the same techniques. Quite consistent with the findings reported in the study II, i*n vitro* analyses confirmed again that triangular and square micropatterns are of potential relevance in directing hMSCs fate towards the osteoblastic lineage.

By combining results from these three studies, we were able to evaluate to which extent triangular and square RGD/BMP-2 micropatterns affect hMSCs osteogenic differentiation. Study III *VS* study II revealed that the spatial distribution of combined RGD/BMP-2 peptides

as triangular and square micro-sized geometries enhanced hMSCs osteogenesis as compared to their homogenous distribution on the material surface. Study III *VS* study II demonstrated that triangular and square RGD/BMP-2 micropatterns improved hMSCs osteogenesis as compared to triangular and square BMP-2, respectively. Taken together, these findings suggest that integrin ligands/growth factors crosstalk and geometric cues are not only potent modulators of hMSCs osteogenic differentiation but can also overlap to further enhance lineage-specific differentiation.

The studies achieved in this thesis project provide new insight into the stem cell-ECM interactions that are likely to contribute to the design of finely-tuned biomaterials capable to meet the current clinical demand in orthopaedic surgery.

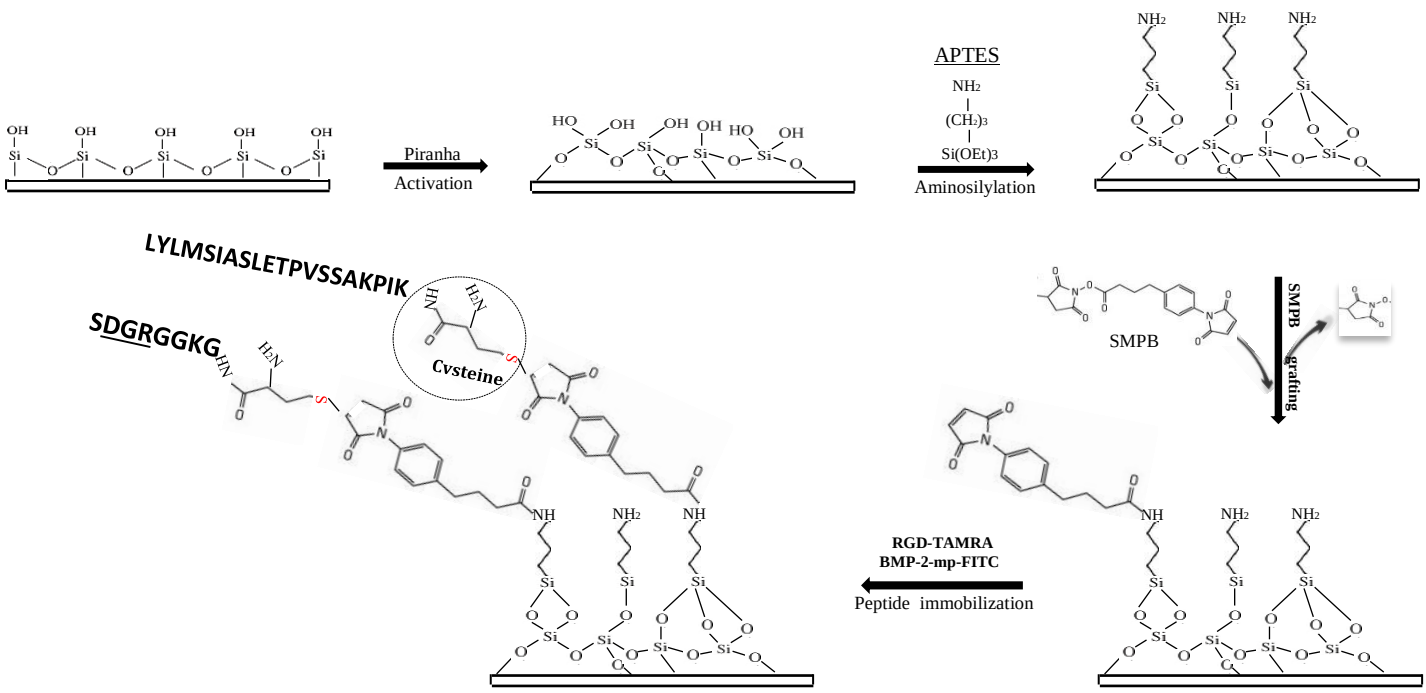

Axis 1. Strategy of the covalent immobilization of RGD and BMP-2 peptides on glass surfaces. For the homogenous peptide grafting, SMPB-NH2-glass surfaces were directly covered with RGD and/or BMP-2 solution. However, the peptide micropatterning required the structuration of SMPB-NH2-glass surfaces using photolithography prior to peptide grafting.

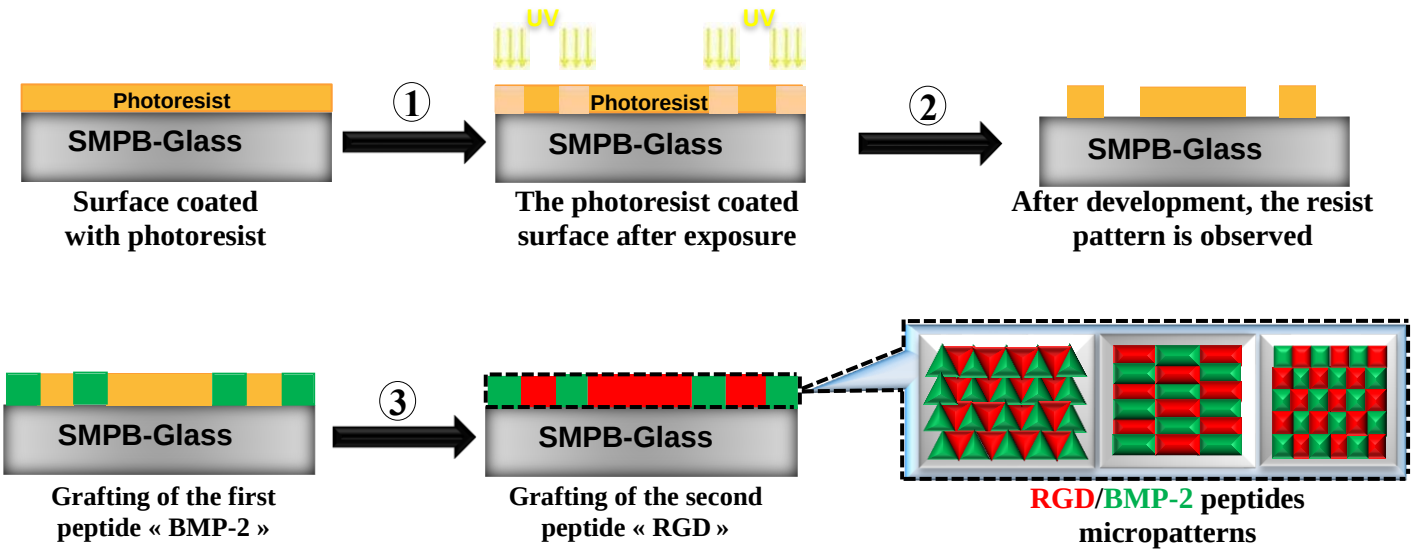

Axis 2. Microscale patterning of RGD and/or BMP-2 peptides using photolithography.

Figure 1: Schematic summary of the main guidelines of the thesis project

Some details regarding the articles achieved during the three years of the thesis as well as the role of the co-authors in the accomplishment of this work are given bellow.

Paper 1:

Title: RGD and BMP-2 mimetic peptide crosstalk enhances osteogenic commitment of human bone marrow stem cells.

Authors: I. Bilem, P. Chevallier, L. Plawinski, E.D. Sone, M.C. Durrieu, G. Laroche.

Journal: Acta Biomaterialia, 36 (2016) 132-42.

State: Submitted 2015, Dec 8th. Published 2016, Mar 18th .

Author's contribution: The first author designed the experiments based on the instructive discussion with all the authors. The first author performed all the experiments, analyzed and interpreted the data and drafted the manuscript. P. Chevallier characterized most of the samples under XPS and significantly contributed to the interpretation of XPS data. All the authors reviewed the manuscript.

Paper 2:

Title: The spatial distribution of RGD and BMP-2 mimetic peptides at the subcellular scale modulates of human mesenchymal stem cells osteogenesis.

Authors: I. Bilem, L. Plawinski, P. Chevallier, E.D. Sone, G. Laroche, M.C. Durrieu.

Journal: ACS Nano.

State: Submitted 2016, Mar 19th.

Author's contribution: The first author designed the experiments based on the instructive discussion with all the authors. The first author performed all the experiments, analyzed and interpreted the data and drafted the manuscript. The difference between the submitted article and that inserted in the thesis is that ALP results are provided as supplementary data only in the thesis manuscript. L. Plawinski collected the raw ALP data and converted them into ALP values (pmole). All the authors reviewed the manuscript.

Paper 3:

Title: Interplay of geometric cues and RGD/BMP-2 crosstalk in directing stem cell fate.

Authors: I. Bilem, P. Chevallier, L. Plawinski, E.D. Sone, M.C. Durrieu, G. Laroche.

Journal: Biomaterials.

State: Submitted 2016, Apr 13th.

Author's contribution: The first author designed the experiments based on the instructive discussions with all the authors. The first author performed all the experiments, analyzed and interpreted the data and drafted the manuscript. All the authors reviewed the manuscript.

LITERATURE REVIEW

I. Physiology of bone tissue

Bone is a complex organ composed of several tissues working together: osseous tissue, cartilage, dense connective tissues, epithelium, adipose tissue and nervous tissue. Bone tissue is a highly specialized and dynamic living tissue that contributes significantly to the homeostasis of the body. It continuously grows and repairs itself since it is subjected to a regular process of breaking down of old bone and building of new bone tissue. This turnover is called *bone remodeling* [13].

1. Bone tissue functions

Bone tissue plays an important role within the body, both biomechanically as metabolically. It has three main functions:

Mechanical function. Since the bone has high mechanical properties, it plays an important role in supporting the body and protecting organs, nervous system and stem cells in the marrow.

Metabolic function. Bone plays a vital role in maintaining mineral homeostasis. It stores and releases several minerals, especially calcium and phosphate, which contribute to the bone strength.

Hematopoietic function. Embryonic bone and some adult bones such as hip bones, ribs, breastbone, vertebrae (backbones) and skull contain hematopoietic stem cells which are responsible for generating blood cells (red and white blood cells and platelets).

2. Bone components

Bone is a connective tissue that comprises various cell types entrapped in a mineralized extracellular matrix (ECM), occupying about 90% of the tissue volume and conferring rigidity and strength to the skeleton while still maintaining some degree of elasticity.

2.1 Cellular components of bone tissue

Bone tissue is composed of four different cell types, osteoblasts, osteocytes, osteoclasts and bone-lining cells [13] [14].

Osteoblasts. They originate from the differentiation of MSCs that reside in the periosteum, endosteum and bone marrow [15]. MSCs maintain their stemness until they are stimulated (due to injury or bone development) to gradually become mature osteoblasts. Osteoblasts express different osteogenic factors, including alkaline phosphatase (ALP), type I collagen, osteopontin (OPN), osteocalcin (OCN) and bone sialoprotein (BSP)

which are involved in the formation of an organic bone matrix (osteoid) and its mineralization **(Figure 2)**.

Osteocytes. These cells are osteoblasts that have reached a high level of maturation. They are surrounded by a mineralized bone matrix and have the capacity not only to synthesize, but also to resorb the bone matrix to a limited extent, thus regulating bone remodeling process. Osteocytes are also responsible for the transmission of mechanical and biochemical stimuli, essential for bone metabolism.

Osteoclasts. They are giant multinucleated cells (diameter ≈ 100 microns) derived from the self-fusion of macrophages. These macrophages (pre-osteoclasts) express RANK receptor (Receptor Activator of Nuclear factor Kappa-B) and then merge under the activation of (RANKL) ligand, which leads to their differentiation into multinucleated active cells (osteoclasts). The main function of osteoclasts is to digest the old mineralized bone matrix by releasing tartrate-resistant acid phosphatase, cathepsin K, matrix metalloproteinase 9 and gelatinase [16] **(Figure 2)**.

Bone-lining cells. These cells are flat, elongated and inactive. They cover bone surfaces that undergo neither bone formation nor resorption. Their principle function is to protect bone matrix against the osteoclast action. However, during bone remodeling, these cells degrade the osteoid by secreting collagenases. Bone-lining cells are also a source of osteoblasts. Indeed, under the action of various stimuli, such as parathyroïd hormone (PTH), they can dedifferentiate into active osteoblasts.

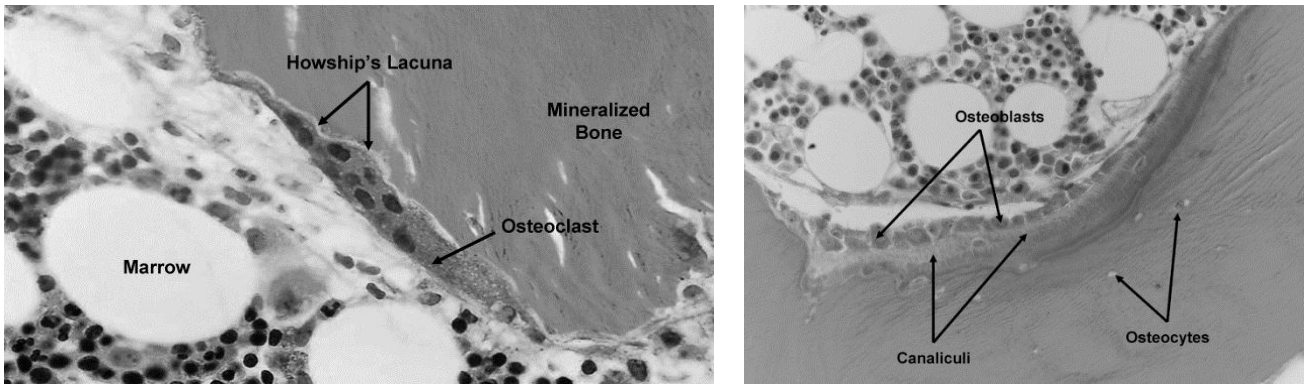

Figure 2: Bone tissue remodeling. Osteoclasts resorb bone to form resorption pits known as Howship's lacunae (left). Osteoblasts synthesize the inorganic matrix (osteoid), rich in type I collagen, to fill in resorption pits (right). The osteoid is gradually mineralized to form new bone [14].

2.2 Extracellular matrix of bone tissue

Bone ECM is made of non-mineralized organic components (predominantly type I collagen) and mineralized inorganic components (mineral crystals) [17].

Organic matrix. Type I collagen constitutes approximately 80-90% of the organic matrix. It confers bone tissue its hierarchical structure and ensures its viscoelasticity. The remaining 10-20 % correspond to other types of collagen (collagen type III, V, X) and over 200 different non-collagenous proteins such as proteoglycans, osteonectin (ON), BSP, OCN, OPN and ALP, all of them contribute to the maintenance of bone tissue. Other molecules have a direct action on the activity of bone cells, such as Bone Morphogenetic Proteins (BMPs), known to induce the differentiation of osteoblast precursors or osteoprotegerin (OPG) glycoprotein that inhibits the differentiation of osteoclast precursors. Organic matrix also comprises specific proteins involved in bone remodeling and vasculature, such as TRAP (tartrate-resistant acid phosphatase) and VEGF (Vascular Endothelial Growth Factor), respectively [16] [18].

Mineral matrix. About 50-70% of the weight of bone tissue corresponds to mineral matrix that ensures its rigidity. The mineral content in bone is mostly a crystalline calcium phosphate deposited in thin apatite platelets, with small amounts of carbonate, magnesium, and acid phosphate. Bone mineral is initially deposited in the form of hexagonal apatite nano-crystals in small gaps generated by the regular stacking pattern of collagen molecules in a fiber [19]. As the hexagonal apatite nano-crystals mature they take on a plate shape. Although this process is mediated by bone cells and the organic phase, it may also be facilitated by ECM vesicles in bone in which calcium and phosphate concentrations can increase sufficiently to precipitate apatite crystals [20].

3. Bone tissue structure: From the macro- to nanometer scale

The squeleton is made up of more than 206 different bones that can be classified depending on their shape into short, flat and long bones. As with all organs in the body, bone tissue is hierarchically organized over length scales that span several orders of magnitude from the macrometer scale to the nanometer scale [21] [22] [23] **(Figure 3)**:

- At the macrometer scale, bone is made of 80% of cortical (compact) bone and 20% of trabecular (cancellous) bone. Cortical bone is much denser and less porous (5% to 30 %) than trabecular bone (30% to 90%). Cortical bone forms the outer shell (cortex) of most bones and provides mechanical and protective functions, while trabecular bone is typically found at the ends of long bones (epiphysis) and provides metabolic functions.

- At the micrometer scale (10 to 100 µm), osteon and trabeculae are the anatomical and functional units of cortical and trabecular bone, respectively.
- At the sub-micrometer scale (1 to 10 µm), an osteon is organized in concentric flat sheets of mineralized collagen fibers, called lamellae. An osteon or Haversian system consists of a set of 8-15 lamellae surrounding the Haversian canal. In cortical bone, lamellae are highly organized and oriented in parallel to the longitudinal axis of bone, while in trabecular bone their arrangement is irregular.
- At the nanometer scale (~100 nm to 1 µm), mineralized collagen fibers of ~200 nm in diameter are the structural unit of bone tissue.
- At the sub-nanometer scale (<100 nm), the main components are the apatite nano-crystals, type I collagen proteins and non-collagenous proteins. Apatite nano-crystals exhibit typical average dimensions of 50 x25x3 nm. Depending on their maturity, their dimensions can vary from 15 to 150 nm in length, 10 to 80 nm in width and 2 to 5 nm in thickness. On the other hand, triple helices collagen molecules have average dimensions of 200 nm in length and 2–3 nm in diameter.

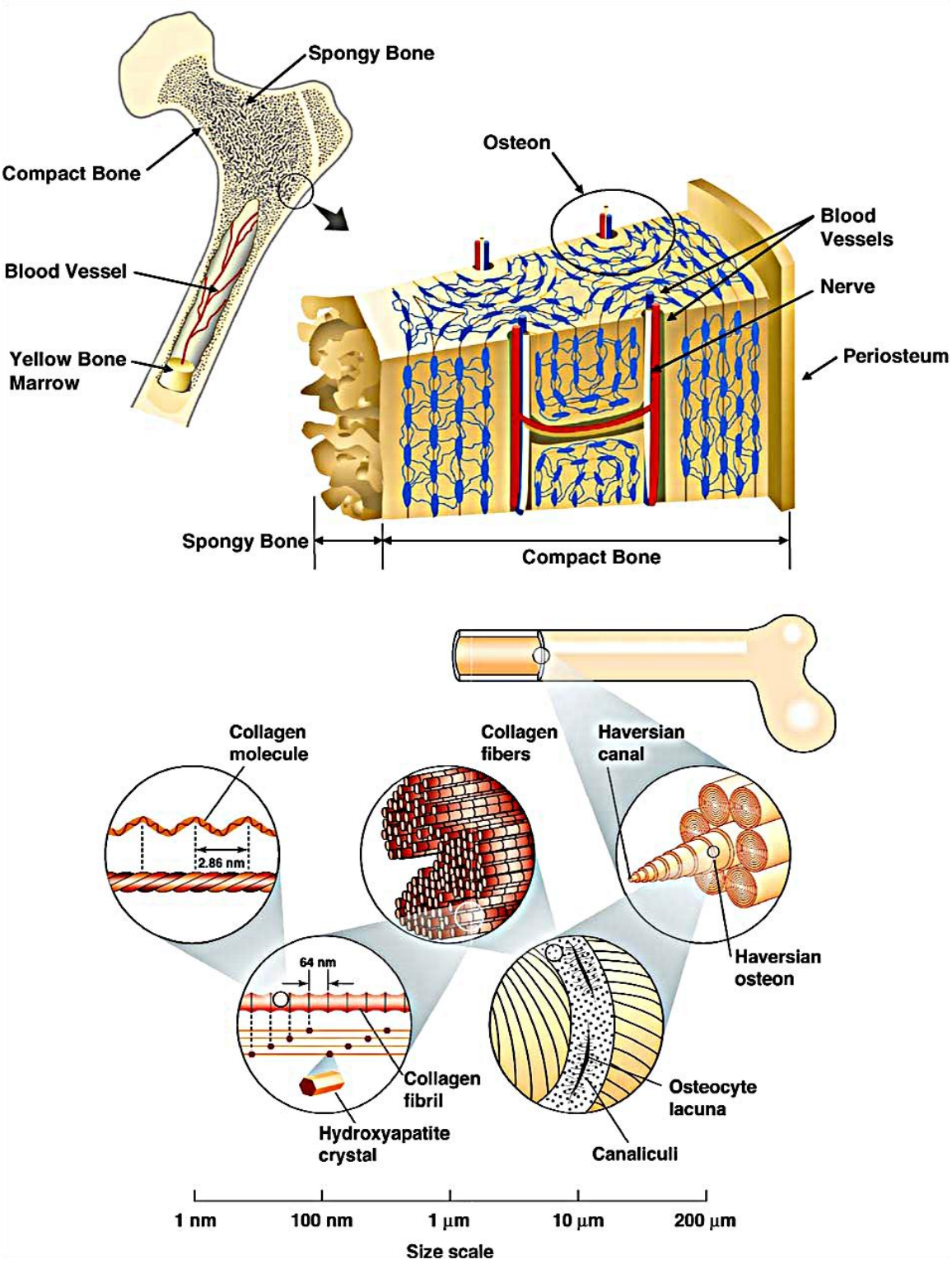

Figure 3: Hierarchical structure of human cortical/compact bone [24].

II. Bone development and repair

1. Physiology of bone development

During life, bone undergoes processes of longitudinal and radial growth, modeling (re-shaping) and remodeling, as described below [25].

1.1. Osteogenesis

Normal bone develops through two mechanisms that can act independently or together during bone formation: endochondral and intramembranous ossification [26] [27] **(Figure 4) (Figure 5)**.

The process of endochondral bone formation involves different phases of cell proliferation, differentiation, migration and ECM remodeling. This begins with the differentiation of MSCs into chondrocytes that synthesize a hyaline cartilage model, rich in type II collagen, whose shape resembles a small version of the bone to be formed [28]. Gradually, chondrocytes in the primary ossification center -in the middle of diaphysis- grow, differentiate into hypertrophic chondrocytes and begin secreting ALP, thus allowing for the calcification of the cartilaginous matrix. Simultaneously, a vascularized periosteal bone -rich in osteoprogenitor cells that later become osteoblasts- appears around the diaphysis of the hyaline cartilage model. At this moment, hypertrophic chondrocytes (before apoptosis) secrete VEGF, leading to blood vessels sprouting from the periosteal bone to the primary ossification center. Blood vessels, forming the periosteal bud, invade cavities left by apoptotic chondrocytes, thus carrying hematopoietic cells, osteoprogenitor cells and other cells inside the cavities. While hematopoietic cells will later form the bone marrow, osteoprogenitor cells specialize into osteoblasts that form osteoid over the calcified cartilage [26]. Subsequently, the primary ossification center progresses in the direction of the epiphysis, leading to a secondary ossification center. Osteoprogenitor cells invade epiphyseal cartilage, differentiate into osteoblasts and secrete osteoid onto the cartilage matrix -cartilage tissue remains in two places: articular cartilage and epiphyseal plate- [29]. Finally, a woven bone (immature bone) is formed which will be replaced by lamellar bone at the next steps of bone development [27].

The bone development via endochondral process occurs in initial bone formation in an embryo and fetus as well as in bone growth during infancy, childhood and adolescence. Indeed, it is involved in growth in length of the most bones in the body, mainly long bones such as femur, tibia, humerus and radius [26].

Unlike the endochondral ossification, the intramembranous ossification does not involve a cartilaginous tissue formation. This process begins by the aggregation of MSCs into layers at specific regions of a highly vascular connective tissue, called center of ossification. MSCs proliferate, condense around a profuse capillary network and differentiate into osteoblasts. The latter secrete organic matrix (osteoid), get surrounded by collagen fibers and transform into osteocytes. At this stage, the collagen fibers of osteoid form a woven bone that gradually thickens. Eventually, woven bone is remodeled and replaced by lamellar bone [26] [27]. The intramembranous ossification mainly occurs in embryogenesis during formation of the flat bones such as skull, mandible, maxilla and clavicles [26].

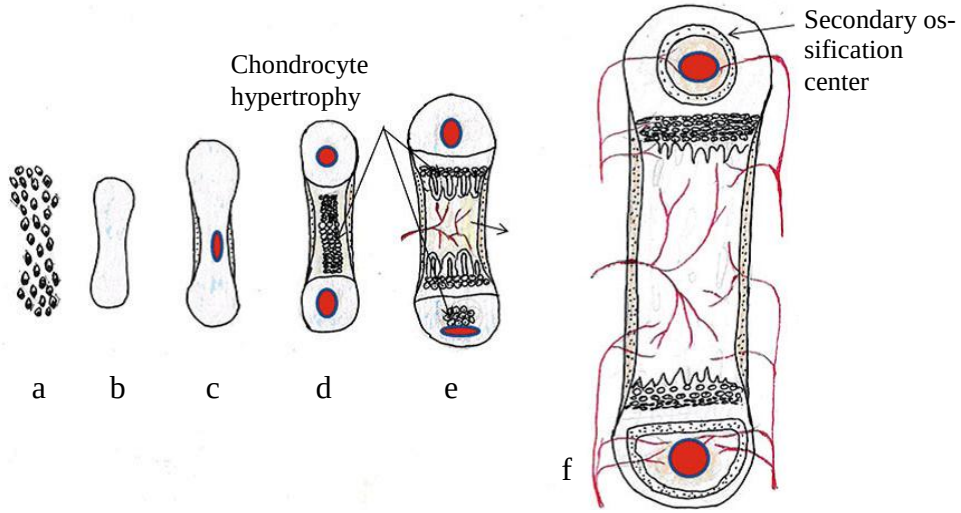

Figure 4: Endochondral ossification process. (a) Aggregates of osteoprogenitor cells (b) Model of hyaline cartilage (c) Primary center of ossification (d) Secondary center of ossification (e) Bone with medullary cavity and epiphyseal ends (f) Highlighting feeding blood vessels [26].

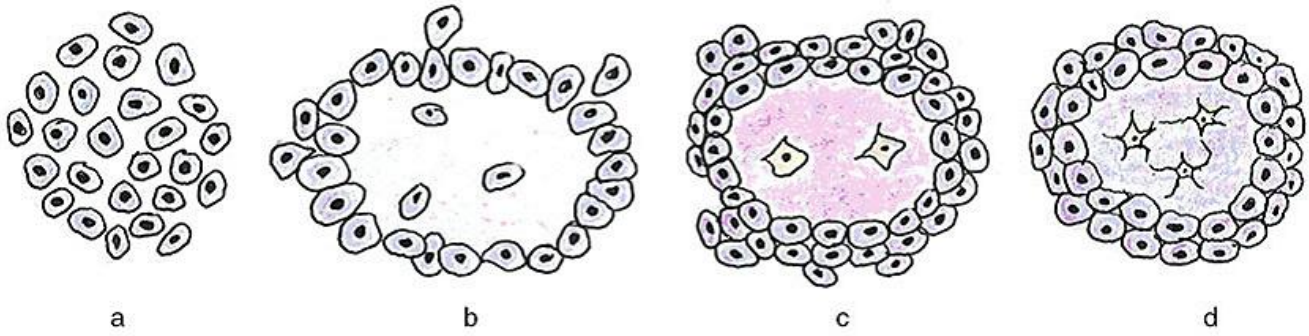

Figure 5: Intramembranous ossification process. (a) Aggregates of mesenchymal stem cells (b) Amorphous ground substance and collagen network formed in the center and between the cells. (c) Mesenchymal stem cells transform to osteoblasts which synthesize organic matrix (osteoid) in the center of the aggregate. (d) Organic matrix mineralization and the transformation of some osteoblasts incorporated within the osteoid into osteocytes [26].

1.2. Calcification

This stage of bone development involves the calcification of woven bone previously formed osteogenesis process. The mineralization of woven bone occurs 24-74 h after organic matrix synthesis, through two main steps: nucleation of calcium phosphate crystals and crystal growth [20]. This results in the precipitation of calcium phosphate, the formation of small apatite nano-crystals and their growth along the collagen fiber axis under the effect of ALP and several non-collagenous proteins, including as OCN, OPN, ON and BSP [25] [30].

1.3. Remodeling

Bone remodeling ensures the transformation of woven bone to mature lamellar bone. This process is a lifelong phenomenon that permits the maintenance of bone tissue, the repair of damaged tissue and the homeostasis of the phosphocalcic metabolism. It is achieved by the combination of bone resorption/formation process (**Figure 6**). Bone resorption involves removal of an old bone while bone formation involves the synthesis of a newly organic matrix and its subsequent mineralization to form new bone which replaces the removed one. Thus, approximately 5–10 % of total bone is renewed per year [13].

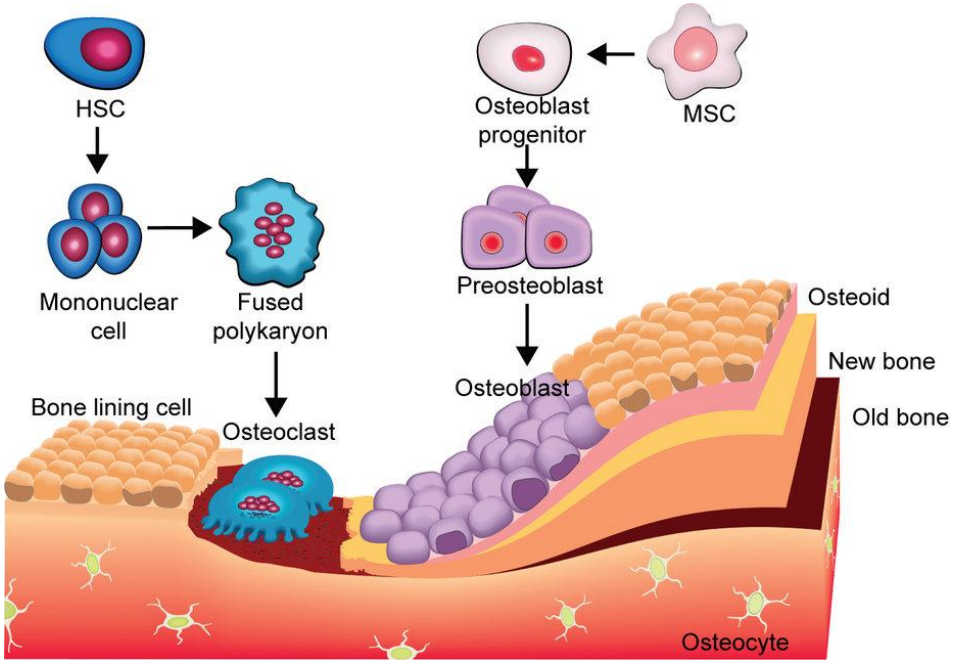

Figure 6: Schema showing evolution of osteoblasts and osteoclasts during bone formation. HSC: Hematopoietic Stem Cells [31].

2. Physiology of bone fracture healing

Bone fracture repair is similar in many ways to pre- and post-natal bone development. For example, fractures heal via the endochondral ossification when the fracture is not really stabilized, as in the case of fractures treated by cast immobilization [26] [27]. On the other hand, the intramembranous ossification is involved in the repair of bone fractures of size between 0.25 and 0.5 mm, stabilized by metal plate and screws [26] [32]. However, in contrast to the natural bone development, bone healing begins with an inflammatory reaction due to bone injury caused by a trauma or surgical procedure to introduce an implant or bone graft **(Figure 7)** [33].

First, vascular lesions result in the formation of blood clot and granulation tissue as well as the accumulation of platelets. Platelets start then to secrete cytokines and growth factors, thus triggering an inflammatory response that manifests itself by the migration of leucocytes, lymphocytes and monocytes to the site of injury. Among cytokines and growth factors that play an important role during fracture repair are Interleukins-1 and -6 (IL-1 and IL-6) and TNF-α as pro-inflammatory cytokines, BMPs -mainly BMP-2, BMP-4 and BMP-6- as osteoinductive factors and VEGF as angiogenic factors. The involvement of the underlying regulators during the different stages of fracture healing is well reviewed in [34].

Then, the repair process begins when MSCs, from the periosteum, endosteum and bone marrow, migrate to the lesion area, proliferate and differentiate to cover the blood clot [35]. If the fracture is mechanically stable, MSCs differentiate into osteoblasts that eventually ensure the production of organic matrix and its mineralization. If the fracture is unstable, MSCs differentiate into chondrocytes that secrete a cartilaginous matrix, called fracture callus, to temporarily stabilize the fracture [28] [36]. The cartilaginous matrix is then replaced by woven bone via endochondral ossification.

Finally, the vascularization of newly formed tissues permits the resorption of woven bone, which is gradually replaced with more resilient lamellar bone during the remodeling phase.

Given that fracture healing requires the migration of inflammatory cells and MSCs to the site of lesion, bone repair takes place only when the fracture gap is too small. However, in the case of critical-size bone defects, the recourse to bone grafts and biomaterials is usually advocated.

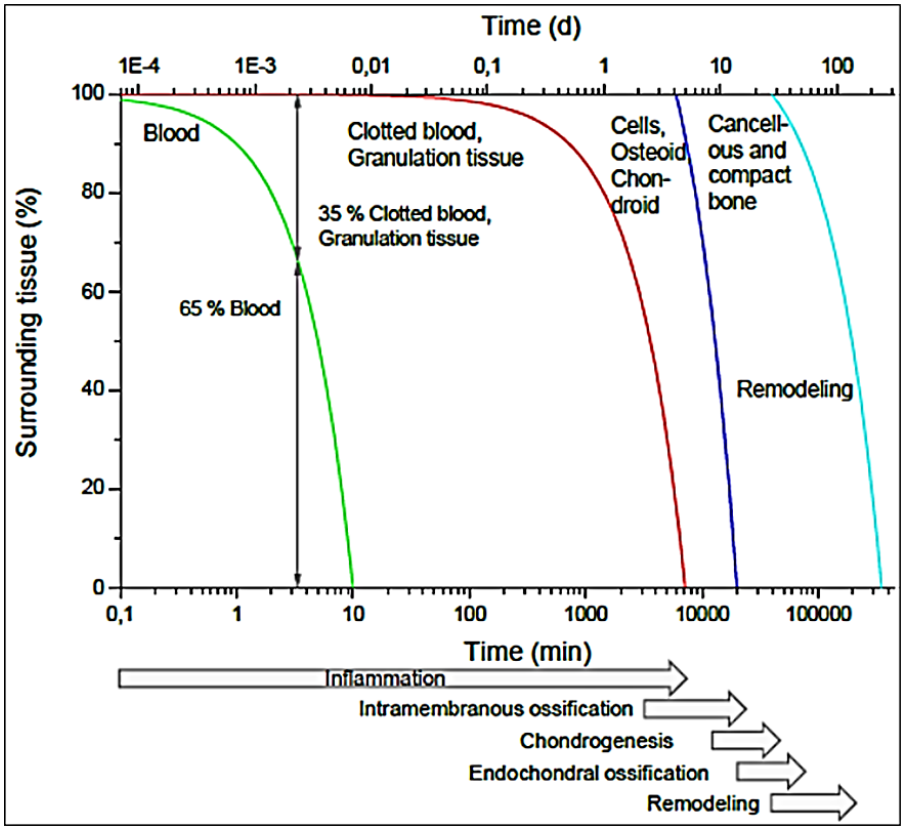

Figure 7: Physiological wound healing in bone [33]

III. Clinical needs in the bone replacement/regeneration

Trauma has been recognized as a major healthcare epidemic by the World Health Organization (WHO), with over 16, 000 people die each day and injury accounting for 16 % of the global burden of disease [37]. Injuries affecting the musculoskeletal system are the most common and hence significantly contribute to the increase of musculoskeletal disease prevalence, that is already affecting roughly 20% of the population [38]. This has been endorsed by the United Nations and WHO, as they recognized musculoskeletal disease as a major burden on individuals, health systems and social care systems with a high financial impact [39]. For instance, osteoporosis is a major risk factor for fractures of the hip, vertebrae, and distal forearm [40], resulting in more than 8.9 million fractures around the world annually; i.e. an osteoporotic fracture every 3 seconds [41].

Among these skeletal fractures, many heal spontaneously in the first 6 to 8 weeks and require short-term and low-cost treatment. However, a fracture can be clinically considered as a delayed union or nonunion if no bony healing is observed after 4 months and 6 months, respectively. Such fractures has been estimated at 100,000 annually in the United

States [42]. They are difficult and slow to heal and significantly harm the national economy, with respect to medical resources (hospitalization, medical equipment, medical implants, diagnostic tests, outpatient follow-ups, therapies and drugs) [43].

Overall, bone injuries, aging population and lifestyle factors, such as obesity are unquestionable risk factors that drastically accentuate musculoskeletal disease burden and consequently boost the demand for the orthopaedic devices market. In term of costs, the global market of therapeutics and orthopaedic biomaterials for musculoskeletal disease has approached $45 billion in 2010 with a compound annual growth rate (CAGR) forecasted to be about 5 %, bringing the total market to more than $57 billion by 2014 **(Figure 8)** [38]. Therefore, medical approaches that help to accelerate bone healing in critical-size bone defects will not only improve medical outcomes for the patient, but they will also contribute to reduce the financial burden related with musculoskeletal disease.

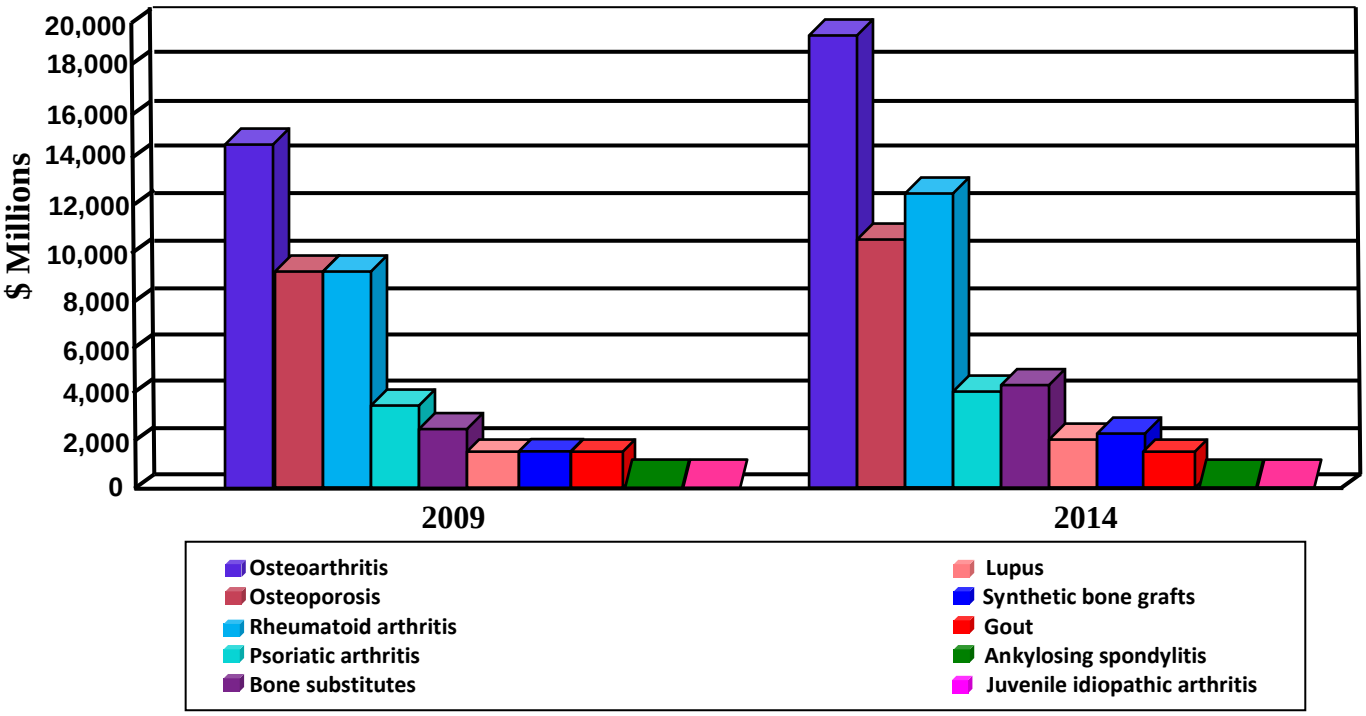

Figure 8: Global potential market of therapeutics and biomaterials for musculoskeletal disease, 2009 and 2014 [38].

IV. Strategies for bone regeneration and replacement

Among approaches currently employed for the treatments of bone injuries are the excision of the fibrous tissue formed at the bone defect site, the use of internal and external skeletal fixation devices for fractures stabilization or the recourse to bone grafts and orthopaedic biomaterials to replace or restore damaged bone.

1. Bone grafts (auto-, allo-, xeno-grafts)

As previously highlighted, the high regenerative capacity of bone tissue ensures a natural facture healing in small bone defects. Unfortunately, diseases such as osteogenesis imperfecta, osteoarthritis, osteomyelitis, along with fractures and traumas as well as tumor resections may lead to critical-size defects (gap size beyond 2-2.5 times the radius of the affected bone) that require surgical intervention to restore or replace lost bone [44]. Currently, the gold standard treatment is the use of autologous bone graft, taken from another part of the patient's own body. These grafts integrate reliably with the host bone, lack the immune-related complications and provide osteogenic cells as well as osteoinductive factors needed for bone healing and regeneration [44] [45]. Nevertheless, the use of this strategy is mainly hampered by the limited supply of autologous bone and the risk of necrosis at the donor site. Allograft (i.e. bone from a human cadaver) and xenograft (i.e. bone from an animal source) represent an alternative since larger bone grafts could be provided. However, these grafts should be sterilized, which leads to the loose of osteoinductive factors and living cells. In addition, they present a potential risk of viral and bacterial infections and immune rejection after implantation [45].

Although these grafts are of great interest in reconstructive orthopaedic surgery, their potential to repair large bone defects is limited and, as consequence, an incomplete graft/host tissue osseointegration was observed in several clinical cases [46] [47].

2. Biomaterials

2.1. Biomaterials market

Owing to the pressing clinical need in orthopaedics highlighted above, the market of biomaterials-based treatments is growing at a rapid rate. Predominantly based in North America, the biomaterials market is expected to be worth $88.4 by 2017 and is forecasted to increase at a CAGR of 16% to reach $130.57 Billion by 2020. Several factors contribute to the growth of the overall market, including increased funds & grants by government bodies worldwide, technological advancements, population ageing and the growth of the implantable devices market (www.marketsandmarkets.com).

Specifically, the global orthopaedic devices market was valued at $34.9 billion in 2014 by Frost & Sullivan's research and at $57.9 billion in 2016 by marketsandmarkets. The North America is the largest orthopaedic market, especially the United States that stands as the leadership with its 60 % of contribution in the market. Indeed, orthopaedic biomaterials are the most implanted materials, especially load-bearing implants such as artificial hip and knee joints and fixation devices. These have been designated as "the orthopedic success story" by the *American Academy of Orthopaedic Surgeons,* representing 52% of all implantations [48].

2.2. Load-bearing biomaterials and their limitations

During the last decades, many bone substitute materials have been evaluated with the aim of resolving the need for autologous or allogenic grafts. The strength of implantable materials is their large availability, safety (no potential diseases transmission), handling characteristics as well as the possibility to incorporate drugs and bioactive molecules in the bulk or the surface of materials.

The choice of a suitable material, exhibiting a high level of biocompatibility, is crucial to successfully replace or support bone repair. Actually, materials used in load-bearing parts are often made of metals or ceramics due to their resistant to the load and their high fracture toughness. The use of polymeric materials in such applications is more restricted due to the limited number of polymers exhibiting adequate mechanical properties.

2.2.1. Metallic materials

Traditionally, metallic implants have been widely used in partial and total joint replacement, fracture fixation devices as well as dentistry. In general, they consist of metals such as stainless steel, cobalt chromium alloy, titanium and titanium alloys.

Stainless steel-based materials. Stainless steel was the first material used in the early days of arthroplasty [49]. It is an alloy consisting mainly of nickel, chromium, manganese, molybdenum and nickel. This material was primarily used for the manufacture of internal fixation devices such as fracture plates, screws, wires, pins, hip nails or rods. More recently, it was used in femoral stems. Among the available stainless steel (SS) alloys, 316L SS remains one of the most used materials in orthopaedic surgery due to its biocompatibility, availability, great strength, and cost effectiveness [50].

The main drawback of SS alloys is corrosion that leads to the release of toxic metal ions such as nickel (Ni) and chromium (Cr). In addition, 316L SS alloy possesses much higher modulus (200 GPa) than cortical bone (≈ 20 GPa), which causes stress shielding effect and the subsequent implant loosening due to the bone resorption [51].

Cobalt/Chromium-based materials. These alloys, basically composed of cobalt and chromium, are generally used in hip arthroplasty to manufacture femoral heads. They are also used as acetabular cups, tibia trays and dental implants [52]. The main advantage of cobalt/chromium (Co-Cr) alloys is their high fatigue strength [53]. However, these alloys release cobalt and chromium metals from the material surface due to corrosion phenomenon. These metal particles can become integrated into the periprosthetic tissue, triggering local inflammatory reactions and the formation of soft tissue at the interface bone/implant, thus impairing a strong implant osseointegration [54]. In addition, the high modulus of Cr–Co alloys (230 GPa) results in bone resorption (stress shielding), which leads to the implant loosening after some years of implantation [55].

Titanium-based materials. In the early 1970s, titanium (Ti) and its alloys have been a great success in orthopaedic surgery, being attractive materials for manufacturing bone fracture fixation devices, dental implants and joint replacement parts for hip, knee, and shoulder [56]. In addition to the interesting properties observed in materials previously cited, titanium quickly reacts with oxygen to form a titanium oxide layer (TiO_2) on the surface, making it more corrosion resistant as compared to other metallic materials. Indeed, titanium is considered as the most corrosion resistant non-noble metal and became the most popular orthopaedic material in the biomedical industry [3]. In addition, titanium

alloys exhibit lower Young modulus (55-110 GPa) than those of 316 L stainless steel and Cr–Co alloys. Pure titanium (ASTM F67) was the first to be introduced in the market but due to its limited strength, other alloys were developed such as *Ti-6Al-4V ELI* (Extra Low interstitial), *Ti-6Al-7Nb* and *Ti-5Al-2.5Fe* that exhibit better strength properties [57] [58]. Nevertheless, the cytotoxicity of vanadium and aluminum has encouraged the development of newer titanium alloys such as *Ti-35Nb-7Zr-5Ta*. This alloy seems to be very promising due to its low elastic modulus (55 GPa) close to that of cortical bone [55]. Despite all advantages that titanium and its alloys offer, the level of osseointegration required to reach a strong adhesion at the interface bone/implant remains of concern [58].

Magnesium-based materials. Another interesting class of metallic materials which has recently attracted much attention consists of biodegradable magnesium alloys. In addition to the good biocompatibility of these materials, they exhibit excellent mechanical properties, being among the lowest elastic modulus of metallic materials reported to date (≈ 45 GPa), thus minimizing stress shielding effect [59]. Furthermore, implants made of magnesium alloys such as screws and plates obviate the need of a second surgical intervention for implant removal, thanks to their biodegradable nature. However, the major drawback of magnesium alloys is their low corrosion resistance, which was intensively studied during the last few years [59].

2.2.2. Bio-inert ceramics

Alumina (Al_2O_3) and zirconia (ZrO_2) are the most popular inert ceramics used in THR (Total Hip Replacement) and TKA (Total Knee Arthroplasty) to manufacture femoral heads. The latter are often coupled to acetabular cup made from UHMWPE (Ultra High Molecular Weight Polyethylene). Al_2O_3 Alumina and zirconia ceramics are also used as maxillofacial bone substitutes, post dental implants, bone screws, blade screws and keratoprosthesis. These materials have been widely investigated due to their desirable mechanical properties, as they possess high compressive strength and hardness, excellent corrosion and wear resistance and an acceptable level of biocompatibility [60]. Nevertheless, their use as orthopaedic biomaterials is constrained by their high elastic modulus (Al_2O_3 ≈ 400 GPa and ZrO_2 ≈ 200 GPa) and bio-inertness. These limitations affect the long-term performance of these materials for several reasons, including the fracture of femoral heads, stress shielding and formation of a fibrous tissue at the interface bone /implant, leading to implant failure [61].

In contrast to inert ceramics, bioactive ceramics such as hydroxyapatite (HA) or tricalcium phosphates (TCP) bound better to the native bone tissue. Unfortunately, they are not good candidates in load-bearing parts due to their brittle nature, hence these materials are often applied only as coating on load bearing implant [62] [63].

2.2.3. Polymeric materials

Polymers are interesting candidates for biomedical devices employed in several fields, including orthopaedic, dental, craniofacial, cardiovascular, drug delivery systems and tissue engineering applications [64]. In joint replacement applications, synthetic polymers with high stability, strength and stiffness such as UHMWPE, PTFE (Polytetrafluoroethylene) or PEEK (polyetheretherketone) are frequently used. PMMA (polymethyl methacylate) is commonly used as bone cement due to its excellent elastic modulus, close to that of bone [65]. Poly-HEMA (poly-hydroxyethylmethacrylate) has also been reported as a potential candidate for bone regeneration, since a subcutaneous bone formation was observed following the implantation of this material in pigs [66], however the osteoinductive potential of this polymer is not well-documented in the literature. To date, only a limited number of polymeric materials have been approved by the U.S. Food and Drug Administration for orthopaedic clinical use. Moreover, most of them have raised some concerns, especially the lack of osseointegration and the low wear resistance [64].
A scheme of the mains factors responsible of implant failure that may lead to revision surgery is shown in **Figure 9**.

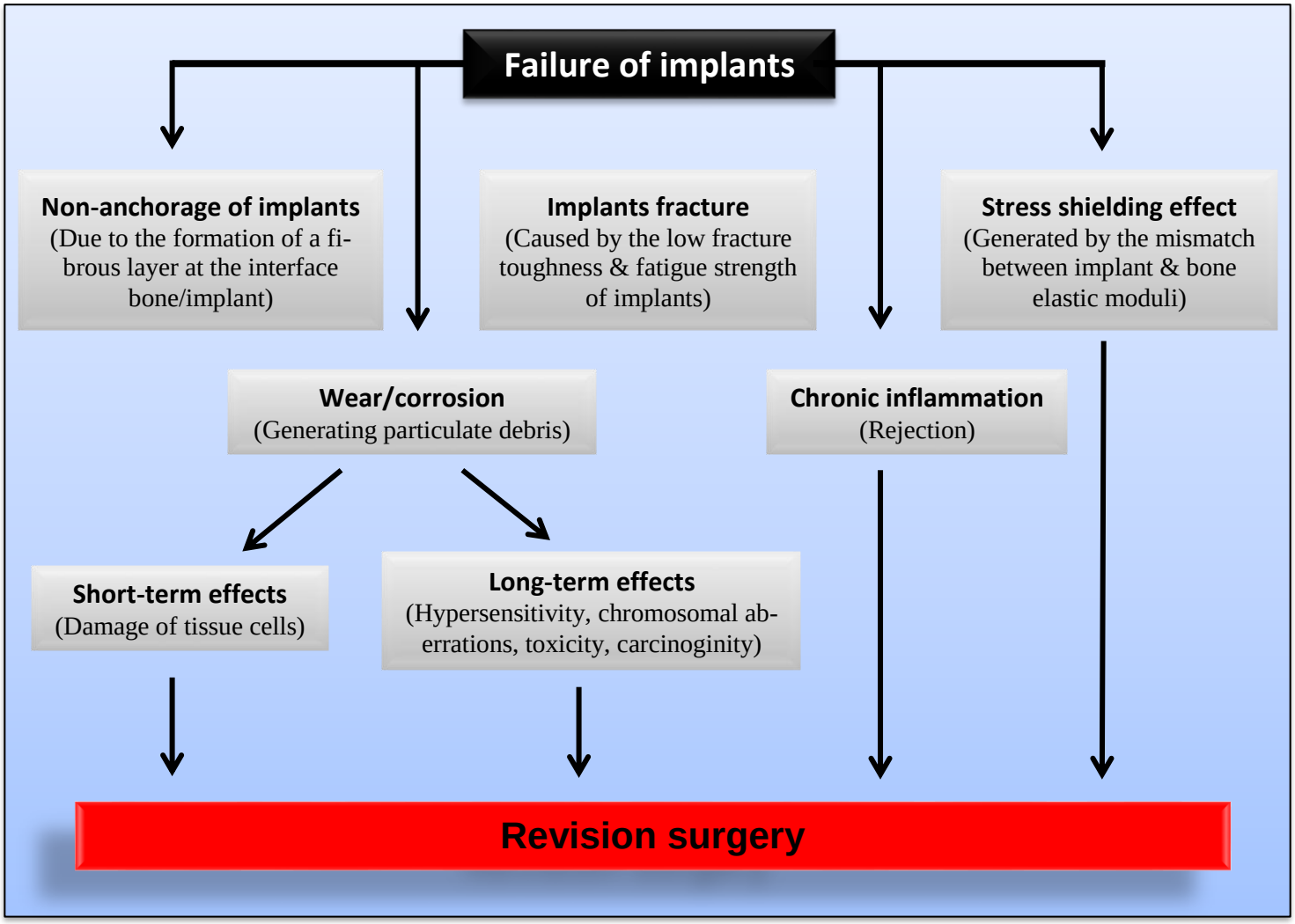

Figure 9: Factors of risk of implants failure that may require revision surgery (adapted from[8]).

3. Bone tissue engineering

The reconstruction of damaged bone remains a real clinical issue in the case of large bone loss caused by trauma, musculoskeletal disease and surgical treatment of tumors. Although, several therapeutic treatments are proposed today, such as bone graft transplants (auto-, allo-, xeno-grafts), bone marrow transplant, Ilizarov technique, load-bearing implants and bone-defect-filling materials, none has proven to be fully satisfactory [67] [68-70] [8]. For example, complications and non-union fractures are common in clinical practice, when bone grafts are used to reconstruct large bone defects [46] [47] [71]. Also, orthopaedic biomaterials, such as those discussed above, meet some clinical needs due to their large availability and acceptable biocompatibility, however their lack of osteoinductivity restrict their application in large bone defects. Therefore, due to these conventional routes limits, tissue engineering has emerged as a promising alternative intended to meet the demand in surgical reconstruction of large bone defects.

Historically the term tissue engineering dates back to the fall of 1987, when it was "coined" at a meeting at the National Science Foundation in Washington, D.C. Few months later, the first conference called "tissue engineering" was held in early 1988 at Lake Tahoe, California [72]. The field of tissue engineering is highly multidisciplinary and draws on experts from clinical medicine, mechanical engineering, materials science, genetics and related disciplines from both engineering and the life sciences. This approach aims to obtain a fundamental understanding of structure-function relationships in normal and pathological mammalian tissue and the development of biological substitutes to restore, maintain, or improve tissue functions.

The tissue engineering paradigm is the belief that cells can be isolated through a small biopsy from a patient, expanded *in vitro* and then seeded in a scaffold material. The resulting tissue-engineered construct (hybrid material) is then grafted back into the desired site in the patient's body to restore damaged tissues. Tissue engineering is also of particular interest in investigating aspects of the structure-function relationship *in vitro* and to predict the clinical outcome of specific medical treatments.

The first commercial tissue engineering product was a bioartificial skin for burn treatment, introduced in 1990 [73]. Since then, the global tissue engineering and regeneration market is steadily growing, reaching $17 billion in 2013, according to BCC Research. This market is expected to increase to nearly $56.9 billion by 2019, with a compound annual growth rate (CAGR) of 22.3%. The key areas of tissue engineering, where a high

rate of success has been reported, are skin [73] [74], bladder [75], airway [76] and bone [77] [78] engineering.

In bone tissue engineering applications, cells harvested from the patient, ranging from primary adult osteoblasts to mesenchymal stem cells, are either incubated for only few hours in 3D scaffold prior to implantation or cultured for sufficient time to induce their differentiation into mature osteoblasts and the production of an ECM rich in proteins and growth factors. The second approach is more advantageous than the first one for several reasons. First, the cultured cells have already started to produce a bone matrix *in vitro* and will continue this process *in vivo*, resulting in an accelerated regeneration of damaged bone. Second, the synthetized bone matrix will contain various proteins and growth factors essential to induce osteogenesis *in vivo*. The key components of a bone tissue-engineered construct are depicted in **(Figure 10)**.

The first implantation of a bone tissue-engineered construct, made of autologous bone marrow stromal cells expanded *in vitro* and loaded in a hydroxyapatite (HA) scaffold, was performed in 2001 to repair large bone diaphysis defects of three patients (bone defect size: from 4 to 7 cm) [79]. Complete fusion between the implant and the host bone occurred 5 to 7 months after surgery [80]. Long-term analyses by means of radiographs and computed tomography (CT) scan at different post-surgery time intervals revealed that the implants were not resorbed and their integration to the host tissue was maintained in all patients after 6 to 7 years post-surgery [80]. During the same year, Vacanti et al. tried to restore a phalanx of a patient's thumb using an engineered construct made of a coral scaffold and autologous cells harvested from the periosteum [81]. In 2004, Warnke et al. described a clinical study where the concept of tissue engineering was applied to reconstruct a mandible of a 56 year-old patient who has undergone a mandibulectomy, leading to a critical-size bone defect greater than 7 cm [78] [82]. A titanium mesh, having the shape of the patient's mandible, was filled with HA blocks containing BMP-7 and autologous bone marrow stromal cells. The patient's body served as his own bioreactor since the construct was first implanted in its dorsal muscle. After 7 weeks, the hybrid material was placed in the lesion site and 4 weeks later the patient has regained his chewing capacity [83]. Tissue engineering has also been employed for maxillary sinus augmentation. This procedure was tested on twenty seven patients using a periosteum-derived tissue-engineered bone. Three months following the implantation, bone biopsy evaluation revealed the formation of mineralized trabecular bone, with remnants of the biomaterial in eighteen patients [77].

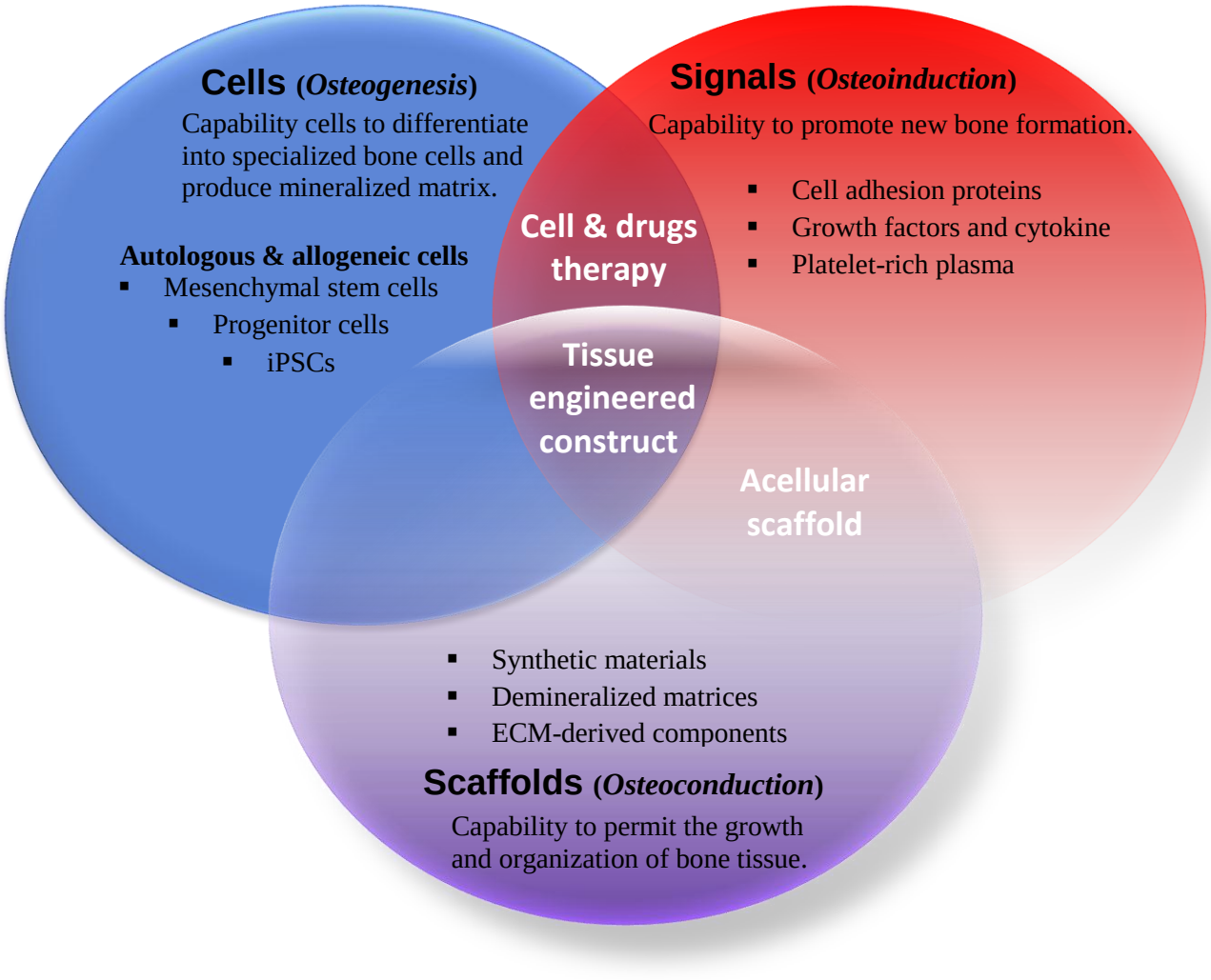

Figure 10: Principle of bone tissue engineering.

3.1. Cell sources for bone tissue engineering

3.1.1. Mesenchymal stem cells

A part of the use of an adequate scaffold material, the choice of a reliable source of cells is critical to ensure the regeneration of bone tissue. An ideal cell source should be easily isolated, expandable to higher passages, non-immunogenic and have an osteogenic phenotype or can acquire it. From a rational point of view, the adequate cells for bone tissue engineering are osteoblasts. However, these cells could not only be harvested from the patient only in few amounts, but they also have a relatively low expansion rate *in vitro.* Furthermore, the surgical procedure to harvest osseous biopsy is very painful for the patient [84]. Alternatively, mesenchymal stem cells (MSCs) seem to be the most valid and more promising cell source to overcome some of the above mentioned limitations. MSCs are undifferentiated cells with high proliferative potential, able to self-renew and to differentiate to committed lineages, including osteoblasts (bone cells), chondrocytes (cartilage cells) and adipocytes (fat cells) [85]. Another astonishing property of MSCs is their ability to escape disease transmission and immuno-rejection after their implant/injection, making them suitable for allogenic and xenogenic transplantation [86]. Ten years ago, Taupin. [87] reported that a USA company, Osiris Therapeutics, has developed a stem cell therapy based on allogeneic MSCs derived from bone marrow (BMSCs). This treatment has been awarded the Orphan Drug status for its potential benefit in enhancing bone marrow transplants in cancer patients, for the prevention of graft versus host disease (GVHD) and for the treatment of Crohn's disease. However, the use of stem cells is still very restricted and controversial in tissue engineering and regenerative medicine applications due to conflicting clinical outcomes. In 2008, one patient in Spain was successfully transplanted with a re-engineered trachea. Trachea from a donor was first decellularized using a detergent and then this scaffold was re-cellularized in a bioreactor using the patient's MSCs [76]. In a second case, the cerebellum of a boy with a neurodegenerative hereditary disorder (ataxia telangiectasia) was injected with human fetal neural stem cells. Nevertheless, four years later, a glio-neuronal brain tumor of stem cell origin was found [88].

MSCs are present through the entire body and can be isolated from perinatal tissues (i.e., placenta, umbilical cord and blood from the umbilical cord) and postnatal tissues (bone marrow, trabecular bone, alveolar bone, cartilage, hair follicles, fat, skin and dental pulp) [89] [90]. However, in bone tissue engineering field, MSCs located in bone marrow,

known as Bone Marrow Mesenchymal Stem cells (BMSCs) have gained a special notoriety taking advantage from their high osteogenic potential [91] [92]. MSCs can be harvested from bone tissue bits or bone marrow using mechanical or chemical approach or both of them. Mechanically, the bone tissue is cut into small pieces using surgical blades and then either suspended or plated. Chemically, bone chips are exposed to an enzymatic digestion, with a combination of trypsin and collagenase to obtain a cell suspension.

Although BMSCs are of great interest for tissue engineering and regenerative medicine applications, there are still some issues that need to be addressed. For instance, Bernardo et al. reported that MSCs frequency in bone marrow exhibits an age-related behavior from 1:10,000 in a new-born to 1:1,000,000 in an 80-year-old subject. This would make the expansion tricky and time consuming. It has also been shown that the amount and the differentiation potential of MSCs decrease with increasing patients age [9].

Alternatively, adipose tissue represents a potential source of MSCs due to its abundance in adult subjects. In addition, lipoaspirates are very easy to perform compared to bone marrow aspiration which is somewhat a laborious and painful procedure. Regarding the differentiation potential of adipose tissue derived stem cells (ADSCs), comparative *in vitro* studies revealed that the multilineage potential of ADSCs and BMSC was similar according to cell morphology and histology [93], however, ADSCs exhibit an inferior potential for both osteogenesis and adipogenesis than BMSCs [93] [94]. Contradictory results regarding the differentiation potential of MSCs from different sources have also been reported. For instance, Dicker et al. compared the adipogenic differentiation potential of MSCs derived from adipose tissue and bone marrow and concluded that ADSCs can be differentiated into fully functional adipocytes with a similar, if not identical, phenotype as that observed in stem cells derived from bone marrow (BMSCs) [95].

3.1.2. Other sources of osteogenic cells

Peripheral blood is also a source of cells that could be used in bone tissue engineering applications. These cells, known as blood mesenchymal precursor cells (BMPCs), circulate in physiologically significant numbers in peripheral blood and their concentration is markedly higher during pubertal growth or bone fracture healing [96]. Phenotypically, they resemble but are distinguishable from BMSCs. *In vitro*, It has been shown that BMPCs acquire an osteoblastic phenotype when grown in osteogenic media [97] and promote bone formation *in vivo* when loaded in an osteoconductive scaffold (a mixture of HA/β-TCP) [96].

The formation of ectopic bone within skeletal muscle is a widely observed phenomenon, therefore suggesting the presence of bone-forming in this tissue. Indeed, this hypothesis was confirmed both *in vitro* and *in vivo* [98]. Among muscle cell subpopulations that can give rise to osteoprogenitor cells are myosatellite cells [99], side population cells, multipotent adult progenitor cells (MAPCs) and pericytes. Preclinical studies have already been conducted using skeletal muscle-derived osteoprogenitor cells as therapeutic cells for bone tissue engineering [100].

Others cells that hold great interest in regenerative medicine and tissue engineering are the induced pluripotent stem cells (iPS), discovered in 2006. These cells were generated *in vitro* by reprograming somatic cells, using a combination of several transcription factors [101]. iPS cells have gained considerable notoriety due to their high *in vitro* self-renewal, genomic stability and high differentiation capacity to form several mature lineages. However, most human iPS cells are made by viral vectors, such as retrovirus and lentivirus, which integrate the reprogramming factors into the host genomes and may increase the risk of tumor formation [101].

3.2. Osteoinductive growth factors

Commonly, biomaterials used in bone tissue engineering are osteoconductive and lack osteoinductivity. Therefore, incorporating osteoinductive growth factors in the bulk of biomaterials or on their surfaces seems to be an interesting way to stimulate the formation of new bone tissue around the biomaterial, thereby enhancing its osseointegration. Two osteoinductive growth factors have gained Food and Drug Administration (FDA) approval, recombinant human rhBMP-7 and rhBMP-2, for use in orthopaedic applications. rhBMP-7 is marketed under the name “OP-1” by Stryker-Biotec. rhBMP-7 is also commercially available under the name “OP-1 putty, Stryker” product which consists of a tissue-engineered construct (rhBMP-7/collagen matrix) used as an alternative to autograft. OP-1 putty was evaluated in clinical trials for the treatment of tibial nonunions. It provided clinical and radiographic results comparable to those achieved with bone autograft [102]. OP-1 putty has also been investigated in posterolateral spinal fusions. This biomaterial led to a solid fusion rate of 55 % compared with 40 % for iliac crest autograft during the study period [103].

Medtronic Sofamor Danek developed INFUSE® Bone Graft which is an osteoinductive and osteoconductive bone graft substitute composed of rhBMP-2 loaded in absorbable collagen sponge scaffold. In an integrated study based on three similar large-scale clinical

trials, the osteoinductive potency of INFUSE® Bone Graft was compared to that of autograft. Results of 2-year follow-up were impressive as they stated a significant superiority of using synthetic INFUSE® Bone Graft over naturally transplanted bone (autograft). Indeed, patients treated with BMP-2 spent statistically significant shorter times in the operating room, lost less blood, had shorter hospital stays and returned to work earlier than patients who received autograft [104]. INFUSE® Bone Graft has registered $750 million annually in sales due to its widespread use in several medical applications, including spinal fusion procedures, tibial shaft fractures and oral-maxillofacial procedures [105].

Despite of the success and FDA approval of BMP-2- and BMP-7-based scaffolds in clinical practices, they have raised some concerns. These tissue-engineered products provide supraphysiological doses of rhBMPs, 10 to 1,000 fold higher than the concentration of the native BMPs, over a limited period (60-240 min) [106]. For example, one vial of OP-1, commercialized by Stryker-Biotec, contains 3 mg of BMP-7 embedded in 1 g of bovine collagen I. Consequently, such treatments are highly expensive, taking into account the short shelf life and the price of rhBMP-7 (OP-1 ≈ $5,000 *per* one time use) and rhBMP-2 (Infuse ≈ $3,500-4,900 depending on the quantity used) [107]. In addition, the high concentration of rhBMPs loaded within the scaffolds can induce undesired ectopic bone formation and lead to immunological reactions. Such side-effects could be harmful for the patient, specifically in cervical spine surgery when the margin for error is minimal [108] [109]. Therefore, a careful choice of growth factors and the identification of patients who are more likely to receive such treatments are critical for satisfactory clinical outcomes.

3.3. Materials used as scaffolds for BTE and their limitations

Scaffolds design and development represent the most active research area in the field of bone tissue engineering [110]. These biomaterials have to fulfill more stringent requirements than load-bearing biomaterials since cells are in contact with both the bulk and material surface. In addition to the adequate biocompatibility and mechanical properties, these biomaterials require a 3D structure, high porosity and controllable biodegradation parallel to bone growth [111]. These properties are intended to permit the colonization of the scaffold with cells while providing them with nutriments and ensuring their growth and differentiation in a biomimetic three dimensional environment.

Typically, three groups of materials, ceramics, synthetic polymers and natural polymers, are proposed as scaffolds for tissue engineering. Metallic and ceramic materials are less

attractive than polymers for bone tissue engineering due to two major drawbacks. They are not biodegradable, except biodegradable ceramics such as β-tricalcium phosphate (β-TCP), and their processability is very limited due to their high toughness [111] [112]. Therefore, we will mainly focus on the use of biodegradable polymers as materials for bone tissue engineering.

3.3.1. Bioactive ceramics

Unlike inert ceramics frequently used as load-bearing biomaterials, bioactive ceramics are rather used for bone tissue engineering applications, especially as bone filling substitutes. They can be natural such as coral or synthetic such as hydroxyapatite (HA) and α-/β-TCP. These biomaterials possess some specific properties not necessarily observed in metallic or polymeric materials. Indeed, they are highly resistant to deformation and bound better to the bone tissue than metals or polymers due to their osteoconductive property [62]. More interestingly, some of synthetic calcium phosphate ceramics such as α-TCP, β-TCP, tetracalcium phosphate (TTCP) and octacalcium phosphate (OCP) undergo progressive degradation, while the new bone tissue regenerates [113]. In addition, several works have shown that by using ceramics with or without bone marrow cells, acceptable results regarding bone regeneration could be obtained [79] [112].

Another promising material that belongs to the category of bioactive ceramic is Bioglass which is a kind of silica glass containing calcium and possibly phosphate elements. Recent *in vitro* studies have shown that some compositions of glass, containing a specific amounts of SiO_2, Na_2O, CaO, and P_2O_5 bind strongly to bone tissue and may induce neovascularization [114] [115]. Furthermore, it was shown that silicon (Si) found in glass induces the activation of complex gene transduction pathways, leading to enhanced cell differentiation and osteogenesis [116] [117]. To date, bioactive ceramics are one of the few biomaterials that have led to acceptable outcomes in term of inducing osteogenesis and integration with the native bone tissue. However, their brittle nature and low mechanical stability prevent their use in large bone defects. In addition, it is difficult to control their degradation rate *in vivo* due to the presence of multiple factors that affect the biomaterial behavior such as the osteoclastic activity [115].

3.3.2. Biodegradable polymers

Biodegradable polymers have received considerable attention and are considered the ideal material for bone tissue engineering, owing to their interesting properties discussed above. As ceramic materials, polymers can be categorized as natural and synthetic polymers as well as their copolymers [65] [111] [118].

Among natural biodegradable polymers, collagen, fibrinogen, chitosan, starch, hyaluronic acid (HA) and poly(hydroxybutyrate) are the most popular ones.On the other hand, the most widely used synthetic biodegradable polymers are Poly(α-hydroxy acids), including poly glycolacid (PGA), polylactic acid (PLA), and their copolymer PLGA [111] [112] [118]. These polymers have gained FDA approval for certain clinical applications and they are often used as degradable surgical sutures. The main advantage of these materials is their biodegradability since some of them contain chemical bonds that undergo hydrolysis within the body's aqueous environment such as PGA, while others degrade by cellular enzymatic pathways such as collagen. Furthermore, they can be moldable, shapeable and injectable to ensure a good fit in the defect site [111] [112] [118]. These astonishing properties permit to reduce the surgical cost and patient suffering since only a minimally invasive surgery is required to introduce the implant. Further, no additional surgical procedure is needed to remove it [65]. However, the use of both natural and synthetic polymers has some limitations too. For example, the isolation of natural polymers from biological tissue while preserving their native properties is still of concern and some of them such as collagen and chitin are not easy to melt by heat treatment but require special solvent. Also, there is less control in their biodegradability and reproducibility as compared to synthetic polymers and they may exhibit immunogenicity and contain pathogenic impurities. Regarding synthetic polymers, they exhibit reduced bioactivity and are less mimicking the native cellular environment, as compared to natural polymers. In addition, concerns exist regarding the toxicity of polymers byproducts. For example, lactic acid and glycolic acid monomers, resulting from the degradation of PLGA, lead to local inflammatory reaction and potential poor tissue regeneration [119]. Furthermore, both biodegradable natural and synthetic polymers exhibit poor mechanical properties (0.8-16 GPa) [111] [120].

One of the attempts to expand the limited use of ceramics and polymers, due to their limitations, is the fabrication of composite scaffolds comprising two or more materials. Different types of composite scaffolds have been developed by combining, for example, polymeric and ceramic materials or synthetic and natural polymers in order to enhance their mechanical and/or biological properties [65] [121]. While composite scaffolds have shown some successful and promising outcomes, they all have associated problems with biocompatibility, biodegradability or both [65] [63] [121].

Another interesting category of materials used in bone tissue engineering are hydrogels which are a class of highly hydrated polymers. These materials have been proposed as an alternative to polymeric materials that are often hydrophobic in their native state and require surface and/or bulk modification to become hydrophilic. In addition, biomolecules incorporation and cells encapsulation within hydrophobic polymers is a potential challenge [122]. Therefore, a variety of hydrogels composed of hydrophilic polymer chains were developed and employed as scaffold materials. The most frequently used ones are degradable and are either from natural origin such as agarose, alginate, chitosan, collagen, fibrin, gelatin, and hyaluronic acid (HA) or synthetic such as poly(ethylene oxide) (PEO), poly(ethylene glycol) (PEG), poly(vinyl alcohol) (PVA), poly(acrylic acid) (PAA) and poly(propylene furmarate-co-ethylene glycol) (P(PF-co-EG)) [121] [123] [124]. Another exciting property of many hydrogels such as alginate, PEO, chitosan and P(PF-co-EG) is their ability of jellify *in vivo* meaning that cells and molecules can be mixed with hydrogel *in vitro*, mini-invasively delivered and gelled *in situ*. Also, most of synthetic hydrogels undergo degradation through hydrolysis mechanism which facilitates the control of their degradation kinetic since hydrolysis occurs at a constant rate *in vivo* and *in vitro* [121] [122] [124]. However, as the majority of polymeric materials, hydrogels require their association with osteoinductive molecules and cells to support bone tissue formation. In addition, these biomaterials lack an adequate initial strength, preventing their use in load bearing parts [125].

While the introduction of orthopaedic biomaterials in the market has significantly improved the living conditions of patients, there are still many challenges to be met by scientists and engineers in order to improve the integration of biomaterials within the body. Clinically, these challenges address two main issues, amongst others. Currently, orthopaedic surgeons are faced with. *(i)* Commercially available orthopaedic biomaterials exhibit poor osseointegration potential, which restricts their long-term performance to 10-15 years [48] and *(ii)* the real need of reliable materials that support a rapid and sufficient

expansion of stem cells as well as their effective specification into homogenous bone cells population.

On this basis, it seems that the source of the problem is the biomaterial itself, which means that an ingenious design of both the structure and the composition of biomaterials is crucial to ensure a perfect implant osseointegration at the lesion site and successfully repair or replace damaged bone. Nevertheless, the design of biomaterials is far from easy since an in-depth comprehensive knowledge of material science and cell biology is required to understand phenomena occurring at the cell-biomaterial interface. In the next chapter of this literature review, the focus will be made on the most investigated approaches during the last two decades, as tools to better understand cell/material interactions with the aim of improving the osteoinductive potential of conventional biomaterials.

V. Recent advances in biomaterial design to enhance stem cells/progenitors osteogenesis

In the early days of biomaterials research, the major efforts to enhance orthopaedic implants osseointegration have been mainly made on tailoring their bulk properties, including the shape, inner structure and mechanical properties. For example, in the case of biomaterials used in load bearing part, one great challenge was to enhance their mechanical compatibility by matching the mechanical constants of biomaterial and bone tissue to be replaced. The reason being that, when the Young's modulus of hard tissue biomaterials is much higher than that of cortical bone, the load bearing is not ideal and the risk of stress shielding and fibrous encapsulation of the implant is greater [126].

More recently, much attention was paid to the properties of the material surface to improve the biological compatibility. This new direction stems from the fact that the biological host tissue interacts, in any case, with the outermost atomic layers (thickness ≈ 0.1-1 nm) of 2D/3D biomaterials [127]. In other words, when an implant is inserted into the host bone, tissue fluids first come into contact with its surface. Hence, surface features are of particular interest in determining the adsorption of biomolecules from the body fluids and the subsequent cells/material interaction event that dictate implant fate. It is worth noting that the surface modification of biomaterials can also affect the mechanical properties of their bulk, thus controlling indirectly several risk factors of implant failure, such as stress shielding, wear debris or fatigue failure [128].

Therefore, this chapter provides an overview of recent advances in surface modification technology while seeking to improve the osteogenic potential of orthopaedic biomaterials. This literature survey will serve as a general scope for the original work presented later in this thesis.

1. Surface modification strategies for enhanced osteogenesis

Surface science is one of the most popular fields applied in biomaterials and tissue engineering research to improve the biological response at the interface bone/implant [127]. Nowadays, accumulating evidences suggest that biomaterial surface features, including but not limited to nano/micro-topography, chemistry, wettability and electrical charges are potent modulators of cellular behaviors, including adhesion, proliferation, migration and differentiation [128] [129] **(Figure 11)**.

Therefore, the surface modification strategy has captured the interest of many scientists, clinicians and manufacturers as tool to induce and accelerate osteogenesis on biomaterials surfaces [130]. The most commonly used approaches to alter the surface properties are categorized into two major axes; the chemical and physical surface modification. The chemical surface modification includes the surface chemistry/biochemistry and chemical patterning, while the physical surface modification includes the surface roughness, stiffness and topographical patterning [128] [129] [131] [132].

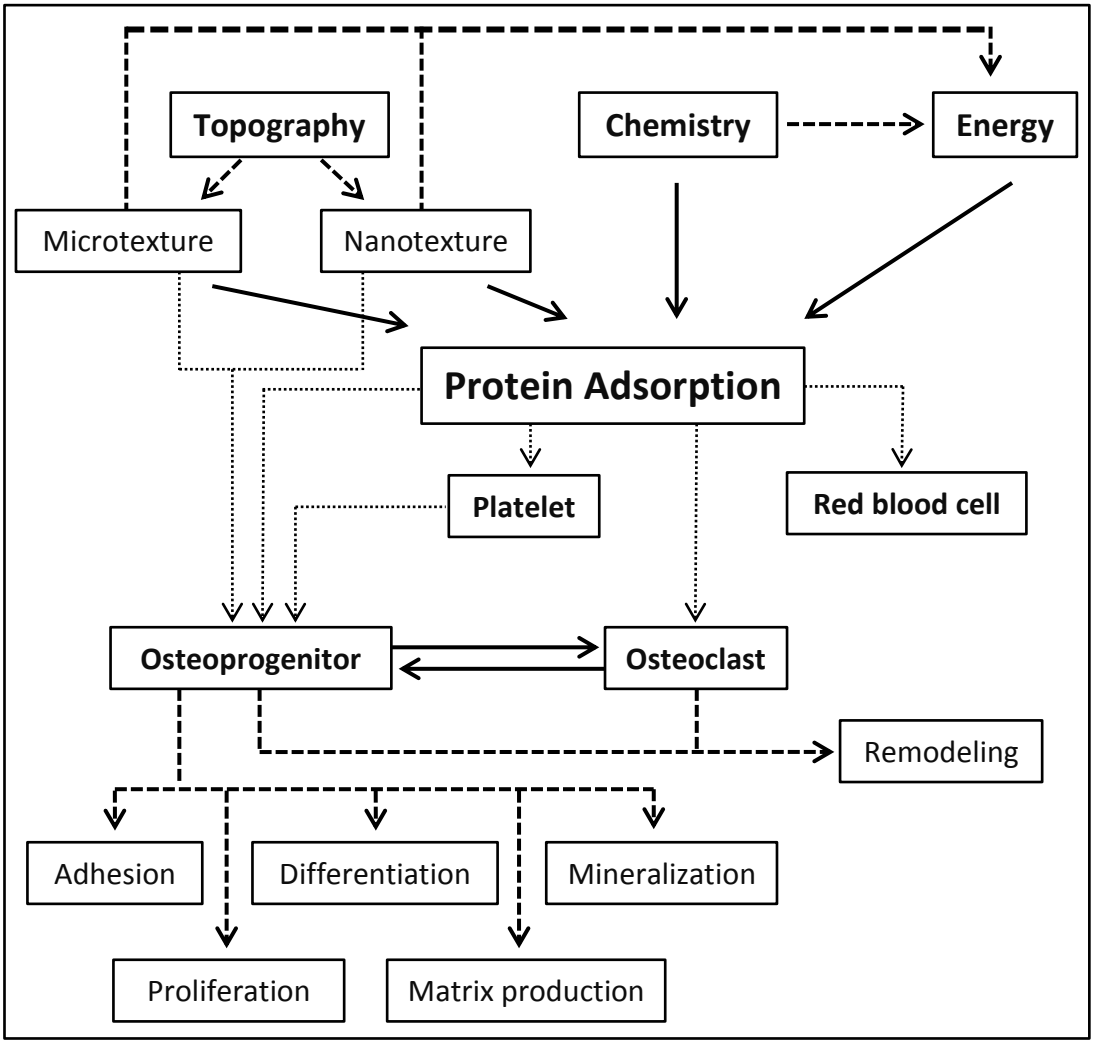

Figure 11: Effect of surface features on cell behavior at the interface bone/ implant [133].

1.1. Physicochemical surface modification

Basically, the physicochemical surface modification seeks to control the surface free energy, wettability and electric charges onto biomaterials. These properties have been shown to influence protein adsorption kinetics and their spatial conformation, which in turn affect cellular functions [131] [134].

Several groups have focused on altering the surface wettability with the aim of drawing an optimal surface wettability profile that positively affect cell behaviors at the interface of biomaterials. In this regard, it has been shown that highly hydrophilic surfaces are more desirable than hydrophobic ones owing to their interactions with biological fluids, cells and tissues [135]. Accordingly, *in vitro* studies demonstrated that cell adhesion, differentiation and ECM production are better mediated on hydrophilic surfaces [136] [137] [138]. In an *in vitro* experiment, it has been shown that human BMSCs exhibited higher gene expression of osteogenic markers, such as Runt-related transcription factor 2 (Runx-

2) and bone sialoprotein (BSP) on hydrophilic chemically modified-titanium surfaces, as compared to hydrophobic ones [139]. In another study, Benoit et al. also investigated the differentiation of hMSCs in response to hydrophobic and hydrophilic modified-poly(ethylene glycol) (PEG) hydrogels. They found that hydrophobic hydrogels containing *t*-butyl chemical groups promoted hMSCs adipogenesis, while hydrophilic negatively charged hydrogels functionalized with phosphate groups favored hMSCs differentiation towards the osteoblastic lineage [140]. Consistent with these *in vitro* studies, some *in vivo* and clinical trials demonstrated that hydrophilic surfaces accelerate implants osseointegration [141] [142] [143]. For example, Buser et al. demonstrated, in an animal model, that hydrophilic titanium implant surfaces, implanted in the maxillae of miniature pigs, yielded higher bone/implant contact than a standard titanium surfaces [144].

Although these results are promising and have led to further investigations, contradictory results have been reported regarding the influence of the surface wettability on cell behaviors. Guehennec et al. cultured osteoblastic MC3T3-E1 cells on hydrophilic a biphasic calcium phosphate coated titanium material and a commercially available titanium material which was less hydrophilic. They failed to demonstrate the advantageous effect of hydrophilic surfaces since insignificant differences in osteogenic markers expression on hydrophobic and hydrophilic titanium surfaces were reported [145]. More surprising, Bauer et al. observed that on nanotubular titanium surfaces having different degrees of wettability, rat MSCs exhibited increased adhesion from super hydrophilic to super hydrophobic surfaces [146]. *In vivo*, other studies have shown that hydrophilic material surfaces exhibited statistically similar bone-to-implant contact and removal torque results, as compared to hydrophobic surfaces [147] [148]. Similarly, some clinical trials have demonstrated that implants with both hydrophilic and hydrophobic surfaces were well-integrated and exhibited high survival rate in patients' mouths [149] [150].

Contradictory results have also been reported regarding the impact of surface energy [151] [152] and charges [153] [154] [155] on promoting osteogenesis at the interface bone/implant. One key reason leading to this controversy is the vast differences in cell lines, serum components, underlying substrates, culture procedures, time points and characterization techniques used by the different groups. In addition, it is difficult to dissect the individual contribution of each surface parameter in modulating cell behaviors since the modification of one surface feature such as the surface wettability may also elicit

changes in the surface chemistry and topography. Therefore, a biologically relevant surface wettability is yet to be established, hence rigorous modification and characterization of the surface parameters with respect to their biological relevance will be necessary.

1.2. Chemical surface modification

The objective behind the chemical surface modification is to allow for direct interactions between the material surface and the chemical nature of bone tissue. To date, several chemical moieties have been claimed as modulator of stem cell fate, since they are inherently present within the native ECM [140] [156]. For example, carboxylic acid groups, phosphate groups and hydrophobic moieties are widely present in cartilaginous matrices, mineral phase of bone tissue and adipose tissues, respectively [140] [156]. The role of these chemical functionalities in directing both short- and long-term cellular functions has been obviously evidenced through several *in vitro* studies. The most popular method for investigating the effect of specific surface chemistries on stem cell fate, *in vitro*, lies on the use of self-assembled monolayers (SAMs) [157]. Among several SAMs available to modify biomaterial surfaces, SAMs of alkanethiolates created on gold-coated substrates are recognized as the most reliable class of model organic surfaces, owing to their significant control over material chemical properties [158]. A key advantage of this system is the high reproducibility of well-defined surfaces, created throughout the use of simple protocols, that nicely control protein deposition and cell interactions at the interface of biomaterials [158].

In this context, Phillips et al. [158] demonstrated that (–CH_3)-, (–OH)-, (–COOH)- and (–NH_2)-terminated SAMs substrates affected fibronectin adsorption and conformation as well as the osteogenic differentiation of human MSCs (hMSCs). In fact, they demonstrated that fibronectin adsorbed onto self-assembled monolayers with terminal -OH groups had more accessible cell-binding domains than did the fibronectin on surfaces with terminal -CH3 and-NH2 groups. In addition, they found that fibronectin-coated NH_2-SAMs induced the highest level of hMSCs osteogenic differentiation under osteogenic cell culture conditions, as revealed by alizarin red staining and osteogenic markers Runx2, BSP, OCN expression. They also revealed that CH_3-, OH- and COOH-SAMs affected hMSCs osteogenic differentiation, however their osteogenic potential was visible on only one or two phenotypic markers. For instance, COOH-SAMs enhanced Runx2 and OCN expression but not BSP and calcium phosphate (CaP) deposition, while OH-SAMs enhanced Runx2 and CaP deposition but not BSP and OCN [158].

In another study, Curran et al. [159] analyzed the effect of thiols (-SH) groups, in addition to the four chemical groups investigated Phillips and coworkers, using silane-modified glass surfaces. Similarly, NH_2 surfaces favored the differentiation of hMSCs along the osteogenic lineage. At day 7, hMSCs cultured on NH_2 surfaces showed higher cell viability as compared to day 1, associated with a significant increase in Cbfa-1 (bone transcription factor) expression and decrease in type II collagen (cartilaginous matrix marker) expression. However, hMSCs grown on $-CH_3$, -SH and -OH surfaces did not demonstrate any up-regulation of osteogenic differentiation markers throughout the test period. It is noteworthy that, in this study, cells were cultured in basal growth medium, free of soluble osteogenic factors, thus allowing a direct correlation between surface chemistry and cell behavior. In addition, it has been suggested that the conformation of adsorbed serum proteins, specifically vitronectin, on NH_2 surfaces might have contributed to the specification of hMSCs towards the osteoblastic lineage [159]. In a subsequent work, the same authors extended the culture time to 28 days and evaluated hMSCs differentiation in both growth and osteogenic medium [156]. Again, NH_2 surfaces were shown to elicit the strongest osteogenic stimulatory effect on hMSCs, as revealed by higher expression of osteoblast lineage-specific genes and proteins on NH_2 surfaces as compared to other chemically modified surfaces. However, other results from this study are somewhat questionable. In fact, the authors highlighted an up-regulation of osteogenic OCN and Cbfa-1 markers on SH surfaces at different time points and in both growth and differentiation medium, however they demonstrated in their previous study [159] that these surfaces did not affect hMSCs osteogenic differentiation after 1 week of culture in growth medium. In addition, all functionalized surfaces up-regulated at least one osteogenic marker at certain time points [156].

In general, although SAMs cannot be used as implant materials, the knowledge gathered from these studies provide valuable insights towards the design of 3D scaffolds or implants able to achieve a fine control over MSCs differentiation.

Other chemical moieties are thought to control cell fate due to their abundance within the native ECM. As highlighted above, it has been speculated that providing mimetic chemical functionalities on material surfaces might help to guide stem cells towards distinct lineages. This hypothesis was verified *in vitro* by seeding hMSCs on material surfaces functionalized with phosphate groups, carboxylic groups and *t*-butyl, which somewhat mimic the chemical composition of bone matrix, glycoaminoglycans in cartilage and lipids in adipose tissues, respectively. It was demonstrated that acid-, phosphate- and t-

butyl-functionalized surfaces increased the expression of chondrogenic collagen II marker, osteogenic OPN marker and adipogenic PPAR-γ (peroxisome proliferator-activated receptor gamma) marker, respectively [140]. As another example, Granja et al. [160] immobilized phosphorus-containing groups onto cellulose surfaces in order to compared three different substrates for their ability to induce calcium phosphate mineral formation; untreated cellulose surfaces, phosphorylated cellulose surfaces and phosphorylated/calcium-pre-incubated cellulose surfaces. Each disc was immersed in stimulatory body fluid (SBF) for a period ranging from 12 hours to 15 days, prior to assessing mineral deposition. They demonstrated that phosphorylated/calcium-pre-incubated surfaces mineralized at a higher extent than materials only phosphorylated. In addition, phosphorylated surfaces, which are negatively charged and highly hydrophilic showed reduced hMSC attachment and proliferation and poor osteogenic potency, as evidenced by a slight ALP activity and OCN and type I collagen expression [160]. Indirectly, this study confirms the aforementioned issue regarding the difficulty of dissecting the individual contribution of each surface property in regulating stem cell fate. The ultimate question then arises from this study is: which surface parameter, amongst the surface charge, wettability and chemistry, affected hMSCs osteogenic differentiation?

Another approach, also inspired from the physiological situation and broadly used to enhance cellular activities at the interface bone/implant, consists of coating material surfaces with CaP. This approach was initially proposed by de Groot and Geesink in the mid-1980's [161]. CaP ceramics have long been a potential candidate for deposition as coating onto inert metallic implants [161] [162]. Introduced in 1985, the Furlong^{R} (JRI, London, UK) has been the first implant worldwide coated with hydroxyapatite for use in total hip replacement [163]. As a general rule, following the implantation of a CaP-coated implant, the release of CaP into the peri-implant region increases the saturation of body fluids, which consequently causes the deposition of a biological apatite containing endogenous proteins onto the implant surface [164] [165].

During the past decades, serious efforts have been undertaken to optimize the performance of CaP coating by adjusting several parameters such as the Ca/P ratio or the investigation of several types of CaP-based coatings, including pure HA, tricalciumphosphate (TCP), biphasic calcium phosphate (BCP), Si-doped HA, Mg-substituted HA and carbonated HA [131] [166].

In clinical and preclinical trials, these CaP coatings were found to stimulate the formation of new bone tissue and facilitate the bridging of small gaps at the interface bone/implant [167] [162].

For example, Rajaratnam et al. [163] have reported the clinical outcomes of 331 Furlong HA-coated femoral prosthesis consecutively implanted between 1986 and 1991. The global survival rate, including all causes of revision, was 97.4 % after a mean follow-up of 17.5 years. In an experimental study carried out in animals, Manders et al. [162] inserted titanium implants, coated in one side with CaP and left without coating in the other side, into goat's femoral condyle. They demonstrated that CaP-coated surfaces had a significantly higher amount of bone contact than uncoated surfaces, as bone ingrowth occurred from both the surrounding bone tissue and the coated implant surface. **Figure 12** shows light photomicrographs of histological sections of uncoated and CaP-coated titanium implants.

Although the use of CaP as coating has led to faster and more robust bone formation, there are major concerns with CaP coatings such as the coating delamination and adhesive failures at the interface CaP coating/implant [167].

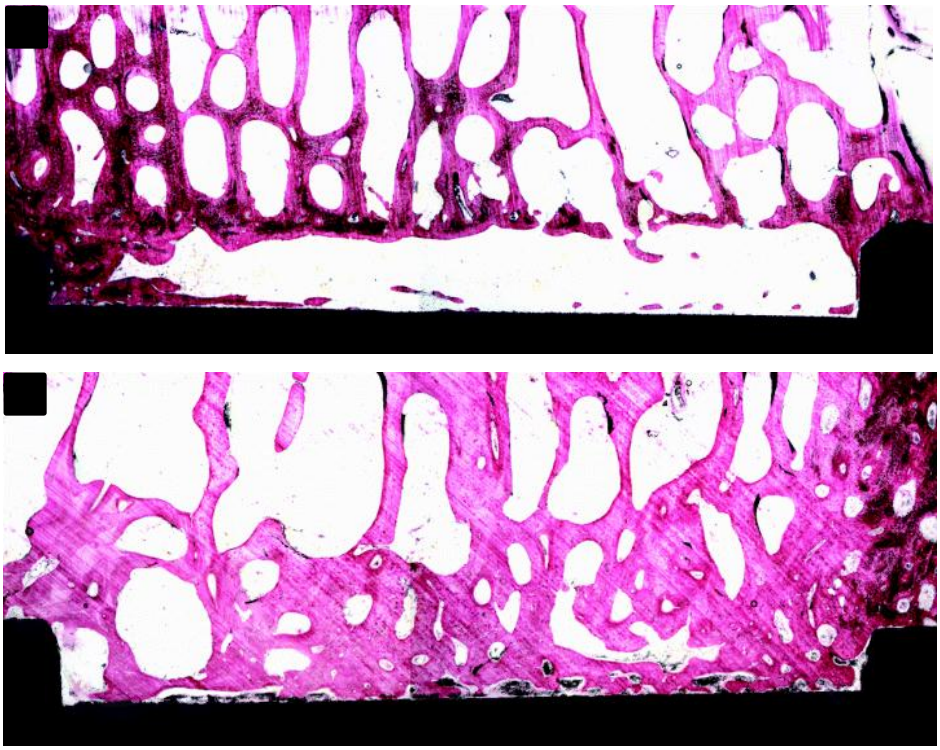

Figure 12: Light micrographs showing bone ingrowth at **(A)** uncoated titanium implant and **(B)** plasma-sprayed hydroxyapatite coating, gaps 1 mm (original magnification × 2.5) [162].

1.3. Biochemical surface modification

Tissue culture polystyrene (TCPS) substrates are frequently used in laboratory to amplify, differentiate or characterize various cell types including hMSCs. However, such substrates are bioinert and usually require the use of highly saturated culture medium with proteins, growth factors and cytokines to modulate the behavior of adherent cells [168]. The drawback of this type of cell culture platforms is the limited control of biochemical cues (proteins, growth factors and cytokines) distribution, concentration and bioactivity over material surfaces. Consequently, cause/cell response correlation is usually hardly established. Alternatively, biochemical surface modification of synthetic and natural materials has gained a particular interest as tool to create a well-defined microenvironment on material surfaces to better control cell/biomaterials interactions, even at the molecular level. biochemical surface modification approaches currently investigated include the immobilization of adhesion proteins, growth factors and enzymes on biomaterial surfaces in order to invoke the desired short- and long-term cellular responses [131]. Specifically, the principle motivations behind the use of this approach are as following; *(1)* limiting the adsorption of proteins adsorption, thus minimizing the risk of ligands denaturation and unspecific protein deposition, and therefore favoring specific cell adhesion on implanted biomaterials *(2)* providing persistent stimulatory effect on biomaterial surfaces through the immobilization of growth factors.

Two well-documented methods can be used to immobilize biomolecules onto biomaterial surfaces. The first one aims to physically adsorb biomolecules (hydrophobic interactions, hydrogen bonding, ionic (or electrostatic) bonding and Van der Walls interactions). Although this method is very simple, ligands anchorage to the material surface is highly dependent on experimental parameters such as pH, temperature, solvent, reaction period and initial concentration of biomolecules. In addition, the physical adsorption often lacks the deposition of uniform coatings on material surface. Moreover, biomolecules desorb from the surface in an uncontrolled manner. Consequently, the correlation between the intensity of cellular response and the coating characteristics is difficult to establish.

The second approach aims to immobilize biomolecules on the material surface through a covalent link. This method is probably more laborious and time consuming, but it offers several advantages over the physical adsorption. In fact, the covalent immobilization permits to manipulate the local concentration of ligands in a well-controlled manner, provides a control over their spatial orientation and leads to sustained cell/ligand interactions.

Krijgsman et al. evaluated human umbilical vein endothelial cells (HUVEC) attachment on polymeric materials containing RGD and/or heparin adhesive peptides, which were either adsorbed or grafted to the surface. They revealed that ligand grafting enhanced cell attachment after 90 min, while their simple coating (via physical adsorption) conferred no advantage over uncoated materials [169]. In another study, Dettin et al. investigated HUVEC adhesion on grafted or adsorbed RGD peptide on electrospun polymer fiber after 24 h. They found that RGD peptide enhanced HUVEC adhesion, only when grafted [170]. Interestingly, the advantage of the covalent grafting over the physical adsorption was also reported in *vivo*. It has been shown that alginate hydrogels, loaded with covalently grafted BMP-2 peptide, induced the formation of new bone tissue and vascular channels ectopically, while hydrogels containing adsorbed peptide did not [171].

Given that the thesis project presented here seeks to investigate stem cell fate in response to covalently immobilized mimetic peptides, this sub-section will mainly provide an overview of studies exploring the biological relevance of adhesive and osteoinductive ligands, conjugated to biomaterials through a covalent link.

1.3.1. Extracellular matrix derived proteins/growth factors and mimetic peptides

The early works in this research field have been focused on decorating biomaterial surfaces with full-length ECM proteins such as collagen, fibronectin, vitronectin, and laminin to promote cell adhesion and proliferation [172], or with growth factors such as transforming growth factor-beta (TGF-β) and bone morphogenetic proteins (BMPs) to induce osteogenesis [173]. Growth factors can be classified in term of their bioactivity in three categories, from mitogenicity (fibroblast growth factor (FGF), platelet-derived growth factor (PDGF), insulin-like growth factor (IGF)) to increasing activity of bone cells (TGF-β1) to osteoinduction (BMPs) [115].

BMPs are believed to be the most effective growth factors to induce bone formation, hence their extensive use in fundamental research and bone tissue engineering applications [174]. Originally discovered by Urist in 1965 [175], BMPs are a group of 20 proteins, belonging to the TGF-β family. Indeed, it has been proposed that BMP-2, -6 and -9 may be the most potent inducers of MSCs differentiation to osteoblasts, while the remaining BMPs promote the maturation of committed osteoblasts [176]. The binding of these BMPs to their cell receptors (BMPR-I and BMPR-II) promotes osteogenesis via

two regulatory pathways: the Smads-dependent pathway and the Smads-independent mitogen activated protein kinase (MAPK) pathway. The first pathway is initiated by the formation of BMP ligand/BMPR-I/BMPR-2 complex, leading to the phosphorylation of BMPR-I by BMPR-II and the subsequent phosphorylation of cytoplasmic transcription factors Smads1/5/8 by BMPR-I. Afterwards, phosphorylated Smads associate with Smad4 and the complex is then transported from the cytoplasm into the cell nucleus. This complex can cooperate with other transcriptional factors in the nucleus, such as Runx-2 to modulate the transcription of target genes, like those encoding bone ECM proteins (type I collagen, OPN, BSP, OCN) [31] [177] [178]. (MAPK) pathway also plays an important role in BMP-induced osteogenesis. The transduction of MAPK signal into the nucleus can be achieved through three different cascades: the extracellular signal-regulated kinase (ERK), c-Jun N terminal kinase (JNK) and p38 MAPK cascades [31] [179]. As discussed in the subsection **[IV.3.2. Osteoinductive growth factors]**, BMP-2 and BMP-7 are so far the only BMPs approved by FDA for use in spinal fusion, non-union fractures and oral-maxillofacial treatments due to their high osteoinductive potential as compared to other BMPs [103] [106] [107].

Although the effectiveness of ECM derived proteins and growth factors in enhancing biomaterials biocompatibility has been proven in several instances, the use of only their bioactive domains, termed as mimetic peptide, is thought to be more advantageous for numerous reasons. A major opportunity when using mimetic peptides is the possibility to precisely target specific cell receptors, therefore eliciting the desired cell response, while avoiding undesired responses. Interestingly, mimetic peptides can promote specific cellular responses as stronger as their full-length forms [172] [180]. Their small size permits a higher coating density and makes them generally more resistant to denaturizing insults and proteolysis [48] [181]. On the financial side, mimetic peptides are cost-effective and can be readily produced synthetically. Furthermore, nearly all immobilized short ligands (peptides) are available for cell receptors, in contrast to the full-length biomolecules where epitopes are not always sterically available [182].

Of a long list of mimetic peptides developed during the last decades, the arginine-glycine-aspartic acid sequence “RGD” remains the most popular and investigated peptide mimetic peptide. RGD is the main integrin-binding domain, derived from several ECM proteins such as fibronectin, vitronectin, fibrinogen, osteopontin and bone sialoprotein [131] [183]. Eight integrins have been identified as RGD-binding receptors: all five α_V, two β_1 (α_5 and α_8) and $\alpha_{IIb}\beta_3$ integrins [184]. To date, there is an exhaustive literature review

emphasizing the role of RGD peptide in promoting the adhesion of MSCs and other cell types to a wide range of materials, including glass [185], metal oxide [186] and polymers [187]. Although the capacity of RGD peptide to modulate cell adhesion is widely accepted, there is still no consensus with respect to its osteoinductive effect, mainly at the *in vivo* level. Indeed, several studies have demonstrated enhanced osteogenesis and implant osseointegration on RGD-modified materials [188], while others have failed to evidence the underlying effect [189]. Besides RGD, several other peptides derived from the bone ECM proteins have been designed and used to improve cell adhesion on biomaterial surfaces **(Table 1)**.

Although some of these peptides have also been reported to possess an osteogenic activity *in vitro*, further investigations are needed to confirm their stimulatory effect *in vivo* as well.

Table 1: Biological effect of peptides derived from ECM proteins and growth factors covalently immobilized on biomaterials.

Peptide sequence	Origin	Function	Ref.
ECM proteins derived peptides			
RGD	Fibronectin, vitronectin, type I collagen, bone sialoprotein	Cell adhesion	[181]
YIGSR, IKVAV	Laminin	Cell adhesion	[190]
PHSRN, REDV, LDV	Fibronectin	Cell adhesion	[191] [192] [193]
*RGD	Fibronectin, vitronectin, type I collagen, bone sialoprotein	Cell adhesion & osteogenic differentiation *in vitro* and *in vivo*	[194] [195] [196]
*GFOGER	Type I collagen	Cell adhesion & osteogenic differentiation *in vitro*	[197] [198]
*FHRRIKA, KRSR	Heparin binding domain	Cell adhesion & osteogenic differentiation *in vitro*	[199] [200]
*HVP	Human vitronectin	Cell adhesion & osteogenic differentiation *in vitro*	[201]
*CGGNGEPRGDTYRAY	Bone sialoprotein	Cell adhesion & osteogenic differentiation *in vitro*	[202] [203]
*DVDVPDGRGDSLAYG	Osteopontin	Cell adhesion & osteogenic differentiation *in vitro*	[204] [205]
Growth factors derived peptides			
NSVNSKIPKACCVPTELSAI	68–87 BMP-2	Ectopic bone formation in rats	[171]
KIPKASSVPTELSAISTLYL	73–92 BMP-2	MSCs osteogenic differentiation *in vitro* & new bone formation in tibial bone defects	[206] [207] [208]
S^{PO4}KIPKASSVPTELSAIS TLYLDDD	73–92 BMP-2	MSCs osteogenic differentiation *in vitro* & ectopic bone formation in rats	[209]
RKIPKACCVPTELSAISMLYL	73–92 BMP-2	MSCs and preosteoblasts osteogenic differentiation *in vitro*	[210] [187] [211]
DWIVA	30–34 BMP-2	Osteogenic differentiation of myoblasts *in vitro*, new bone formation in rabbit calvarial defect and in periodontal defects in dogs	[212] [213] [214] [215]
AISVLYFDDSSNVILKKYRN	111-130 BMP-7	Foetal rat calvaria cells osteogenic differentiation *in vitro*	[216]
RTVPKPSSAPTQLNAISTLYF	98-117 BMP-7	Preosteoblasts osteogenic differentiation and matrix mineralization *in vitro*	[187]
KPSSAPTQLN KAISVLYFDDS SNVILKKYRN	101-110 BMP-7 110-120 BMP-7 121-130 BMP-7	Increased ALP activity and calcium deposition in human osteoblasts *in vitro*	[217]
CGGKVGKACCVPTKLSPIS-VLYK	68-87 BMP-9	Increased ALP activity in mouse preosteoblasts in 1 day of culture	[218]
RKVGKASSVPTKLSPISILYK	68-87 BMP-9	Preosteoblasts osteogenic differentiation and matrix mineralization *in vitro*	[187]

Note: Results from studies demonstrating an osteoinductive effect of peptides highlighted with an asterisk should be interpreted with some caution due to the contradictory opinions and the scarcity of relevant *in vivo* and clinical trials reporting the effectiveness of such mimetic peptides.

In addition to adhesive peptides, short sequences derived from the bioactive domains of several growth factors have been proposed to meet some issues related to the use of full-length growth factors. In clinics, growth factors are often used in supraphysiological doses to reach the therapeutic level; i.e. to induce bone regeneration. This is due to their short half-life as well as their diffusion away from the site of regeneration. Consequently, undesired ectopic bone formation has been reported in several clinical cases [106] [108]. BMP-2 and BMP-7 mimetic peptides are, of course, the most investigated sequences as their full-length proteins have gained a particular interest for clinical use. Several peptides derived from the knuckle epitopes of human BMPs have been recently designed and assessed for their osteogenic activity **(Table 1)**. The first well-documented study highlighting the osteoinductive potential of BMP peptides was performed by Suzuki et al. in 2000. They conjugated a mimetic peptide, derived from the knuckle epitope of human BMP-2 (68–87 residues), to alginate hydrogels through the interaction of activated alginate carboxyl groups and the $N_{terminal}$ serine amino acid of the peptide. BMP-2 modified-alginate hydrogels promoted the recruitment of osteocalcin-positive osteoblasts and induced ectopic calcification of rat calf muscle *in vivo* after 8 weeks [171]. Few years later, Saito et al. [206] developed a slightly different BMP-2 peptide sequence, corresponding to 73-92 residues. Similarly, Alginate hydrogels containing BMP-2 peptide, implanted in the same animal model, induced prolonged ectopic bone formation for up to 7 weeks [207]. *In vitro*, this peptide was shown to interact with BMPR-1 and BMPR-2 receptors, leading to elevated ALP activity in mousse MSCs [206]. Subsequently, the same group revealed that BMP-2 peptide combined with either polymeric and ceramic materials effectively induced new bone formation in tibial bone defects created in small animals [208] [219]. In addition, they observed further enhancement and acceleration of new bone formation when BMP-2 modified-polymers were loaded with MSCs [219]. While these studies clearly evidenced BMP-2 (residues 73-92) effectiveness in inducing osteogenesis both *in vitro* and *in vivo*, Kloesch et al. [220] reported contradictory results both *in vitro* and *in vivo*. They demonstrated that BMP-2 peptide was not able to induce osteogenic differentiation in mouse myoblast cell line (C2C12) after 5 days of culture *in vitro*. *In vivo*, BMP-2/collagen scaffolds implanted in the back muscle of Sprague–Dawley rats led to poor ectopic bone formation for up 4 weeks. The conflicting outcomes may due to the difference in materials (alginate vs. collagen) and BMP-2 doses (75 µg vs. 50 µg) used by Santo [206] [207] and Kloesch [220].

It is likely that the reader will notice that *in vivo* studies presented above are somewhat beyond the scope of this subsection **[V.1.3. Biochemical surface modification]** since in the aforementioned examples, BMP-2 peptides were used to modify, not only the surface, but also the bulk material. This is due to the lack of *in vivo* studies focused on the modification of material surfaces with osteoinductive mimetic peptides. One of the few examples highlighting the biological relevance of BMP-2 modified material surfaces was carried-out by Seol et al. [221]. In this study a novel peptide containing the sequence DWIVA (residues 30-34), which corresponds to both wrist and knuckle epitopes of BMP-2, was either adsorbed or covalently linked to titanium surfaces through a silane coupling agent. *In vitro,* MC3T3-E1 preosteoblasts proliferation and alkaline phosphatase activity peaked on BMP-2 grafted surfaces at different time points during 4 weeks of cell culture. *In vivo,* BMP-2 grafted titanium surfaces promoted higher new bone formation and rapid bone maturation, as compared to control materials, in 3x3x5 mm^3 canine mandibular bone defects, after 4 weeks [221]. Subsequently, the same group examined whether the modification of osteoconductive material surfaces with DWIVA containing peptide enhances osteogenesis. Throughout a set of *in vivo* assays, authors reported that the coating of deproteinized cancellous bovine bone mineral (BBM) surfaces with DWIVA peptide induced ectopic calcification in New Zealand white rabbits [212] and significantly enhanced new bone formation in rabbit calvarial defects [213] and in one-wall [214] and three-wall [215] intrabony defects in beagle dogs.

In another study, Lin et al. modified the BMP-2 peptide, developed by Saito et al. [206], by adding polyaspartic acid (DDD) and phosphorylated serine amino acid ($S^{[PO4]}$) to create the sequence $S^{[PO4]}$KIPKASSVPTELSAISTLYLDDD (designated as P24) [209]. The incorporation of these residues at the terminal amino-acids of BMP-2 peptide is thought to promote apatite nucleation and enhance mineralization. P24 peptide was conjugated to poly(lactic-co-glycolic acid) (PLGA) copolymer through PEG-aspartic acid spacer. *In vitro,* PLGA polymers bearing P24 peptide were shown to induce higher levels of ALP activity and ECM mineralization in rat MSCs in the presence of osteogenic differentiation medium, as compared to controls. *In vivo,* the subcutaneous implantation of P24-PLGA materials in rats promoted ectopic bone formation, as demonstrated by radiographic and histological examination, western blotting and mRNA expression of type I collagen and OPN [209]. More recently, Poh et al. demonstrated that the covalent immobilization of BMP-2 peptide on cobalt-chromium surfaces led to two-fold higher ALP activity and

four-fold higher mineral deposition in MC3T3-E1 preosteoblast cells, as compared to untreated surfaces [222]. Although, the authors have proposed BMP-2-cobalt chromium materials as potential candidate in orthopaedic surgery, no subsequent investigations using the underlying material were found.

In summary, **Figure 13** recapitulates some of the most important findings on BMP-2 in biology and materials science during the last two decades.

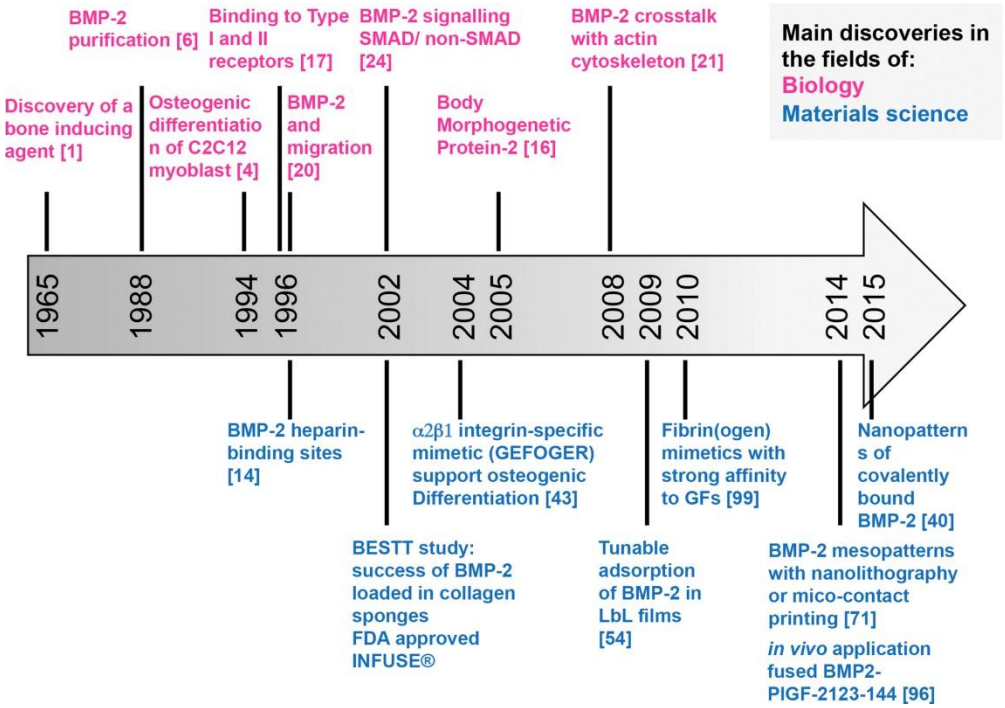

Figure 13: Time-line showing few of the most important findings on BMP-2 in biology (in red) and in material sciences (in blue) [223].

Besides BMP-2 peptides, other peptide sequences derived from the knuckle epitope of several BMPs have been developed by our group and others. In particular, BMP-7 [187] [217] [216] and BMP-9 [187] [218] mimetic peptides are the most investigated ones for their osteoinductive potential both *in vitro* and *in vivo*.

1.3.2. Integrin ligands and growth factors crosstalk

Cell adhesive ligands and growth factors are not independent systems for modulating osteogenic differentiation since compiling evidence highlights to the existence of a bidirectional crosstalk between many growth factor receptors and integrins [224]. Lai and Cheng reported increased expression of β_1 integrin subunits and $\alpha_v\beta_3$, $\alpha_v\beta_5$, $\alpha_v\beta_6$ and $\alpha_v\beta_8$ integrins at the surface of human osteoblasts, in the presence of BMP-2 protein. In addition, they demonstrated that blocking α_v integrins, using L230 antibody, inhibited BMP-2 induction of matrix mineralization [225]. Drevelle et al. revealed that mouse preosteoblasts MC3T3-E1 grown on polycaprolactone (PCL) surfaces functionalized with RGD containing peptide respond to BMP-2 through Smads pathway, while those cultured on PCL surfaces functionalized with scrambled RGD (negative control: RGE containing peptide) did not [202]. BMPs mimetic peptides have also been investigated for their capacity to act synergistically with cell adhesive peptides on enhancing MSCs and progenitor cells differentiation towards the osteoblastic lineage. Marquis et al. examined the crosstalk of BMP-9 peptide with different cell adhesive peptides. On polystyrene (PS) dishes coated with DGEA containing peptide, a type I collagen derived peptide, BMP-9 failed to increase ALP activity in mouse preosteoblasts, while on PS coated with RGD containing peptide, ALP activity was significantly enhanced in the presence of BMP-9, as compared to untreated or DGEA surfaces [226]. Cell adhesion was mediated through α_v and β_1 integrin subunits on RGD surfaces and only by β_1 integrins on GDEA surfaces within 24 h. It is important to mention that in this study DGEA and RGD peptides were adsorbed on PS surfaces [226]. In addition, in the last three studies discussed above (Lai and Cheng, Drevelle et al., and Marquis et al.), BMPs were added in its soluble form to the cell culture media.

He et al. grafted BMP-2, developed by Saito et al. (2003), solely or in combination with RGD peptide on poly (lactide-co-ethylene oxide-co-fumarate) (PLEOF) by click chemistry. They found that RGD and BMP-2 peptides, solely grafted, induced similar extent of ALP activity and ECM mineralization in rat MSCs cultured in osteogenic differentiation medium. However, when the peptides were co-grafted, they acted synergistically to enhance MSCs osteogenic differentiation [227]. More recently, the same group added to their previous cell culture model a third peptide, OPD, corresponding to residues 162–168 of osteopontin protein, which is known to influence vasculogenesis [228]. First, RGD

peptide was conjugated to PLEOF hydrogels, and then BMP-2 and OPD were simultaneously grafted through alkyne and aldehyde moieties, respectively. Rat MSCs were cultured on RGD, RGD+BMP-2 or RGD+BMP-2+ODP hydrogel surfaces in osteogenic differentiation medium supplemented with vasculogenic factors. At 28 days, RGD+BMP-2+ODP hydrogels triggered the highest levels of ALP activity, OPN and OCN mRNA expression and ECM mineralization. In addition, the expression of vascular markers such as PECAM-1, α-SMA and VE-cadherin was mediated with both BMP-2 and OPD peptides. Therefore, this study evidenced that the three peptides (RGD + BMP2 + OPD) acted synergistically to provide a suitable microenvironment for concomitant MSCs osteogenesis and vasculogenesis [228].

In a similar work, Moore and al. tested the combinatory effect of RGD and BMP-2 peptides on MSCs osteogenic differentiation, but in the absence of soluble osteogenic supplements in the medium. Human MSCs were cultured for 21 days on glass surfaces conjugated with RGD and/or BMP-2 or RGD+BMP-2, using alkyne-SAMs. On dually grafted surfaces, a synergistic enhancement of human MSCs was noticed, as revealed by an increase of BSP expression and the appearance of ECM mineralization markers. interestingly, they demonstrated that BMP-2 induced hMSCs osteogenic differentiation at a density ranging from 80 to 120 pmol/cm² when solely grafted, however on bifunctionalized, a density of 65 pmol/cm² of BMP-2 peptide was sufficient to induce osteogenesis [229].

Durrieu group has recently developed several mimetic peptides containing the knuckle epitope of BMP-2 (residues 73-92), BMP-7 (residues 89–117) and BMP-9 (residues 68–87). These mimetic peptides, containing the same number of amino acids, were identified by selecting the region of BMP proteins capable of interacting with their receptors, using crystallographic studies [187]. To evaluate their biological relevance, each peptide was jointly grafted with RGD peptide on oxidized poly (ethylene terephthalate) (PET) by carbodiimide chemistry. The differentiation of murine pre-osteoblastic MC3T3-E1 cells on the different peptide modified surfaces was assessed in growth medium after 24 h and 72 h. The dual peptide grafting; i.e. RGD+BMP-2, RGD+BMP-7, RGD+BMP-9, significantly enhanced the expression of both early and late osteogenic differentiation markers (Runx-2, BSP, OPN) after 24 h, as well as the expression of genes encoding bone ECM proteins and growth factors (OCN, BMP-2, TGF-b1 and VEGF) [187]. Subsequently, the extent of ECM matrix mineralization was evaluated after 5 days of culture in osteogenic medium, using Von Kossa staining. Much more significant mineralization was observed

on bifunctionalized surfaces, than on control PET or RGD surfaces. In addition, enhanced osteogenic differentiation of MC3T3-E1 cells was observed on BMP-2 surfaces as compared to BMP-7 and BMP-9 surfaces [187]. In a subsequent study, the same group reported that changes in cytoskeleton network play an important role in regulating the differentiation of osteoblast precursor into mature osteoblasts through RGD/BMP-2 crosstalk [211]. Together, these studies suggest that a synergistic effect on hMSCs osteogenic differentiation could be obtained when integrin binding proteins and growth factors or their mimetic peptides are used jointly. Further details about ligands crosstalk signaling pathways are provided in **[Results and discussion, study I and III]**.

Although osteoinductive mimetic peptides have proven to effectively induce osteogenic differentiation *in vitro* and new bone formation in animal models, they are not clinically used as an alternative to growth factors. This is partially due to the limited availability of data on structure and function of morphogenic peptides in physiological medium, particularly in tissue-engineered scaffolds.

1.4. Physical surface modification

Physical cues are as crucial as biochemical cues in directing cell behavior. Matrix stiffness is an external biophysical cue that cells perceive and interpret via the initiation of mechanotransduction cascades, which convert physical cues to biochemical signaling [230]. Within the human body, an abnormal alteration of ECM stiffness may result in severe diseases such as Duchenne muscular dystrophy [231] [232]. Unlike, tissue culture plastic, natural and synthetic materials can be produced with fine-tuned mechanical properties, hence their extensive use in investigating the effect of matrix stiffness on MSCs fate, *in vitro* [233] [230] [231] [234]. One early demonstration of the influence of matrix stiffness on cell behavior goes back several decades, where it has been shown that mouse mammary epithelial cells grown on soft collagen exhibited higher differentiation potential than those seeded on tissue culture plastic [235]. These preliminary observations were confirmed more recently in several instances. In an elegant study, hMSCs acquired functions and morphological patterns of distinct tissue-specific cells when exposed to polyacrylamide gels with different stiffnesses [236]. Indeed, after one week of culture in identical growth medium, the morphology of hMSCs cultured on soft substrates, mimicking the stiffness of brain (0.1–1 kPa), was close to neuronal-like cells morphology and those cultured on harder substrates, mimicking muscle stiffness (8–17 kPa), were similar in shape to C2C12 myoblasts, whereas the hardest matrices, mimicking collagenous bone

matrices (25–40 kPa), yielded polygonal MSCs similar in morphology to osteoblasts. Furthermore, early neuronal, myogenic and osteoblastic markers were expressed in each condition respectively [236]. Similarly, material stiffness has been shown to modulate MSCs adipogenic differentiation. Huebsch et al. investigated mouse MSCs differentiation in response to RGD modified alginate gel substrates of different stiffnesses, ranging from 2.5 to 110 kPa [237]. Osteogenic commitment was observed primarily at intermediate stiffness (11–30 kPa) with the expression of osteogenic markers such as OPN and OCN, whereas adipogenic lineage was predominant in softer substrates (2.5–5 kPa), as revealed by the expression of adipogenic markers, such as peroxisome proliferator-activated receptor gamma (PPAR-γ) and adiponectin (Adn). Interestingly, authors evidenced that MSCs feel the stiffness of their microenvironment by regulating integrin binding affinity and adhesion ligands reorganization on the nanoscale [237]. In fact, significant decrease in osteogenesis and enhancing in adipogenesis was observed by blocking the binding of RGD peptide to α_5 integrins [237].

In another study, Winer et al. tested the effectiveness of matrix stiffness on maintaining the stemness character of stem cells [238]. They reported that hMSC stopped progression through the cell cycle, despite the presence of serum, when grown on 250 Pa polyacrylamide substrates that mimic the stiffness of bone marrow tissues. However quiescent hMSCs started to proliferate when transferred to stiff substrates and underwent adipogenic or osteogenic differentiation in the presence of induction medium [238]. Similarly, Li et al. successfully maintained human embryonic stem cells (hESCs) in their stemness state by manipulating the polymer stiffness and the density of tethered RGD ligand. They reported that hESCs remained viable, maintained their native morphology and expressed the markers of undifferentiated hESCs for up to 5 days [239].This study provides valuable insights that can be taken into consideration in biomaterials design since the maintenance of stem cells multipotency *ex vivo* remains a real challenge.

As highlighted in the previous sub-section, we have demonstrated that biochemical cues (RGD and BPM-2 mimetic peptides) act in a synergistic manner on enhancing hMSCs and preosteoblasts osteogenic differentiation [185] [187] [211]. Similarly, Durrieu group has investigated whether biochemical and mechanical cues can act synergistically to regulate hMSCs osteogenic differentiation [210]. RGD and BMP-2 mimetic peptides were grafted separately onto poly (acrylamide-co-acrylic acid) (pACAA) surfaces of various stiffnesses ranging from 0.5 to 70 kPa through carbodiimide chemistry. On RGD functionalized pACAA surfaces, hMSCs commitment was stiffness-dependent, as evidenced

by hMSCs myogenic and osteogenic commitment at 13-17 kPa and at 45-49 kPa, respectively, after 96 h of culture. However, on BMP-2 modified-pACAA surfaces, hMSCs differentiated along the osteogenic lineage regardless the matrix stiffness, when it was higher than 13 kPa. In contrast, BMP-2 failed to induce osteogenic differentiation on very soft substrates (0.5–3.5 kPa). Interestingly, further investigations from this study revealed that on very soft gels, the effect of mechanical cues resulted in a particular reorganization of actin fibers cytoskeleton, which was not favorable for the activation of BMP-2-mediated Smads pathway. One plausible explanation of the underlying cellular behavior is that hMSCs perceived a weak mechanical feedback from the very soft hydrogels, which resulted in an inappropriate integrins distribution and clustering, and therefore inadequate cell spreading and cytoskeleton reorganization and contractility. Indeed, it is currently well-established that integrins and actin-myosin machinery are essential in directing MSCs commitment and differentiation towards the osteoblastic lineage [240] [241] [242]. Soon later, Ding's and Mooney's groups highlighted the interplay between mechanical and biochemical cues [240] [243], which supports the findings reported by Durrieu team. Although these studies and others confirm unambiguously the effect of matrix stiffness on cell adhesion [244] [245], migration [246], proliferation [247] and differentiation [236] [237] [210] [244], these findings were not persuasive for all researchers working on this issue. For example, Trappmann and co-workers criticized the fact that Engler and colleagues [236] as well as other groups ascertained the effective influence of matrix stiffness on stem cell differentiation without decoupling the underlying effect from that of biochemical cues (such as tethered proteins on biomaterials, used as cell adhesion ligands). On the basis of a series of extensive experiments, Trappmann et al. argued that matrix stiffness could not be the key factor itself, but affected stem cell fate through the modification of the surface chemistry (ligands density and distribution) upon the variation of matrix stiffness [248]. They found that polyacrylamide (PA) hydrogels of the same stiffness, but exhibiting different crosslinker concentrations, induced different cellular responses. In addition, stiff PA hydrogels with lower crosslinker density induced similar MSCs behavior, as compared to that observed by Engler [236] on soft PA hydrogels. Moreover, they reported that varying the anchoring point distance for collagen, without altering matrix stiffness, led to cell behavior typically found when cells were cultured on PA substrate of different stiffnesses [248]. Together, these findings clearly associate the triggered cellular responses to the mechanical feedback of tethered proteins, instead of matrix stiffness. However, two years later, Engler group published an elegant study

where they defended their viewpoint by stating that "*differentiation does not depend on tethering*" [249]. Therefore, the precise mechanism of how cells sense the substrate mechanical properties is still under debate and two main concepts have been proposed in the literature. First, Engler and colleagues have put forward the influence of matrix stiffness in dictating stem cell fate by providing direct evidence that the mechanical feedback from PA substrates themselves regulate MSCs fate determination independently of surface chemistry [236] [249]. The second concept, established by Trappmann et al., highlighted that PA stiffness-induced MSCs differentiation is modulated through the mechanical feedback of tethered ECM proteins, such as collagen [248]. Although, significant differences have been reported from these two groups, both of them recognized that MSCs sense mechanical cues applied from their surrounding through integrins. The latter, along with actin-myosin cytoskeleton-based contractile mechanism, play a key role in directing stem cell fate in response to matrix stiffness.

Following this controversy, a novel class of polymers has been recently introduced, offering the advantage of varying the stiffness and ligand density independently. Such materials provide a reliable tool to decouple the effect of matrix stiffness from that triggered by surface chemistry, which will contribute to a clear and robust interpretation of mechanotransduction mechanisms [239] [240] [243] [250].

As an important conclusion from these studies is that both mechanical and biochemical cues are effective modulators of stem cell fate and they may act independently or jointly. Nevertheless, it is still difficult to mimic the mechanical properties of the native ECM, *in vitro*. Therefore, an in-depth understanding of specific or combinatorial effects of ECM properties may significantly contribute to new biomaterial designs, in order to precisely target and potentiate the desired cell response.

1.5. Topographical surface modification

Besides controlling MSC fate by applying the aforementioned surface modification strategies, surface microstructuration, by creating ordered or disordered topographies, has currently generated a great interest in bone tissue engineering application owing to the high sensitivity of cells to such stimuli [251] [252]. Nowadays, it is well-established that altering the surface topography of biomaterials affect early cell responses such as cell adhesion, spreading and migration, by modulating cell integrins distribution and clustering as well as cytoskeleton reorganization, which in turn regulate more complex cellular functions such as cell fate determination [251] [253] [254]. It is also though that topographical cues alone can trigger the same effect as biochemical signals. One simple reason of the biological relevance of topographically structured materials is their resemblance to the native ECM from a structural perspective. Topologically, ECM consists of a heterogeneous mixture of nano- and micro-sized structures, such as pits, pores, ridges, protrusions, crystals and fibers [255] . Typically, the ECM acquires its architecture from the folding or bending of nanoscale topographies to create microscale topographies and even macroscale structures. As highlighted at the beginning of this literature review, bone tissue is a pertinent example that perfectly illustrates this high hierarchical organization over different length scales **(Figure 3)**. As another example, the ECM of human thick skin dermis, examined by scanning electron microscope (SEM), exhibits topographical features spanning several length scales **(Figure 14)** [256]. At the millimeter scale, the ECM consists of alternating wide and narrow grooves, called primary and secondary grooves, respectively. The bottoms of primary grooves are smoother than those of secondary grooves, and these grooves are separated by ridges. Each ridge is composed of submillimeter to several hundred micron finger-like projections, termed dermal papillae. The surface of dermal papillae is covered by folds and pores of approximately 10 microns in dimension. At the nanometer scale, folds consist of dermal collagen fibrils (60-70 nm in diameter) that form a loose honey comb-like network. Further characterizations of the ECM topographical features have been performed on tissue and organs often harvested from animals, including pig aortic heart valve basement membrane [257], rat small intestine ECM [258], canine corneal basement membrane [259] and macaque bladder basement membrane [260]. Therefore, fundamental knowledge on the native ECM topography provides a rational basis for a finely-tuned design of biomimetic material surfaces.

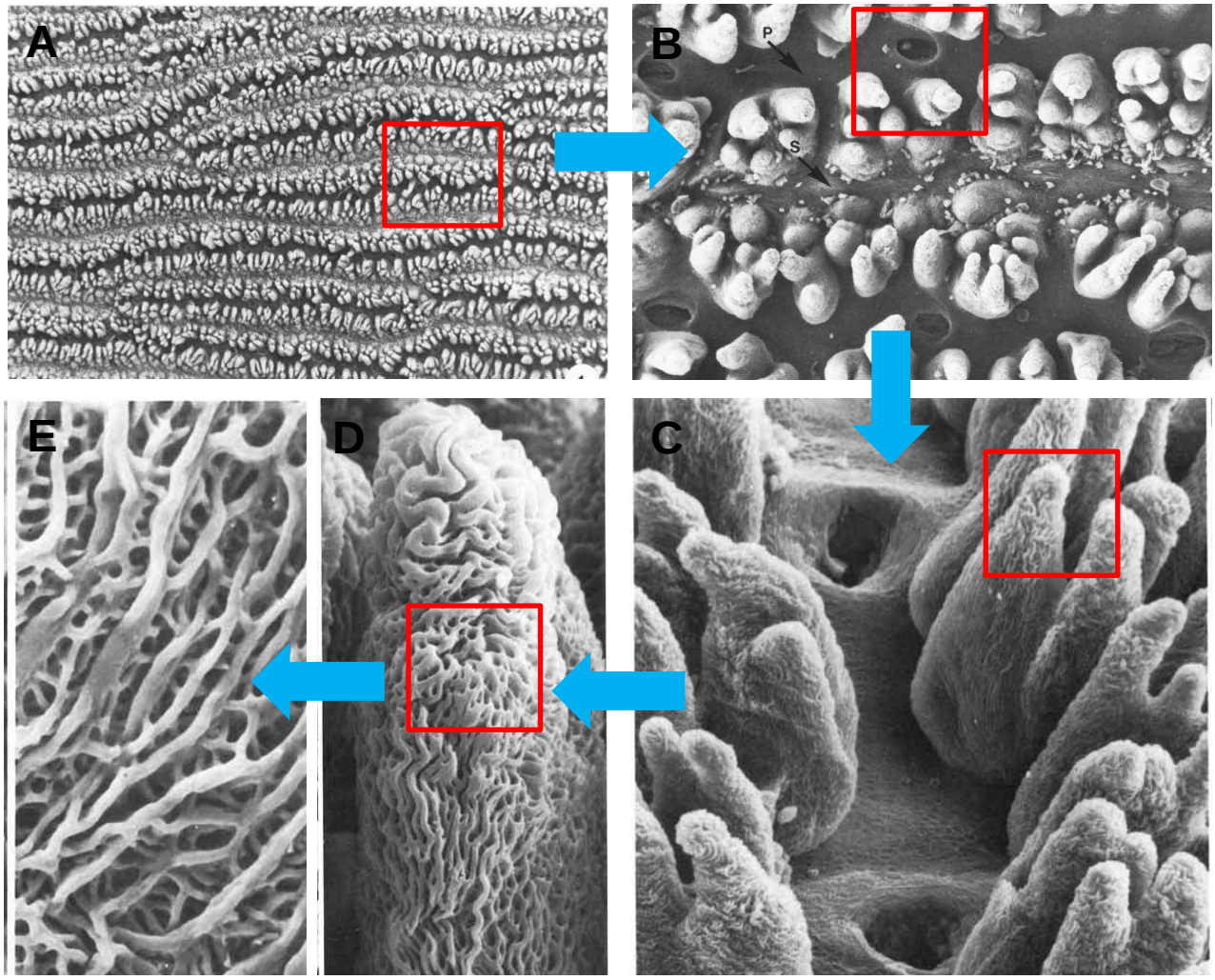

Figure 14: Hierarchical structure of human thick skin dermis surface over different length scales, from millimeter to micron range (Magnification: **(A)** 20x, **(B)** 130x, **(C)** 260x, **(D)** 1,040x, **(E)** 2,800x) [256].

One of the key approaches applied to create topographies onto biomaterials is surface roughening. Altering the surface roughness of orthopaedic implants has gained considerable interest as tool to enhance their osseointegration. Albrektsson and Wennerberg classified the implant surfaces as smooth (0.0-0.4 μm), minimally rough (0.5-1.0 μm), moderately rough (1.0-2.0 μm) and rough (>2.0 μm) [261]. It has been shown that increasing the surface roughness at both the nanometer and micrometer scale is beneficial for bone cells interactions with biomaterial surfaces. However micro- and nano-rough surfaces enhance bone cells responses through different ways.

Micro-roughening elicits an increase in the overall area and irregularities on the biomaterial surface, which facilitates bone cells attachment and adhesion [262]. Conse-

quently, this may promote new bone formation at the interface bone/implant, thus allowing increased bone-to-implant contact and better implant mechanical integrity [263]. On the other hand, nano-roughening leads to higher surface energy as compared to very smooth surfaces [262]. However, the surface energy effect on bone cells behaviors is still under debate, as highlighted in the sub-section **[V.1.1. Physicochemical surface modification]**. It is also thought that bone cells perceive and respond to nano-rough surfaces because such surfaces replicate the nanostructured organization of bone tissue ECM [264].

Actually, the literature provides plentiful information about the positive effects of surface roughening on inducing osteogenesis. For instance, it has been reported that osteoblasts on micro-rough surfaces secreted various factors responsible for their maturation such as osteoprotegerin (OPG), receptor activator of nuclear factor kappa B ligand (RANKL) and TGF-β1, while osteoclast formation and activity decreased [265]. *In vivo*, various orthopaedic implants with micro-rough topographies -generated by different surface modification methodologies such as blasting, etching, blasting/etching, plasma spraying and oxidation- exhibited stronger integration to bone, as compared to smooth implant surfaces [266]. It has also been suggested that an average roughness (Ra) of material surfaces ranging from 1 to 2 µm is optimal for bone/implant interactions [267]. At the nanometer scale, various studies have also proven the effectiveness of on nanostructured materials on enhancing bone cells functions, including cell adhesion and ECM synthesis and mineralization, when compared to conventional materials [262] [264].

Although the positive biological effect of altering the surface roughness has been reported in in several instances, other investigations have failed to confirm the effect of nano- and micro-rough surfaces on MSCs proliferation, differentiation and ECM mineralization [268]. In addition, clinical trials, reported in several systematic reviews, were not able to evidence any positive effect of increasing surface roughness on implant osseointegration. Esposito et al. have reported, in the last Cochrane review, results from 1512 participants and 3230 dental titanium implants [269]. They have concluded that implants with smooth surfaces had a 20% reduction in risk to be affected by peri-implantitis (bone loss) than implants with rough surfaces after 3-year follow-up. Therefore, it remains difficult to draw an appropriate surface roughness profile for orthopaedic implants. This is partly due to the multiplicity of roughening protocols and the lack of a standard procedure to evaluate the surface topography, which makes the comparison of values from one study with another an almost task [267]. Furthermore, it should be not neglected that procedures for

altering the surface roughness may lead to changes in the surface chemistry and wettability, therefore the evaluation of the biological effect of the surface roughness independently from other factors is challenging [266].

Besides surfaces roughening, topographical patterning, which consists of designing regular and well-defined topographies on material surface, represents a powerful tool to deconstruct the complexity of the native ECM and replicate one or a combination of its features on model materials *in vitro*. The introduction of topographical patterning technology, along with super-resolution microscopy to assess the native ECM topography, have offered a unique opportunity to elucidate mechanisms by which MSCs regulate their fate decision in response to topographical cues. One demonstration of the ability to reproduce ECM topographical features *in vitro* has been reported by Pfluger et al., where the complex topography of pig small intestinal basement membrane was precisely replicated **(Figure 15)**. Indeed, they were able to mimic villus (100-200 μm in height & 50-150 μm in diameter), crypt (20-50 μm in diameter), and pore (1-5 μm in diameter) of the basement membrane [270].

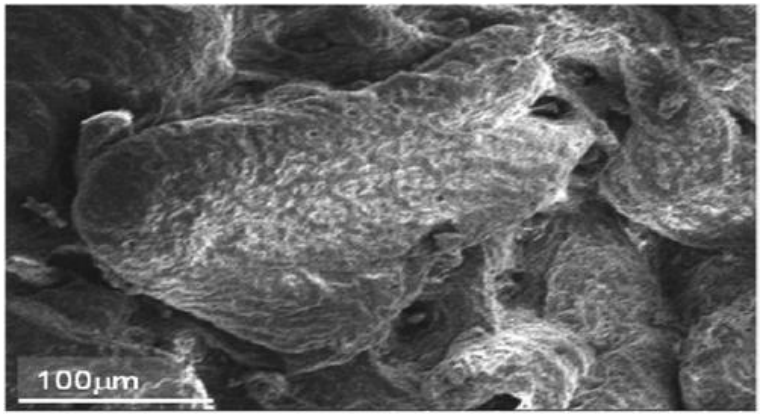

Figure 15: Precise replication of pig small intestinal basement membrane using plasma enhanced chemical vapor deposition (CVD) of poly(2-hydroxyethyl methacrylate) p(HEMA) [270].

So far, a series of micro- and nanofabrication techniques have been developed to engineer topographically structured material surfaces [271]. Photolithography and microcontact printing are the most popular methods to create microscale features with controlled geometry, dimension and periodicity on 2D materials, including grooves, posts and pits. Using these techniques, topographical micropatterns could be generated on both organic and inorganic materials. Organic materials commonly used include silicon, glass and titanium, while organic materials include poly(dimethylsiloxane) (PDMS), polystyrene (PS), poly(methyl methacrylate) (PMMA), polycarbonate (PCL) and poly(ethylene glycol) (PEG) or biodegradable polymers such as PLA, PGA and PLGA [271]. Therefore, such topographically microstructured materials have been used as cell culture substrates to investigate the effect of topographical cues on cellular functions, including cell morphology, adhesion, proliferation, migration and differentiation.

Wan et al. evaluated osteoblast-like cells adhesion and proliferation on pits-patterned surfaces of polystyrene (PS) and islands-patterned surfaces of PLLA of 2.2 μm in diameter. They suggested that cell adhesion could be enhanced on both micropatterned surfaces, as compared to unpatterned surfaces. On micro-scale islands, cells adhered along the surface, while on micro-scale pits cells were located inside the holes. Osteoblast-like cells proliferated in similar trend on micropatterned and unpatterned surfaces [272]. Zinger et al. studied human bone-derived cells (MG63 cells) behavior on titanium surfaces with hexagonal cavities of 10, 30 and 100 μm in diameter. Cells were not able to recognize 10 μm diameter cavities but colonized both 30 and 100 μm cavities and exhibited a three-dimensional shape only on 30 μm cavities. Additionally, cells exhibited dense focal contacts and actin cytoskeleton on all micropatterned surfaces, as compared to unpatterned surfaces [273]. In this study, the authors suggested that cells sense and respond to topographical micropatterns exhibiting at least their own size, since MG63 cells -of approximately 30 μm in size- recognized 30 and 100 μm cavities but not 10 μm cavities. In another study, Hamilton and al. investigated the effect of micropatterns of different geometries and dimensions on bone cells differentiation and ECM mineralization both *in vitro* and then *in vivo*. Osteoblasts isolated from *rat calvaria* (RCOs) were seeded on micropatterned silicon surfaces with trapped pits and inverted pyramids. Patterns depth ranged from 30 μm to 120 μm while patterns pitch was varied from 185 μm to 280 μm. *In vitro*, osteoblasts were shown to be highly migratory, adherent and surrounded by a

mineralized ECM on all micropatterned surfaces. However, mineral deposition was significantly higher on trapped pits-patterned surfaces of 120 µm depth and 280 µm pitch (120TPs280) after 2 weeks. At 4 weeks, some 120TPs280 were completely filled with mineral. Consistent with *in vitro* results, *in vivo* experiments revealed greater bone formation and mineralization on 120TPs280 after 8 weeks [274]. The same group examined the behavior of the same cell type, RCOs cells, on another type of micropatterns, shaped as open square boxes or pillars. Dimensions of open square boxes were varied from 34x34 µm to 65x65 µm in width and fixed at 4 and 10 µm in height. Pillars were separated by a repeated spacing of 20 µm and their height was 4 or 10 µm. Compared with smooth surfaces, both micropatterned surfaces affected osteoblasts adhesion, proliferation and migration at short time points (<1 week) and enhanced matrix synthesis and mineralization at longer time intervals (2–6 weeks) [275]. Ghibaudo et al. also confirmed the underlying effect of pillar micropatterns, as they reported that cells gradually appeared similar in morphology to that cultured on smooth surfaces, as pillars became shorter [276].

Grooves and ridges are among the most studied topographical features as they exert a strong effect on cells, known as contact guidance [277]. This means that cells, when cultured on such structures, align and elongate along the major axis of grooves. Grooves dimensions; i.e. their width and depth greatly affect the degree of cell alignment and elongation [271] [277]. Lu and al. engineered hydroxyapatite micro-grooves of different width (8 and 24 µm) and depth (2, 4 and 10 µm) on silicon substrates. They demonstrated that grooves of 8 µm in width had a strong orientation effect on both osteoblast and myoblast cells, as revealed by well-aligned cells in the direction of grooves axis. Larger grooves (24 µm in width) strongly influenced myoblasts but not osteoblasts. Grooves depth also affected osteoblasts and myoblasts behavior, however cell alignment and orientation were higher on grooves with intermediate depth (4 µm) as compared to grooves of 2 µm and 10 µm depth [278]. López-Bosquerat et al. performed a comparative study between the effect micro- and nano-sized topographies on the contact guidance. PMMA substrates were used to created micro-sized channels (10 µm width, 500 nm depth, 10 µm spacing) and nano-sized channels (200 nm width, 100 nm depth, 200 nm spacing). Results showed that rat MSCs (rMSCs) aligned along the direction of both nano- and micro-scale channels and no difference in term of cell density was observed between these substrates. However, compared to nano-channel substrates, rMSCs cultured on micro-channels exhibited larger morphology, as evidenced by smaller elongation and higher surface area. Cell migration also exhibited different profiles between the underlying substrates, since

rMSCs exhibited persistent spreading and stable cell morphology on micro-channels, while on nano-channels cells had tendency to spread, align, stretch and retract, repeating this pattern along the direction of channels. Interestingly, rMSCs maintained the same behavior even when micro- and nano-structured surfaces were pre-coated with fibronectin, meaning that topographical features effect was not hindered by the presence of biochemical cues [279].

Topographical micropatterns have also been used to direct MSCs fate. Recently, a randomized topographical biomaterials library, designed from mathematical algorithms, was applied *in vitro* to screen 2,176 topographies in order to unravel which induce hMSCs proliferation or osteogenic differentiation [280]. Fu et al. have focused on determining the role micropatterns height on directing hMSCs osteogenic differentiation. PDMS templates were used to create pillars of different heights (0.97 to 12.9 µm) with constant diameter (1.83 µm) and spacing (4 µm). On shorter micropillars (0.97 µm), hMSCs were well-spread with highly organized actin fibers and large focal adhesion (FA), and expressed elevated levels of osteogenic markers. Conversely, hMSCs grown on taller micropillars (12.9 µm) exhibited round morphology, disorganized actin filaments, small FA as well as an adipogenic phenotype, as confirmed by the formation of lipid droplets [281]. Guvendiren and Burdick investigated the effect of micropatterns shape on MSCs commitment and differentiation. hMSCs were grown on microstructured poly (2-hydroxyethyl methacrylate) (pHEMA) hydrogels that have the particularity of spontaneously forming lamellar or hexagonal wrinkles upon swelling. They found that hMSCs, attached to lamellar wrinkles, were well-spread, exhibited high aspect ratio, whilst taking the shape of the pattern. In contrast, cells attached inside the hexagonal patterns remained round with low spreading. Subsequently, hMSCs were cultured for 14 days in 1:1 osteogenic/adipogenic mixed media. Results showed that 91% of cells were positive to ALP staining on lamellar patterns, followed by 74% on flat hydrogels and 61% on hexagonal patterns. On the other hand, 9% of cell were positive to oil droplet staining on lamellar patterns, followed by 26% on flat hydrogels and 39% on hexagonal patterns [282]. In the same context, Wei et al. al examined the influence of micropatterns width on MSCs osteogenesis. They created circular polyvinyl alcohol (PVA) patterns exhibiting three different diameters (40, 60, 80 µm) on polystyrene substrates. hMSCs exhibited the greatest degree of spreading and actin cytoskeleton contractility on the largest micropatterns (80 µm). In osteogenic and adipogenic medium, a monotonic trend of hMSCs differentiation with the

pattern size was observed. In fact, after 21 days of osteoinduction, the percentage of osteogenic differentiation of hMSCs was 17.5%, 40.2% and 53.9% on micropatterned surfaces with 40, 60 and 80 µm circles, respectively. After 7 days of adipogenic induction, the percentage of adipogenic differentiation was inversely correlated to the pattern size, leading to 45.3%, 26.3% and 14.7% of differentiated cells on micropatterns with 40, 60 and 80 µm circles, respectively. This study highlights the importance of cell spreading extent and actin cytoskeleton contractility in guiding MSCs fate decision [283]. In another study, Seo et al. evaluated the osteogenic effect of lattice micropatterns, fabricated on PDMS substrates, on murine MSCs (mMSCs). Lattice micropatterns exhibited different widths, ranging from 0 to 8 µm, but constant height of 1 µm. the distance between lattice micropatterns was 2 µm. Enhanced mMSCs osteogenic differentiation was noticed with the increase of micropatterns width, when comprised between 0 and 3 µm. indeed, micropatterns of 3 µm in width led to the highest levels of ALP after 6 days and type I collagen and OCN after 12 days. Conversely, micropatterns of width ranging from 4 to 8 µm slighted affected the expression of osteogenic markers [284]. The same group performed an another interesting study, where they tried to shed light on signaling pathways triggered following the interaction of MSCs with topographical micropatterns. They found that mMSCs exhibited higher FA maturation, actin cytoskeleton polymerization and focal adhesion kinase (FAK) phosphorylation when cultured on lattice micropatterned surfaces, as compared to unpatterned substrates. In addition, they evidenced that the underlying events were regulated by RhoA/ROCK pathway [285].

Taken together, these studies suggest that focal adhesion, actin cytoskeleton tension and RhoA/ROCK pathway are involved in directing MSCs differentiation into osteoblast lineage. Other signaling pathways have been proposed as potent regulators of topography-mediated osteoblast differentiation, such as the mitogen-activated protein kinase (MAPK) pathway [286]. However, the exact mechanism by which topographical features guide MSCs fate determination is yet to be fully understood.

Overall, the studies presented here provide clear evidence of the potency topographical cues in dictating multiple cell response, thereby such cues should be considered upon the design of biomaterials for stem cell research and bone tissue engineering applications.

1.5. Chemical surface patterning

The difference between topographical and chemical surface patterning is that the first approach aims to modify the surface structure of the material itself by creating ridges, grooves, pores, pits…etc, while the second approach consists of presenting moieties, proteins and growth factors on material surfaces in a spatially controlled manner. In contrast to topographically patterned surfaces, specifically at the microscale level, chemically patterned surfaces induce slight changes in the physical parameters of the material surface (surface roughness for example), with respect to unpatterned surfaces. Within stem cell niches, known as the natural stem cell microenvironment that ensure cell survival and functions, physical cues -such as topography and stiffness- and biochemical cues -such as proteins and growth factors- as well as cell cues overlap to regulate stem cell fate, hence the complexity of delineating their individual contributions [287] [288].

The introduction of microfabrication techniques that permit the functionalization of material surfaces with well-defined chemical patterns of microscale resolution afforded a unique opportunity to elucidate the role of each effector independently. The most popular micropatterning technologies used to engineer 2D chemical patterns are those used for topographical micropatterning; i.e. photolithography and microcontact printing (µCP) techniques. Alternatively, microtransfer lithography has been recently developed to prepare stable chemical micropatterns on hydrogels under wet environment [289]. The fabrication procedure of chemical micropatterns on model materials using µCP and microtransfer lithography is depicted below in **Figure 16**, while the basic principle of photolithography is presented in **[Results and discussion, study I and III]**. Other technologies are also used in microfabrication, such as the computer-assisted laser ablation [290], inject printing [291] and microfluidic patterning [292].

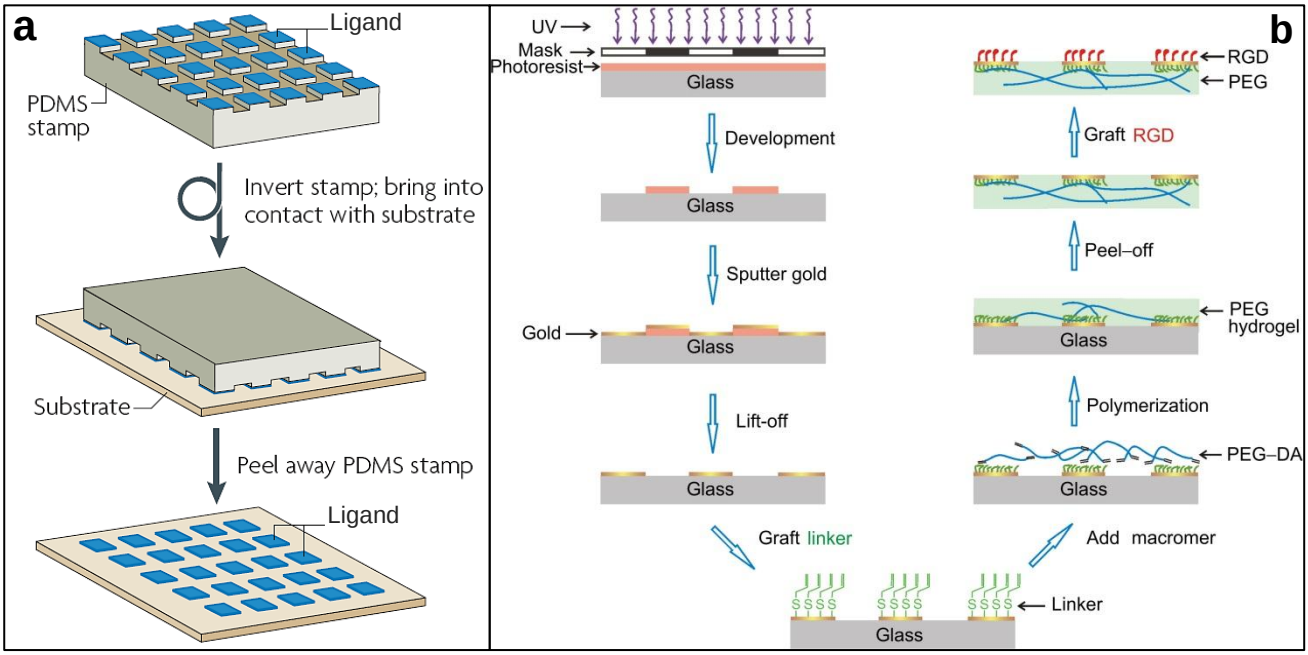

Figure 16: Schematic presentation of two typical micropatterning techniques. (a) Micro-contact printing (μCP) (adapted from [293]). (b) Microtransfer lithography [294].

This subsection will provide a review of the most pertinent studies based on chemical patterning of ECM-derived ligands to mediate MSCs osteogenesis through the fine control of individual cellular events, such as cell morphology, spreading and adhesion at the microscale level.

The application of microfabrication techniques in biology to manipulate cell adhesion can be traced back to Carter's discovery, more than 50 years ago. He observed in a series of experiments that cells had tendency to accumulate on palladium metal micropatterns in preference to cellulose acetate micropatterns [295] [296]. However, micropatterning technology has gained prominence and became accessible to cell biology and biomaterials laboratories more recently. The well-accepted study as a pioneering work in this topic was done in cooperation of two Harvard university groups, Whitesides and Ingber groups [297], using μCP technique introduced by Whitesides group in 1994 [298]. In this study, cell spreading was restricted on adhesive proteins (fibronectin, vitronectin or type I collagen) microislands, fabricated on gold substrates, to investigate to effect of pattern size on cell fate. They found that more cells underwent apoptosis on small microislands, exhibiting an overall area of ≈ 100 μm^2. Their conclusion was that the size of adhesive micropatterns controls cell life and death regardless the type of proteins and integrins involved in mediating cell adhesion. These findings have motivated several other groups

to investigate the effect of chemically patterned ECM-derived ligands on nearly all cellular events, including cell adhesion, migration, polarity, growth and mitosis [288].

Ten years following the discovery of the impressive role of geometric cues in controlling cell life and apoptosis, Lehnert et al. applied the same chemical micropatterning technique (μCP) to investigate the effect of ligand micro-spacing on cell adhesion and spreading [299]. Square vitronectin micropatterns with different sizes (0.1-9 μm^2) and center-to-center spacing (1-30 μm) were created onto a gold-coated coverslip, through SAMs of alkanethiolates. Melanoma cells were then cultured on these substrates for 1 h in serum-free medium, in order to minimize the modification of the substrate pattern due to the deposition of proteins and growth factors secreted by cells or present in the serum. The first important element reported in this study was that the micro-spatial distribution of ECM adhesive ligands drastically affects focal adhesion assembly [299]. In a subtle manner, they were able to localize cells at the border between uniform and micropatterned vitronectin on the same substrate regions (**Figure 17 1-1'**). In the cell side adhered on uniform fibronectin coating, $\alpha_V\beta_3$ integrins (vitronectin receptors) were concentrated and clustered at the cell periphery. On the other side; i.e. on vitronectin micropatterns (1 μm^2 & 5 μm spacing), $\alpha_V\beta_3$ integrin receptors were precisely localized at on the patterns (**Figure 17 1-1'**). In another set of experiments, the authors evaluated the effect of the distance between fibronectin square micropatterns on cell spreading, by varying pattern spacing from 1 to 30 μm (**Figure 17 A-I)**. As long as the spacing between micropatterns was less than 2 μm (center-to-center), cell morphology was similar to that found on homogeneous fibronectin-coated substrates. At a pattern distance ranging from 5 to 20 μm, cells adapted their shape to the spatial distribution of fibronectin micropatterns. In addition, they formed actin fibers tension mainly between adjacent micropatterns. When the distance between micropatterns reached or exceeded 25 μm, cells hardly probed the surrounding micropatterns, and consequently exhibited limited spreading and more rounded morphologies [299]. This study provides evidence that cells are highly sensitive to chemically micropatterned surfaces and adapt their integrins assembly and clustering, cytoskeleton rearrangement and shape in response to the spatial distribution of ECM ligands.

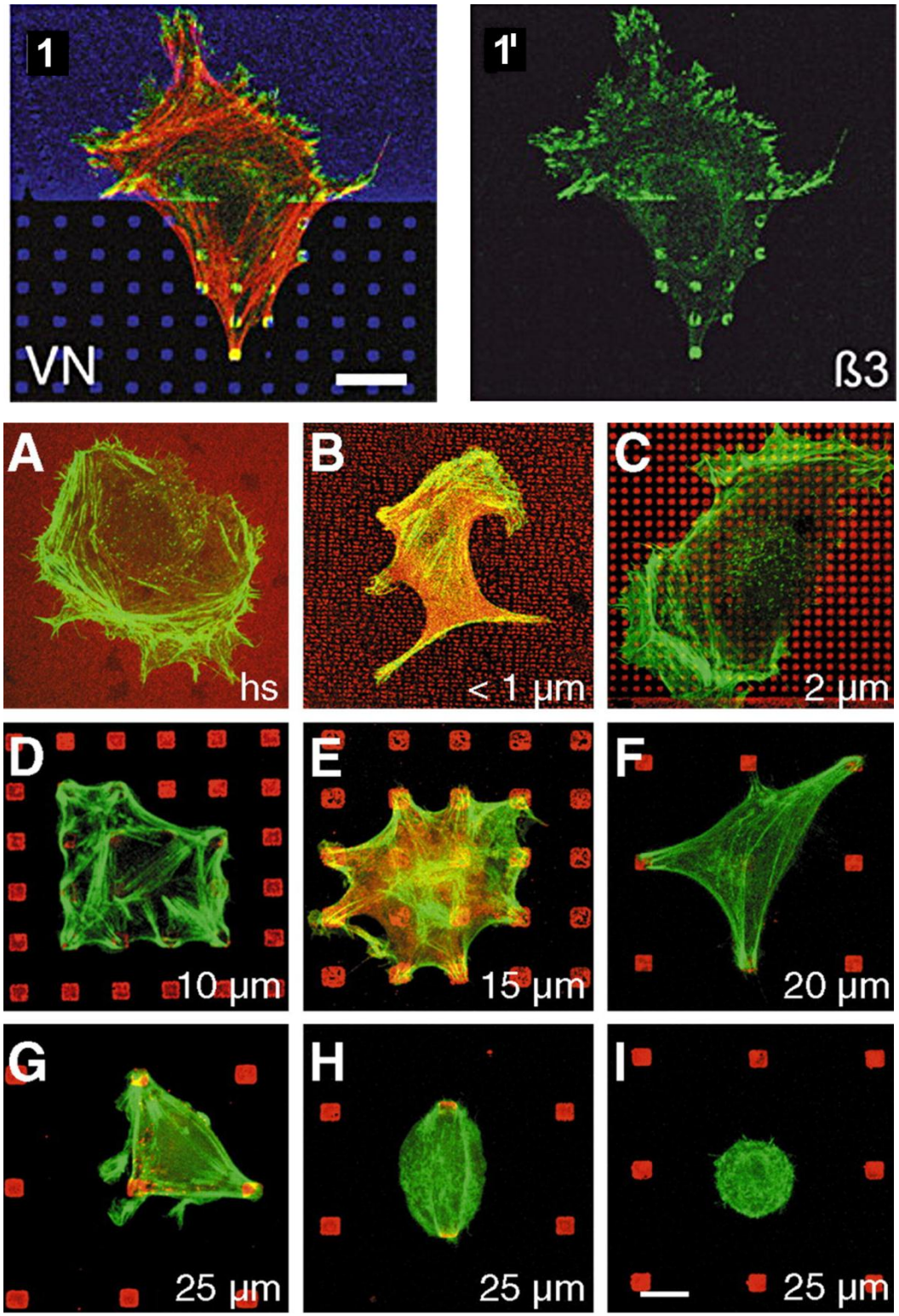

Figure 17: Effect of ligand micropatterning on cell behaviors. (1-1') β3-integrin-GFP (green) distribution in melanoma cell labeled for actin (red) and grown on vitronectin (blue) at the border between a uniform and a micropatterned region. (A-I) cell spreading extent controlled throughout fibronectin micropatterns spacing ranging from 1 to 25 µm. fibronectin and actin fibers were labeled in red and green respectively. (A) homogenous fibronectin-coated substrates. (B) 0.1 µm² fibronectin patterns with 1 µm spacing. (C) 1 µm² fibronectin patterns with 2 µm spacing. (D-I) 9 µm² fibronectin patterns with spacing as indicated in the right-hand corner. Scale bar: 10 µm [299].

In the same context, Healy et al. developed chemically micropatterned surfaces to control the extent of cell adhesion [155]. Rat calvaria bone cells were seeded on line micropatterns of N-(2- aminoethyl)-3-aminopropyl-trimethoxysilane (EDS), separated by parallel line micropatterns of dimethyldichlorosilane (DMS). The width of EDS and DMS micropatterns was 50 and 100 µm, respectively. Although cells were randomly distributed over EDS and DMS micropatterns upon cell plating, they selectively gathered on the EDS regions within 30 min. Matrix mineralization, assessed after 15 and 25 days of culture by Von Kossa staining, preferentially occurred on the EDS regions. The authors suggested that the preferential cell distribution and matrix mineralization was related to the hydrophilicity of the EDS coating. This favored serum proteins adsorption, thus promoting cell attachment, spreading, proliferation and the ECM mineralization. They also evaluated serum proteins adsorption on hydrophobic DMS micropatterns and revealed that the density and activity of proteins adsorbed on these regions were significantly reduced [155].
In stem cell research, chemical micropatterning techniques have gained interest only very recently. In 2004, McBeath et al. examined the effect of cell spreading extent on hMSCs specification into distinct lineages [241]. To manipulate MSCs spreading independently from other effectors, they used µCP technique to create square microislands of fibronectin of different sizes (1,024, 2,015 and 10,000) on a cell-repellent background (Pluronic F108), thus the cell spreading degree was pattern size-dependent. After one week of culture in a mixed adipogenic/osteogenic medium, an interplay between hMSCs fate and pattern size was noticed. Osteogenesis, assessed by ALP staining, occurred on large islands, while adipogenesis, evidenced by oil red staining, occurred on relatively small islands. On intermediate-sized islands, a mixture of both lineages was found. In this excellent study, authors have put forward the influence of cell shape on cell differentiation, however in our opinion the underlying paper was focused on evaluating the "size" effect more than the "shape" effect on stem cell fate. Following the publication of this work, a debate has been raised around this study, arguing that the use of mixed osteogenic/adipogenic medium in cell differentiation experiments is likely to elicit a sort of competition between osteogenesis and adipogenesis, which may hinder the precise evaluation of pattern size mediated-lineage specification. To clarify that point, Peng et al. used their microtransfer patterning technique to prepare circular RGD micropatterns on a PEG background. Six pattern dimensions (177/ 353/ 707/ 1,413/ 2,826/ 5,652 μm^2) and three culture media (osteogenic, adipogenic and 1:1 osteogenic/adipogenic media) were tested. rMSCs maintained under these different conditions for one week exhibited a monotonic increase

of osteogenesis and a monotonic decrease of adipogenesis in relationship with pattern size; i.e. cell spreading size. These trends of MSCs differentiation were observed not only in the presence of mixed medium, but also in medium supplemented with either osteogenic or adipogenic factors [300].

While the above-mentioned studies examined the potency of cell spreading cue on dictating MSC fate for up to 7 days, Song et al. tried to extend cell culture time for up to 21 days, given that cell differentiation is a long-term cellular process [283]. Polystyrene plates were coated with Azidophenyl-derivatized poly(vinyl alcohol) (AzPhPVA) and a photolithographic procedure was applied to created circular micropatterns of 5,024, 11,304 and 20,096 μm². Consistent with McBeath et al. and Peng et al. studies, they found that cell spreading significantly influenced hMSCs fate after one week. In addition, the effect of cell spreading on stem cell fate persisted for up to 21 days [283].

Chemical patterning strategies have shed light on other cues, as crucial as cell size in directing cell fate determination. Kilian et al. reported in a wonderful study that the cell shape alone can dictate lineage-specific differentiation of MSCs [242]. In this work, fibronectin micropatterns shaped as flower, pentagon or star, having the same overall area of 2,500 μm², were created on PDMS substrates. hMSCs cultured for one week in mixed adipogenic/osteogenic medium on the different surfaces took the patterns shape. The extent of osteogenesis and cytoskeleton tension increased from flower to pentagon to star shape. Adipogenesis was inversely correlated with osteogenesis. The pattern shape was also shown to affect focal adhesion (FA) density and distribution, as revealed by larger FA contacts on star-shaped micropattern as compared to flower-shaped micropattern. In addition, the authors stated that the pattern shape was not the only modulator of MSC fate decision and that the pattern subcellular curvature also affected cell differentiation. Indeed, they suggested that concave curvatures were favorable for osteogenic different, while convex curvatures were beneficial for adipogenic differentiation [242]. One year later, Peng et al. published an interesting study, supporting Kilian's conclusions, where they provided further insights into the role of geometric cues in controlling stem cell switching into distinct cell phenotypes [294]. hMSCs differentiation was evaluated after one week of culture in osteogenic or adipogenic medium in response to circular, square, triangular and star micropattern of 900 μm². The highest levels of osteogenesis and adipogenesis were found in star- and circular-shaped cells, respectively. In addition, a linear

relationship of osteogenic and adipogenic differentiations with cell perimeter was established in these four conditions, showing enhanced osteogenesis and diminished adipogenesis as cell perimeter increases [294].

Another cell cue that has recently emerged as a potent regulator of stem cell fate is "cell anisotropy". Similarly to the cell size and shape, the manipulation of this cell feature has been made possible thanks to micropatterning techniques. Both Kilian et al. [242] and Peng et al. [294] investigated the effect of cell anisotropy on mediating MSCs osteogenesis by varying the aspect ratio (AR) of rectangular micropatterns. To facilitate reader's comprehension; AR = 1 corresponds to square shapes, AR = 2 and 4 correspond to rectangles with length/width = 2 and 4, respectively. At first sight, these two studies seem to provide conflicting results as Kilian et al. described a monotonic trend of osteogenesis with AR [242], while Peng et al. found a peak in osteogenesis at AR about 2 [294]. However, it should be noted that Kilian et al. tested the effect of only three pattern aspect ratios (AR 1, 1.5 and 4), while Peng et al. examined six aspect ratios (AR 1, 1.5, 2, 4, 8, and 16). In this case, if Peng et al. compare only the AR tested by Kilian et al.; i.e. AR 1, 1.5 and 4, a monotonic trend could be "found" as well. Therefore, the data from these two studies agree with each other quite well. Furthermore, Peng et al. tried to explain the significant increase of MSCs osteogenesis on micropatterns with AR 2. They measured the mean aspect ratio of free MSCs and osteoblasts cultured on tissue culture plates and found that MSCs exhibited a very heterogeneous AR, while osteoblasts displayed an average AR of 2.1 [294]. On this basis, they suggested that the shape of MSCs on micropatterns with AR 2 resembles to that of osteoblasts, which might be responsible for the significant increase of osteogenic differentiation.

As clearly indicated in the above studies, the effect of cell size, shape and anisotropy on promoting MSCs differentiation was assessed in the presence of induction media. From a critical perspective, the question that arises is whether or not the underlying cell cues maintain their stimulatory effect in the absence of soluble induction factors in the medium. Surprisingly, a very limited number of papers dealing with this issue can be found in the literature. This may due to the unsatisfactory outcomes regarding the biological relevance of these cues in growth medium. The first successful demonstration of the positive cell shape effect on MSCs differentiation in growth medium free of induction factors was reported by Yao et al. three years ago [301]. Rat MSCs were allowed to grow on micro-sized patterns with different AR (1, 2 and 8), but constant area (900 μm^2), for up to 21 days in basal growth medium. At one week, no effect of cell anisotropy was seen,

however a significant increase of MSCs osteogenesis was noticed after 13 and 21 days on all conditions, as compared to the day 7. As compared to AR 1 and 8, anisotropic cells on micropatterns with AR 2 exhibited higher osteogenesis, as revealed by a significant up-regulation of ALP activity [301]. These findings are consistent with those reported by Peng et al. [294] in osteoinduction conditions.

Although the chemical micropatterning seem to be a powerful strategy to control several MSCs features and consequently their lineage-specific differentiation, the complete mechanisms involved in the differentiation process remain to be determined. During the last decade, several groups tried to draft a rough pathway by which microscale geometric cues affect cell shape, cytoskeleton rearrangement, focal adhesion assembly and the subsequent stem cells commitment and differentiation.

The Chen group emphasized the importance of cell cytoskeleton tension in controlling stem cell fate and proclaimed that higher cell tension is beneficial for MSCs osteogenesis [241]. Obviously, they argued that the degree of cell spreading "cell shape", manipulated by chemically micropatterned surfaces, regulates cytoskeleton tension through RhoA/ROCK pathway, which in turn affects cell differentiation. As a short summary of the experimental approach undertaken by the authors to elucidate the underlying mechanism, they first demonstrated that well-spread cells -obtained on large micropatterns- led to high cytoskeleton contractility, while round cells -obtained on small micropatterns- led to low cytoskeleton contractility. Then, they highlighted the importance of actomyosin contractility in regulating MSCs osteogenesis, as revealed by MSCs switch from osteogenesis to adipogenesis when inhibiting myosin-generated cytoskeleton tension by adding Y-27632 drug in the medium. Given that Y-27632 inhibits Rho kinase (ROCK) pathway, they suggested that actomyosin contractility-mediated osteogenesis is ROCK dependent. They also found that RhoA (an upstream activator of ROCK) effectively affected actomyosin contractility-mediated osteogenesis. That is, osteogenesis was abrogated when well-spread cells were infected with dominant-negative RhoA (RhoA-N19), which is an inhibitor of RhoA. On the other hand, they demonstrated that cytoskeleton tension could in turn affect RhoA activity since well-spread cells drastically lost their osteogenic capacity when treated with actin disturbing agent (cytochalasin D) or myosin inhibitors (Y-27632, blebbistatin). Next, they determined that RhoA/ROCK activity was directly affected by cell spreading, since ROCK activity in well-spread cells was significantly greater than that in round cells. Finally, they demonstrated that RhoA is necessary, but not sufficient, to drive the switch in hMSCs commitment, as revealed by the inability of

round cells, infected with active RhoA-V14, to form osteoblasts and well-spread cells, infected with negative RhoA-N19, to form adipocytes. In contrast, ROCK appeared to play a more prominent role than RhoA, given that both round and well-spread hMSCs became osteoblasts when infected with ROCKΔ3 [241]. Therefore, through these remarkable findings, they provided a first insight into the mechanism by which cell shape and cytoskeleton contractility regulate MSCs osteogenesis. Recently, the Ding group supported the speculative signaling pathway drawn by the Chen group and confirmed this scenario even in growth medium [301].

Other mechanisms are thought to be involved in controlling cell shape-mediated cell differentiation, such as the activation of serum response factor (SRF) in response to changes in actin polymerization. For example, it has been reported that the polymerization of cytoplasmic G-actin promotes the release of myocardin-related transcription factor (MRTF), which is a SRF co-factor, and its accumulation in the nucleus. Subsequently, MRTF binds to SRF, thus promoting the transcription of SRF target genes involved in cell differentiation process [302]. In addition, preventing nuclear localization of MRTF, by increasing the amount of cytoplasmic G-actin, inhibits cell differentiation, while decreasing cytoplasmic G-actin concentration, promotes cell differentiation [303].

The Mrksich group has also proposed another molecular mechanism. They demonstrated that geometric cues mediate the differentiation of MSCs towards the osteoblastic lineage through MAPK and Wnt pathways [242].

Taken together, *in vitro* studies discussed here bear witness to the potential of microfabrication techniques in stem cell research. These studies and others have provided valuable insights into the role of the microscale distribution of ECM derived ligands in regulating both short- and long-term stem cell functions. Currently, micropatterning-based products are commercially available and mainly used as *in vitro* miniaturized high throughput platforms (polymer, protein and cell microarrays). Such high throughput systems permit a very rapid screening for the role of single ECM components or a combination of them, within the native stem cell microenvironment.

CYTOO, a French company, has pioneered the ability to reconstitute, *in vitro*, some *in vivo*-like conditions, through the development of finely-tuned micropatterned substrates that offer the unique advantage of evaluating structure/function relationship in a more physiological environment than the conventional tissue cultures plates. One of their principle products is the 96-well CYTOOplates, which consists of thousands of adhesive mi-

cropatterns arrayed on glass substrate, in each well (**Figure 18)**. Nevertheless, the chemical micropatterning is by far a popular approach in preclinical and clinical trials. One promising demonstration of the potential of this technology in reconstructing damaged and dysfunctional tissues has been recently reported by the Chen group [304] [305]. Although their studies are in their infancy, they successfully developed tissue-engineered scaffolds with micropatterned endothelial cell cords of different diameters (50, 150, 500 µm). The *in vivo* performance of the underlying constructs revealed a rapid microvessel network formation. Interestingly, the location and density of the neo-formed capillaries were modulated by the diameter of cords. These *in vivo* studies provide an important insight into the utility of micropatterning techniques to control vascular architecture and density, crucial for tissue oxygenation and function. However, much more research is needed until micropatterned biomaterials can be applied in human.

Given the potential of micropattering technology for reproducing and manipulating many ECM aspects *in vitro*, this approach will undoubtedly contribute towards a clear and deeper understanding of the mechanisms adopted by stem cells to control their fate choice.

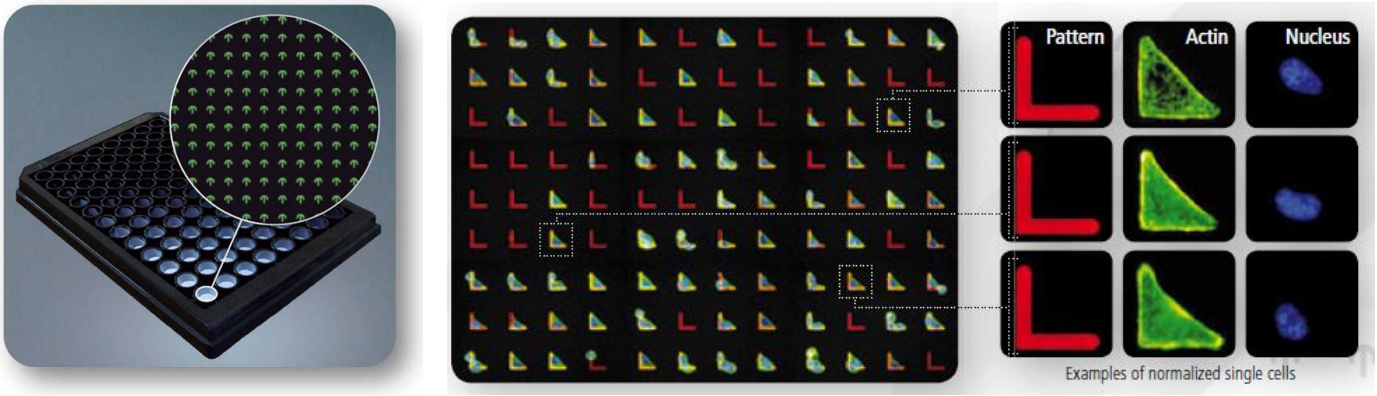

Figure 18: CYTOOplates™ for High Content Screening assays. Several micropattern shapes and sizes could be explored at once.

RESEARCH PROJECT & OBJECTIVES

As highlighted at the beginning of this thesis, there are several unsolved clinical needs in orthopaedic surgery, which are often related to the insufficient osseointegration of implanted biomaterials at the site of bone injury.

This thesis project objective was to reproduce on models materials some features innate to the native ECM, thought to mediate stem cells osteogenesis *in vivo*. These features were evaluated for their capacity to induce hMSCs osteogenic differentiation, independently or in combination. Specifically, we investigated the effect of BMP-2 peptide, RGD/BMP-2 peptide crosstalk, and the microscale distribution of RGD and/or BMP-2 peptides on hMSCs fate decision. Such fundamental studies are believed to provide valuable insights into biomaterials design, which may pave the way towards the development of custom-made orthopaedic biomaterials. The literature review provided above clearly states the considerable efforts dictated to improve the osteogenic potential of orthopaedic biomaterials. While tremendous strategies have been explored in biomaterials and stem cell research to tune ECM/stem cell interactions, the smart biomaterial that perfectly mimics the osteoinductive *in vivo* microenvironment is unfortunately a long way from being clinically available. The reason for this relies on the extreme structural and functional complexity of the native ECM that generates a multitude of stem cell regulatory signals, which are strongly interconnected. Consequently, the *in vitro* translation of signals mediating hMSCs osteogenesis is unsurprisingly a great challenge. Therefore, towards the development of finely-tuned biomaterials, it seems important to start by selecting the adequate tools that enable recapitulating essential ECM features (physical and biochemical cues) on model materials and evaluating their biological relevance, independently. This step of screening for both individual and combinatorial effects of various ECM features, along with sophisticated analysis methods (super-resolution microscopy), will significantly contribute to deeply understand the mechanisms governing MSCs lineage specification, and thereby facilitating the reconstruction of instructive artificial ECM. As a comparison, tissue culture dishes have been used for long time and until now to investigate cellular behaviors and signaling pathways in healthy and diseased tissues. However, such *in vitro* models fail to reproduce many aspects of living tissues, such as the hierarchical structure, cell-cell interactions and elasticity, which make the *in vitro* to *in vivo* extrapolation quite difficult and unreliable. A powerful tool that offers the unique opportunity to evaluate, in a more physiologically relevant condition, how cells recognize and respond to their microenvironment is the micropatterning technology. For example, cardiomyocytes isolated from a healthy human heart exhibit an elongated morphology with highly

ordered and aligned myofibers, while those isolated from the heart of a patient in heart failure are more elongated and less narrow. As depicted in **Figure 9**, cardiomyocytes seeded on conventional cell culture models lack their natural morphology, however the morphology of both healthy and diseased cells can be precisely reproduced using micro-patterned substrates.

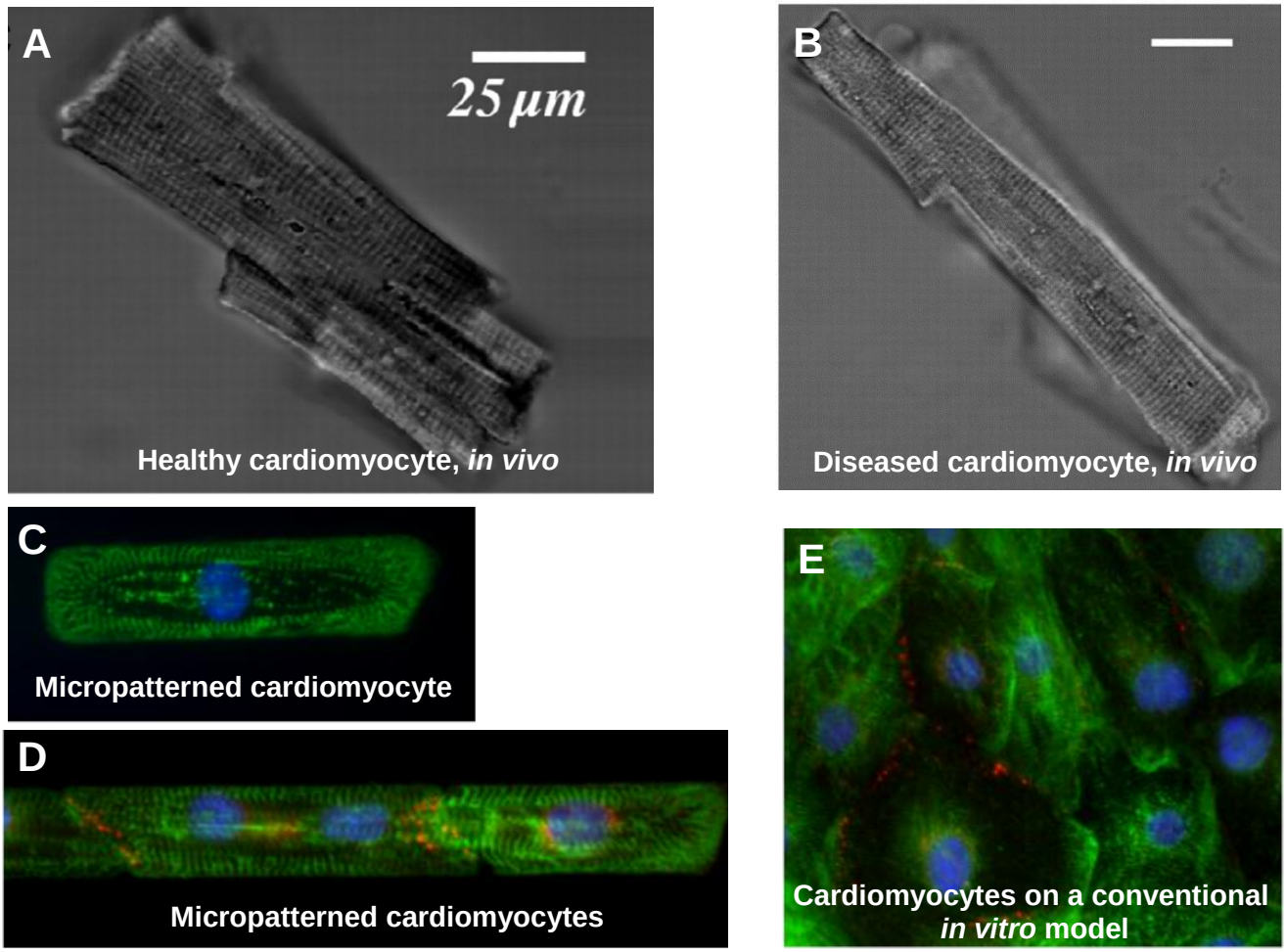

Figure 19: The potential of micropatterning techniques in reconstituting the *in vivo* situation. (A-B) [306] , (C-E) [307].

By taking advantage of the potential of micropatterning strategy for creating well-defined microenvironments, while applying this tool in an innovative way, we investigated for the first time the role of micro-scale spatially distributed and combined ECM ligands in regulating hMSCs differentiation into osteoblasts, following several steps.

Initially, glass surfaces were homogenously functionalized with cell adhesive RGD and/or osteoinductive BMP-2 peptides. These conditions were used to investigate the effect of each peptide as well as their crosstalk on hMSCs osteogenic differentiation (Paper I).

Then, RGD and BMP-2 peptides were solely structured onto glass substrates, so that they form well- ordered micropatterns of different shapes (triangular, square and square geometries), but constant surface area (50 µm² per micropattern). We reported here the role of the microscale distribution of ligands, which somewhat mimic the organization of ECM components *in vivo*, in regulating hMSCs osteogenesis (Paper II).

At last, RGD and BMP-2 were simultaneously micropatterned onto glass materials. The objective of this third study was to investigate hMSCs osteogenesis differentiation in response to the interplay between RGD/BMMP-2 crosstalk and microscale geometric cues (Paper III).

RESULTS & DISCUSSION

I. Study 1: RGD/ BMP-2 mimetic peptides act synergistically to enhance hMSCs osteogenic differentiation.

RGD and BMP-2 mimetic peptide crosstalk enhances osteogenic commitment of human bone marrow stem cells

I. Bilem[abc], P. Chevallier[ab], L. Plawinski[c], E.D. Sone[d], M.C. Durrieu[c*], G. Laroche[ab*]

[a]Laboratoire d'Ingénierie de Surface, Centre de Recherche sur les Matériaux Avancés, Département de Génie des Mines, de la Métallurgie et des Matériaux, Université Laval, 1065 Avenue de la médecine, Québec G1V 0A6, Canada
[b]Centre de Recherche du Centre Hospitalier Universitaire de Québec, Hôpital St-François d'Assise, 10 rue de l'Espinay, Québec G1L 3L5, Canada
[c]Institute of Chemistry & Biology of Membranes & Nanoobjects (CNRS, UMR5248 CBMN), Université de Bordeaux, Bordeaux INP, France
[d]Institute of Biomaterials and Biomedical Engineering, Department of Materials Science and Engineering, and Faculty of Dentistry, University of Toronto, Toronto, ON M5S 3G9, Canada

I. Bilem: Ibrahim.bilem.1@ulaval.ca
P. Chevallier : Pascale.Chevallier@crchudequebec.ulaval.ca
L. Plawinski : l.plawinski@cbmn.u-bordeaux.fr
E.D. Sone: eli.sone@utoronto.ca
M.C. Durrieu: marie-christine.durrieu@inserm.fr

*Corresponding authors (equally contributed):
Email address: Gaetan.Laroche@gmn.ulaval.ca Phone: 1 (418) 656-7983 Fax: (418) 656-5343;
marie-christine.durrieu@inserm.fr Phone: 011 33 5 40 00 30 37 Fax: 011 33 5 40 00 30 68

Key words: Stem cells, biomimetic materials, bone tissue engineering, mimetic peptides, surface modification.

This work has been published in the journal: ***Acta Biomaterialia***

Résumé :

L'engagement des cellules souches mésenchymateuses (CSMs) vers une voie de différenciation est contrôlé par les molécules bioactives séquestrées au sein de leur matrice extracellulaire (MEC). Une des approches fréquemment utilisées pour mimer l'environnement physiologique des cellules souches consiste à fonctionnaliser la surface des biomatériaux avec des séquences peptidiques dérivées de la MEC naturelle, afin de favoriser le recrutement et la différenciation des cellules souches présentes à proximité du biomatériau. L'objectif de cette étude est d'examiner l'engagement des CSMs humaines vers la voie ostéoblastique en réponse à l'effet synergétique de plusieurs molécules bioactives. Les ligands d'intérêt sont le peptide RGD, facilitant l'adhérence cellulaire par l'intermédiaire des récepteurs intégrines transmembranaires, et le peptide BMP-2, correspondant aux acides aminés 73-92 de Bone Morphogenetic Protein-2, connu par son potentiel d'induction de la différenciation des CSMs en ostéoblastes. Le greffage des peptides sur la surface des matériaux a été évalué par Spectroscopie photoélectronique par rayons X (XPS), la densité peptidique a été quantifiée par microscopie à fluorescence et la rugosité de la surface a été évaluée par Microscopie à Force Atomique (AFM). L'engagement des CSMs vers le lignage ostéoblastique sur les différentes surfaces (RGD, BMP-2, RGD/BMP-2) a été déterminé par immunohistochimie, en utilisant STRO-1 comme marqueur spécifique de l'état souche des CSMs et Runx-2 comme marqueur ostéogénique précoce. Les analyses quantitatives des marqueurs cellulaires, effectuées après 4 semaines de culture dans un milieu basal, ont révélé une très faible expression de STRO-1, marquer souche, sur les surfaces greffées BMP-2 ou RGD/BMP-2 et une forte expression sur les matériaux greffé RGD. Concernant l'expression de Runx-2, marqueur ostéogénique, des taux significativement plus élevés ont été constatés sur les surfaces RGD/BMP-2, comparativement aux surfaces contenant que le peptide BMP-2. Tandis que sur les surfaces greffées RGD ont conduit à une très faible expression de Runx-2. Ces résultats ont confirmé que les peptides RGD et BMP-2 agissent d'une manière synergétique pour induire et améliorer l'engagement des CSMs vers la voie ostéoblastique. Ce type de travaux contribue fortement au développement des biomatériaux biomimétiques, permettant une profonde compréhension des mécanismes de signalisation responsables de la transition des cellules souches en ostéoblastes matures.

Abstract

Human bone marrow mesenchymal stem cells (hBMSCs) commitment and differentiation are dictated by bioactive molecules sequestered within their Extra Cellular Matrix (ECM). One common approach to mimic the physiological environment is to functionalize biomaterial surfaces with ECM-derived peptides able to recruit stem cells and trigger their linage-specific differentiation. The objective of this work was to investigate the effect of RGD and BMP-2 ligands crosstalk and density on the extent of hBMSCs osteogenic commitment, without recourse to differentiation medium. RGD peptide promotes cell adhesion via cell transmembrane integrin receptors, while BMP-2 peptide, corresponding to residues 73-92 of Bone Morphogenetic Protein-2, was shown to induce hBMSCs osteoblast differentiation. The immobilization of peptides on aminated glass was ascertained by X-ray Photoelectron Spectroscopy (XPS), the density of grafted peptides was quantified by fluorescence microscopy and the surface roughness was evaluated using Atomic Force Microscopy (AFM). The osteogenic commitment of hBMSCs cultured on RGD and/or BMP-2 surfaces was characterized by immunohistochemistry using STRO-1 as specific stem cells marker and Runx-2 as an earlier osteogenic marker. Biological results showed that the osteogenic commitment of hBMSCs was enhanced on bifunctionalized surfaces as compared to surfaces containing BMP-2, while on RGD surfaces cells mainly preserved their stemness character. These results demonstrated that RGD and BMP-2 mimetic peptides act synergistically to enhance hBMSCs osteogenesis without supplementing the media with osteogenic factors. These findings contribute to the development of biomimetic materials, allowing a deeper understanding of signaling pathways that govern the transition of stem cells towards the osteoblastic lineage.

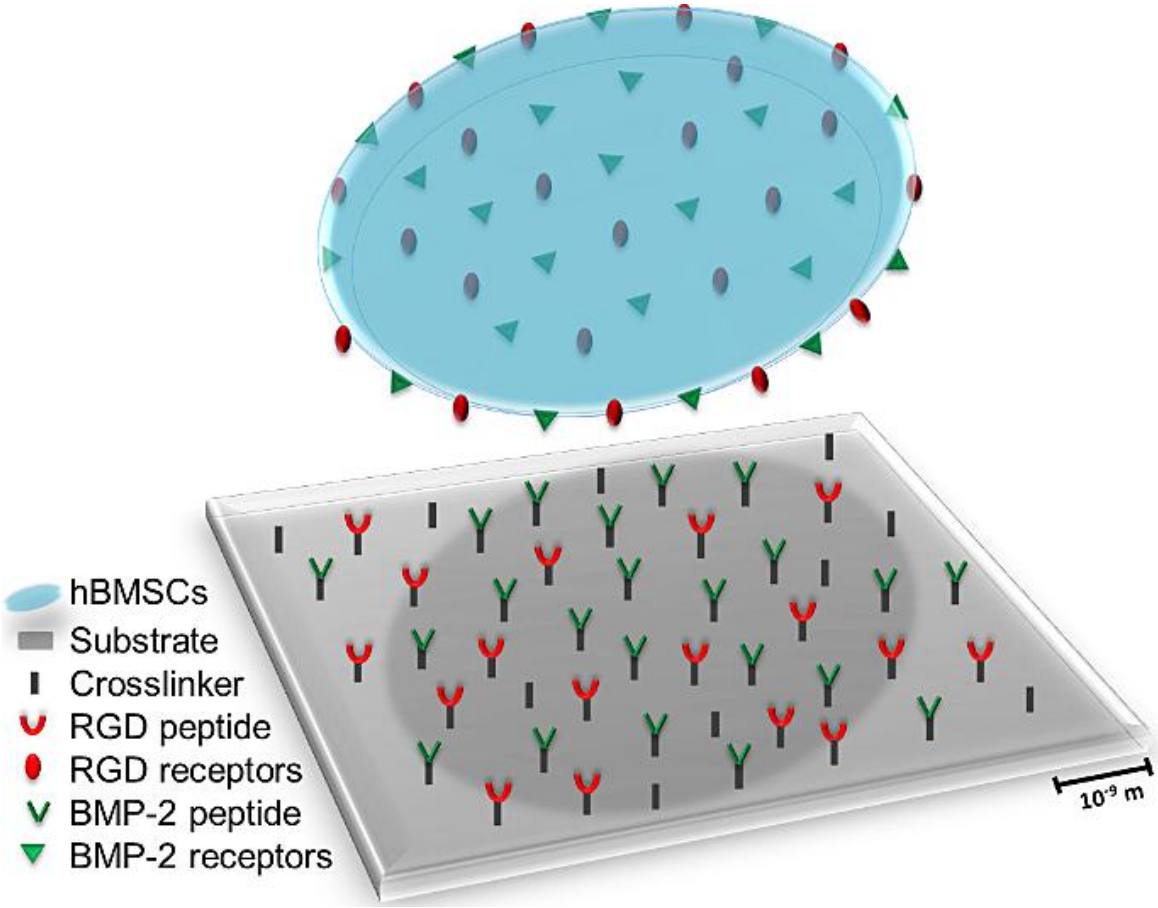

Graphical abstract

1. Introduction

Mesenchymal Stem Cells (MSCs) are considered as a promising cell source for musculoskeletal regeneration due to their high osteogenic differentiation potential when stimulated with growth factors and specific signaling molecules [9] [91]. The first stem cell-based therapies involved the injection of cells directly into bone defect sites. Unfortunately, this approach had limited success due to the high death rate of the cells and their poor engraftment into host tissues [308]. Therefore, much effort has been dedicated to design biomaterials capable of recruiting stem cells, interact with them and drive their fate in a controlled manner towards the osteoblastic lineage.

Up to now, a large panel of natural and synthetic materials has been investigated for bone tissue engineering applications [309] [310] [311]. However, no single material fulfills all the criteria of biocompatibility. For example, natural materials have an acceptable level of cytocompatibility but exhibit poor mechanical properties compared to cortical bone [312]. Synthetic materials are more available and their mechanical properties, degradation rate, shape, and composition, etc. can be tailored [313] [314]. For example, synthetic hydrogels are usually used to mimic pre-calcified bone tissue of approximately 25-40 kPa of stiffness [236]. Nevertheless, most of synthetic materials are intended to be bioinert and lack regulatory signals required to control cell-biomaterial interactions [312].To increase materials bioactivity, several recent works have attempted to create a biomimetic microenvironment on conventional synthetic materials by chemically conjugating bioactive ligands or short peptide sequences derived from the Extra Cellular Matrix (ECM) proteins [315].

During the last decades, biomimetic peptides have gained much more notoriety than full-length native matrix proteins due to their straightforward synthesis, high purity, minimal cost and tight control of their conformation and density when grafted onto biomaterials [316]. In fact, several classes of peptides, mimicking properties of the native ECM components, have been designed, synthesized and exploited for their potential to induce desired cell response [317] [318] [319] [320] [321] [322]. This has, of course, led to develop strategies for functional peptide sequences conjugation to biomaterials [317] [321] [322] [323]. In this work, we propose to develop biomaterials functionalized by one or several biomimetic peptides and subsequently to investigate their effect on hBMSCs osteogenic differentiation. One of the most commonly used peptides to functionalize biomaterials are cell adhesion peptides containing the arginine-glycine-aspartic acid (RGD) sequence,

which is present in several proteins such as collagen I, fibronectin, bone sialoprotein and osteopontin [324] [325] [326]. It was shown in several instances that RGD peptide grafted materials interact with integrin cell surface receptors and enhance adhesion of bone marrow stem cells [325] [186]. Moreover, several studies have demonstrated that this peptide is a mild promoter of osteogenic differentiation *in vitro* [327] [328] and can stimulate bone formation *in vivo* [188].

Beside integrin ligands, growth factors have also been used to improve materials bioactivity due to their ability to stimulate stem cells expansion and differentiation towards a specific lineage [329] [330]. For example, Bone Morphogenetic Proteins (BMPs), belonging to the Transforming Growth Factor beta family ((TGF-β), promote the differentiation of mesenchymal stem cells into mineral-depositing osteoblasts [331], via different signaling pathways [332]. Indeed, BMPs interact with their cell surface receptors through non-covalent bonds [333], leading to the phosphorylation of Smad 1, Smad 5, and Smad 8 signaling pathways. Phosphorylated Smads associate with Smad 4, leading to the translocation of this complex from cytoplasm into nucleus [334], which leads to the transcription of genes mediating cell differentiation such as Runx2 and Osterix [178] [335]. These growth factors can also trigger the activation of the Mitogen-Activated Protein Kinase (MAPK) pathway which plays a critical role in cell commitment and differentiation into osteoblastic lineage [336] [337]. Another pathway that influences osteogenic differentiation mediated by BMPs proteins is the Wnt canonical pathway [338] [339]. The activation of this pathway through the binding of Wnt ligands to their Frizzled receptors and LRP5/LRP6 coreceptors stabilizes β-catenin and causes its translocation to the nucleus [340]. This leads to the activation of specific genes like c-Jun that, in turn, influences the early osteoblast differentiation [341].

Among 20 BMPs identified to date, BMP-2 is considered as the most potent one in terms of inducing osteogenesis, hence its widespread use in the clinic for bone therapy [342] [342]. For instance, the USA Food and Drug Administration (FDA) approved recombinant human BMP-2 delivered in a collagen scaffold, called Infuse Bone Graft ®, as a bone tissue engineering product for spinal fusion surgery [104]. Due to the high cost of BMP-2 and satisfactory clinical outcomes reported using this protein, several peptide sequences derived from the knuckle epitope of BMP-2 protein have been identified, synthesized and used both *in vitro* and *in vivo* [187] [206] [171]. It was shown that these BMP-2 peptides also bind to BMP receptors I and II, thus activating specific signaling pathways similarly

to the full-length BMP-2 protein [206]. Further studies demonstrated that materials functionalized with BMP-2 peptides induced osteoblastic differentiation of mesenchymal stem cells *in vitro* and bone regeneration *in vivo* [179]. In addition, several literature works have shown that integrins and BMP-2 proteins/peptides cooperate synergistically to up-regulate osteogenic differentiation [187] [227] [343] [211] [225]. However, most of studies investigated this synergistic effect on committed pre-osteoblasts or in the presence of osteogenic supplements in the medium. For example, we previously determined that the concomitant immobilization of RGD and BMP-2 mimetic peptides on polyethylene terephthalate (PET) surfaces elicit a synergistic effect that positively affects the osteogenic differentiation and mineralization of mouse calvaria-derived pre-osteoblastic cells [187]. Although such animal models are widely used in basic and applied research, cells from mice are likely to behave differently than human cells. Hence the current study objectives to investigate RGD and BMP-2 ligands crosstalk in more physiologically relevant conditions. In fact, we used more primitive cells, hBMSCs, which are likely to differentiate into pre-osteoblastic cells and more mature bone cells. These cells were harvested from patient's iliac crest and cultured in basal medium free of soluble osteogenic factors. Moreover, to facilitate the interactions of grafted ligands and their cell receptors, hBMSCs were plated and maintained on the different materials in serum-free medium for the first 6 h since we can imagine that serum proteins may adsorb on modified surfaces and mask specific cell/material interactions. In this work, three categories of materials chemically modified were synthesized: glass material surfaces grafted with RGD or BMP-2 peptides and bifunctionalized surfaces with both peptides. Both mimetic peptides used in this work have been reported as potent effectors of cell adhesion [326] and differentiation [187]. The surface physicochemical characterization after each step of peptide grafting was achieved by XPS and AFM while the peptide surface density was quantified using fluoro-tagged peptides. The osteogenic differentiation of hBMSCs was then characterized after four weeks of cell culture by fluorescent staining of two specific markers, STRO-1, the best known mesenchymal stem cells marker and Runx-2 which is an earlier osteogenic marker. The expression level of STRO-1 and Runx2 were evaluated by quantifying the average fluorescence intensity of each marker in hBMSCs on different peptide modified surfaces. This study contributes to the development of biomimetic microenvironment on material surfaces as tool to better understand signaling pathways that govern

the switch of stem cells from their stemness state into differentiated state. This fundamental understanding seems to be essential to improve biomimetic materials, thereby, promoting desired cell response.

2. Materials and methods

2.1 Materials

Borosilicate glass was chosen as a model material because of its transparency, allowing its use for microscopy experiments. Borosilicate glass slides (76 x 26 mm, thickness ≈ 1 mm) were obtained from Schott (Tempe, AZ, USA). These slides were then laser-cut into 10x10 mm pieces to fit in 24 well cell culture plates. H_2O_2 (33 wt %), concentrated H_2SO_4, acetone, ethanol, anhydrous toluene, dimethylsulfoxyde (DMSO), 3-aminopropyltrieth-oxysilane (APTES) and succinimidyl-4-(p-maleimidophenyl) butyrate (SMPB) were all purchased from Sigma-Aldrich, France. The fluorophore-tagged CG-K(PEG3-TAMRA)-GGRGDS adhesion peptide (referred to as RGD-TAMRA; MW 1437 g/mol) was synthesized by Anaspec (Fremont, CA, USA). CKIPKASSVPTELSAISMLYL and fluorophore-tagged CKIPKASSVPTELSAISMLYLK-FITC peptides (referred to as BMP-2 mimetic peptide; MW 2251.75 g/mol and BMP-2-FITC mimetic peptide; MW 2769 g/mol, respectively) were produced by Genecust, Belgium. These peptides were first dissolved at 2 mM in DMSO and stored at -20 °C until use. Peptides, to be conjugated with material surface, were resuspended at 20 µM in a 0.2 µm-filtered Phosphate-Buffered Saline (PBS, Life Technologies, France) solution containing 7.5 % glycerol.

2.2 Methods

2.2.1 Surface conjugation with mimetic peptides

Prior to surface conjugation, borosilicate glass slides were washed with deionized water (DI H_2O), and ultrasonically cleaned in successive baths containing ethanol (30 min), acetone (30 min), ethanol (10 min), and finally acetone (2 min). Glass slides were then activated by a further cleaning in a piranha solution (mixture of 3 mL of H_2O_2 (33% wt) and 7 mL of concentrated H_2SO_4) for 15 min in an ultrasonic bath. Samples were then successively ultrasonically cleaned three times in water for 10 min and in acetone for 2 min. Piranha treatment not only activates glass substrates by providing hydroxyl groups on their surfaces but also reduces the percentage of carbon contamination; so this cleaning

step is essential for the subsequent grafting of aminosilane molecules [344]. Cleaned surfaces were immediately functionalized with aminoalkylsilane molecules according to the protocol of Moon et al. with some slight modifications [345] **(Figure 20)**. Briefly, samples were immersed in a 34.5 mM (1 % v/v) solution of APTES dissolved in anhydrous toluene for 3 h. The reaction was performed under agitation and under inert atmosphere of Argon (Ar). After silanization, a slight wash with anhydrous toluene of glass materials was performed to remove any excess of APTES, followed by three washes of 2 min in an ultrasonic bath. Subsequently, the substrates were outgassed at 120 °C under vacuum (3. 10^{-4} Torr) for 30 min. Aminated glass surfaces were then conjugated with the heterobifunctional SMPB crosslinker **(Figure 20)**. The succinimidyl function of this molecule reacts with the surface amine groups, therefore leaving a maleimidyl group which further reacts with thiol groups from terminal cysteine of both peptides. Briefly, aminated glass surfaces were immersed in a 3 mg/mL solution of SMPB dissolved in DMSO for 2 h away from light. The substrates were then rinsed in DMSO for 10 min in ultrasonic bath. Once washed, the substrates were air-dried and stored in the dark for 24 h prior to peptide grafting to avoid SMPB degradation. Finally, immobilization of mimetic peptides was achieved by covering SMPB grafted surfaces of 1x1 cm^2 with 200 µL of 20 µM solution of RGD-TAMRA, BMP-2-FITC or a mixture of both peptides at a 1:1 ratio in humidified and dark chamber **(Figure 20)**. After grafting, slides were ultrasonically cleaned three times for 15 min in DMSO, and then thoroughly washed in DI H_2O to remove DMSO solvent. The substrates were stored for at most 1 month in PBS until use. All reactions were performed with ≈ 50 rpm agitation, at room temperature.

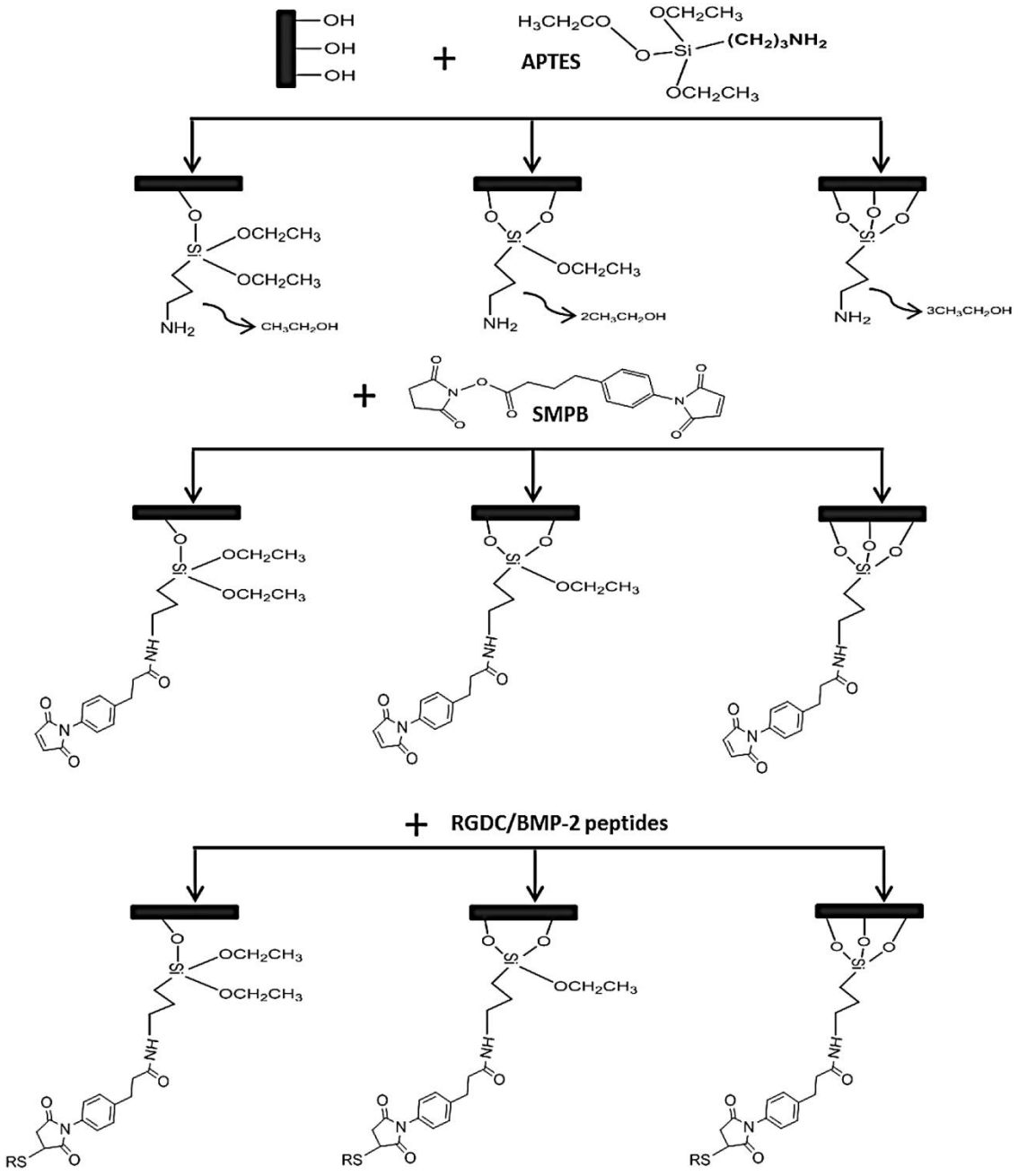

Figure 20: Schematic of the different steps involved in the grafting of each peptide alone or in combination.

2.2.2 Surface characterization

The surface chemical composition was investigated after each step of covalent peptide grafting by XPS using a PHI 5600-ci spectrometer (Physical Electronics, Eden Prairie, MN, U.S.A). The survey spectra were recorded using a standard aluminum X-ray source (1486.6 eV) at 300 W with charge neutralization. High resolution C1s XPS spectra were recorded using a standard magnesium X-ray source (1253.6 eV) at 150 W without charge neutralization and then curve-fitted by referencing each spectrum to carbon at 285 eV. The size of the analytical X-ray spot was about 0.5 mm^2. To ascertain the reproducibility of the surface chemistry, three measurements *per* sample were carried out.

The amine surface density (NH_2) was ascertained on the aminoalkysilane-modified surfaces by vapor-phase chemical derivatization using 4-chlorobenzaldehyde according to Chevallier et al. [346]. Briefly, the substrates were introduced in a sealed glass tube containing the reagent covered with 1 cm thick bed of soda-line to prevent the direct contact between the substrate surface and the reagent. After 2h of reaction at 40 °C, the surfaces were vacuum-dried overnight at 40 °C and analyzed by XPS.

To quantify covalently grafted peptides, glass surfaces were functionalized with RGD-TAMRA, BMP-2-FITC or RGD-TAMRA+BMP-2-FITC mimetic peptides according to the previously described protocol. These surfaces were observed using fluorescence microscopy (Leica DM5500B, Germany) at magnification of 2.5. In parallel, a series of droplets of RGD-TAMRA and BMP-2-FITC mimetic peptides with well-known concentrations (from 5 nM to 10 µM) were deposited on bare glass surfaces. These peptides droplets were then imaged at the same magnification and exposure time and a standard curve was constructed for each peptide. Finally, the fluorescence intensity on different peptide modified surfaces was quantified by Leica MMAF software and the peptide density was evaluated according to the standard curve in pmol/mm^2.

The surface roughness and morphology were evaluated on 20x20 μm^2 scanned areas using tapping mode AFM (line scan rate = 1 Hz). Three measurements *per* sample were carried out at room temperature in clean room with a Dimension 3100 Atomic Force Microscope (Veeco, Santa-Barbara, CA, USA) using etched silicon tips (OTESPA, tip radius of curvature < 10 nm, aspect ratio ≈ 1.6/1). The surface roughness was calculated by the root mean square (R_{rms}) parameter using Nanoscope software.

2.2.3 Cell culture

Commercially available hBMSCs (Lonza, France) were grown on gelatin coated culture flasks in MSCs growth medium (MSCGM) (Lonza, France), subcultures using trypsin/EDTA 1x (Sigma-aldrich, France) and maintained in a humidified atmosphere containing 5 % CO_2 at 37 °C. Modified glass substrate of 1x1 cm^2 were sterilized with 70 % ethanol and rinsed by PBS, then placed in cell culture plates 24 well. To induce osteogenic differentiation, hBMSCs at passage 4 were seeded on different peptides grafted surfaces at a density of 10^4 cells/cm^2 for 6 h in serum free α-MEM medium (Life technology, France). This allows the interactions between grafted peptides and their cell surface receptors without hassle of serum proteins. Serum-free medium was then removed and replaced with α-MEM medium containing 10 % fetal bovine serum (FBS) and 1 % penicillin/streptomycin. The culture media was changed twice *per* week during four weeks of cell culture.

2.2.4 Immunocytochemical analysis

At four weeks of cell culture, hBMSCs were rinsed in PBS, and fixed in 4 % paraformaldehyde at 4 °C for 20 min. Samples were then permeabilized with 0.5 % Triton X-100 in PBS for 15 min and blocked with 1 % Bovine Serum Albumin (BSA) in PBS for 30 min at 37 °C. Next, samples were incubated with 10 µg/mL of primary antibodies mouse monoclonal anti-STRO-1 (R&D Systems, France) and mouse monoclonal anti-Runx-2 (abcam, UK) in 1 % BSA in PBS overnight at 4 °C. After washing in PBS containing 0.05 % Tween 20, samples were incubated with the secondary antibody Alexa Fluor 647 goat anti-mouse IgG (H+L) (1:400 dilution) for 1 h at 37 °C. To visualize cell cytoskeletal filamentous actin (F-actin), cells were incubated with Alexa Fluor 488 phalloidin on RGD-TAMRA and RGD-TAMRA/BMP-2 surfaces or Alexa Fluor 568 phalloidin on BMP-2-FITC surfaces (Invitrogen, France) (1:400 dilution) for 1 h at 37 °C. The substrates were then rinsed three times with PBS containing 0.05 % Tween 20, and counterstained and mounted on glass microscope slides with a ProLong Gold antifade reagent with DAPI (Sigma, France). Finally, surfaces were examined using a Leica microsystem DM5500B, microscope with a motorized and programmable stage, and a CoolSnap HQ camera controlled by Metamorph 7.6. Quantitative analyses of the expression levels of STRO-1 and Runx-2 were performed using Image J freeware (NIH, http://rsb.info.nih.gov/ij/), using a slightly modified version of the Jensen's protocol

[347]. Briefly, all images of stained markers were acquired at the same exposure time, using a 40X objective. Image files were opened with Image J and converted to 16-bit files. These fluorescence images were then used to determine the intensity of the red color emitted by the label from which was subtracted the background signal measured on hBM-SCs cultures on glass surfaces and only incubated with the secondary antibody Alexa Fluor 647. Fluorescence intensity measurements were performed on at least 60 cells *per* each type of surface.

2.2.5 Statistical analysis

Data are expressed as mean values ± standard deviation (SD). Statistical analysis was performed by one-way analysis of variance (ANOVA) and Tukey's test for multiple comparisons, using GraphPad Prism version 6.07 for Windows, (GraphPad software, San Diego California USA, www.graphpad.com). Differences were considered statistically significant for P value of at least < 0.01.

3. Results and discussion

3.1 Characterization of the biochemical modification of glass surfaces

3.1.1 XPS analyses

The grafting of peptides on glass substrates was confirmed by XPS after the different steps of surface modification. XPS survey analyses are given in **Table 2** while high resolution C1s XPS spectra are shown in **Figure 21**. At first sight, piranha-treated glass surfaces exhibited the expected silicon (Si: 23.7 ± 0.3 %) and oxygen (O: 65 ± 2 %) elements with a slight carbon contamination of 10 ± 4 % **(Table 2)**, which remains acceptable compared to the carbon surface pollution reported in previous works [52, 56]. High resolution C1s spectra allowed detailed chemical characterization of this carbon pollution. Indeed, it mainly consists of CH/ C-C/ C=C bonds at 285 eV and a mixture of oxidized carbonaceous species as evidenced by the presence of contributions at 287 eV assigned to C-O/C=O moieties **(Figure 21)**.

On aminosilane grafted surfaces, XPS survey spectra showed a substantial increase of carbon compounds (19 ± 2 %), a slight decrease of oxygen (54 ± 1 %) and silicon (22 ± 1 %) as well as the appearance of nitrogen (1.4 ± 0.4 %) **(Table 2)** which can be assigned to the formation of an aminosilane monolayer on the surface. However, the experimental N/C ratio of 0.08 ± 0.01 was quite lower than the theoretical one which is around 0.14 -

0.33 depending on the number of ethoxy groups that are eliminated upon functionalization with APTES **(Figure 20)**. The amount of primary amine moieties available on aminated glass surfaces was evaluated by chemical derivatization reaction, and calculated based on the relative percentage of chlorine atoms detected in XPS. The percentage of amino groups was estimated at 0.9 ± 0.4 %, meaning that ~ 64 % of nitrogen atoms available onto glass surfaces are primary amine functions.

These amino groups allowed the subsequent grafting of SMPB linking arms, to provide terminal maleimide groups for peptide grafting, thereafter raising the carbon and nitrogen amounts from 19 ± 2 % and 1.4 ± 0.4 % to 25 ± 1 % and 2.2 ± 0.6 %, respectively **(Table 2)**. However, the oxygen amount did not significantly increase in spite of the presence of 3 oxygen atoms on the crosslinker chain. This may due to the relative percentage of oxygen which was already high on aminated glass substrates. Indeed, these variations observed in the surface chemical composition after SMPB grating match well with its structure, composed of C, N and O atoms. Interestingly, the experimental N/C ratio of reacted SMPB, estimated at 0.09, was close to that expected (0.1-0.12) **(Figure 20)**, which confirmed that the increase of N/Si ratio is due to the coverage of Si substrates with a layer of SMPB crosslinker **(Table 2)**. XPS high resolution of C1s also evidenced the grafting of SMPB linking arm, as revealed by the appearance of a new peak at 288.2 eV **(Figure 21)**. This peak corresponds to the imide (O=C-N-C=O) and amide (NH-C=O) groups present on grafted SMPB crosslinker.

Finally, fluorescent RGD and BMP-2 mimetic peptides were covalently attached through their $N_{terminal}$ cysteine amino-acid on SMPB modified surfaces. On the one hand, XPS survey spectra mainly showed significant increase in nitrogen amount and decrease in silicon percentage from 2.2 ± 0.6 % and 21 ± 1 % on SMPB treated surfaces to 5.9 ± 0.3 % and 15.2 ± 0.5% on BMP-2-FITC grafted surfaces, respectively. Moreover, higher N/C and N/Si ratios were noticed after BMP-2-FITC peptide grafting compared to SMPB grafted surfaces **Table 2**. The experimental N/C ratio of 0.15 ± 0.01 was close to the theoretical one (~ 0.19), thus confirming the presence of BMP-2-FITC peptide onto the surface. These observations were further supported through C1s high resolution analyses since the grafting of BMP-2-FITC peptide led to a greater contribution of the peak at 288.2 eV. Indeed, the percentage of amide groups, characteristic of peptide bonds, increased from 1.9 % on SMPB modified surfaces to 6.5 % on BMP-2-FITC surfaces **(Figure 21)**.

On the other hand, the grafting of RGD-TAMRA peptide was difficult to assess by XPS survey analyses due to the slight variations in the surface chemical composition before and after RGD-TAMRA grafting. For instance, N/C and N/Si ratios slightly increased from 0.09 ± 0.02 and 0.10 ± 0.03 on SMPB treated surfaces to 0.12 ± 0.02 and 0.14 ± 0.03 on RGD-TAMRA surfaces, respectively **(Table 2)**. However, high resolved C1s spectra clearly evidenced the peptide grafting, as demonstrated by a significant increase of NH-C=O bonds from 1.9 % to 3.3 % on peptide modified surfaces **(Figure 21)**. Compared to RGD-TAMRA surfaces, it is reasonable that the grafting of BMP-2-FITC peptide elicited more important changes in the surface chemical composition, since BMP-2 peptide sequence contains many more amino-acids than RGD sequence.

From XPS results, it could be concluded that glass materials were effectively functionalized with a thin and homogenous aminosilane layer, leading to a surface concentration of primary amines intended to be sufficient to conjugate biological molecules such as peptides, proteins or growth factors [326] [348]. On SMPB treated surfaces, XPS analyses clearly showed that the variation in the atomic surface composition closely matches with the chemical structure of the SMPB crosslinker, thus evidencing its immobilization on aminated glass substrates. Finally, the grafting of peptides elicited changes in the surface chemical composition as revealed by a significant increase of amide bonds after peptide grafting with higher amount on BMP-2-FITC surfaces than RGD-TAMRA surfaces. Therefore, it seems reasonable to postulate that the conjugation of RGD-TAMRA and BMP-2-FITC mimetic peptides with glass material was successfully achieved.

3.1.2 Atomic Force Microscopy

The surface topography and roughness obtained by tapping mode AFM after each step of surface modification are shown in **Figure 22** and **Table 3**. The surface functionalization with SMPB did not lead to an important surface roughness change with respect to aminosilane and piranha treated glass surfaces [344] [349]. Indeed, statistical analyses of the data showed no significant increase in surface roughness during these three steps of surface modification; i.e. from piranha to SMPB treated surfaces. In contrast, after peptide grafting, significant change in the surface topography was noticed, leading to an increase in surface roughness from 1.3 ± 0.3 nm on SMPB surfaces to 2.2 ± 0.2 nm and 2.5 ± 0.4 nm after RGD-TAMRA and BMP-2-FITC mimetic peptides grafting, respectively. This could be due to the fact that the sequences of grafted peptides are much longer than APTES or SMPB chains. Even though the surface roughness significantly increased after

peptide grafting, it remains relatively low, thus confirming that peptides were homogeneously grafted without the formation of aggregates on the surface. On the other hand, there was no significant difference in surface roughness between the different peptide modified surfaces, therefore ruling out the possibility that cells behave differently due to surface topography features [252] [350] [351] .

3.1.3 Peptide surface density

Peptide densities were evaluated by fluorescence microscopy on glass materials solely or dually functionalized with fluorescent peptides. On substrates containing only one peptide, the total peptide surface density was estimated to 1.8 ± 0.2 pmol/mm² and 2.2 ± 0.3 pmol/mm² on RGD-TAMRA and BMP-2-FITC surfaces, respectively **(Figure 23)**. The measured peptide densities were in agreement with those reported in some previous works. For example, Chollet et al. [352] estimated the RGD peptide density at 1.7 pmol/mm² on polyethylene terephthalate (PET) surfaces, while Boivin et al. [353] showed that the density of RGD peptides on polytetrafluoroehylene (PTFE) was 1.5 pmol/mm². Kim et al. evaluated hMSCs osteogenic differentiation on modified tissue culture plastic (TCP) surfaces where the density of BMP-2 peptides was 0.69 pmol/mm² [354]. In the same context, Moore et al. fabricated a linear gradient of BMP-2 peptide (0-1.4 pmol/mm²) on glass surfaces and showed that at least 0.8 pmol/mm² is required to up-regulate Runx-2 gene expression [229]. On the other hand, the dual peptide grating; i.e. RGD-TAMRA+BMP-2-FITC surfaces led to lower individual peptide densities as compared to the sole peptide grafting, which was expected. Indeed, on bifunctionalized surfaces, the surface density of RGD-TAMRA and BMP-2-FITC mimetic peptides was estimated at 0.7 ± 0.1 pmol/mm² and 1.0 ± 0.1 pmol/mm², respectively, representing almost half the density of peptides grafted alone. In other words, the global peptide density on bifunctionalized surfaces, estimated at 1.7 ± 0.1 pmol/mm², was close to that measured on surfaces containing only RGD-TAMRA or BMP-2-FITC. These results are consistent with previous literature works showing that the grafting of pre-mixed RGD and BMP-2 peptides at equimolar concentration leads to a 50:50 combination, such that each peptide covers half of the whole surface [229] [354].

In this work, RGD-TAMRA and BMP-2-FITC mimetic peptides were covalently grafted onto glass surfaces in controlled manner leading to a quite similar total peptide density on the different peptide modified surfaces. In addition, changes in the surface roughness, recognized to greatly influence cell behaviors, was statistically not significant between the different type of peptide grafted surfaces [252] [350] [351]. Thereby, the probability that cells may behave differently in response to the surface peptide densities and surface roughness can be eliminated, thus keeping the specific effect of each peptide and their synergistic cooperation as the main parameters influencing hBMSCs fate. Therefore, creating a well-defined biochemical microenvironment on material surfaces is crucial to subsequently investigate stem cell differentiation and signaling pathways governing this cell behavior.

Table 2: XPS survey analyses of glass surfaces at each step of peptide grafting.

	Si	C	O	N	N/C	N/Si
Glass "Piranha"	23.7 ± 0.3	10 ± 4	65 ± 2	—	—	—
+ APTES	22 ± 1	19 ± 2	54 ± 1	1.4 ± 0.4	0.08 ± 0.01	0.07 ± 0.02
+ SMPB	21 ± 1	25 ± 1	49 ± 1	2.2 ± 0.6	0.09 ± 0.02	0.10 ± 0.03
+ RGD-TAMRA	20.4 ± 0.5	25 ± 2	50 ± 2	2.9 ± 0.5	0.12 ± 0.02	0.14 ± 0.03
+ BMP-2-FITC	15.2 ± 0.5	39 ± 2	38 ± 2	5.9 ± 0.3	0.15 ± 0.01	0.40 ± 0.03

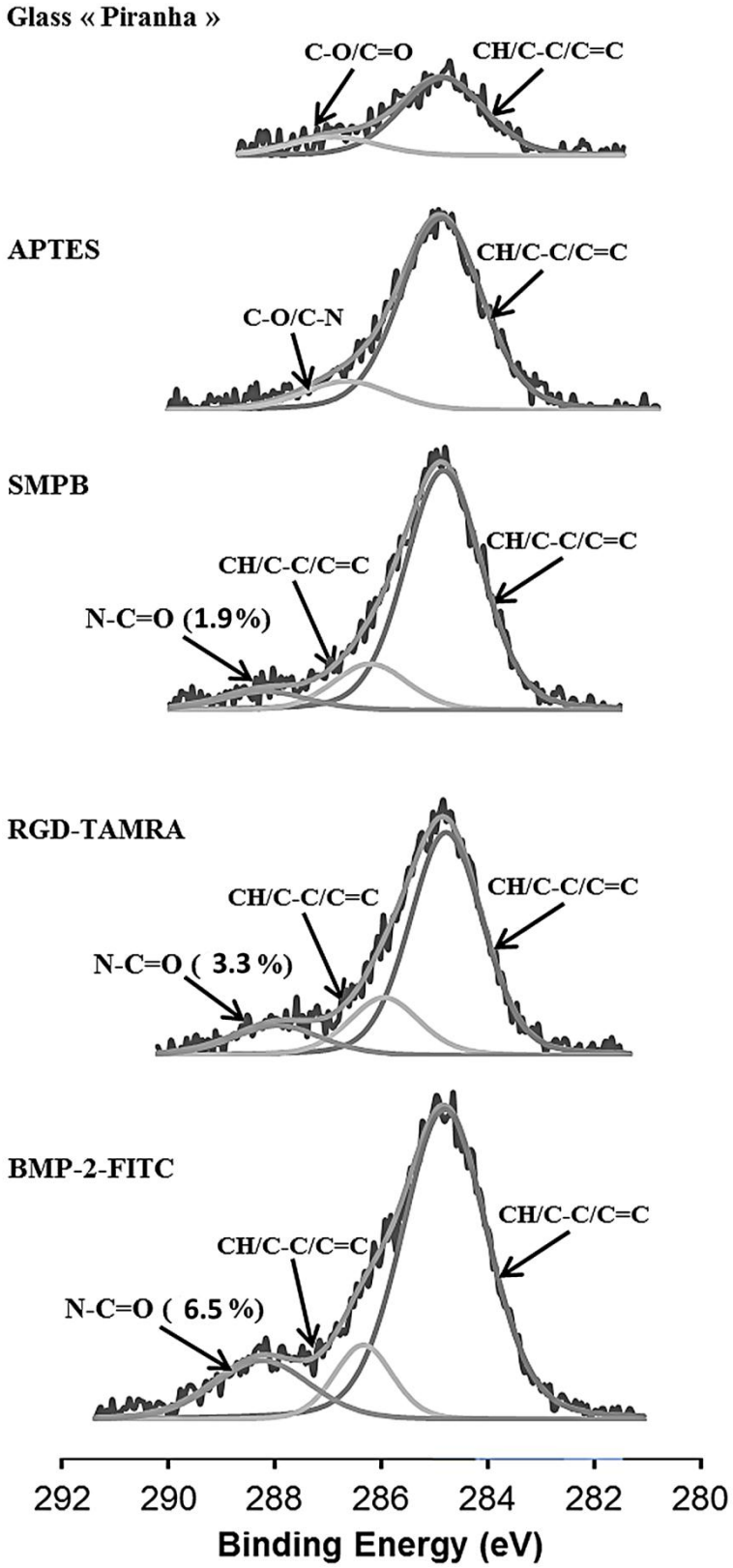

Figure 21: C1s XPS spectra obtained at each step of RGD-TAMRA and BMP-2-FITC peptide grafting.

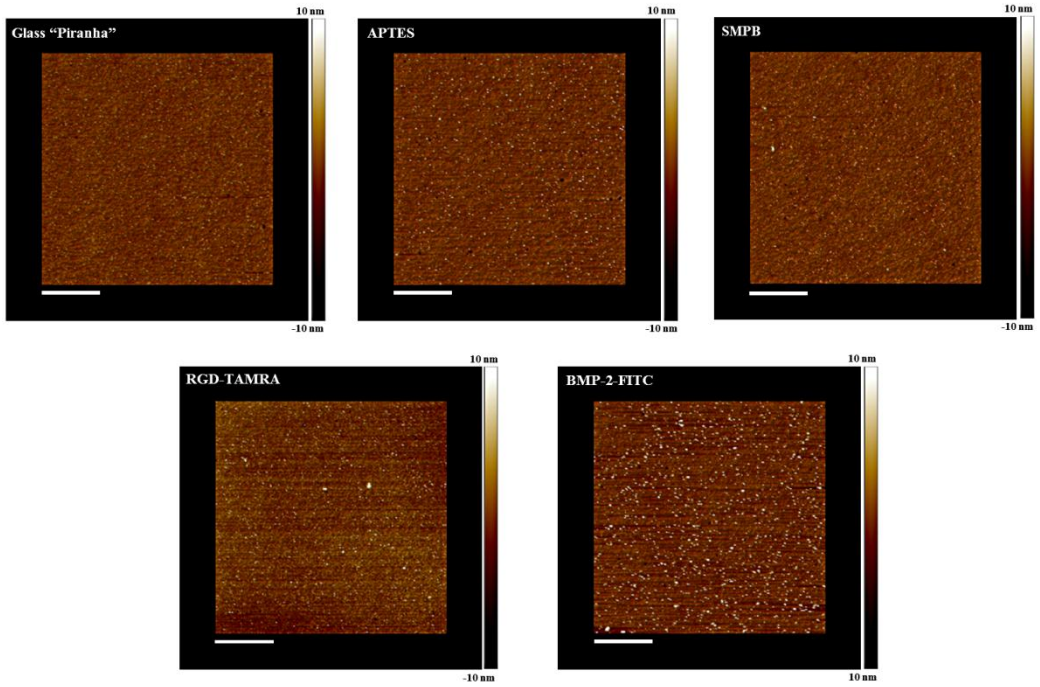

Figure 22: AFM images of the surface topography on different modified glass surfaces Scale bar: 5 µm.

Table 3: Surface roughness measurements after each step of surface modification.

	Glass "Piranha"	APTES	SMPB	RGD-TAMRA	BMP-2-FITC
R_{rms} *(nm)*	1.1 ± 0.1	1.4 ± 0.3	1.3 ± 0.3	2.2 ± 0.2	2.5 ± 0.4

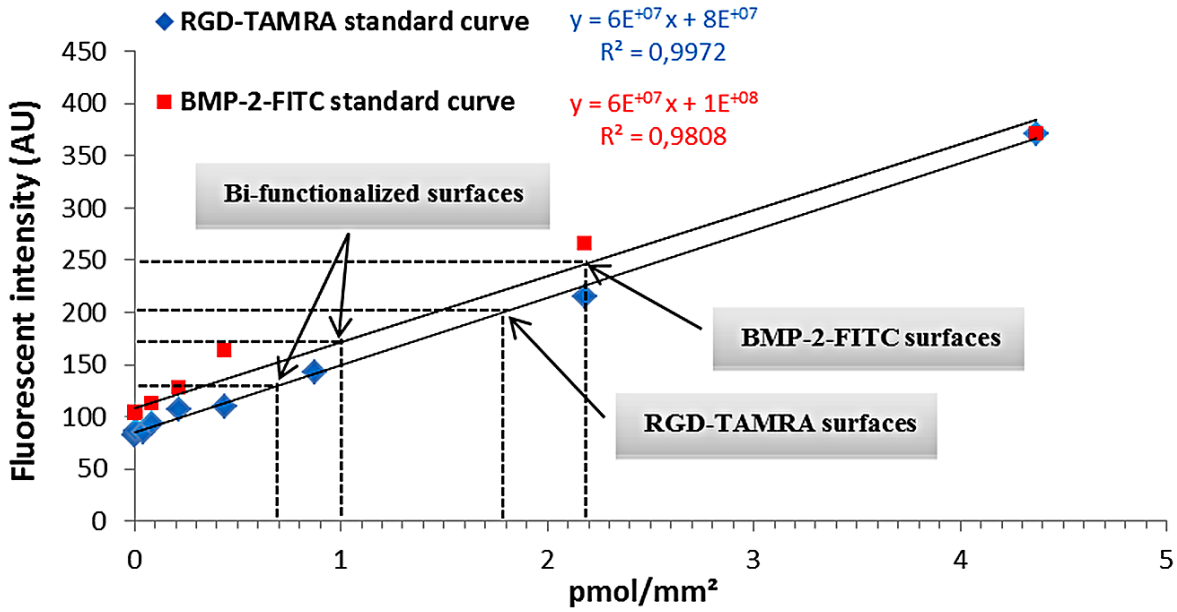

Figure 23: Fluorescent measurements of peptide surface density on different peptide modified surfaces using a standard curve with well-known peptide concentrations *per* mm^2.

3.2 hBMSCs osteogenic differentiation

Identification of biochemical cues that precisely control the switch of stem cells into mature cells exhibiting osteoblast phenotype is crucial to the advancement of biomaterials used as bone tissue-engineered scaffolds. Surface modification of biomaterials by covalent binding of signaling molecules and growth factors derived from the natural ECM provides a useful model to identify these biochemical features and to understand the signaling pathways triggered by their interactions with stem cells. In a previous study, PET (Polyethylene Terephthalate) was conjugated with different ECM-derived peptides. It was demonstrated that RGD peptide enhances the osteoinductive potential of BMP-2 peptide on mouse calvaria-derived preosteoblast-like cells (MC3T3-E1) [211] [355]. The present study focuses on the response of more primitive cells derived from human bone marrow (hBMSCs) to these peptides, either alone or combined together. All cell culture experiments were performed in serum-free media for the first 6 h and in the absence of soluble osteogenic factors over 4 weeks of cell differentiation. These cell culture products, frequently used in biological experiments, are not physiologically relevant, greatly influence cell behavior and might mask the specific effect of immobilized ligands on stem cells fate.

To screen for potential changes in hBMSCs phenotype on the various peptide modified surfaces, the number of stemness (STRO-1) and osteogenic (Runx-2) markers expressed by cells was measured using fluorescence microscopy. hBMSCs seeded on bare glass substrates, in the same cell culture conditions as modified surfaces, were used as negative control. No release of cells from the different materials was noticed after 4 weeks of cell culture. At first sight, images of fluorescently stained markers showed that hBMSCs express STRO-1 marker only on bare glass and RGD surfaces **(Figure 24.a-d)**. Quantitative analyses confirmed these observations since we noticed a decrease of STRO-1 expression on substrates containing RGD and/or BMP-2 mimetic peptides compared to control condition, with stronger effect on BMP-2 and RGD+BMP-2 surfaces **(Figure 24.i)**. The difference in STRO-1 expression was statistically significant between the control and surfaces containing RGD peptide, while the difference between surfaces containing BMP-2 mimetic peptide was not significant **(Figure 24.i)**. This indicates that the population of hBMSCs that have lost their stemness was greater on surfaces presenting BMP-2 peptide compared to RGD or control surfaces. Therefore, it could be hypothesized that these cells underwent a lineage-specific commitment, probably a commitment towards the osteoblastic lineage. To confirm this hypothesis, hBMSCs were stained for Runx-2 marker, considered to be the first transcription factor required for determination of osteoblast lineage. Indeed, fluorescent images showed that the expression profile of the osteogenic marker Runx-2 exhibits an opposite trend compared to that of stem cells marker STRO-1 **(Figure 24.e-h)**. Quantitative analysis clearly evidenced the underlying trend as revealed by an overexpression of Runx-2 on BMP-2 and RGD+BMP-2 surfaces and a slight expression on RGD and control surfaces, suggesting that surfaces containing the mimetic peptide of BMP-2 are osteoinductive. Specifically, significantly higher expression of Runx-2 was noticed on RGD+BMP-2 surfaces with respect to BMP-2 surfaces, meaning that RGD peptide up-regulates the stimulatory activity of BMP-2 mimetic peptide **(Figure 24.j)**. Together, the expression profile of STRO-1 and Runx-2 markers demonstrated that RGD peptide alone weakly affected stem cells commitment, as confirmed by decreased STRO-1 and equivalent Runx-2 levels compared to the control. In contrast, BMP-2 peptide effectively induced hBMSCs osteogenic commitment, as revealed by a down-regulation of STRO-1 and an up-regulation of Runx-2 markers. Specifically, RGD and BMP-2 mimetic peptides synergistically enhanced BMP-2-mediated osteoblast differentiation of hBMSCs.

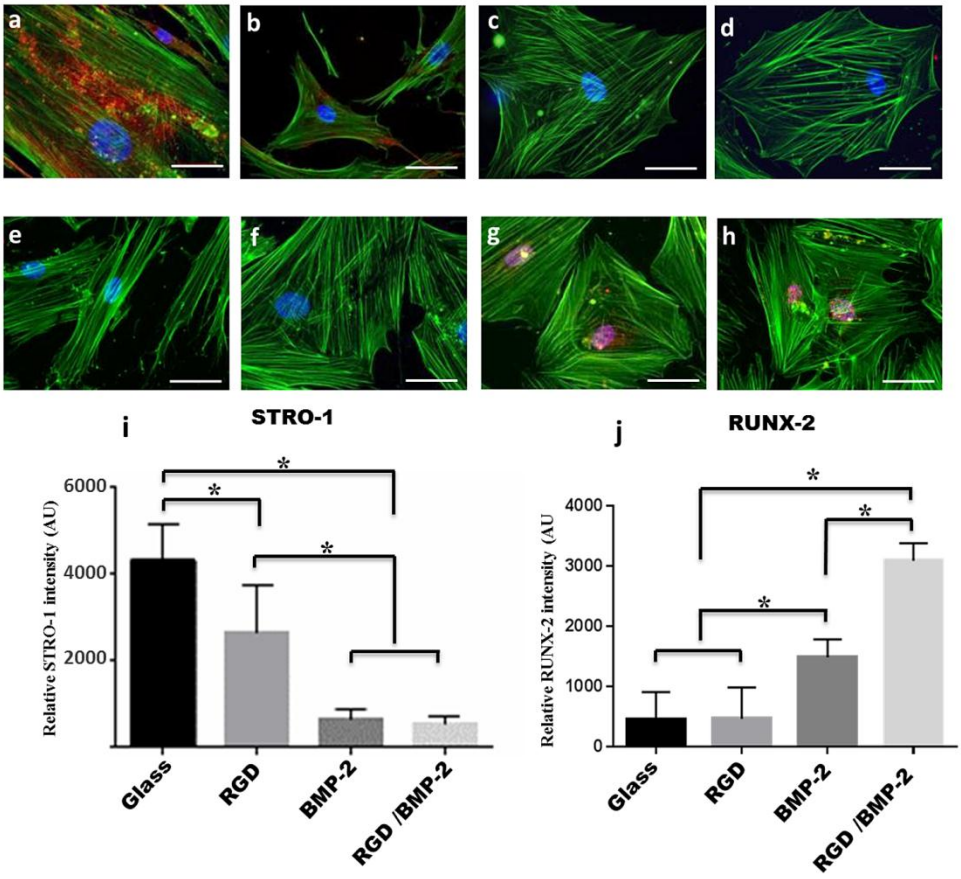

Figure 24: Osteogenic commitment of hBMSCs after 4 weeks of culture on Bare glass surfaces (a, e), RGD surfaces (b, f), BMP-2 surfaces (c, g) and RGD/BMP-2 surfaces (d, h). Cells were stained for STRO-1, a hBMSCs marker (A-D) and Runx-2, an osteoblast marker (E-F) in red, with F-actin stained in green and cell nucleus in blue. Scale bar: 50 µm. (i, j) Quantitative analysis of the total cellular STRO-1 (i) and Runx-2 (j) immuno-fluorescence intensity in hBMSCs cultured on various types of modified surfaces (*P < 0.01).

Basically, the RGD peptides were commonly used for their ability to mediate cell adhesion and spreading [325] [186], however, conflicting results were reported as to whether RGD peptides promote osteoblast differentiation. The osteogenic effect of RGD peptides was often demonstrated on osteoblast and committed pre-osteoblasts [349] [356] than more primitive uncommitted cells such as BMSCs [227] [229] [357]. He et al. observed increased ALP and calcium in rat BMSCs cultured on hydrogels containing 0.02 pmol/mm² of RGD peptides [227], while Moore et al. found that hBMSCs seeded on RGD peptide gradient substrates (0-1.4 pmol/mm²) down-regulated the expression of Runx-2 mRNA compared to the negative control [229]. However, it should be noted that in contrast to the Moore et al. study, He et al. tested the osteogenic effect of RGD peptide in the presence of osteogenic medium, which can explain the difference in stem cells

response to RGD between these two studies. Our results are in agreement with those published by Moore et al. Indeed, we demonstrated that the RGD peptide alone, at a density of 1.8 pmol/mm², effectively reduced the stemness phenotype of hBMSCs but weakly induced their osteogenic commitment, in the absence of osteogenic medium **(Figure 24.i-j)**. The RGD peptide may thus promote osteogenic differentiation of hBMSCs in the presence of soluble osteogenic factors in the culture media.

The differentiation of MSCs and progenitors towards the osteoblastic lineage is usually accomplished in response to BMP proteins or their mimetic peptides. BMPs interact with BMPR-I and BMPR-II receptors leading to the phosphorylation of BMPR-I by BMPR-II, which in turn activate Smad 1/5/8 signaling pathways [334] [179]. This Smad-dependent pathway leads to an up-regulation of Runx-2 transcriptional factor, which in turn regulates the expression of other osteoblast-specific proteins such as bone sialoprotein (BSP) and osteopontin (OPN) [358]. Indeed, quantitative analysis of osteogenic markers expression showed that surfaces containing BMP-2 mimetic peptide alone at a density of 2.2 pmol/mm² (surfaces 2) up-regulated Runx-2 levels in hBMSCs, consistent with previous works [104] [354] [229] [359] [360]. On the other hand, bifunctionalized surfaces exhibited a significant decrease of each peptide surface density compared to the sole peptide grafting. Indeed, because bifunctionalized surfaces were obtained from a 50:50 peptide mixture, the BMP-2 density on these surfaces was 1 pmol/mm², which is almost half the density measured on surfaces containing only BMP-2 mimetic peptide. However, results showed that the osteogenic effect of BMP-2 is still maintained, suggesting that the density of BMP-2 mimetic peptide ranging from 1 to 2.2 pmol/mm² was sufficient to promote hBMSCs osteogenic commitment. These observations are supported by Moore et al. where they investigated the extent of hBMSCs osteogenic differentiation as a function of BMP-2 surface density in basal medium. Indeed, they noticed increased fluorescence intensity of Runx-2 as BMP-2 concentration increases along a peptide gradient ranging from 0 to 1.4 pmol/mm² [229].

The combination of RGD and BMP-2 mimetic peptides at a density of 0.7 pmol/mm² and 1 pmol/mm², respectively, noticeably influenced the expression of osteogenic markers, leading to 2 fold increases in Runx-2 level compared to surfaces containing BMP-2 mimetic peptide alone. The up-regulation of Runx-2 expression strongly suggested that hBMSCs were switched towards the osteoblast lineage and that RGD and BMP-2 mimetic peptides act synergistically to accelerate hBMSCs osteogenic commitment. This synergetic effect has been previously observed by He et al. on rat BMSCs cultured on hydrogels

functionalized with RGD+BMP-2 mimetic peptides. They hypothesized that RGD peptide provides sites for cell attachment to the substrates, which facilitates the interaction of BMP-2 mimetic peptides with their transmembrane receptors, BMPR I and BMPR II, thereby, leading to enhanced osteogenesis [227]. This assumption seems reasonable since Lai and Cheng demonstrated that BMP-2 receptors co-localize/overlap with α_v and β_1 integrin subunits at focal adhesion points, which makes easier the interaction between BMP-2 receptors and their ligands sequestered within the ECM [225]. Moreover, it was shown that integrin signaling plays an essential role in the activation of BMP-2 receptors since blocking $\alpha_v\beta$ integrins using α_v integrin antibodies L230 suppressed the Smad signaling elicited by the activation of BMP-2 receptors. Koepsel et al. also confirmed these findings; they showed that hBMSCs could not interact with BMP-2 when cells are seeded onto gold surfaces presenting a cell adhesion peptide mutant (GRGESP) in combination with BMP-2 mimetic peptide [361]. This means that the osteogenic effect of BMP-2 mimetic peptide is not only related to BMP-2 receptors activation as suggested in several previous works [332] [334], but is also integrin signaling dependent. Suzawa et al. provided further details about the mechanism involved in the cooperation between RGD and BMP-2 mimetic peptides. Indeed, they clearly demonstrated that Ras-ERK signals potentiate BMP-2 bioactivity through their direct effects on Smad 1 transcriptional activity, and that Ras-ERK might be downstream signals of activated α2β1-integrin [362].

Although this synergetic effect was highlighted in several studies, the scientific literature also provides contradictory results [354] [361]. For example, Kim et al. prepared modified tissue culture polystyrene (TCP) surfaces with BMP-2, RGD+BMP-2 or scRDG+BMP-2 peptides, where scRDG was used as a negative control sequence of RGD. Results showed that the density of BMP-2 ranging from 0.33 pmol/mm² on sc-RDG+BMP-2 surfaces to 0.69 pmol/mm² on BMP-2 surfaces promotes hMSCs osteogenic differentiation, without any influence of osteogenic differentiation extent within this range. However, on RGD+BMP-2 surfaces, having the same BMP-2 density as sc-RDG+BMP-2 surfaces, the osteogenic effect of BMP-2 peptides was clearly reduced causing a down-regulation of Alkaline Phosphatase (ALP) activity and calcium deposition compared to BMP-2 and sc-RDG+BMP-2 surfaces [354]. Kim et al. and Koepsel et al. reported that this discrepancy between the results regarding the effect of RGD peptides on stem cells and progenitor response to BMP-2 peptide could be due to differing peptide densities that can significantly impact cell behavior, the way to attach peptides on the biomaterial as well as the medium conditions used for biological experiments [354] [361].

Taken together, our data demonstrate that RGD and BMP-2 mimetic peptides work in synergistic manner to enhance the osteogenic differentiation of hBMSCs, without the need of additional osteogenic supplements.

With regard to potential applications, these osteoinduction systems can be used in regenerative medicine, tissue repair or even tissue engineering. For example, such systems could be proposed as cell culture models to induce lineage-specific differentiation of MSCs into bone cells. Differentiated cells might be harvested and then loaded in a bioreactor to maintain their phenotype and produce bone-like tissues for cell-based therapies. It could also be conceivable to develop 3D biodegradable matrices simultaneously loaded with osteoinductive combined ligands (RGD/BMP-2) and hMSCs. Interestingly, mechanical properties of these scaffolds could be tailored to mimic the stiffness of immature bone tissue [236]. Such materials could be used as tissue engineered products to repair bone defects throughout two strategies. The constructs could be either incubated *in vitro* for only a few hours or cultured for sufficient time to produce osseous entities prior to implantation. One can also imagine functionalizing the surface of metallic and ceramic materials, used as bone fixation and/or replacement implants, with these ligands. Osteoblasts are likely to colonize implants and produce a mineralized ECM, which may avoid the formation of a fibrous layer at the interface bone/implant, therefore improving the integration of implants with the surrounding bone tissue. In addition, this osteoinduction system would be an insightful tool for an in-depth understanding of MSCs interactions with their microenvironment.

4. Conclusion

The effect of RGD and/or BMP-2 mimetic peptides on osteogenic differentiation of hBMSCs was evaluated. RGD peptide is known to promote hBMSCs adhesion to glass surfaces through their integrins, while BMP-2 mimetic peptide induces hBMSCs commitment and differentiation towards the osteoblastic lineage. The results demonstrated that BMP-2 mimetic peptide at a density in the pmol/mm² effectively induced the switch of hBMSCs into osteoblast cells. Importantly, compared to BMP-2 grafted surfaces, the co-grafting of both RGD and BMP-2 mimetic peptides on glass surfaces increased the expression of Runx-2 levels by 2 fold after 4 weeks in the absence of osteogenic media, thus suggesting that these peptides synergistically enhanced the extent of hBMSCs commitment towards the osteoblastic lineage. These findings contribute to the sum of efforts

deployed by researchers to design biomaterials capable of fostering the response of stem cells toward bioactive molecules for bone tissue engineering applications.

Acknowledgments

I. Bilem acknowledges funding from the NSERC CREATE Program of Regenerative Medecine (NCPRM). The authors also express their gratitude to Andrée-Anne Guay-Bégin for her assistance for XPS analyses. This research was supported by the National Research and Engineering Research Council of Canada (G.L.).

II. Study 2: Microscale geometric cues enhance osteogenic differentiation on BMP-2-, but not RGD-modified surfaces.

The spatial distribution of RGD and BMP-2 mimetic peptides at the subcellular scale modulates of human mesenchymal stem cells osteogenesis

Ibrahim Bilem[abcf], Laurent Plawinski[cde], Pascale Chevallier[ab], Eli D. Sone[f], Gaétan Laroche[ab†], Marie-Christine Durrieu[cde†]

[a]Laboratoire d'Ingénierie de Surface, Centre de Recherche sur les Matériaux Avancés, Département de Génie des Mines, de la Métallurgie et des Matériaux, Université Laval, 1065 Avenue de la médecine, Québec G1V 0A6, Canada.
[b]Centre de Recherche du Centre Hospitalier Universitaire de Québec, Hôpital St-François d'Assise, 10 rue de l'Espinay, Québec G1L 3L5, Canada.
[c]Université de Bordeaux, CBMN, UMR 5248, F-33600, Pessac, France.
[d]CNRS, Institute of Chemistry & Biology of Membranes & Nanoobjects (CBMN 5248), F-33600, Pessac, France.
[e]Bordeaux INP, CBMN, UMR 5248, F-33600, Pessac, France
[f]Institute of Biomaterials and Biomedical Engineering, Department of Materials Science and Engineering, and Faculty of Dentistry, University of Toronto, Toronto, ON M5S 3G9, Canada.

[†]Corresponding authors (equally contributed):
Gaetan.Laroche@gmn.ulaval.ca Phone: 1 (418) 656-7983 Fax: (418) 656-5343
marie-christine.durrieu@inserm.fr Phone: +33 5 40 00 30 37 Fax: +33 5 40 00 22 00

Keywords: chemical patterning· mimetic peptides· BMP-2· stem cell differentiation· bone tissue engineering.

This work has been submitted to the journal: ***ACS Nano***

Résumé:

Le développement de matrices extracellulaires (MECs) artificielles, *in vitro*, basé sur la récapitulation de la distribution temporaire et spatiale des facteurs biochimiques *in vivo* (tel que les gradients des protéines et facteurs de croissance au sein de la MEC naturelle) semble être une étape importante vers une meilleure compréhension des mécanismes de régénération des tissus vieillissants ou endommagés.

Dans la présente étude, la technique de photolithographie a été utilisée afin de mimer l'organisation spatiale des biomolécules séquestrées dans la MEC. Deux ligands dont l'effet biologique est différent ont été sélectionnés ; le peptide RGD, facilitant l'adhérence cellulaire, et le peptide BMP-2, connu pour sa capacité à induire la différenciation ostéoblastique des cellules souches mésenchymateuses (CSMs). Chaque peptide a été greffé sur la surface d'un matériau sous forme de micro-motifs afin d'étudier l'effet de la distribution spatiale des ligands à bioactivité différente sur la différenciation des CSMs en ostéoblastes. Les résultats ont révélé que la modification de la forme des micro-motifs peptidiques influence la différenciation des CSMs, dépendamment de la nature du ligand présenté aux cellules. En effet, contrairement au peptide RGD, la distribution spatiale du peptide BMP-2 à l'échelle micrométrique a significativement amélioré la différenciation ostéoblastique des CSMs, comparativement à la distribution aléatoire des ligands. Ces résultats confirment que l'effet de la microstructuration des ligands dépend considérablement de leur nature et bioactivité.

Ce type de systèmes *in vitro* représente un outil très intéressant pour explorer les mécanismes par lesquels les cellules souches perçoivent et répondent à leur microenvironnement, ce qui pourrait contribuer au développement des biomatériaux de nouvelle génération, capables de répondre aux besoins cliniques actuels en chirurgie orthopédique.

Abstract

Engineering artificial extracellular matrix (ECM) based on the presentation of proteins and growth factors in a spatially controlled manner, mimicking the distribution of biochemical cues within the native environment, is of great importance for understanding mechanisms of bone tissue regeneration. Herein, photolithography was used to decorate glass surfaces with subcellular patterns of RGD and BMP-2 ligands; two mimetic peptides recognized to be involved in stem cells osteogenesis. Well-defined micropatterned surfaces were used to compare the effect of the micro-scale distribution of these ECM-derived ligands on directing human mesenchymal stem cells (hMSCs) differentiation into osteoblasts, in the absence of induction media. By manipulating micropatterns shape while keeping their overall area constant, the differentiation of hMSCs was affected differently depending on the type of ligand presented to cells. Obviously, the micro-scale distribution of BMP-2, but not RGD peptide, significantly enhanced the extent of hMSCs differentiation, suggesting that geometric cues guide stem cells specification into specialized cells in a ligand type dependent manner. Such cell culture models provide an interesting tool to investigate how stem cells perceive and respond to their microenvironmental cues and may contribute to the development of next-generation biomaterials capable of producing clinically relevant volume of bone tissue.

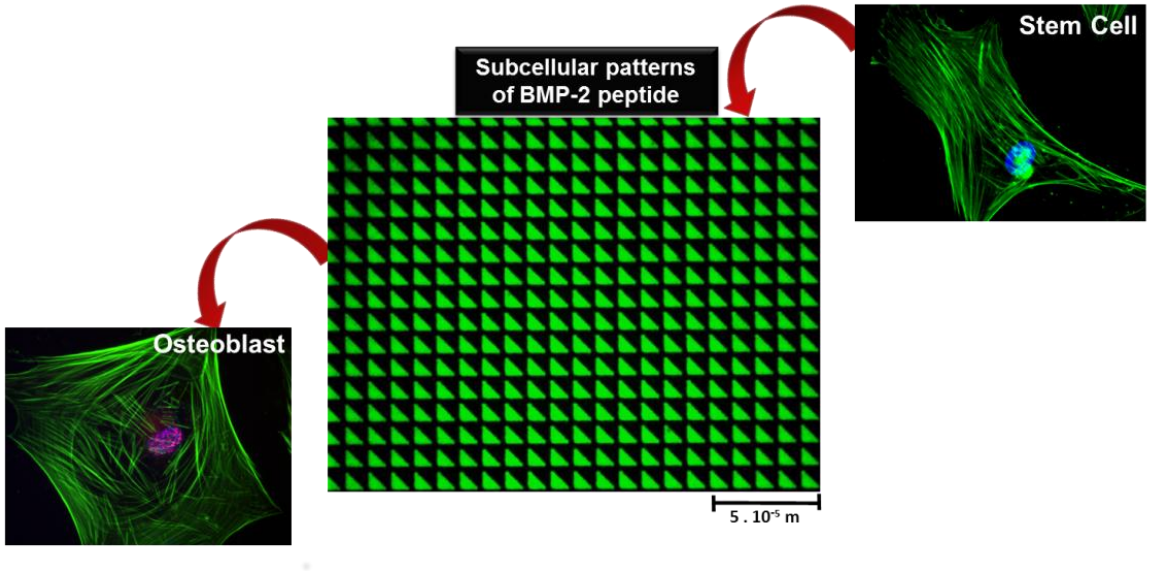

Graphical table of content

Stem cell commitment and differentiation into specialized cells is governed by their local microenvironment known as the stem cell niche [363] [364]. The ECM, a key component of the stem cell niche *in vivo*, has emerged as a crucial regulator of extracellular signals mediating the maintenance of stem cells or their differentiation [365] [366]. So, identifying ECM cues dictating cell-fate decision and understanding how stem cells perceive and respond may help to recapitulate the complexity of the native ECM and eventually mimic their physiologically relevant properties *in vitro*. During the last decades, it has become evident that cell behaviors are influenced by biochemical cues such as ligands type and density [367] [368] as well as physical cues such as matrix stiffness, surface topography, free energy, wettability and electric charges [138] [155] [236]. Biochemical cues are the most studied and the best characterized ECM features affecting stem cells fate [369]. Indeed, different signaling molecules were found to be tethered within the ECM during mesenchymal stem cells (MSCs) differentiation into distinct lineages, such as fibroblast growth factor (FGF) during proliferation [370], bone morphogenetic protein-2 (BMP-2) during osteogenenic differentiation [371], transforming growth factors (TGFβ) during chondrogenic differentiation [372], and vascular endothelial growth factor (VEGF) during angiogenic differentiation [373]. Therefore, growth factors and other bioactive molecules such as adhesive ECM-derived proteins, including fibronectin, vitronectin, collagen, and Laminin [374] have been extensively used as ECM mimics to induce, guide and control lineage-specific differentiation of stem cells [375] [376].

Beside biochemical properties of the native ECM, many literature works have reported that cells *in vivo* are exposed to both nano- and micro-sized structures of different geometries such as pits, pores, ridges, protrusions, crystals and fibers [257] [259] [377] [378]. For instance, bone tissue is hierarchically organized from nanometer to centimeter scale, with an average roughness of 32 nm [379]. Therefore, within a very brief time-frame, the idea of designing biomaterials that closely mimic the complex architectural conditions *in vivo* has excited many scientists over the world and attracted interest in various biomedical applications including tissue engineering, drug discovery, permanent implants, high throughput microarrays, cell-based biosensors, and fundamental studies in cell biology. Structuring material surfaces consists of creating either topographical or chemical patterns, thanks to the microfabrication techniques [380]. Topographical patterns have long been recognized to control short and longer cellular functions such as cell adhesion and differentiation, respectively [251]. However, the effect of chemical patterns has been less

addressed and mainly focused on controlling early cell responses (cell adhesion, proliferation and migration) [299]. This may be related to the fabrication process complexity, poor reproducibility, restricted range of materials suitable for chemical patterning and risks of affecting ligands bioactivity due to the use of harsh organic solutions and heat treatment.

Although the existing literature exploring the impact of chemical patterns on stem cells fate is quite limited, some few recent studies clearly revealed that MSCs and progenitor cells sense and response to spatially distributed ligands, when pattern features are carefully selected and designed to target a lineage-specific differentiation. For example, it has been shown that maintaining the stemness character of stem cells or eliciting their differentiation can be regulated by varying the features of chemical patterns, including their shape, aspect ratio, or size at both nano- and micro-scale [242] [381] [382] [383] [384]. These recent studies have shown that chemical micropatterning has a more profound impact on cell behavior than had previously been recognized, however most of them have been focused on investigating MSCs differentiation in response to the spatial distribution of adhesive ligands, such as fibronectin or RGD peptide rather than growth factors [385]. Additionally, micropattern systems have been mainly used to manipulate stem cells commitment and differentiation at single cell scale [241] [242] [381] [383]. Even though these *in vitro* models are used as tool to decipher the complexity of ECM-cell interactions and shed light on new mechanisms by which stem cells recognize their microenvironment and respond to, they do not likely reflect the physiological situation for several reasons, including: (i) cells interactions are neglected, while cell-cell contact are known to play an important role in mediating MSCs differentiation, (ii) it is very challenging for materials, used for single cell patterning, to keep their anti-adhesion properties for long time, thereby restricting usually the time of cell differentiation to 1 week (iii) the osteogenic differentiation of MSCs and signaling pathways assumed to be modulated by the pattern features are usually assessed in induction media, which may mask the specific effect of the pattern.

In the present study, the osteogenic differentiation of human mesenchymal stem cells (hMSCs) was evaluated on glass surfaces decorated with a checkerboard of adhesive RGD or osteoinductive BMP-2 patterns at subcellular scale. RGD and BMP-2 mimetic peptides have proven as potent effectors of cell adhesion [326] and differentiation [187], respectively. Peptide patterns of different geometries but similar overall area were created using photolithography technique, in such a way that cells are allowed to communicate with each other and move freely over the substrate, without imposing to cells specific

physical features (shape and/or dimension). The osteogenic differentiation of hMSCs, grown during 4 weeks in a medium free of soluble osteogenic factors, was assessed on the different patterned surfaces by determining the expression levels of STRO-1, as specific stemness marker, and Runt-related transcription factor 2 (Runx-2), Osteopontin (OPN) and Alkaline Phosphatase (ALP) activity, as specific markers of osteoblast phenotype.

In this study the following questions were explored: 1) Is the effect of geometric cues alone sufficient to modulate stem cells fate? 2) Does the spatial distribution of cell adhesion peptide, RGD, affect hMSCs differentiation? 3) At what extent the spatial distribution of BMP-2 peptide affect its bioactivity?

Results

Characterization of peptide patterned surfaces. The spatial distribution of peptides was ascertained at different stages, before and after peptide grafting and patterning. In a previous study, the covalent grafting of fluoro-tagged RGD-TAMRA and BMP-2-FITC peptides was evidenced using XPS [185]. Herein, the same protocol of peptide grafting was used to immobilize RGD-TAMRA and BMP-2-FITC peptides as specific patterns. First, the creation of resist patterns on glass substrates, using photolithography, was visually confirmed under fluorescence microscopy due to the S1818 resist auto-fluorescence. Images depicted in **(Figure 25**) clearly showed well defined geometries shaped as triangles, squares and rectangles. The size of resist patterns size was measured using optical interferometry. The obtained X and Y surface profiles revealed that the overall area of resist patterns was close to the originally defined micro-sized features of 50 µm², thus demonstrating high fidelity of pattern transfer **(Table 4) (Figure 26**). Fluorescent images and interferometric measurements were acquired at different locations on material surface to verify the reproducibility of resist patterns.

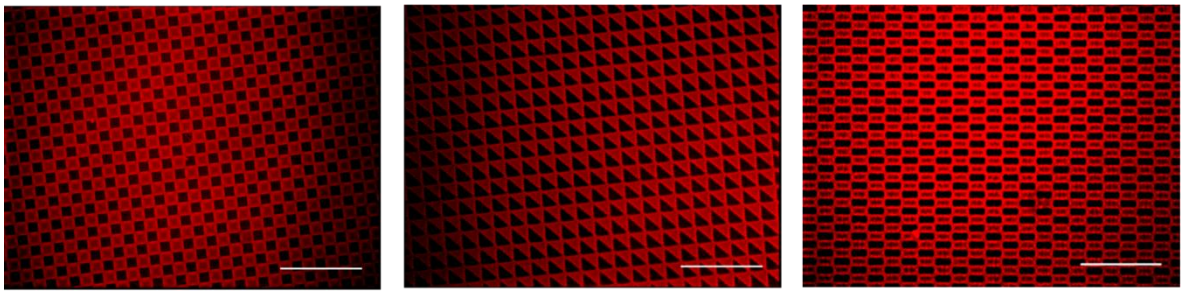

Figure 25: Fluorescence microscopy images of resist micropatterned surfaces showing three different pattern geometries (Triangle, rectangle, square) with a constant surface area. Scale bar: 50 µm.

Table 4: Measurements of pattern dimensions obtained on X and Y interferometry profiles and compared to the pattern features defined by the photomask.

Micropatterns shape	Replicated feature dimensions	Photomask feature dimensions	
Triangle (µm²)	9.8 ± 0.2 x 9.9 ± 0.1	10 x 10	
Square (µm²)	7 ± 0.2 x 7 ± 0.2	7.07 x 7.07	***50 µm²***
Rectangle (µm²)	10 ± 1 x 5 ± 1	10 x 5	

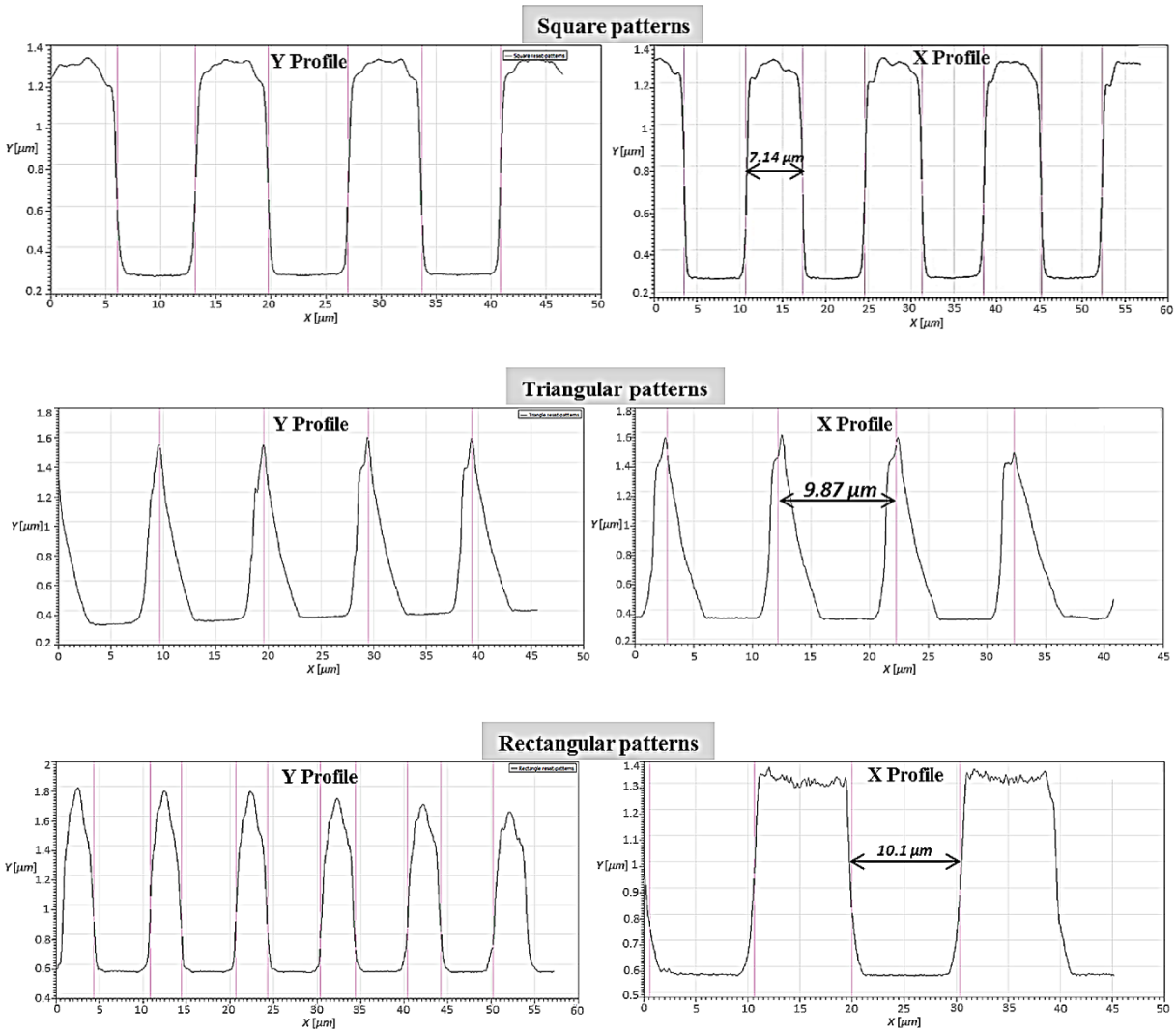

Figure 26: X and Y surface profiles obtained on different resist micropatterned surfaces using optical interferometry.

Subsequently, well-characterized resist micropatterned surfaces were used as a template to spatially distribute fluorescent RGD and BMP-2 peptides onto glass substrates. The efficiency of peptide patterning was confirmed by fluorescence microscopy. As shown in **Figure 27**, RGD-TAMRA and BMP-2-FITC micropatterns are readily identifiable and exhibit the expected shapes (triangular, square and rectangular geometries) and size (~ 50 µm²). It is worth noting that fluorescent images of micropatterned peptides are representative of pattern features on the entire surface of 150 samples used for cell culture experiments. Such criterion seem of outmost importance to ensure a high reproducibility of biological results, given that these pattern systems are used as cell culture model to investigate stem cells response to their microenvironment.

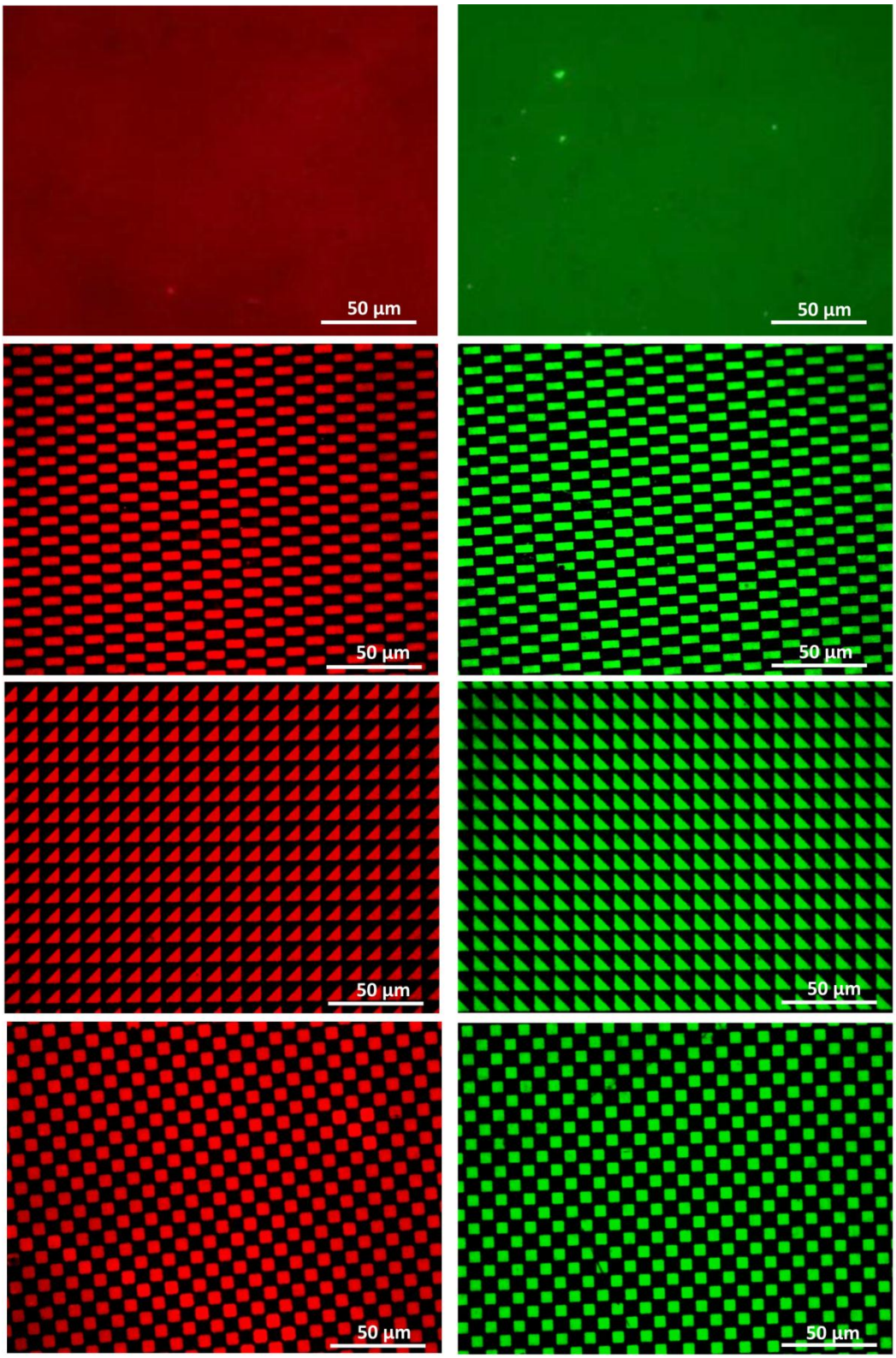

Figure 27: Fluorescence images of the different patterned and unpatterned surfaces with RGD-TAMRA (labeled in red) and BMP-2-FITC (labeled in green). Dark background corresponds to SMPB regions.

Osteogenic differentiation of hMSCs mediated by patterns shape. Given that the surface roughness has been recognized for long time to greatly affect stem cells behavior and functions [350] [351], we previously evaluated the surface roughness of RGD-TAMRA and BMP-2-FITC peptides distributed in homogenous way on glass surface [185]. Results showed no significant difference in the surface roughness between these two conditions. In the present work, the same protocol of peptide grafting was used to immobilize these peptides on glass material as specific patterns. Also, attention was paid to the fact that hMSCs seeded on peptide micropatterned surfaces are exposed not only to peptide patterns but also to the surrounding crosslinker regions, as shown in **Figure 27**. Indeed, the peptides were grafted through SMPB crosslinker, previously demonstrated by our team to exert no specific effect on cell behavior [344]. The focus was, therefore, made on comparing the effect of the spatial distribution of peptides as specific geometries on hMSCs osteogenesis. The extent of stem cell osteogenic differentiation was evaluated after 4 weeks of cell culture by measuring expression levels of stemness marker (STRO-1) and osteogenic markers (Runx-2, OPN, ALP) on patterned and unpatterned surfaces. Negative controls consisted of hMSCs cultured on bare glass surfaces.

On one hand, results showed that most of hMSCs maintained their stemness state on RGD-TAMRA surfaces, regardless the peptide pattern geometry. Indeed, fluorescence images indicated that hMSCs expressed STRO-1 marker on all RGD-TAMRA micropatterned surfaces **(Figure 28)** while only a slight expression of Runx-2 and OPN was noticed (Data not shown). Quantitative analysis also confirmed these observations, as revealed by an inverse correlation between the expression profile of stem cells marker and osteogenic markers, *i.e*. high expression of STRO-1 and very low expression of Runx-2 and OPN **(Figure 32-S1)**. ALP activity, which is the most frequently used marker for osteogenic differentiation, was also measured. Compared to the pattern of expression of fluorescently stained osteogenic markers, a similar trend of ALP expression, determined by colorimetric assay, was observed **(Figure 32-S1)**, thus confirming again that the distribution of RGD-TAMRA peptide at subcellular scale weakly induced the differentiation of hMSCs towards the osteoblasts lineage.

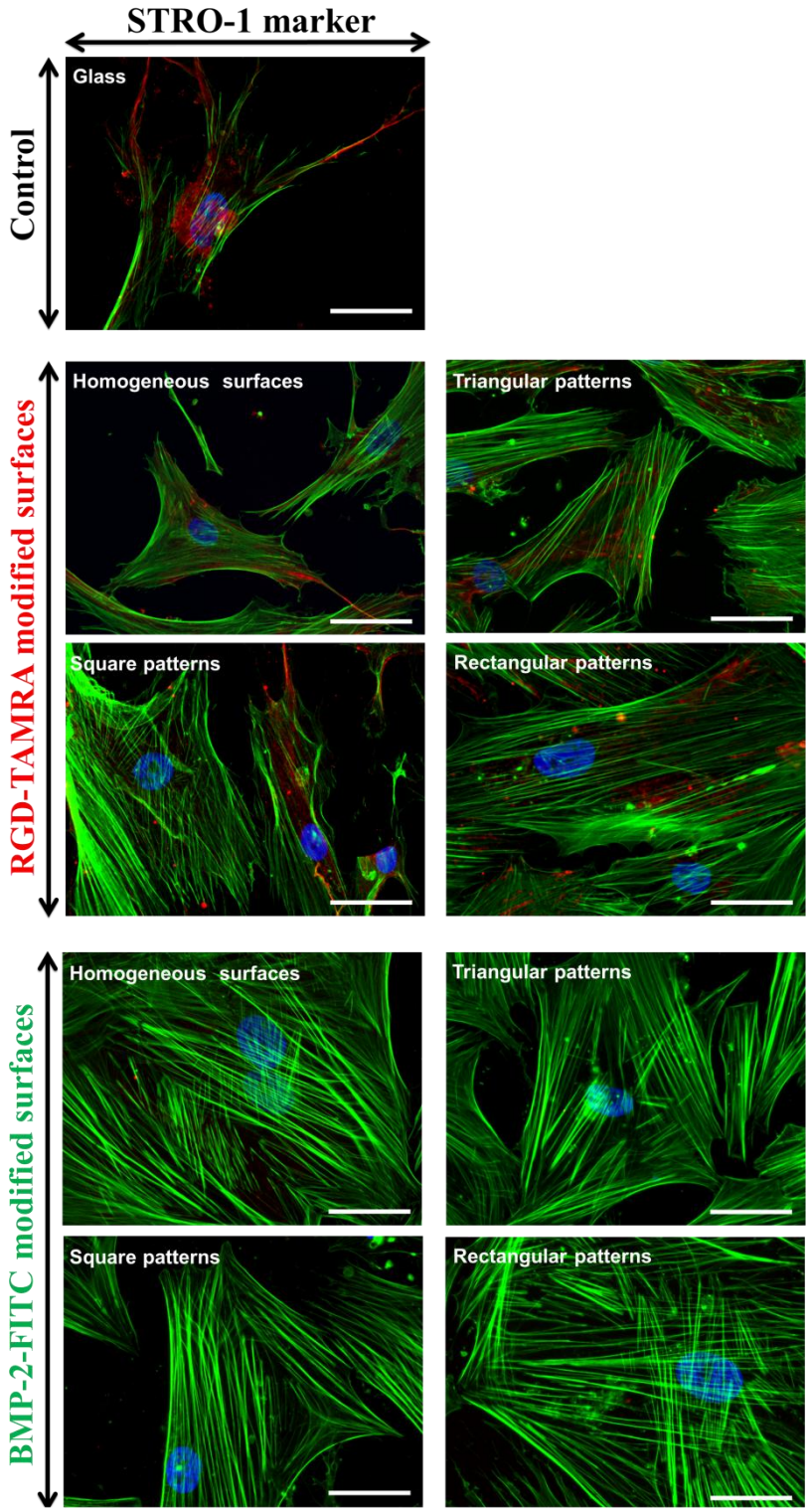

Figure 28: Fluorescent images of hMSCs cultured for 4 weeks on homogeneous and micropatterned surfaces with peptides. Cells were stained for stem cells marker (STRO-1) in red, with F-actin stained in green and cell nucleus in blue. Scale bar: 50 µm.

On the other hand, the extent of hMSCs differentiation into osteoblasts was evaluated in response to micropatterned surfaces with osteoinductive ligands. Herein, the purpose was to verify whether the stimulatory effect of BMP-2-FITC is still maintained or enhanced when the peptide is spatially distributed as specific geometrical cues at subcellular scale. The cell phenotype was analyzed using the same stemness and osteogenic markers as those employed for the evaluation of hMSCs fate in response to RGD-TAMRA patterns. Fluorescent images of stained markers revealed that all pattern geometries of BMP-2-FITC induced hMSCs osteoblast differentiation, as revealed by the suppression of STRO-1 marker **(Figure 28)** and the expression of both earlier Runx-2 and late OPN osteogenic markers **(Figure 29)**. Specifically, quantitative analysis showed significant increase in the expression yield of osteogenic markers depending on the pattern shape of BMP-2-FITC peptide. Indeed, the expression levels of Runx-2 and OPN markers were significantly higher on BMP-2-FITC patterns shaped as triangles and squares and similar on rectangular micropatterns as compared to unpatterned surfaces **(Figure 30)**. The underlying expression profile of fluorescently stained osteogenic markers was also observed on ALP results, showing the highest levels ALP activity on triangular and square patterns **(Figure 33-S2)**.

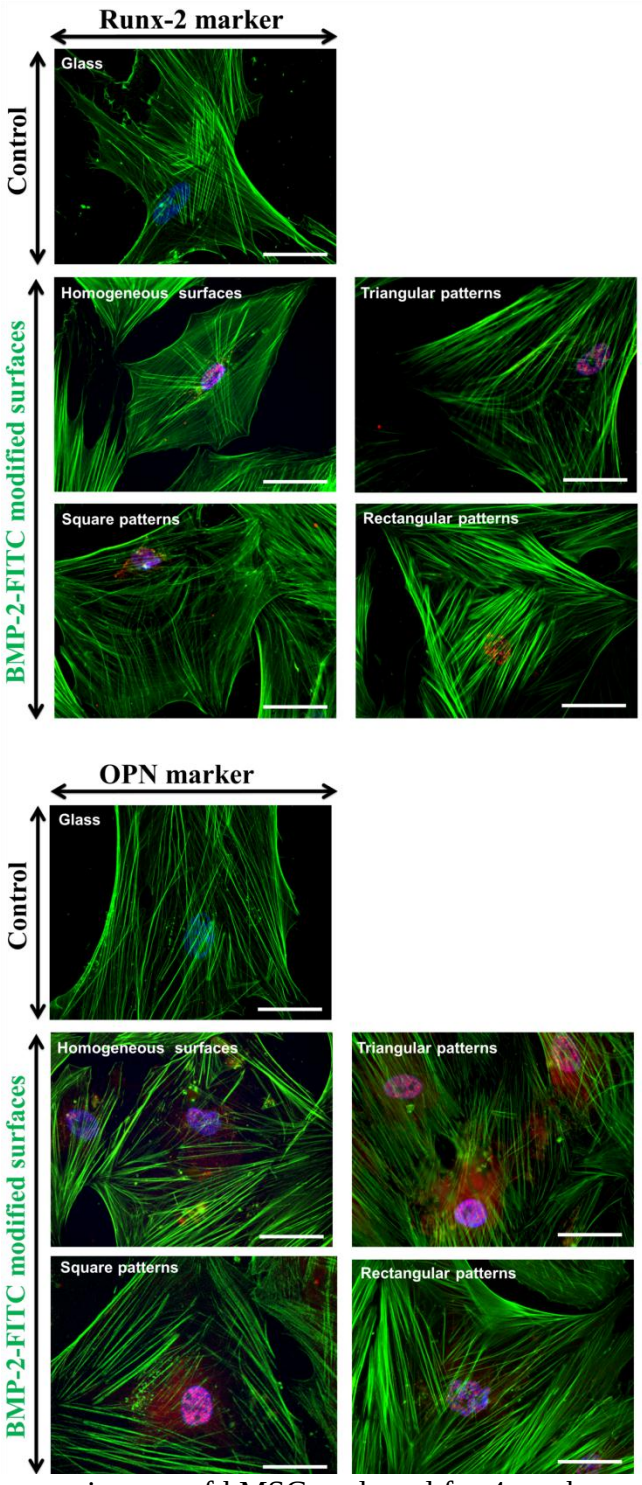

Figure 29: Fluorescence images of hMSCs cultured for 4 weeks on glass surfaces containing spatially distributed BMP-2-FITC peptide. Cells were stained separately for osteogenic markers Runx-2 and OPN in red, with F-actin stained in green and cell nuclei in blue.

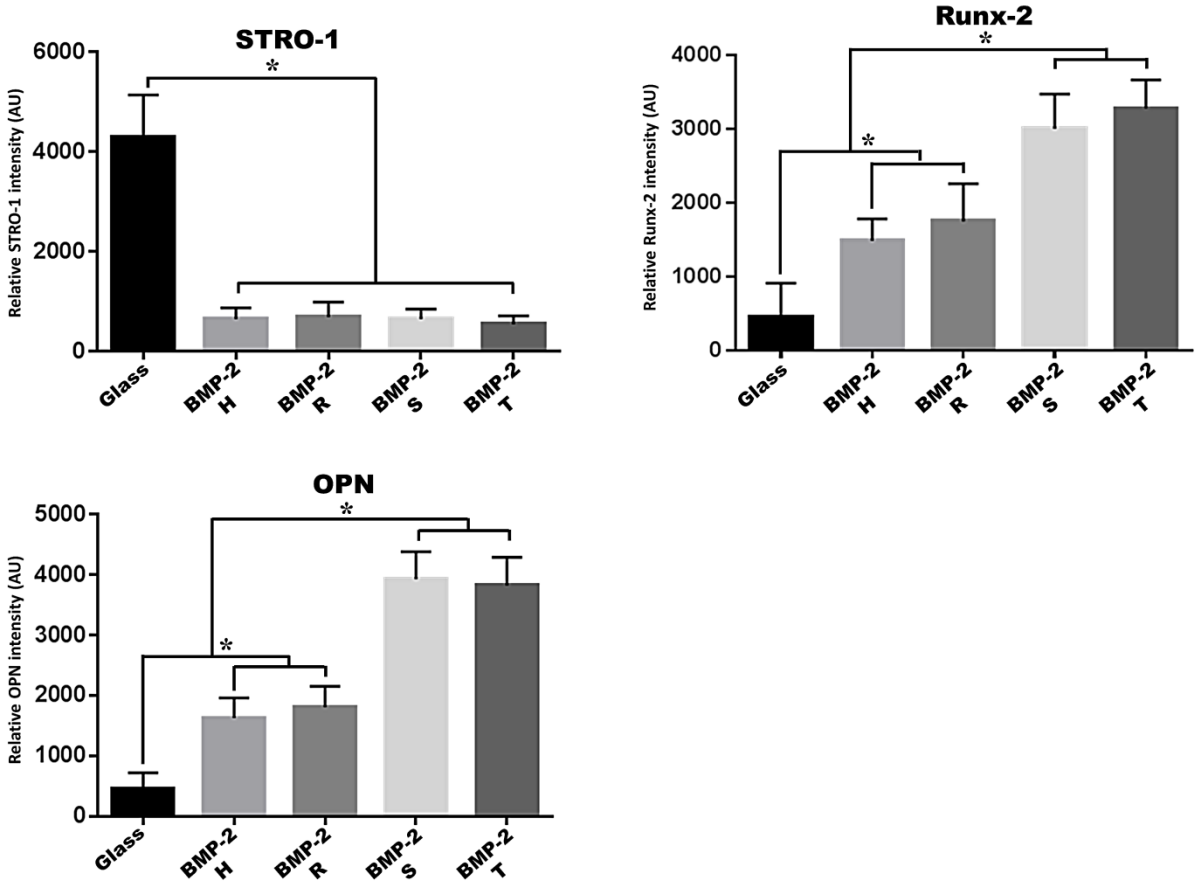

Figure 30: Quantitative analysis of the total cellular immunofluorescence intensity of STRO-1, Runx-2, and OPN in hMSCs cultured on patterned and unpatterned BMP-2-FITC surfaces.

Discussion

Identifying ECM cues that direct MSCs differentiation towards the osteoblastic lineage is crucial for the design of *in vitro* cell culture models that closely mimics the extracellular microenvironment of bone cells, which may help to produce clinically relevant quantities of bone tissue. Indeed, modulating chemical, topographical and mechanical properties of biomaterial surfaces are the most investigated approaches in an effort to recapitulate key aspects of the native ECM dictating MSCs fate, thus applying the acquired knowledge for bone tissue engineering application [315] [364]. The present work aims to investigate whether the grafting of BMP-2-FITC mimetic peptide as specific patterns with defined shapes and sizes, which somewhat mimics the organization of the native ECM components, enhances hMSCs osteogenic differentiation. Adhesive RGD-TAMRA peptide was also spatially distributed to examine whether geometrical cues effects are peptide dependent or influence hMSCs fate regardless ligand bioactivity. hMSCs were seeded on glass surfaces containing RGD-TAMRA or BMP-2-FITC patterns with different shapes but constant surface area at subcellular scale. To rule out the interference of the external cues beyond pattern shapes, all experiments were performed in serum-free media during the first six hours and in the absence of osteogenic soluble factors along the cell culture experiment, thus all of cells were exposed to the same local environments except geometrical cues. Quantitative and qualitative investigation of hMSCs differentiation provided two main information. First, the effect of the patterns shape is peptide-dependent as revealed by relevant changes in cell behavior on BMP-2-FITC patterns, unlike RGD-TAMRA patterns. Second, patterning of BMP-2-FITC mimetic peptide improves its bioactivity and consequently enhances hMSCs osteogenesis, depending on the pattern shape. The insensitivity of cells to RGD-TAMRA patterning demonstrated that the spatial distribution of RGD-TAMRA peptide was not a potent cue to sufficiently induce hMSCs differentiation **(Figure 33-S2)**. Although the nano-scale presentation of adhesive ligands has been widely recognized to affect stem cell fate [350] [386] [387], little is known regarding the biological effect of their distribution at subcellular scale. Indeed, some literature studies reported that the distribution of RGD peptide and other adhesive ligands at the micro-scale level is not sufficient to direct MSCs towards mature cell lineages. Hence, soluble growth factors are usually added to the media in such cell culture models to push stem cells to become terminally differentiated cells [236] [241] [351] [294]. In addition, cell differentiation in response to RGD peptide was mainly observed on pre-committed

cells such as pre-osteoblasts [349] rather than more primitive cells such as MSCs [227] [229].

Although patterning of RGD peptide as different shapes (rectangle, triangle, square) did not affect hMSCs fate, BMP-2-FITC peptide patterns exhibiting similar subcellular shapes significantly enhanced hMSCs differentiation towards osteoblastic lineage. Indeed, both ALP activity and levels of early and late fluorescently stained osteogenic markers were substantially up-regulated on triangular and square BMP-2-FITC patterns. However, on rectangular BMP-2-FITC patterns hMSCs expressed similar levels of osteogenic markers compared to those cultured on unpatterned BMP-2-FITC surfaces. Specifically, the correlation of the pattern shapes with a physical factor, known as the aspect ratio (AR), revealed that square and triangular patterns exhibit higher AR of 1 and 0.7, respectively, compared to rectangular micropatterns (AR = 0.5). The aspect ratio is defined as the Feret's minimum length to the Ferets's maximum length [388]. Therefore, experimental data demonstrate that; *(i)* the spatial presentation of BMP-2-FITC peptide as specific geometries is a strong regulator of cell differentiation and *(ii)* higher feature aspect ratios accentuate osteoblastic phenotype on differentiated hMSCs. Changing patterns geometry locally changes the distribution of BMP-2-FITC peptide and this may in turn change the binding affinity of the ligand with its receptors. It is important to reiterate that all patterns exhibited a constant subcellular size of 50 μm^2, so the differences observed in cell behaviors can be attributed directly to differences in pattern shapes and their aspect ratio. Creating a well-defined microenvironment by controlling the distribution of ligands on biomaterial surfaces remains a recent topic of biomaterials science, introduced by Whitesides and Ingber groups in 1994 [298]. The first investigations, using chemical patterning techniques, were focused on modulating the early cell responses such as cell adhesion, spreading, migration, proliferation and apoptosis [382] [389] [390]. Since 2004, this approach began to be applied to regulate more complex cell behaviors, such as cell differentiation and cell-cell communication [351] [383]. Some elegant works described in detail how stem cells respond to spatially distributed ligands as patterns of specific shapes and dimensions. For example, McBeath *et al*. [241] observed that MSCs seeded on large square micropatterns of fibronectin and exposed to mix osteogenic/adipogenic media differentiate preferentially towards osteoblast phenotype, while those cultured on relatively small square micropatterns (10 fold smaller) undergo adipogenesis. In this work, it was demonstrated that the signaling pathway governing lineage specific commitment of MSCs is mediated by the degree of cell spreading which is controlled by the

patterns size. Consequently, RhoA and ROCK activity is regulated, which in turn affect myosin-generated cytoskeleton tension. Therefore, high and low cytoskeleton contractility induces MSCs osteogenic and adipogenic commitment, respectively.

Kilian *et al.*[27] and Peng *et al*. [242]reported in insightful works that geometrical cues (pattern shape) also influence MSCs commitment into distinct specific lineages. Although some of the conclusions from the two groups are similar, such as signals mediating MSCs fate in response to pattern features, contradictory results were also reported. For example, Kilian *et al*. showed enhanced osteogenesis with decreased aspect ratio (AR 1:1 to 1:4) of rectangular micropatterns, while Peng *et al*. revealed that higher level of osteogenesis, determined by measuring ALP activity, was found at aspect ratio of 1:2 among a series of rectangular micropatterns of aspect ratios ranging from 1:1 to 1:16. Conflicting results were also reported regarding the impact of isotropic geometries (aspect ratio = 1:1) on stem cells fate. Indeed, Peng *et al*. [294]observed that the osteogenic differentiation of MSCs, based on ALP activity measurement, was higher on star micropatterns followed by triangular and square micropatterns of the same pattern dimension. However, in a similar recent work done by Wang *et al*. [381], it has been shown that MSCs maintained their stemness regardless the shape of micro-sized patterns (circle, triangle, square, pentagon, and hexagon).

Although some experimental conditions and results vary between these works such as material matrices, strategy of ligand immobilization, culture media composition, pattern size and shape and their effects, the golden rule says that pattern features that promote high cytoskeleton tension and cell spreading favor osteogenic differentiation. To date, the best-known mechanism by which geometric features influence stem cells fate was described by Kilian *et al*. [242] suggesting that MSCs commitment into osteoblasts in response to geometrical cues is modulated by cytoskeleton rearrangement leading to a high actomyosin contractility, which in turn stimulates the expression of the non-canonical Wnt signaling molecules, their receptors, and their downstream effectors, including RhoA and ROCK. Subsequently, expression of genes involved in MAP kinase pathways (ERK/JNK) is enhanced by either mechanical stimuli (cytoskeleton tension) or biochemical stimuli (Wnt signaling), leading to an up-regulation of master osteoblast regulators expression. Therefore, this signaling pathway might be involved in enhancing hMSCs osteogenesis on BMP-2-FITC micropatterned surfaces, since induced cells were well spread, presenting highly organized and contractile F-actins and exhibited cuboidal shape characteristic of mature osteoblasts.

In our cell culture model, other factors may also come into play to improve the specification of hMSCs towards osteoblast phenotype. Among these parameters, cell-cell interactions, known to play a crucial role in stem cells differentiation [391], may contribute in enhancing hMSCs osteogenesis since in the present study cells were allowed to interact with each other's, unlike to previous cited works where cells were confined in adhesive micro-islands for single cell manipulation. In this regard, Ding group [300] [392] investigated differentiation of stem cells in response to controlled and pre-defined cell contact extents, using micro-contact printing technique. Their results clearly demonstrated that the osteogenic differentiation of MSCs was significantly enhanced by cell-cell contact gap junction signaling. In addition, Jeon *et al*. demonstrated that structured materials can, in turn, influence cell-cell interactions extent, as revealed by a significantly higher gene expression of Cadherin 1 in MSCs cultured on 3D micropatterned hydrogels with the 50, 100, and 200 µm patterns compared to those grown on unpatterned hydrogels or the 25 µm pattern [382]. Moreover, they noticed a linear correlation between pattern features and cell behavior since osteogenic and chondrogenic differentiation increased with increasing pattern size and cell-cell contact. Therefore, it should be taken into account the contribution of such cell cues in regulating osteogenesis in our cell culture systems.

The third likely scenario involved in regulating the extent of hMSCs differentiation could be related to the modulation of BMP-2 bioactivity through the geometrical distribution of this ligand. Assuming that cells are highly sensitive to the spatial distribution of adhesive ligands, thus modulating integrin/ligands interactions, focal adhesion formation and maturation as well as the subsequent cell behaviors, it is likely that the spatial distribution of BMP-2 as specific shapes may also affect the binding affinity of this peptide to its receptors and the downstream signaling pathway [393]. This is supported by Zouani *et al*. work where they demonstrated that MSCs sense the stiffness of their microenvironment and respond to by modulating cytoskeleton contractility as well as BMP-2-induced smads signaling pathway, which in turn regulates the extent of MSCs osteogenic differentiation [210]. Moreover, it should be not neglected that the pattern shape and BMP-2 peptide can act synergistically to induce and enhance osteogenesis since both of them have been shown to trigger the activation of Mitogen-Activated Protein Kinase (MAPK) pathway known to play an important role in directing stem cell fate towards osteoblast phenotype [242] [336].

To summarize, we have demonstrated for the first time that spatially distributed BMP-2-FITC peptide as specific geometries at subcellular scale, even in the absence of any induction media, enhances the osteogenic differentiation of hMSCs as compared to uniformly distributed BMP-2-FITC peptide onto material surfaces. Molecular events that govern lineage-specific differentiation of hMSCs, in response the geometric distribution of growth factors, would be of interest for future studies using these cells culture models.

Conclusion

Microfabrication techniques offer a unique and versatile tool to explore and dissect the role of distinct cues within stem cells niches, including cell shape and dimension, matrix stiffness and topography as well as the spatial distribution of proteins and growth factors. In this study, structured glass surfaces were developed using photolithography by manipulating pattern geometry of RGD-TAMRA or BMP-2-FITC peptide at subcellular scale while keeping the overall area constant. When hMSCs were grown for 4 weeks on RGD-TAMRA micropatterned surfaces, most of them have kept their stemness character similarly to those cultured on homogenous surfaces, meaning that the spatial distribution of adhesive RGD-TAMRA peptide did not affect stem cells fate. Unlike RGD-TAMRA peptide, our results clearly demonstrated that the extent of hMSCs osteogenic differentiation can be modulated only by controlling the presentation of BMP-2-FITC peptide on material surfaces. Indeed, hMSCs acquired osteoblast phenotype on both homogenous and micropatterned surfaces containing BMP-2-FITC peptide, however, triangular and square peptide patterns, *i.e*. geometric features with aspect ratio of 1 and 0.7 significantly enhanced hMSCs osteogenesis.

These findings suggest that the effect of subcellular geometrical features is peptide dependent and that an optimal control of growth factors distribution over biomaterials surfaces may help to precisely guide stem cells commitment and differentiation into osteoblast cells, without recourse to osteogenic differentiation media.

Experimental Details

Materials. BorosilicateBorosilicate glass slides (76 x 26 mm, thickness ≈ 1 mm) were obtained from Schott (Tempe, AZ, USA). These slides were laser-cut into 10x10 mm pieces, to fit in 24 well cell culture plates, by ALPhANOV, France. H_2O_2 (33 wt %), concentrated H_2SO_4, acetone, ethanol, anhydrous toluene, dimethylsulfoxyde (DMSO), 3-aminopropyltriethoxysilane (APTES) and succinimidyl-4-(p-maleimidophenyl) butyrate (SMPB) were all purchased from Sigma-Aldrich, France. The fluorophore-tagged CG-K(PEG3-TAMRA)-GGRGDS adhesion peptide (referred to as RGD-TAMRA; MW 1437 g/mol) was synthesized by Anaspec (Fremont, CA, USA). CKIP-KASSVPTELSAISMLYL and fluorophore-tagged CKIPKASSVPTELSAISMLYLK-FITC peptides (referred to as BMP-2 mimetic peptide; MW 2251.75 g/mol and BMP-2-FITC mimetic peptide; MW 2769 g/mol, respectively) were produced by Genecust, Luxemburg. These peptides were first dissolved at 2 mM in DMSO and stored at - 20 °C until use. Peptides, to be conjugated with material surface, were resuspended at 20 µM in a 0.2 µm-filtered Phosphate-Buffered Saline (PBS, Life technologies, France) solution containing 7.5 % glycerol.

Preparation of resist patterned surfaces. Resist patterns were created on glass substrates using photolithography technique. Briefly, photosensible resist S1818 (CHIMIE TECH, France) was coated on glass surfaces and spun at 4000 rpm for 30 s, leading to a homogenous photoresist of approximately 2 µm. The surfaces were then baked at 110 °C for 60 s prior exposure to a pattern of light emitted by UV lampe (365 nm, 19,5 mW/cm², contact mode, 50 Hz, exposure time: 5 s) through photomasks with checkerboard patterns of different geometries (Département de génie électrique et de génie informatique, université de Sherbrooke, QC, Canada). Subsequently, the exposed resist was developed by emerging the substrates in Microposit Developer solution (MF319, CHIMIE TECH, France) for 40 s. Finally, the samples were slightly washed with deionized water to remove any traces of developed resist and dried with nitrogen gas **(Figure 31)**.

Peptide grafting and patterning. The covalent grafting of peptides was achieved as described in a previous work [185]. Briefly, glass substrates were first cleaned using a piranha treatment. Then, material surfaces were immediately aminated by immersing in APTES solution (34.5 mM in anhydrous toluene) for 3 hours, under Argon (Ar) atmosphere. The samples were washed three times with anhydrous toluene to remove unattached aminosilanes and vacuum dried at 120 °C for 30 min. Subsequently, aminated surfaces were conjugated with the heterobifunctional SMPB crosslinker by emersion in SMPB solution (3 mg/mL in DMSO) for 2 h, and then rinsed in DMSO for 10 min. This step was followed by creating resist patterns on SMPB surfaces using photolithography as described in the aforementioned section. Finally, resist patterned surfaces were covered with 200 µL of 20 µM solution of RGD-TAMRA or BMP-2-FITC peptides. After 3 h of reaction, samples were washed with deionized water under agitation, and then immersed in acetone for 1 min to remove the resist pattern, resulting in peptide patterns surrounded with SMPB domains **(Figure 31)**. Finally, the substrates were rinsed three times for 15 min in DMSO, thoroughly washed with deionized water, and stored for at most 1 month in PBS until use. Unless otherwise indicated, all reactions needed for surface modification were carried out with ≈ 50 rpm agitation, at room temperature, away from light, and cleaning steps were performed in ultrasonic bath. Patterns of RGD-TAMRA and BMP-2-FITC peptides developed using this protocol are shaped as triangles, squares or rectangles and exhibit a constant overall area at subcellular scale. In other words, each sample of 10 mm^2 is composed of 10^5 peptide patterns of 50 μm^2, regardless the pattern shape. Unpatterned glass surfaces functionalized with RGD-TAMRA and BMP-2-FITC were also prepared and served as controls for biological experiments.

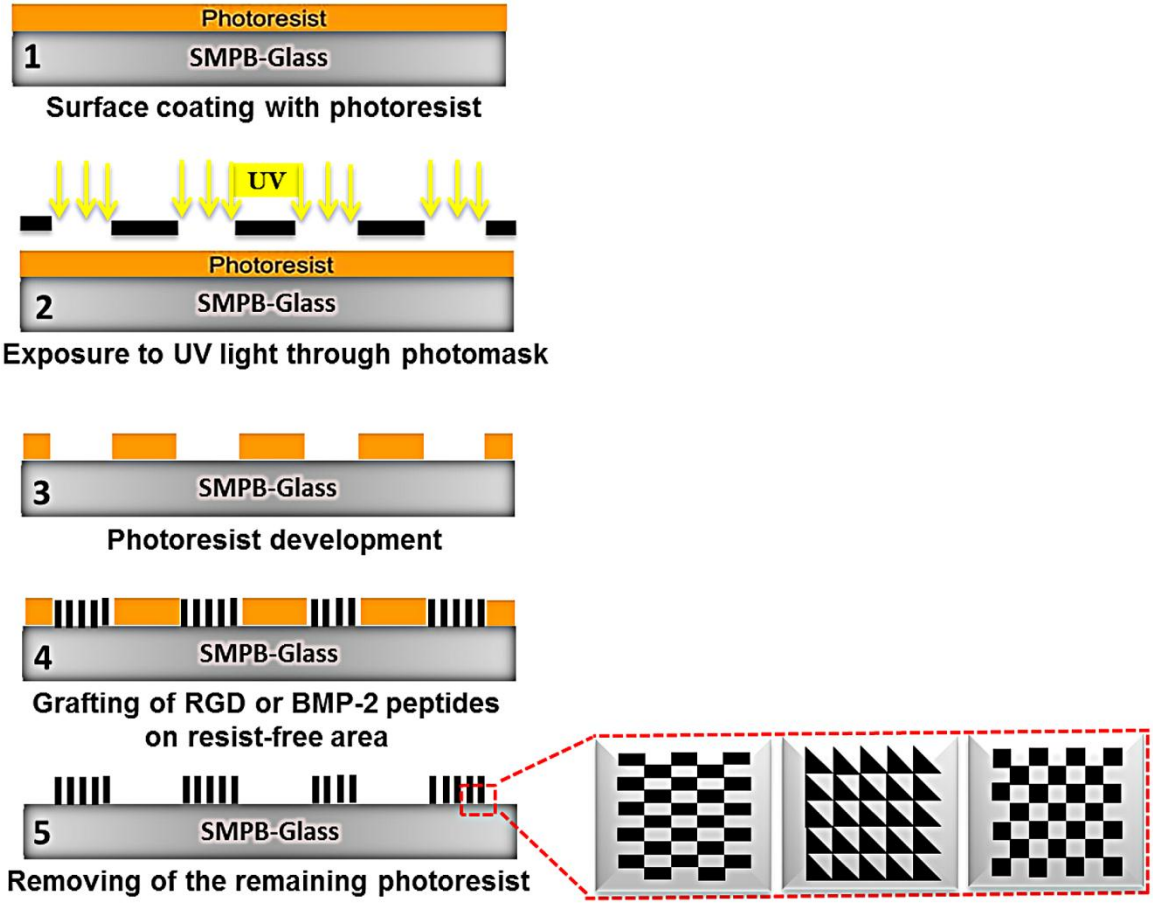

Figure 31: Schematic representation of peptide micropatterning onto glass surfaces using photolithography technique.

Surface characterization. The covalent grafting of peptides, the density of grafted peptides as well as the surface roughness after each step of surface modification were evaluated in a previous work on unpatterned glass surfaces using X-ray Photoelectron Spectroscopy (XPS), fluorescence microscopy and Atomic Force Microscopy (AFM), respectively [185]. In the present work, we have focused on evaluating the efficiency of peptide patterning using fluorescence microscopy and optical interferometry.

On resist patterned surfaces (materials corresponding to step 3 of surface patterning protocol **(Figure 31)** fluorescence microscopy was used to characterize the shape of resist patterns while optical interferometry (Bruker Nano-NT9080) was employed to measure the pattern dimensions. Resist patterns were visible under fluorescence because the S1818 resist is auto-fluorescent when excited with a 543 nm laser line. Optical interferometry measurements were carried out on dry samples, at room temperature, using the vertical

scanning interferometry mode with a vertical resolution of approximately 2 nm. The interferograms were digitalized with a CCD camera and converted into 2D topographic maps. Pattern dimensions, according to the X and Y axes, were measured on these maps using Veeco software.

Well-characterized glass surfaces containing resist patterns were then used as template for fluorescent RGD and BMP-2 patterning. Finally, the spatial distribution of peptides (samples corresponding to the step 5 of surface patterning protocol, shown in **Figure 31** was visualized under fluorescence microscopy (Leica microsystem DM5500B, microscope with a motorized, programmable stage using a CoolSnap HQ camera controlled by Metamorph 7.6).

Cell culture. hMSCs purchased from Lonza, France were maintained in MSCs growth medium (MSCGM) (Lonza, France), subcultured once a week using trypsin/EDTA 1x (Sigma-Aldrich, France) and incubated in a humidified atmosphere containing 5 % (vol/vol) CO2 at 37 °C. Subconfluent cultures of hMSCs at low passage (passage 4) were used; the cells were seeded at a density of 10^4 cells/cm² on patterned and unpatterned glass surfaces, sterilized with 70% ethanol prior to cell plating. All cell culture experiments were performed in serum free α-MEM medium (Life technologies, France) for the first 6 h of culture. This allows for interactions between grafted peptides and their cell surface receptors without interference of serum proteins. Once this time has elapsed, the medium was completed with 10 % fetal bovine serum (FBS) and 1 % penicillin/streptomycin, without addition of soluble osteogenic growth factors. The growth medium was changed twice per week for up to 4 weeks.

Lineage-specific differentiation assays. The extent of hMSCs osteogenic differentiation and cell morphology were evaluated on different conditions using immunocytochemistry staining. Briefly, at 4 weeks, cells were fixed in 4 % paraformaldehyde at 4 °C for 20 min, permeabilized with 0.5 % Triton X-100 in PBS for 15 min and blocked with 1 % Bovine Serum Albumin (BSA) in PBS for 30 min at 37 °C. The osteogenic differentiation of hMSCs was assessed by incubating cells overnight at 4 °C with 10 µg/mL monoclonal anti-STRO-1 (R&D Systems, France), 10 µg/mL monoclonal anti-Runx-2 (abcam, UK) and 1/200 (v/v) monoclonal anti-OPN (Santa Cruz Biotechnology, USA), primary antibodies produced in mouse. Subsequently, cells were treated with the secondary antibody Alexa Fluor 647 goat anti-mouse IgG (H+L) (1:400 dilution) for 1 h at 37 °C. To visualize

cytoskeleton organization, filamentous actin (F-actin) was stained with 1/200 (v/v) Alexa Fluor 488 phalloidin on RGD-TAMRA surfaces and with 1/200 (v/v) Alexa Fluor 568 phalloidin (Invitrogen, France) on BMP-2-FITC surfaces for 1 h at 37 °C. The cell nuclei were counterstained with DAPI (Sigma, France). Finally, samples were mounted on glass microscope slides with ProLong Gold antifade reagent (Sigma, France) and imaged using fluorescence microscopy (DM5500B, Germany) and MetaMorph software.

The osteogenic differentiation was also evaluated by measuring the ALP activity of hMSCs using an ALP Assay kit (Abcam, UK), according to the manufacturer's protocol. To measure intracellular ALP activity, cells were detached from the different modified glass surfaces, centrifuged at 300 g for 3 min and the supernatant was carefully removed. The cell pellets were then homogenized in the assay buffer and 80 µL of cell suspension were incubated with 50 µL of 5 mM of p-nitrophenyl-phosphate (pNPP) solution in 96-well plate at 25 °C for 60 min, away from light. The reaction was stopped by adding 20 µL of stop solution to each sample, then the absorbance (OD) was measured at 405 nm in a plate reader and compared to a standard curve obtained from simultaneously prepared pNPP solutions of known concentrations. Basically, three samples per condition were prepared for ALP assay. However, due to the low density of cells initially plated on materials (10^4) compared to that recommended by the manufacturer to measure intracellular ALP activity (10^5), we pooled cells harvested from the three samples of each condition for ALP measurements. Therefore, preliminary ALP results were obtained from only one sample per condition.

To quantify the expression levels of fluorescently stained STRO-1, Runx-2, OPN markers, we used ImageJ freeware (NIH, http://rsb.info.nih.gov/ij/). Fluorescent images to be analyzed were acquired at the same exposure time and 40x magnification. These images were opened with ImageJ software and the area of interest, which corresponds to the region of marker expression within the cell, was identified by setting a threshold. The average fluorescence density was then measured on selected area of interest. A minimum of 60 cells per condition were analyzed.

The background signal was measured on hMSCs incubated with only the secondary antibody Alexa Fluor 647; three measurements of the average fluorescence intensity per sample were performed (n=3). Finally, the background signal was subtracted from the average fluorescence density measured on all images of stained markers.

Statistical analysis. All data are expressed as mean values ± standard deviation (SD). Statistical analysis was performed by one-way analysis of variance (ANOVA) and Tukey's test for multiple comparisons, using GraphPad Prism version 6.07 for Windows, (GraphPad software, San Diego California USA, www.graphpad.com). A difference was regarded as significant when $P < 0.01$.

Acknowledgements. The authors would like to thank Dr. C. Sarra-Bournet for the photolithography mask fabrication and Dr. C. Ayela for his help for interferometric analyses. I.B. is the recipient of a scholarship from the NSERC CREATE Program on Regenerative Medicine. This work was supported by the National Science and Engineering Research Council (NSERC-Canada) (G.L) and the French "Agence Nationale de la Recherche" (ANR) (M.C.D).

Supporting Information.

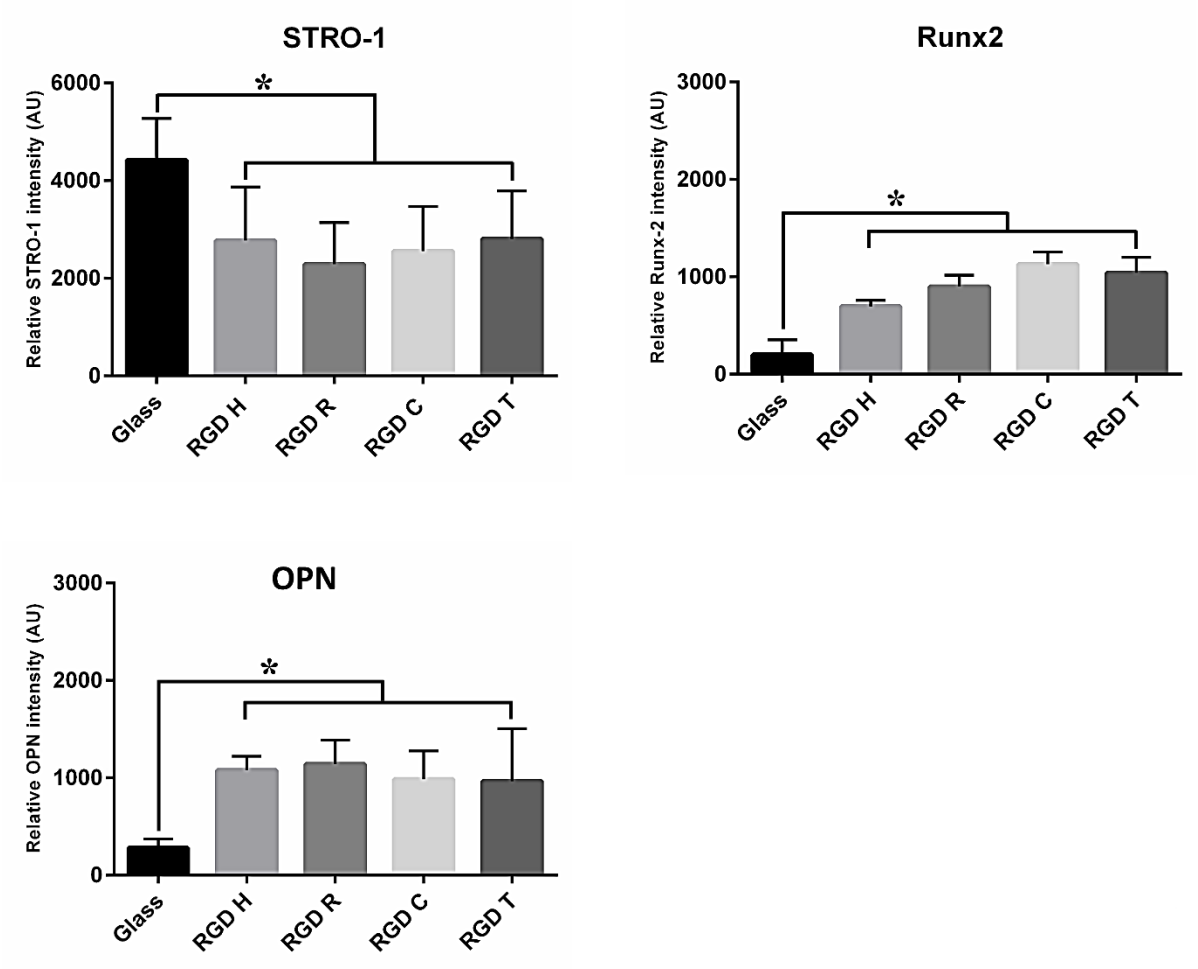

Figure 32-S1: Quantitative analysis of the total cellular immunofluorescence intensity of STRO-1, Runx-2, and OPN in hMSCs cultured on patterned and unpatterned RGD-TAMRA surfaces. ALP activity measured by colorimetric assay on the different RGD-TAMRA modified materials. H: homogenous surfaces, R: rectangular patterns, S: square patterns, T: triangular patterns.

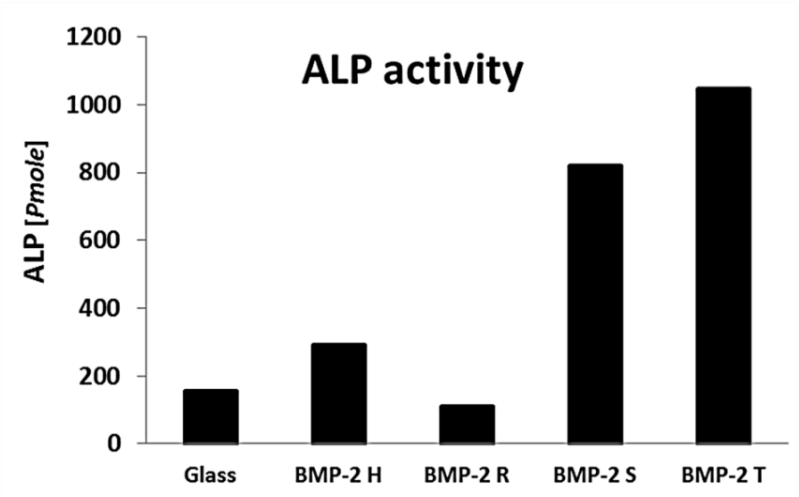

Figure 33-S2: ALP activity measurements on patterned and unpatterned surfaces containing BMP-2-TAMRA mimetic peptide.

III. Study 3: Microscale geometric cues enhance RGD/BMP-2 crosstalk-mediated hMSCs osteogenesis.

Interplay of geometric cues and RGD/BMP-2 crosstalk in directing stem cell fate

Ibrahim Bilem[abcd], Pascale Chevallier[ab], Laurent Plawinski[cde], Eli D. Sone[f], Marie-Christine, Durrieu[cde†]Gaétan Laroche[ab†]

[a]Laboratoire d'Ingénierie de Surface, Centre de Recherche sur les Matériaux Avancés, Département de Génie des Mines, de la Métallurgie et des Matériaux, Université Laval, 1065 Avenue de la médecine, Québec G1V 0A6, Canada.
[b]Centre de Recherche du Centre Hospitalier Universitaire de Québec, Hôpital St-François d'Assise, 10 rue de l'Espinay, Québec G1L 3L5, Canada.
[c]Université de Bordeaux, CBMN, UMR 5248, F-33600, Pessac, France.
[d]CNRS, Institute of Chemistry & Biology of Membranes & Nanoobjects (CBMN 5248), F-33600, Pessac, France.
[e]Bordeaux INP, CBMN, UMR 5248, F-33600, Pessac, France
[f]Institute of Biomaterials and Biomedical Engineering, Department of Materials Science and Engineering, and Faculty of Dentistry, University of Toronto, Toronto, ON M5S 3G9, Canada.

[†]Corresponding authors (equally contributed):
Gaetan.Laroche@gmn.ulaval.ca Phone: 1 (418) 656-7983 Fax: (418) 656-5343
marie-christine.durrieu@inserm.fr Phone: +33 5 40 00 30 37 Fax: +33 5 40 00 22 00

Keywords: chemical micropatterning, BMP-2 mimetic peptide, adhesive ligands, RGD/BMP-2 crosstalk, stem cell niche, bone tissue engineering.

This work has been submitted to the journal: ***Biomaterials.***

Résumé:

Au sein du microenvironnement naturel, les cellules souches mésenchymateuses (CSMs) humaines régulent leur devenir suite à leurs interactions avec la matrice extracellulaire (MEC). Cette dernière joue non seulement le rôle de support cellulaire via les interactions intégrines/ligands mais sert également de réservoir de facteurs de croissance. De plus, ces dernières années ont apporté des informations instructives sur la façon dont les intégrines s'associent aux récepteurs de facteurs de croissance et modulent leur activité, ainsi générant un effet synergétique qui joue un rôle crucial au cours du processus de différenciation cellulaire. Jusqu'à présent, la plupart, voire l'ensemble des études décrivant cet effet synergétique ont été réalisées avec des matériaux fonctionnalisés simultanément et d'une manière aléatoire avec des protéines d'adhésion et facteurs de croissance. Cependant, il est actuellement bien admis qu'au sein de la MEC naturelle, les biomolécules sont distribuées d'une manière hétérogène.

Afin de mimer à la fois l'organisation spatiale des protéines et facteurs de croissance et leur coopération *in vivo*, nous avons greffé simultanément le peptide d'adhésion RGD et le peptide ostéo-inducteur BMP-2 sous forme de motifs juxtaposés, à l'échelle micrométrique. Cela a permis d'évaluer l'effet combiné de la microstructuration des ligands et leur coopération sur la différenciation des CSM humaines vers la voie ostéoblastique. En variant la forme géométrique des micro-motifs peptidiques tout en maintenant leur taille constante, la différenciation ostéoblastique a été considérablement affectée. En effet, les micro-motifs triangulaires et carrés ont significativement amélioré la différenciation des CSMs, comparativement aux micro-motifs rectangulaires. Ces résultats suggèrent que l'organisation spatiale des molécules bioactives peut changer la façon par laquelle les CSMs perçoivent et répondent aux signaux biochimiques. Ce type de systèmes *in vitro* présente un outil intéressant pour explorer des nouveaux mécanismes responsables de la régulation de la différenciation des CMS, ainsi contribuant à la conception et au développement des biomatériaux mimant intimement la situation physiologique.

Abstract:

Within the native microenvironment, human mesenchymal stem cells (hMSCs) regulate their fate by binding to the extracellular matrix (ECM) that not only acts as support for adherent cells through integrin ligands but also as reservoir of growth factors. In fact, there is compelling evidence that integrin ligands such as RGD and growth factors such as BMP-2 are not independent systems but rather cooperate and crosstalk to regulate osteogenic differentiation. By far, cell behaviors in response to this synergistic effect have been investigated only when these ligands are homogenously distributed on material surfaces. However, recent advances in stem cell biology highlighted a heterogeneous distribution of ligands within the native environment, spanning over different length scale. Towards recapitulating the complexity of the native ECM, we present a strategy for the simultaneous patterning of RGD and BMP-2 mimetic peptides to understand the interplay of geometric cues and ligands combination in regulating hMSCs osteogenesis. RGD and BMP-2 were covalently bound to glass surfaces in patterned micro-scale regions using photolithography. By manipulating pattern shape while keeping the overall area constant, the osteogenic differentiation of hMSCs was significantly enhanced on triangular and square peptide micropatterns, as revealed by a very low expression of stemness markers (STRO-1) and an up-regulation of osteogenic markers (Runx-2 and osteopontin (OPN)) as compared to rectangular peptide micropatterns. These results demonstrate that the spatial organization of ECM-derived ligands can change how hMSCs perceive and interpret biochemical signals. Such *in vitro* systems provide an interesting tool to investigate mechanisms by which the spatial organization of ECM cues dictate hMSCs fate, thereby contributing to the design of synthetic, biomimetic versions of *in vivo* microenvironments for bone tissue engineering applications.

1. Introduction

Mesenchymal stem cells (MSCs) are considered as potential candidate in tissue engineering and regenerative medicine due to their high proliferative rate, multipotency, immunocompatibility and convenient sources with respect to ethical and religious issues [90]. *In situ*, in response to injuries, trauma or diseases, MSCs migrate from their niche to the lesion site where they repair damaged tissues and restore their functions [394]. These biological events, including stem cells self-renewal, migration and differentiation are orchestrated by a highly structured and complex cell microenvironment, so-called stem cell niche [287]. Specifically, the extracellular matrix (ECM), a key component of the stem cell niche, provides various stimuli that drastically influence MSCs fate decision [395]. Biochemical cues are the most explored and best characterized stimuli. Their distribution and abundance within the native ECM depend on the type of the targeted cell response as well as the location of the stem cell niche in the body [396]. For instance, a continuous remodeling in the composition and organization of the native ECM has been noticed at different stages of MSCs proliferation and differentiation, including the ECM enrichment with fibroblast growth factor (FGF) during proliferation [370], bone morphogenetic protein-2 (BMP-2) during osteogenenic differentiation [371], transforming growth factors (TGFβ) during chondrogenic differentiation [397] and vascular endothelial growth factor (VEGF) during angiogenic differentiation [373].

On this basis, it has been hypothesized that the translation of the *in vivo* ECM features to *in vitro* models may help to effectively and precisely control MSCs fate [10] [398]. The common approach to do so consists of decorating bioinert material surfaces with specific signaling molecules derived from the native ECM. Of a long list of these biochemical cues, fibronectin, vitronectin, collagen and laminin are the most widely used as cell adhesive ligands, while growth factors including, but not limited to, BMPs, TGFβ, VEGF, FGF are of particular relevance in guiding stem cells/progenitors towards specific lineages [180]. The particular strength of this approach rely on the concept of "solid induction mode", based on tethering functional ligands to biomaterials rather than their delivery in soluble form [211, 399]. The solid induction mode is thought to mimic the physiological situation since *in vivo* growth factors associate with ECM components such as proteoglycans and are released by cell-initiated proteolytic degradation of the matrix [395] [400]. In addition, cell exposure to matrix-bound growth factors has been shown to delay the internalization of growth factor receptors, resulting in continuous receptor activation, thereby promoting persistent signaling [395] [211] [401]. Moreover, this strategy requires smaller amounts of expensive ligands while increasing their local concentration. For example, it

has been shown that matrix-bound BMPs promote bone formation at dosages lower than those used in soluble delivery [402].

Such progress in biomaterials research, in parallel with the development of mimetic peptides, have significantly contributed in reducing experimental costs, thus offering further opportunities for scientist to deeply invest in understanding mechanisms by which biochemical cues affect stem cell fate. Indeed, a bidirectional crosstalk between growth factors and integrins ligands has been highlighted three years ago [403] [404], however, the underlying mechanism has been seriously investigated only more recently. Among evidences suggesting the existence of such crosstalk are: (i) various growth factor binding sites have been found in ECM proteins, such as the heparin binding domains identified in fibronectin [395] [405], (ii) αV integrins, an RGD-binding integrins, form physical complexes with several growth factor receptors, such as IGF, PDGF, VEGF, FGF and TGFβ1 receptors [406] [407] [408], (iii) growth factors receptors/ligands binding elicits a preferential activation of receptors fraction which is integrin-associated [406] and (iv) Integrins/ligands binding promotes cell adhesion to the matrix, which in turn induces tyrosine phosphorylation and the subsequent activation of several tyrosine kinase proteins such as focal adhesion kinase (FAK) [409] and PDGF, FGF-R, EGF receptors [410] [411]. Specifically, the synergistic cooperation between integrins ligands and growth factors has been exploited in bone tissue engineering applications and promising results have been reported both *in vitro* and *in vivo* [343] [412] [413] [414]. In spite of these considerable progresses in biomimetic materials engineering, it is still difficult to produce clinically relevant amount of MSCs *in vitro* and obtain, from these cells, a homogenous and fully differentiated cell population.

One promising direction towards resolving this hurdle involves the consideration of other properties of the native ECM such as geometric and mechanical cues that also have a distinct impact on stem cell fate. So far, most of biomimetic materials used in tissue engineering impose to the cells a homogenous microenvironment while in the physiological situation, stem cells are thought to encounter complex, spatially and temporally controlled biochemical mixtures of chemokines, cytokines and growth factors, as well as ECM proteins [415] [416]. This has been proven following the characterization of several niches in various mammalian tissues as described elsewhere [287] [417] [418] [419] [420]. In addition, several recent *in vitro* studies supported these observations, as it has been reported that varying the spatial presentation of functional ligands elicits very distinct patterns of cellular response [132]. Therefore, presenting proteins and growth factors in a spatially controlled manner is an additional step toward recreating the natural cellular microenvironment by combining both biochemical and topographical properties. Creating finely-

tuned *in vitro* microenvironments can be achieved thanks to the recent progress in micro-engineering techniques. The extent of these techniques during the last couple decades can be easily noticed by a rapid growing body of literature on the use of surface micropatterning as tool to decipher the complexity of stem cell niche [288].

In stem cell research, microfabrication techniques have been applied to (i) dissect combinatorial effects of multiple ligands on stem cell fate using high throughput protein microarrays [31], (ii) recapitulate the spatial complexity of ECM components, including biomolecules gradients and distribution [315] (iii) investigate the behavior of individual, spatially confined stem cells using high-throughput single-cell handling techniques [132] [288] [415]. The study presented here belongs to the second category of micropatterning applications given that the objective is to evaluate hMSCs fate in response to dually grafted and micropatterned RGD/BMP-2 peptides on glass surfaces. This work is a continuity of a recent published study reporting enhanced hMSCs osteogenesis in response to the synergistic cooperation of RGD and BMP-2 peptides, when homogenously grafted [185]. Herein, the issue is to investigate whether RGD/BMP-2 crosstalk and geometric cues cooperate together to accelerate MSCs osteogenesis. Directing MSCs fate towards the osteogenic lineage by controlling the spatial organization of ECM-derived ligands has been achieved either on confined single cells [241] [242] or at the multicellular level [421] [422]. However, most, if not all studies have been conducted using individual spatially distributed ligands, mainly cell adhesion proteins/peptides [385]. In this study, the designed *in vitro* systems consist of combined and spatially distributed RGD and BMP-2 peptides, thereby imposing defined cell adhesion pattern, while promoting osteogenic differentiation. Such *in vitro* systems, which somewhat closely mimic the native ECM, are of particular interest to better understand stem cell biology, whereby contributing to the development of optimized cell culture substrates.

2. Materials and methods

2.1 Materials

Borosilicate glass slides (76 x 26 mm, thickness ≈ 1 mm) were purchased from Schott (Tempe, AZ, USA). To fit in 24 well cell culture plates, these slides were laser-cut into 1 cm² pieces by ALPhANOV, France. H_2O_2 (33 wt %), concentrated H_2SO_4, acetone, ethanol, anhydrous toluene, dimethylsulfoxyde (DMSO), 3-aminopropyltriethoxysilane (APTES) and succinimidyl-4-(p-maleimidophenyl) butyrate (SMPB) were all purchased from Sigma-Aldrich, France. The fluoro-tagged CG-K(PEG3-TAMRA)-GGRGDS adhesion peptide (referred to as RGD-TAMRA; MW 1437 g/mol) was synthesized by Anaspec (Fremont, CA, USA). CKIPKASSVPTELSAISMLYL and fluoro-tagged CKIPKASSVPTELSAISMLYLK-FITC peptides (referred to as BMP-2 and BMP-2-FITC mimetic peptides, respectively) were produced by Genecust, Luxemburg. Peptides, to be conjugated with glass surfaces were first dissolved at 2 mM in DMSO and then resuspended in a 0.2 µm-filtered Phosphate-Buffered Saline (PBS, Life Technologies, France) solution containing 7.5 % glycerol to reach a final concentration of 20 µM.

2.2. The creation of RGD/BPM-2 micropatterns onto glass surfaces

2.2.1. Surfaces functionalization

The grafting of spatially distributed RGD and BMP-2 peptides was achieved by conjugating glass surfaces with an aminosilane coupling agent ($C_9H_{21}O_3Si$-NH2), thus allowing the creation of covalent link between the NH_2 terminated aminosilane and the $N_{terminal}$ cysteine-containing peptides through a heterobifunctional crosslinker. Briefly, glass substrates were, first, cleaned using piranha treatment and subsequently immersed in APTES solution (34.5 mM in anhydrous toluene) during 3 hours, under agitation and Argon atmosphere. After silanization, the samples were successively washed and ultrasonically cleaned with anhydrous toluene to remove unattached APTES. Aminated glass substrates were then vacuum-dried at 120 °C for 30 min and subsequently conjugated with the heterobifunctional SMPB crosslinker by emersion in SMPB solution (3 mg/mL in DMSO) for 2 h under agitation. SMPB-modified surfaces were then ultrasonically cleaned in DMSO for 10 min, air-dried and finally stored under vacuum and away from light for a maximum of 24 h prior to peptide micropatterning. More details regarding the strategy of peptide grafting are published in a previous work [185].

2.2.2. Microstructuration of functionalized surfaces using photolithography

Photolithography was used for the dual grafting of RGD and BMP-2 peptides in a spatially controlled manner. Photosensible resist S1818 (CHIMIE TECH, France) was coated on functionalized glass substrates, spun at 4000 rpm for 30 s and then baked at 110 °C for 60 s to drive off excess resist solvent. After baking, photosensible resist was exposed to a pattern of light emitted by a UV lamp (365 nm, 19.5 mW/cm², contact mode, 50 Hz, exposure time: 5 s), which allows the transfer of geometric patterns from a photomask to resist-coated glass surfaces. Predesigned patterns on the photomask were shaped as triangles, squares or rectangles, exhibiting a constant overall area of 50 µm². The exposed resist was then removed by immersion in Microposit Developer solution (MF319, CHIMIE TECH, France) for 40 s, thus allowing the appearance of micro-sized resist patterns on glass surfaces. Finally, the samples were slightly washed with deionized water (DI H_2O) and dried with nitrogen gas. Under optical microscopy, microstructured surfaces resemble to a checkerboard of resist micropatterns surrounded with SMPB-grafted regions. The steps involved in the photolithographic process are shown in **Figure 34**.

2.2.3. Dual peptide grafting and micropatterning onto glass materials

Peptide micropatterning was performed in two steps. First, resist microstructured surfaces with photosensible resist were covered with 200 µL of 20 µM fluoro-tagged RGD-TAMRA solution for 3 h. This permits the interaction of SMPB crosslinker via its maleimide function with the $N_{terminal}$ cysteine of each peptide, in resist-free regions. The substrates were then thoroughly washed with DI H_2O to remove any excess of peptide solution. In a second step, materials were immersed in acetone bath for 1 min to remove photosensible resist, thus allowing the immobilization of BMP-2-FITC peptide between RGD-TAMRA micropatterns, using the same protocol of peptide grafting **(Figure 34)**. Finally, the substrates were ultrasonically cleaned three times for 15 min in DMSO, thoroughly washed with DI H_2O and stored for at most 1 month in PBS until use. In short, three types of structured surfaces were developed; triangular, square and rectangular micropatterned surfaces containing co-grafted RGD-TAMRA and BMP-2-FITC peptides. Glass surfaces homogenously functionalized with RGD-TAMRA and BMP-2-FITC peptides were also prepared to be used as controls for cell differentiation experiments.

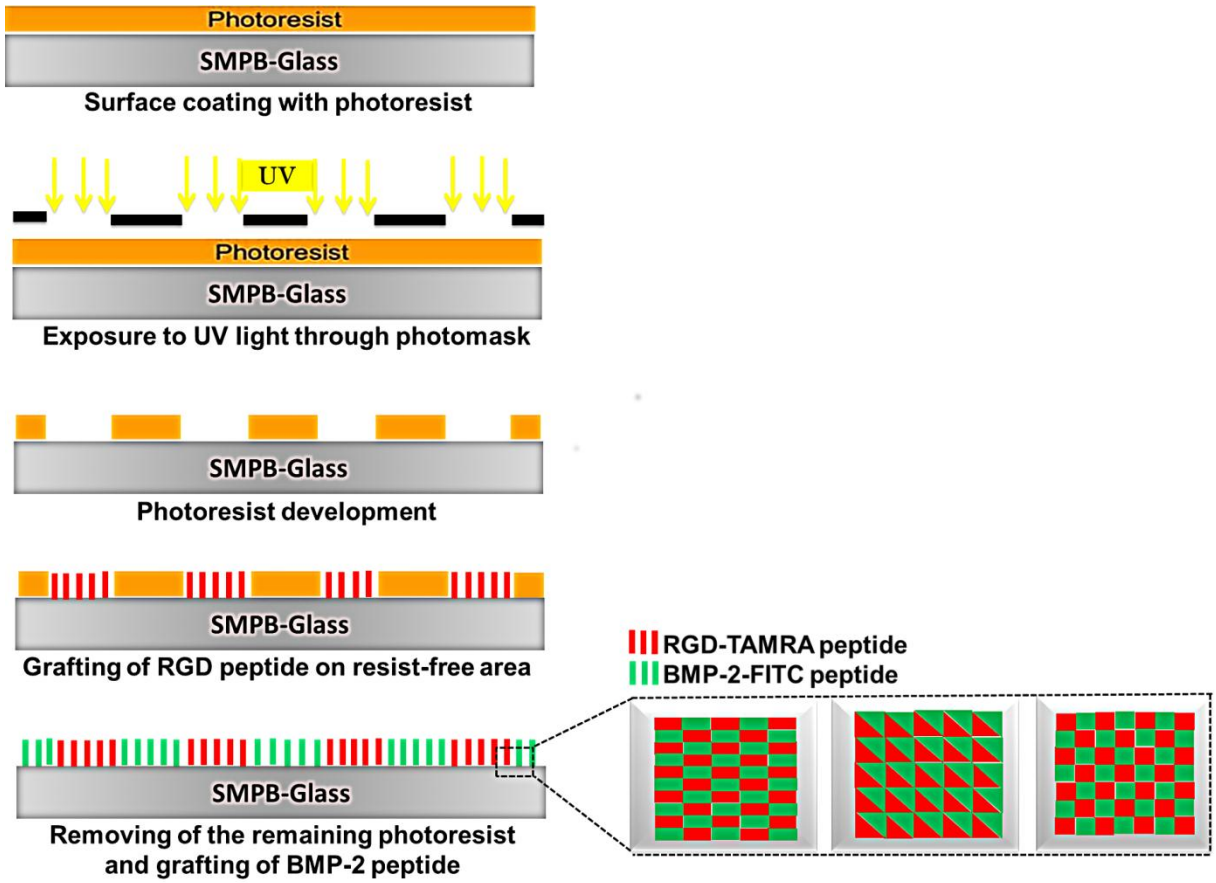

Figure 34: Schematic representation of peptide micropatterning onto glass surfaces using photolithography.

2.4. Surface characterization

Peptide micropatterned surfaces were characterized using optical interferometry and fluorescence microscopy. At first, optical interferometry, a non-contact 3D surface mapping instrument (Bruker Nano-NT9080), was used prior to peptide grafting on glass substrates containing resist micropatterns. Analyses of surface features were carried out on dry samples, at room temperature, using the vertical scanning interferometry mode with a vertical resolution of approximately 2 nm. The interferograms were digitalized with a CCD camera and converted into 2D topographic maps. As previously mentioned, these structured surfaces were used as template for peptide micropattering. Peptide micropatterns were evaluated using fluoro-tagged RGD-TAMRA and BMP-2-FITC peptides under fluorescence microscopy (Leica microsystem DM5500B, microscope with a motorized, programmable stage using a CoolSnap HQ camera controlled by Metamorph 7.6).

2.4. Cell culture

Materials used for cell differentiation experiments were slightly different from those shown in **Figure 36**, since the RGD peptide was labeled with a fluorescent tag (RGD-TAMRA), but not the BMP-2 peptide. In fact, hMSCs differentiation was evaluated on patterned and unpatterned glass surfaces containing RGD-TAMRA/BMP-2 peptides. By this way, cells were fluorescently stained for several components (nuclei, cytoskeleton and osteogenic differentiation markers), whilst tracking their interactions with readily identifiable peptide micropatterns. Later in this study, peptides will be referred as RGD and BMP-2 for the sake of simplification.

Commercially available hMSCs, purchased from Lonza, France, were maintained in MSCs growth medium (MSCGM) (Lonza, France), subcultured once a week using trypsin/EDTA 1x (Sigma-Aldrich, France) and incubated in a humidified atmosphere containing 5 % (vol/vol) CO_2 at 37 °C. For differentiation experiments, hMSCs at low passage (passage 4) were seeded at a density of 10,000 cells /cm² on patterned and unpatterned glass surfaces, all previously sterilized with 70 % ethanol. hMSCs were cultured in α-MEM growth medium (Life Technology, France) containing 10 % fetal bovine serum (FBS) and 1 % penicillin/streptomycin for 4 weeks, except for the first 6 h where cells were exposed to serum free α-MEM medium. This permits the interactions between grafted peptides and their cell surface receptors without interference of serum proteins. Cell culture medium was changed every three days.

2.5. Lineage-specific differentiation assays

The extent of hMSCs osteogenic differentiation was evaluated using specific markers of both hMSCs (STRO-1) and osteoblastic cells (Runx-2, osteopontin (OPN)).

The expression of these markers in hMSCs was assessed by immunocytochemistry staining after 4 weeks of cell differentiation. Cells were fixed in 4 % paraformaldehyde at 4 °C for 20 min, permeabilized with 0.5 % Triton X-100 in PBS for 15 min and blocked with 1 % Bovine Serum Albumin (BSA) in PBS for 30 min at 37 °C. Subsequently, cells were incubated overnight at 4 °C with 10 µg/mL monoclonal anti-STRO-1 (R&D Systems, France), 10 µg/mL monoclonal anti-Runx-2 (Abcam, UK) or 1/200 (v/v) monoclonal anti-OPN (Santa Cruz Biotechnology, USA), primary antibodies produced in mouse. Cells were washed in PBS containing 0.05 % Tween 20 and then incubated with the secondary antibody Alexa Fluor 647 goat anti-mouse IgG (H+L) (1:400 dilution) for 1 h at 37 °C. The cell morphology and cytoskeleton organization were evaluated by labeling filamentous actin (F-actin) with Alexa Fluor 488 phalloidin (Invitrogen, France) [1/200 (v/v), 1 h, 37 °C]. Samples were then mounted on glass microscope slides and stained for nuclei using Fluoroshield™ with DAPI (Sigma, France). Fluorescently stained cells

were examined by fluorescence microscopy (DM5500B, Germany) and MetaMorph 7.6 software.

The expression levels of STRO-1, Runx-2 and OPN markers in differentiated hMSCs were quantified using ImageJ freeware (NIH, http://rsb.info.nih.gov/ij/), using a slightly modified version of the Jensen's protocol [46]. Fluorescent images to be analyzed were acquired at the same exposure time and 40x magnification. Fluorescently stained cells were imaged at the same exposure time and 40x magnification. Image files were opened with Image J, converted to 16-bit files, and the area of interest, which corresponds to the red color emitted by the label, was selected by setting a threshold. The average fluorescence density was then measured on selected area of interest on a minimum of 60 cells *per* condition. The background signal, measured on hMSCs only stained with the secondary antibody Alexa Fluor 647, was subtracted from the average fluorescence density of stained STRO-1, Runx-2 and OPN markers.

2.6. Statistical analysis

The data of fluorescence intensity were expressed as the mean ± standard deviation (SD) and were analyzed by one-way analysis of variance (ANOVA) and Tukey's test for multiple comparisons, using GraphPad Prism version 6.07 for Windows (GraphPad software, San Diego California USA, www.graphpad.com). Significant differences were determined for *P* values of at least < 0.01.

3. Results

3.1. Characterization of micropatterned surfaces

Prior to the characterization of peptide micropatterned surfaces, the completion of peptides conjugation was monitored using X-ray Photoelectron Spectroscopy (XPS), Atomic Force Microscopy (AFM) and fluorescence microscopy. These results were presented in a previous work [185]. In the present study, the same protocol of peptide grafting was used to immobilize RGD and BMP-2 on glass surfaces as specific micropatterns, and therefore, the attention was focused on the evaluation of pattern features (shape and size) by optical interferometry and fluorescence microscopy. Pattern shapes were first verified through the observation of structured surfaces containing photosensible resist micropatterns **(Figure 35)**. Indeed, images clearly showed well defined geometries shaped as triangles, squares, and rectangles, which demonstrates the high fidelity of pattern transfer from the photomask to the substrate. Well-characterized resist micropatterned surfaces were then used as a mold for the dual micropatterning of RGD and BMP-2 peptides. Fluorescent images, depicted in **Figure 36**, showed readily identifiable micropatterns of

fluoro-tagged RGD/BMP-2 peptides. Indeed, they exhibited the expected geometries with dimension, measured using ImageJ, close to the originally defined features size of 50 µm² **(Figure 36**). In addition, uniform fluorescence intensity across micropatterned surfaces was observed, suggesting that the peptides were evenly distributed.

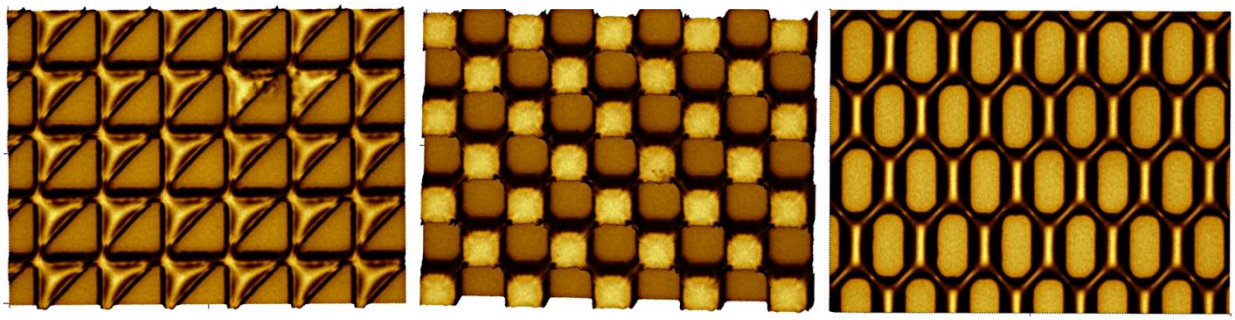

Figure 35: Optical interferometry 2D maps of the resist micropatterns of varied geometries created onto glass substrates.

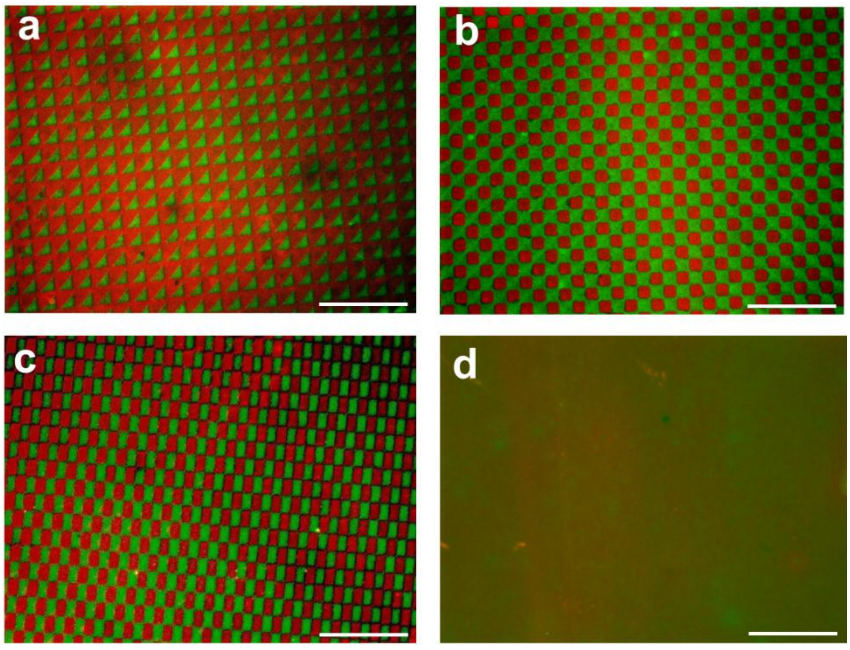

Figure 36: Fluorescence photomicrographs of triangular (a), square (b), rectangular (c) micropatterned glass surfaces containing combined fluoro-tagged RGD-TAMRA (red) and BMP-2-FITC (green) peptides. (d) corresponds to RGD-TAMRA and BMP-2-FITC peptides homogenously grafted onto glass substrates. Scale bar: 50 µm.

3.2. Osteogenic differentiation of hMSCs mediated by micropatterns shape

The extent of hMSCs differentiation in response to the spatial distribution of combined RGD/BMP-2 peptides, known to act synergistically in regulating osteogenesis, was evaluated on hMSCs grown on peptide micropatterns of different geometries. The early lineage commitment of hMSCs towards the osteoblastic lineage was evaluated after 4 weeks of culture in basal medium by assessing the expression of fluorescently stained STRO-1 and Runx-2 markers. STRO-1 is known as the most frequently used stem cells marker, while Runx-2 is considered as an early marker of osteogenic commitment. Negative controls consisted of hMSCs cultured on bare glass surfaces. At first sight, the vast majority of hMSCs have lost their stemness state on RGD/BMP-2 surfaces, regardless the spatial distribution of grafted peptides. Indeed, fluorescent images indicated that hMSCs did not express STRO-1 marker on both patterned and unpatterned glass substrates with peptides, while those cultured on control materials maintained their stemness state (STRO-1 positive) **(Figure 37)**. These observations were in agreement with quantitative analyses, as they showed very low levels of STRO-1 in all conditions, except the controls **(Figure 37)**.

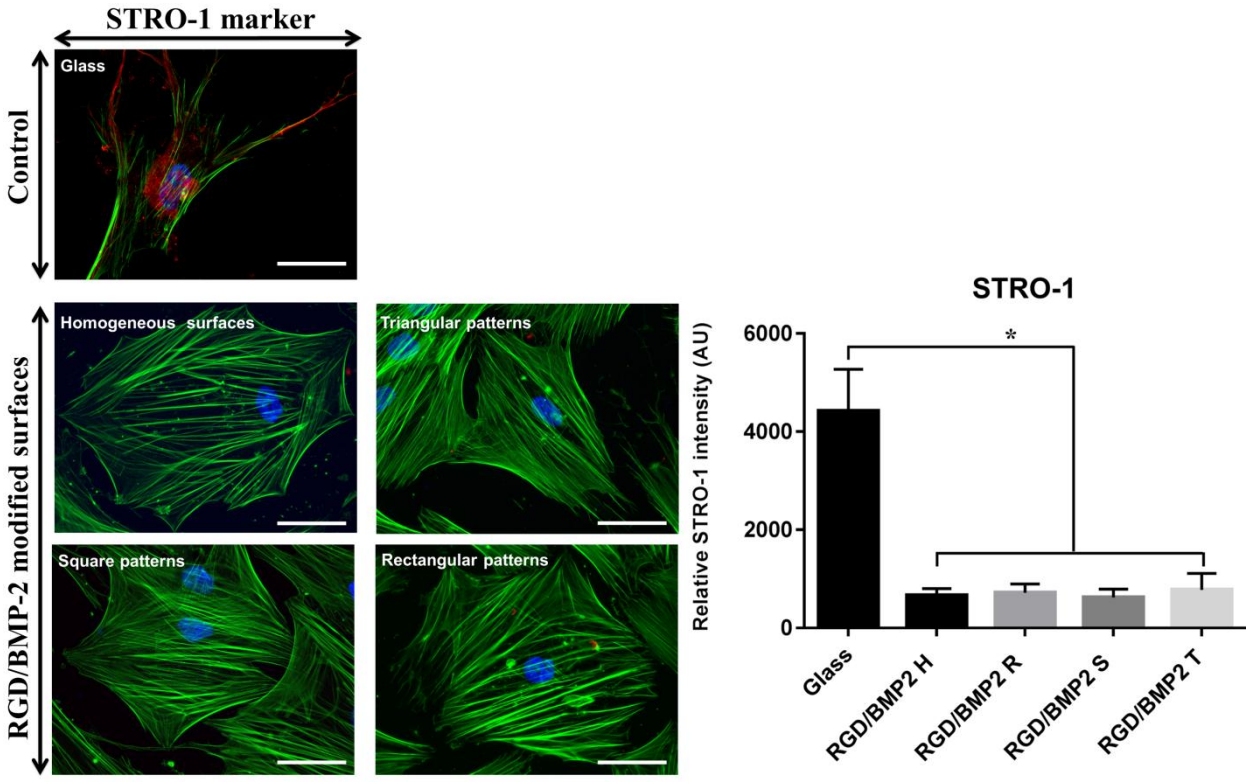

Figure 37: hMSCs cultured for 4 weeks on micropatterned and unpatterned surfaces containing combined RGD/BMP-2 peptides. Cells were stained for stemness (STRO-1) marker in red, with F-actin stained in green and cell nucleus in blue (left). Quantitative analyses of the total cellular immunofluorescence intensity of STRO-1 in hMSCs (right). H: homogenous surfaces, T: triangular patterns, S: square patterns, R: rectangular patterns. Scale bar: 50 µm.

To verify whether hMSCs that have lost their stemness character underwent osteoblast lineage commitment, the expression profile of Runx-2 was evaluated. Based on qualitative analyses, hMSCs expressed Runx2 on all peptide modified surfaces, but not on bare glass surfaces **(Figure 38)**. However, quantitative analyses revealed noticeable differences in Runx-2 intensity which varies by varying the shape of peptide micropatterns. Specifically, the highest Runx-2 intensities were observed on triangular and square geometries, conversely to rectangular ones, where the expression level was similar to that observed on unpatterned surfaces **(Figure 38)**. Compared to bare glass materials, all of the four conditions exhibited significantly higher levels of Runx-2 **(Figure 38)**.

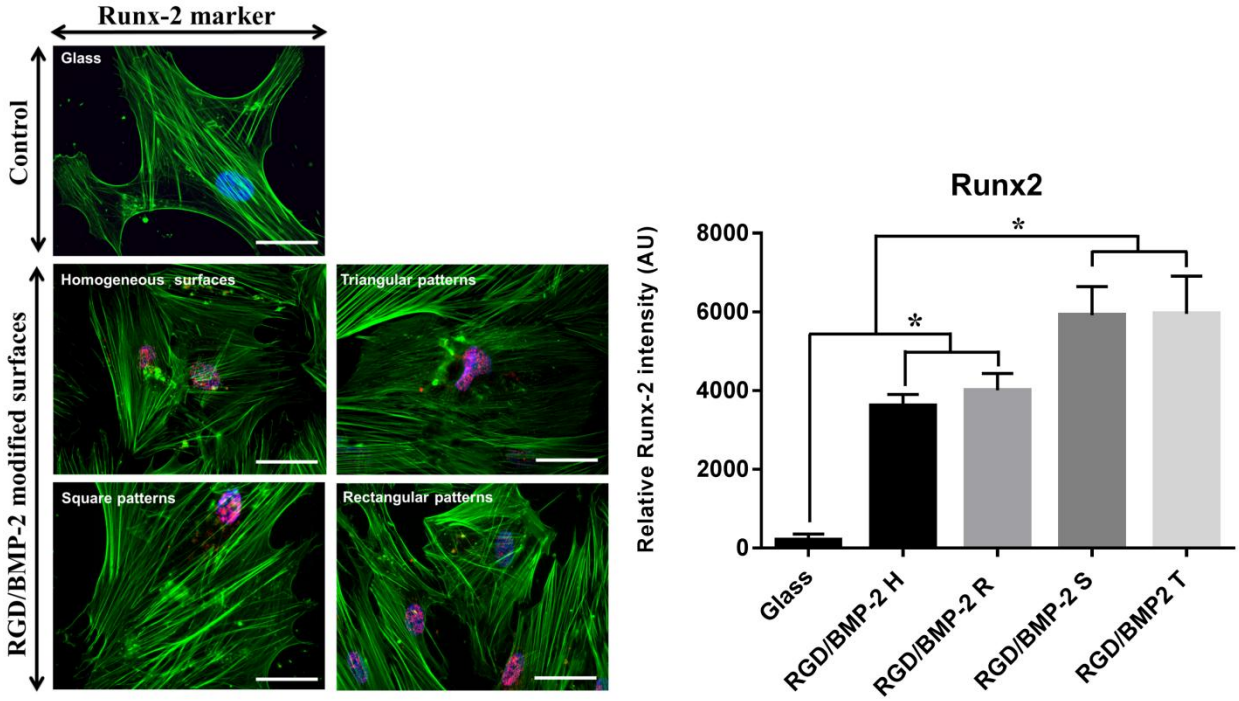

Figure 38: hMSCs cultured for 4 weeks on micropatterned and unpatterned surfaces containing combined RGD/BMP-2 peptides. Cells were stained for the early osteogenic (Runx-2) marker in red, with F-actin stained in green and cell nucleus in blue (left). Quantitative analyses of the total cellular immunofluorescence intensity of Runx-2 in hMSCs (right). H: homogenous surfaces, T: triangular patterns, S: square patterns, R: rectangular patterns. Scale bar: 50 µm.

Taken together, the expression profile of STRO-1 and Runx-2 markers confirmed that the micro-scale distribution of RGD/BMP-2 peptides can regulate hMSCs commitment towards the osteo-blastic lineage. These interesting observations conducted towards further analyses in order to verify whether committed hMSCs reached a mature osteoblast phenotype on the different peptide modified glass surfaces. To do this, cells were stained for OPN, which is a later stage osteogenic marker, and analyzed both qualitatively and quantitatively. The expression of OPN was first vis-

ually observed on hMSCs grown for 4 weeks on peptide micropatterned surfaces as well as unpatterned surfaces, as depicted in **Figure 39**. By quantifying marker expression yield, data clearly showed that triangular and square micropatterns of RGD/BMP-2 had significantly higher impact on up-regulating the expression of OPN than rectangular micropatterns **(Figure 39)**. Compared to unpatterned surfaces, rectangular micropatterned surfaces induced similar levels of OPN, meaning that rectangular geometries had no significant influence on regulating hMSCs osteogenic differentiation **(Figure 39)**. hMSCs cultured on bare glass substrates exhibited very low expression of OPN marker. Taken together, these results obviously demonstrated that hMSCs cultured on RGD/BMP-2 micropatterns exhibiting triangle and square shapes had entered a more mature stage of osteoblast lineage differentiation than those cultured on rectangular micropatterns. It is worth noting that micro-geometrical distribution of combined RGD/BMP-2 peptides can greatly affect hMSCs osteogenesis without the need of supplementing culture media with soluble osteogenic factors.

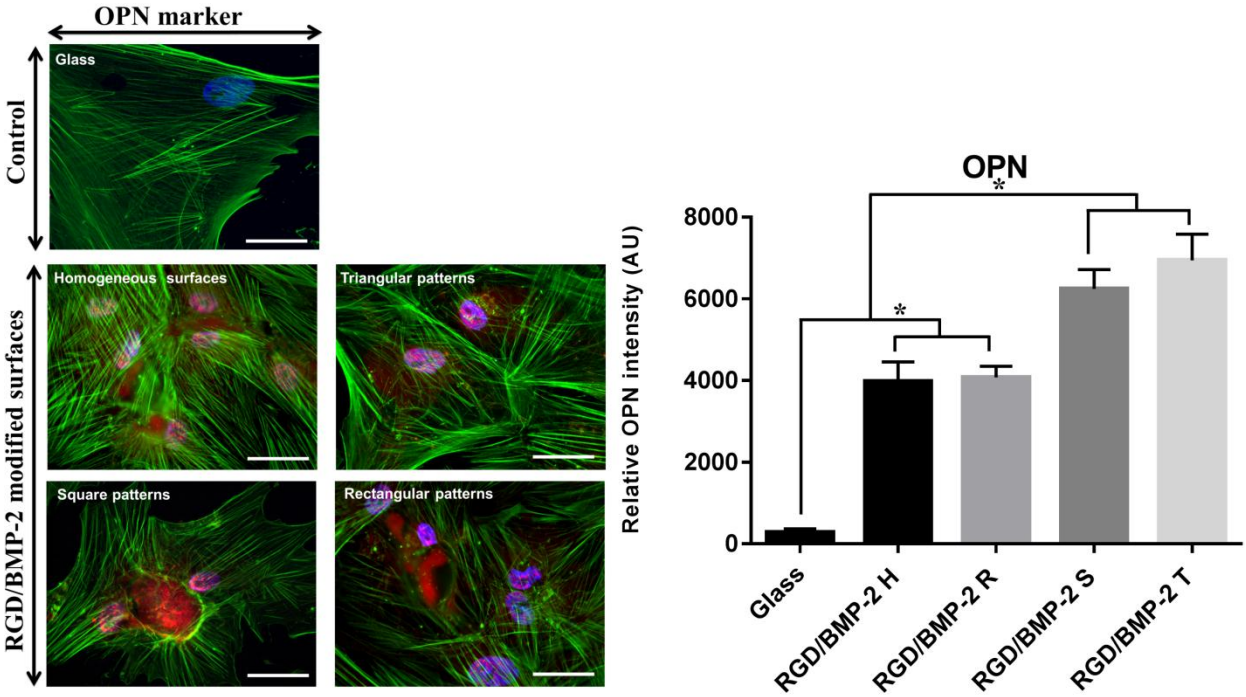

Figure 39: hMSCs cultured for 4 weeks on micropatterned and unpatterned surfaces containing combined RGD/BMP-2 peptides. Cells were stained for the late osteogenic (OPN) marker in red, with F-actin stained in green and cell nucleus in blue (left). Quantitative analyses of the total cellular immunofluorescence intensity of OPN in hMSCs (right). H: homogenous surfaces, T: triangular patterns, S: square patterns, R: rectangular patterns. Scale bar: 50 µm.

4. Discussion

Directing fate-specific differentiation of MSCs is a complex process involving subtle changes in cell morphology, gene expression and ECM proteins abundance. *In vivo*, this process is governed by various stimuli, chemical or physical in nature, originating from stem cell niches [287] [395] [396]. *In vitro*, biochemical cues are the most explored ECM feature for guiding MSCs towards the desired cell phenotype. For example, BMP-2, belonging to the Transforming Growth Factor beta family ((TGF-β), has been successively tested *in vitro* [342], in animal models [423] and has gained USA Food and Drug Administration approval for spinal fusion procedure, tibial shaft fracture treatment and oral-maxillofacial reconstruction [424]. However, the current strategy relies on the principle of presentation-dependent ligand activity. Obviously, this vision, inspired from the physiological situation, highlights the combinatorial effect of a mixture of ligands intended to synergize together and elicit faster and more robust cell differentiation. To date, several reports have proved the importance of presentation-dependent ligand activity. The Wang et al. study, amongst others, demonstrated that collagen IV proteins enhance the interactions of Decapentaplegic, a BMP-4 homologue, with its receptors in *Drosophila* early embryo [401]. Ligand crosstalk has also been observed between partial sequences of the ECM proteins and morphogen (mimetic peptides). For instance, He et al. investigated the effect of several combinations of RGD, BMP-2 and OPN peptides on rat MSCs osteogenic differentiation. They demonstrated a significant continuous increase of ALP activity (at 14 days) and calcium content and OPN expression (at 28 days) from RGD, RGD+BMP-2 to RGD+BMP-2+OPN hydrogels [228]. Consistent with these findings, we recently demonstrated that RGD peptide enhanced BMP-2-induced hMSCs osteogenesis, without recourse to differentiation media [185]. In addition, a bidirectional crosstalk has been reported between integrins and growth factors receptors, resulting in the regulation of integrins expression by growth factors, such as α_2 and α_3 by hepatocyte growth factor (HGF) [425] or the activation of growth factors receptors by the integrin/ligand interactions, even in the absence of soluble growth factors [411]. Therefore, accumulating evidences suggested that integrins control the functional activities of growth factor receptors and act synergistically with them, to activate the same signaling pathway.

Towards the design of the next-generation biomaterials, it seems of great interest to not only recapitulate the biochemical composition of the native ECM, but also its hierarchical organization. Indeed, it is now well-established that biochemical cues distribution within the bone ECM span several orders of magnitude, taking as an example the organization of fibronectin into 5-20 nm diameter fibrils that extend for several µm [426].

On this basis, we investigated here whether the micro-scale distribution of dually grafted RGD and BMP-2 peptides accentuates hMSCs lineage specification as compared to the homogenous distribution of these peptides. Indeed, well-defined artificial microenvironments, comprising highly organized and co-localized patterns of RGD/BMP-2 peptides, were developed **(Figure 36**).

Patterns size, leading to a center-to-center spacing varying from 5 to 10 µm, was chosen so that they can probe the size of mature focal adhesions of approximately 1-5 µm [53]. Patterns shape (triangle, rectangle, square) has been inspired from the characteristics of geometric cues reported to preferentially promote multipotent MSCS to differentiate into osteoblastic cells [242] [294] [301]. Other parameters have also been carefully controlled to eliminate the maximum of interferential factors that may influence cellular responses, thereby allowing a reliable evaluation of hMSCs differentiation in response to micro-scale spatially distributed peptides. First, the efficiency of peptide micropatterning was checked on all materials. Indeed, fluorescent images of RGD/BMP-2 micropatterns, shown in **Figure 36**, are representative of the pattern quality on the 150 samples employed for cell differentiation experiments. Second, hMSCs were plated on patterned and unpatterned surfaces in serum-free medium during the first 6 h of cell culture in order to allow the interactions of peptides with their receptors, thus avoiding the effect of adsorbed serum proteins. Third, the differentiation of hMSCs was evaluated after 4 weeks of culture in the absence of osteogenic differentiation media, known to greatly influence cell differentiation. Therefore, all of cells were exposed to the same local environments, thus ruling out the probability that cells may behave differently in response to external factors besides RGD/BMP-2 micropatterns. Regarding the characterization of hMSCs state, stemness (STRO-1) marker and both early (Runx-2) and late (OPN) osteogenic markers were employed to ascertain the degree of which geometric cues influence the extent of hMSCs osteogenesis.

Cell differentiation data clearly demonstrated that hMSCs sense peptide micropatterns of specific geometric cues and respond to. Indeed, square and triangular RGD/BMP-2 micropatterns significantly enhanced hMSCs osteoblast-lineage differentiation, while rectangular micropatterns induced similar trend of hMSCs differentiation as compared to unpatterned surfaces **(Figure 37) (Figure 38)**. These findings provide evidence that both biochemical and geometric cues are involved in regulating the osteogenic differentiation of hMSCs.

RGD peptide, derived from fibronectin ECM proteins, and BMP-2 peptide, corresponding to residues 73-92 of Bone Morphogenetic Protein-2, were successfully tested for their ability to promote cell adhesion [326] and osteogenic differentiation [185] [187], respectively, and syner-

gistically enhance hMSCs osteogenesis when combined [211] [185] . BMP-2-mediated osteogenesis begins by the interactions of BMP-2 ligand with type I and type II transmembrane serine/threonine kinase receptors. The activation of BMP-2 receptors induces the phosphorylation of smads 1/5/8 and their translocation into the nucleus. This smad-dependent pathway promotes the expression of early and critical transcription factors regulating osteoblast differentiation such as Runx-2 [187] [211], which in turn regulates the expression of late osteoblast phenotype markers such as bone sialoprotein (BSP) and osteopontin (OPN) [358]. Although BMP-2 ligands can modulate cell differentiation independently, they can also affect cell fate in cooperation with integrins binding ligands. Several signaling pathways have been suggested as modulators of cell differentiation through integrins/growth factors receptors interactions, including Ras-MAPK (mitogen-activated protein kinase) pathway, phosphoinositide 3-kinase (PI3K)-Akt pathway, regulation of Rho family GTPases, activation of focal adhesion kinase (FAK) and its downstream targets such as ERK and JNK/MAPK pathways. For a more comprehensive understanding of these signaling pathways, we refer readers to several recent reviews [427] [375] [224]. Very recently, Fourel et al. demonstrated in an impressive work that Smad signaling is also involved in controlling cell migration and fate commitment through BMP-2 receptors and β3 integrin crosstalk [413]. Besides RGD/BMP-2 crosstalk, the spatial distribution of functional ligands as specific micro-sized geometric patterns seems to play a crucial role in dictating lineage-specific differentiation of hMSCs. Although, the use of geometric cues to control MSCs fate is a recent topic of debate, interesting findings have been reported regarding the specification of MSCs into specialized phenotypes in response to micro-scale spatially distributed ligands. For example, McBeath et al. [241] cultured MSCs on different micro-sized fibronectin islands (1024 μm², 2025 μm² and 10 000 μm²) for one week in mixed osteogenic/adipogenic media. They found that MSCs seeded on the largest micro islands differentiate preferentially towards osteoblast phenotype while those on relatively small micro

islands tend to differentiate into adipocytes. Peng et al. [294] investigated the effect of patterns shape on MSCs fate by creating RGD micropatterns of different geometries (circles, squares, triangles and stars) on poly (ethylene glycol hydrogel) (PEG). They observed that the optimal osteogenesis and adipogenesis happened on star and circular micropatterns, respectively, after one week of induction. In contrast to Peng et al. Wang et al. explored the possibility of maintaining the stemness character of MSCs by manipulating patterns shape [381]. Although the precise mechanism by which geometric cues induce the switch of stem cells into osteoblasts is still not fully understood, efforts have been dedicated to draw a rough signaling pathway [241] [242] [294] [301]. The tentative explanation is constructed on the basis that geometric cues, eliciting

high cell spreading, activate RhoA pathway and Rho Kinase Effector (RhoA/ROCK), which in turn stimulates myosins-mediated actin stress fibers contraction. Consequently, the activation of RhoA/ROCK stimulates osteogenesis while inhibiting adipogenesis.

Although our data provide clear evidence that hMSCs perceive geometric cues in their microenvironment, it is quite intriguing that RGD/BMP-2 micropatterns shaped as triangles and squares significantly enhanced hMSCs osteogenesis while those shaped as rectangles exerted no specific effect on hMSCs fate. Even though further investigations are required to elucidate these findings, one possible explanation lies in the fact that varying the shape of RGD/BMP-2 micropatterns elicits different tensile stresses and cytoskeleton reorganization of hMSCs, which ultimately caused different degrees of differentiation. Another likely scenario may involve the modulation of the interactions of RGD and BMP-2 peptides with their receptors, thus regulating the downstream signaling pathways. Indeed, it is well-established that the spatial distribution of adhesive ligands greatly affects integrin/ligands interactions and focal adhesion formation and maturation, which in turn influences cell commitment and differentiation [385]. In addition, Zouani et al. [210] demonstrated that matrix stiffness modulates BMP-2-induced smads signaling pathway, suggesting that the spatial distribution of BMP-2 peptide as specific geometric cues may also affect the binding affinity of this peptide to its receptors and the downstream effectors.

As a final point, a careful interpretation of these data indirectly provides new insights regarding the crosstalk between integrins and growth factors. Indeed, the synergistic effect of RGD and BMP-2 peptides to enhance hMSCs osteogenic differentiation does not necessarily require ligands co-localization at the molecular scale.

Overall, it was demonstrated for the first time that geometric cues intensify the osteoinductive potential of combined RGD/BMP-2 peptides, even in the absence of any induction media. Enhanced hMSCs osteogenesis may result following an eventual synergistic effect of biochemical and geometric cues since both of them activate Mitogen-Activated Protein Kinase (MAPK) [242] [336] [337] and RhoA [241]; two signaling pathways recognized to play an important role in directing stem cell fate towards osteoblast phenotype.

5- Conclusion

Novel artificial ECMs were engineered on 2D model material to examine the osteogenic differentiation of hMSCs in response to the micros-scale distribution of co-grafted RGD/ BMP-2 mimetic peptides. We recently demonstrated that combined and homogenously grafted RGD/ BMP-2 peptides onto glass substrates significantly enhanced hMSCs osteogenesis as compared to solely grafted BMP-2 peptide. Herein, we determined that the same peptides further accentuate the osteoblastic phenotype on hMSCs, when spatially distributed as specific micro-sized geometric cues.

Taken together, the findings suggest that the combination of biochemical and geometric cues, when carefully selected, are of great interest in directing stem cell fate towards the desired cell response, without having to use osteogenic differentiation media. Therefore, geometric cues should be taken into consideration in tissue engineering and regenerative medicine in conjunction with biochemical signals. In addition, these *in vitro* systems provide an interesting tool to elucidate how MSCs perceive and respond to stimuli from the surrounding microenvironment.

Acknowledgements: The authors would like to thank Dr Christian. Sarra-Bournet for the photolithography mask fabrication and Dr Cedric Ayela for his help for the photolithography technique. IB is the recipient of a scholarship from the NSERC CREATE Program on Regenerative Medicine. This work was supported by the National Science and Engineering Research Council (NSERC-Canada) (GL) and the French Agence Nationale de la Recherche (ANR) (MCD).

CONCLUSION & PERSPECTIVES

I. General discussion

The rapid growing of orthopaedic biomaterials market, along with the long-term failure of implants reflect the real need for biomaterials with higher levels of biocompatibility to ensure their long-term performance.

In total joint replacement surgery, clinicians are still faced to the lack of implant osseointegration due to the formation of a fibrous layer, instead of bone tissue, at the interface bone/implant. In tissue engineering applications, tissue-engineered constructs often fail to restore large bone defects caused by fractures of critical size, musculoskeletal diseases and tumors resection. This is mainly due to the poor osteogenic potential of currently available biomaterials. In both cases, the problem relies on the inadequate and incomplete instructions emitted by the biomaterial and perceived by the surrounding cells. Therefore, the desired new bone formation "osteogenesis" around the implanted material is often compromised owing to irrelevant cell-material interactions. One exciting approach that may pave the way towards a definitive solution for the underlying issues is to engineer artificial ECM *in vitro*, with the aim of deconstructing and then reconstructing the *in vivo* microenvironment that intimately control the decision of quiescent or proliferative MSCs to undergo osteoblast lineage differentiation.

During the last decade, three areas of research have been dedicated to the identification of the key ECM properties that guide MSCs during their lineage-specific differentiation.

The first area concerns the physical properties of the ECM, including stiffness, porosity, mechanical load (compression, stretching, and fluid-induced shear), microgeometry, micro/nano-topography and ordered/disordered topography.

The second area is related to the biochemical aspects of the ECM. Various biochemical cues have been extensively studied for their biological relevance, such as ligands nano-/micro-spacing, density, gradient, clustering, affinity to cell receptors and co-signaling [11] [12] [10].

The third area regards the properties inherent to MSCs themselves, such as cell shape, anisotropy, spreading, subcellular geometries and cytoskeleton tension [241] [242] [300] [294] [301].

All these factors have been recognized as potent modulators of MSCs commitment and differentiation towards the osteoblastic lineage [11] [12] [10]. In addition, it is believed that the underlying properties are strongly interconnected and one can influence the others to target specific cellular responses that neither individual cues can elicit alone.

The studies presented in this thesis fall, of course, in the second area of research as the focus was made on evaluating the effect of various biochemical cues on directing hMSCs osteogenesis. To ovoid a repetitive interpretation of results, already reported in the three papers, we will provide

in the next paragraph a brief summary of the key achievements made in this project and their relevance in stem cell and biomaterials research progress.

Controlling hMSCs osteogenic differentiation through RGD/BMP-2 cross-talk:

As discussed in the first paper, BMP-2 mimetic peptide, homogenously immobilized on glass surfaces, induced hMSCs differentiation towards the osteoblastic lineage after 4 weeks of culture. Currently, BMP-2 peptides are widely recognized as potent osteoinductive factors. Several groups have attempted to conjugate these mimetic peptides to biomaterials for bone tissue engineering purposes, as nicely reviewed in [179]. We evidenced that the stimulatory effect BMP-2 can be improved in the presence of adhesive RGD ligand, without the help soluble osteogenic factors. Interestingly, BMP-2-mediated osteogenic differentiation was significantly enhanced on bifunctionalized surfaces (RGD+BMP-2), as compared to BMP-2 surfaces, despite the significant decrease of BMP-2 surface density from 2.2 on BMP-2 surfaces to 1 pmol/mm² on RGD+BMP-2 surfaces. These findings suggest the establishment of a sort of combinatorial effect or crosstalk between RGD and BMP-2 peptides that effectively enhanced hMSCs osteogenic differentiation. However, it would be interesting to verify throughout further experiments whether BMP-2 density of 1 pmol/mm² on RGD+BMP-2 surfaces was sufficient to induce hMSCs osteogenic differentiation or the presence RGD triggered a compensatory effect. The underlying synergistic effect of integrin ligands and growth factors becomes even more evident by taking advantage of such new insights to interpret some clinical outcomes reported in previous studies. For example, in the seminal Urist's work, it has been reported that demineralized bone matrices induced ectopic bone formation when transplanted *in vivo* [175]. The osteoinductive factors within the bone ECM, known as BMP-2, have been later isolated and their amount was estimated at 1-2 µg/kg [428]. In clinics, however, supraphysiological doses of BMPs, -in the order of mg/kg- have been used to achieve satisfactory outcomes. One possible explanation for this obvious difference may be related to the crucial role of ECM components in regulating growth factors bioactivity. Therefore, signals triggered via the crosstalk between adhesive ligands (RGD) and growth factors (BMP-2) are likely to play a key role in regulating hMSCs osteogenic differentiation during bone formation. During the last two decades, distinct mechanisms of integrin ligands and growth factors cooperation have been proposed. **Figure 40** provides a simplified schematic representation of some suggested signaling scenarios, even though the exact mechanism is yet to be elucidated.

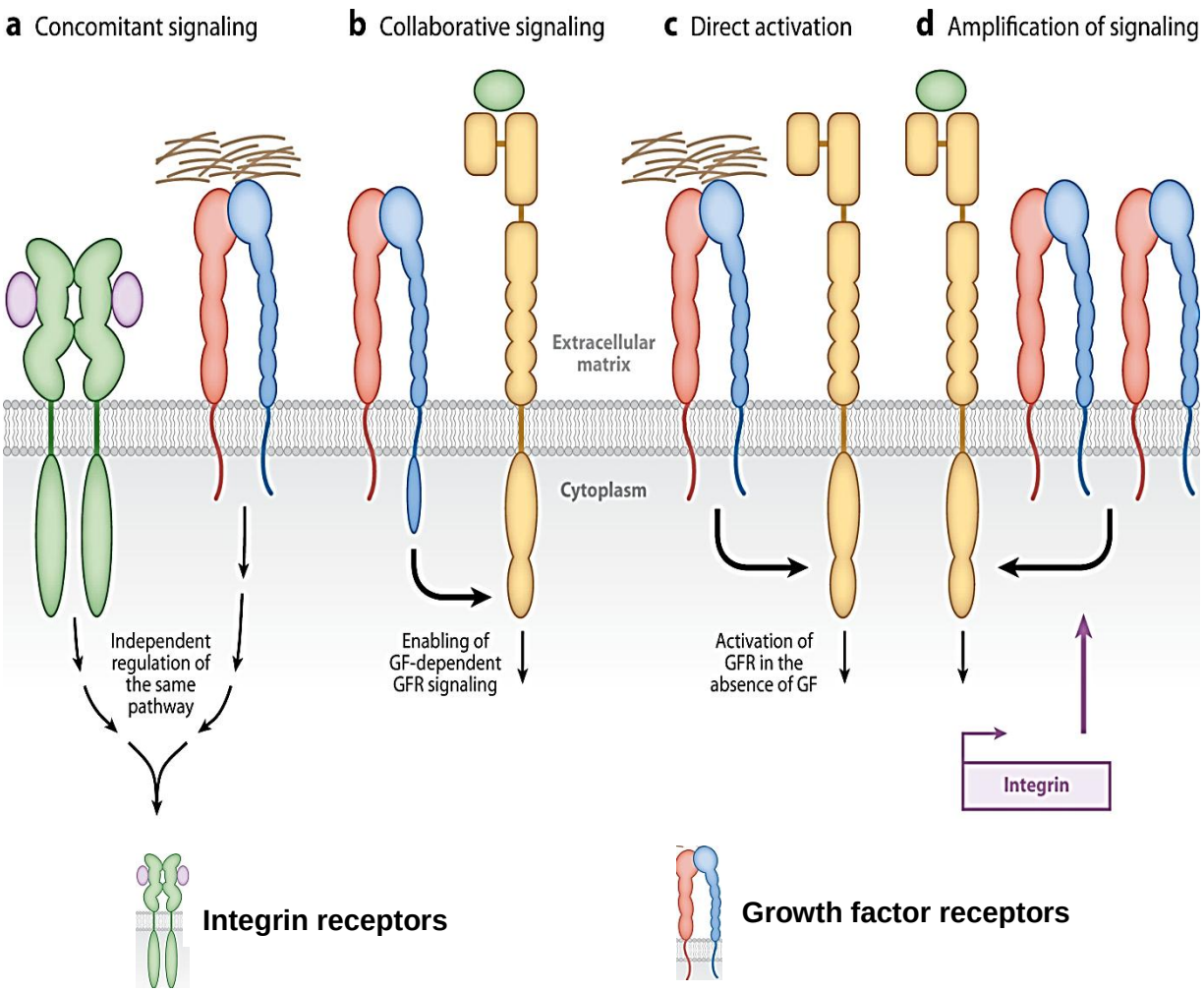

Figure 40: Some expected mechanisms involved in triggering integrin and growth factor receptors interactions-mediated signaling pathways. (a) The activation of the two receptor systems can take place independently to regulate the same pathway. (b) Given that the activation of growth factor receptors (GFRs) often requires cell adhesion, integrins, along with focal adhesion signaling proteins, may support growth factors-dependent signals. (c) Integrins have also been reported to activate GFRs even in the absence of growth factors [411]. (d) Growth factors-dependent signals are known to increase integrins expression. Consequently, the amplification of integrin signals may accentuate the activation of GFRs and the downstream pathway. [427]

Controlling hMSCs osteogenic differentiation through the spatial control of BMP-2 presentation

The second paper highlighted the significant contribution of geometric cues in regulating BMP-2-mediated osteogenic differentiation. Specifically, peptide micropatterns exhibiting triangular and square shapes enhanced hMSCs osteogenesis, while rectangular micropatterns did not. To date, it is still difficult to provide a definite interpretation of changes in MSCs differentiation extent in response to the shape of BMP-2 micropatterns. Indeed, further experiments are needed to elucidate mechanisms by which microscale geometric cues affect hMSCs fate. As discussed in the paper II, several factors may influence the extent of cell differentiation on BMP-2 micropatterned surfaces, including BMP-2 receptors distribution and binding affinity, cytoskeleton remodeling, cell-cell interactions and integrins expression. In addition, it should be not neglected that, inversely to homogenous surfaces, micropatterned surfaces promote BMP-2 clustering in well-defined regions, which may favor receptors oligomerization and BMP-2 signals amplification. To the best of our knowledge, no similar work, in term of the choice of ligand, pattern size, cell type and lineage specification, was published in the literature. Indeed, we found only two studies in bone tissue engineering research area, where BMP-2 was patterned on material surfaces at the subcellular scale. However, these studies are quite far from our objective. In the first study, 25 µm-wide patterned stripes of BMP-2 were created on glass substrates by microcontact printing. The objective of this work was to compare between the effect of immobilized and soluble BMP-2 on myoblasts migration and osteogenic differentiation. BMP-2 tethering resulted in prolonged Smad phosphorylation over a period of 90 min, leading to a sustained localization of the Smad complex in the nucleus, as compared to soluble BMP-2 [429]. In the second study, circular BMP-2 micropatterns were created onto gold substrates using microcontact printing and dip-pen nanolithography. The distance between the micropatterns was 5 µm or 22 µm and their diameter was 4-5 µm. After 24 h of cell culture, myoblastic cells exhibited higher osteogenic marker (osterix) expression on BMP-2 micropatterns with small center-to-center spacing (5 µm). However, the authors reported that the local BMP-2 density was similar in micropatterns with 5 and 22 µm interspacing, while the overall ligand density was significantly higher on micropatterns with 5 µm interspacing. Therefore, it is not clear, in this work, whether the extent of osteogenic differentiation was affected by the density BMP-2, micropattern spacing or both of them [421]. These studies, even though interesting, do not provide insightful information about the role of geometric cues in modulating BMP-2-mediated osteogenesis.

Overall, we believe that the microscale distribution of BMP-2 and others biologically relevant molecules more closely mimics the organization of ECM components *in vivo*, than conventional

cell culture models (homogenous ligands presentation). In addition, our findings suggest that geometric features should be carefully selected to favor the desired cell response, which means that an in-depth understanding of the spatially distributed ligand and stem cells is of great benefit.

Controlling hMSCs osteogenic differentiation through the dual action of RGD/BMP-2 crosstalk and microscale geometric cues

The focus in the third paper was made on the design of novel *in vitro* cell culture models to investigate the intriguing cooperation of ECM cues in regulating one cell behavioral pattern. In the paper I, we evidenced that the homogenous cografting of RGD and BMP-2 peptides effectively enhanced hMSCs osteogenic differentiation. Interestingly, we demonstrated here, for the first time, that cell differentiation could be further enhanced when the distribution of RGD and BMP-2 is finely controlled at the microscale length. Again, triangular and square RGD/BMP-2 micropatterns appeared more effective in inducing osteogenic differentiation than rectangular geometries. In this study (paper III), RGD/BMP-2 micropatterned surfaces were compared to homogenous RGD/BMP-2 surfaces, but not to BMP-2 micropatterned surfaces, in term of their biological relevance. Therefore, in the paragraph below, the comparison will be also made with BMP-2 micropatterned surfaces in order to provide a broader results interpretation than that given in the paper III.

On one hand, the comparison between homogenous and micropatterned RGD/BMP-2 surfaces revealed the importance of microscale geometric cues in regulating RGD/BMP-2 crosstalk-mediated osteogenesis.

On the other hand, the comparison between micropatterned surfaces with both peptides (paper III) and micropatterned surfaces with only BMP-2 peptide (paper II) determined that BMP-2 micropatterning-mediated osteogenesis was effectively enhanced in the presence of RGD peptide, as revealed by significantly higher levels of osteogenic markers (Runx-2, OPN, ALP) on RGD/BMP-2 micropatterns, as compared to BMP-2 micropatterns. Thereby, our data provide obvious evidence of the interplay between ligands/growth factors crosstalk and geometric cues in modulating hMSCs specification towards the osteoblastic lineage.

As discussed in the paper III, actin-myosin machinery and integrins may play a key role as transducers of inside-out and outside-in signaling. In a study carried-out by Kolodziej et al., it has been demonstrated that 1 µm square RGD/FGF patterns, with a center-to-center spacing of 3 µm, significantly enhanced human umbilical vein endothelial cells (HUVECs) spreading, as compared to micropatterned substrates containing only RGD ligand [430]. Although, cell spreading was the only cell behavior investigated in this study, this finding emphasizes the importance of

cytoskeleton rearrangement in mediating cellular events, in response to combined and micropatterned adhesive and growth factors ligands.

Besides, a growing body of evidence points at ECM ligands clustering in predefined regions as an important parameter in regulating cellular behavior, given that cells within their *in vivo* microenvironment are exposed to temporal and spatially distributed ligands. For example, it has been shown that the morphogen Hedgehog, known for its role in tissue patterning during embryonic development, exhibits a hierarchical organization and its clustering is essential for a correct activation of downstream signals [431]. Another physiological phenomenon, witnessing ECM proteins clustering *in vivo*, is the formation of growth factor gradients during morphogenesis, such as long range BMP-2 gradient along the ventral and dorsal axis [432]. Accordingly, several groups have attempted to mimic the spatial distribution of ligands *in vivo*, by creating a wide range of gradients and micro-/nanopatterns of proteins and growth factors on material surfaces. For example, Spatz group investigated the effect of ligand clustering on integrins assembly. They developed RGD patterned gold surfaces with micro/nano-sized features. RGD nanopatterns arranged in 2 μm^2 squares (with 1.5 µm spacing) [433] or in 1.5 µm diameter circles (with 1.7 µm spacing) [434] were compared with substrates containing a homogenous layer of RGD nanopatterns. Although, micro/nano-patterned substrates exhibited lower peptide density than homogenously nanopatterned substrates, they were more supportive for focal adhesion formation and clustering. These observations highlight the importance of ligand clustering at the microscale in modulating cell adhesion strength.

Currently, there is an extensive body of literature focusing on the effect of ligand clustering at the nanoscale on MSCs fate, however little is known about its biological relevance at the microscale.

On the basis of the above-mentioned studies, micropatterned surfaces developed in our study could be considered as a template for RGD and BMP-2 clustering. Therefore, ligand clustering is likely to have a prominent role in enhancing osteogenic differentiation on RGD/BMP-2 and BMP-2 micropatterned surfaces, through the following schema. Based on Spatz group studies [433] [434], RGD peptide clustering may promote focal adhesion formation and clustering, which may in turn regulate BMP-2 signaling pathways through RGD/BMP-2 crosstalk previously discussed (see **Figure 40**).

Overall, our findings, reported in the study III, provide evidence of the high hMSCs sensitivity to integrin ligands/growth factors crosstalk and micro-sized geometric cues as well as their concerted action. Such ECM cues interplay has been previously reported in several instances, in-

cluding the interplay between biochemistry and topography [435] [436], biochemistry and stiffness [210] [240], micro- and nanoscale topography [437], micro- and nanoscale chemical patterns [433] [434] [438], chemical patterns and stiffness [439] and stiffness and topography [440].

II. Conclusion

Stem cells within the human body are constantly receiving a plethora of information from their niches that are precisely interpreted and applied to ensure the maintenance of tissues homeostasis. ECM is a key component of stem cell niches since it provides, through its physical and biochemical properties, supportive and regulatory functions for cells. Following an injury, bone tissue can repair itself by establishing a sort of bridge or bone-like matrix, rich in structural proteins and growth factors essential for the recruitment of stem cells and osteoprogenitor cells at the site of injury. However, the regenerative capacity innate to bone tissue is drastically lost in critical size defects, which requires in such clinical case the use of biomaterials. In initial steps towards the development of clinically relevant biomaterials, it seems inevitable to understand the complexity stem cells interactions with their microenvironment *in vivo*. In this regard, a body of research in regenerative medicine and bone tissue engineering has been recently dictated to the reconstruction of the native ECM complexity by engineering artificial matrices as *in vitro* models for dissecting the role of single ECM cues or a combination of them on stem cell behaviors.
From this perspective, we designed different *in vitro* models that allowed for evaluating of three main ECM aspects: integrin ligands/growth factors crosstalk signaling, microscale presentation of individual ligands and the interplay between ligands crosstalk and microscale geometric cues.

Regarding the synergistic effect of RGD and BMP-2 peptides on hMSCs fate

In this study, RGD and/or BMP-2 were homogenously immobilized on glass substrates. The covalent peptide immobilization was ascertained by physical-chemical characterization (XPS, AFM, fluorescence microscopy). Fluorescence measurements of peptide density revealed quite similar RGD and BMP-2 densities on glass surfaces containing only one peptide. On bifunctionalized surfaces (RGD/BMP-2 ratio 1:1), the density of each peptide was almost half the density measured on the corresponding surfaces containing only one peptide. Given that the surface topography may affect cellular responses, we measured the surface roughness after each step of peptide grafting. Results showed slight differences in the surface roughness between RGD and BMP-2 materials.

Cell differentiation experiments were performed for all studies in the absence of soluble osteogenic factors in the medium in order to exclude the interference of external factors that may influence the extent of hMSCs, and thus mask the biological relevance of biomimetic surfaces.
The characterization of osteogenic differentiation, by staining cells for STRO-1 as stemness marker and Runx-2 and OPN as osteogenic markers, showed that hMSCs acquired an osteoblast phenotype on BMP-2 surfaces, but not RGD surfaces. Interestingly, the combination of RGD and BMP-2 peptides significantly enhanced the expression of osteogenic makers in hMSCs, as compared to the sole grafting of BMP-2 peptide.

Regarding the effect of the single peptide micropatterning on hMSCs fate

Micropatterned surfaces with RGD or BMP-2 peptide were developed using photolithography. The spatial distribution of peptides as specific micro-sized patterns of varied shapes but constant surface area was assessed using optical interferometry and fluorescence microscopy. Highly ordered and well-defined micropatterns exhibiting triangular, square or rectangular geometries were obtained.
RGD and BMP-2 micropatterned surfaces were evaluated for their potency to induce hMSCs osteogenic differentiation. RGD did not affect hMSCs osteogenic regardless the pattern geometry, as revealed by the expression of stemness and osteogenic markers at levels equivalent to those observed on homogenous RGD surfaces. On the hand, the influence of geometric cues on stem cell fate was distinguishable on BMP-2 surfaces. Unlike rectangular micropatterns, triangular and square micropatterns resulted in enhanced hMSCs osteogenic differentiation, as compared to the homogenous distribution of BMP-2.

Regarding the effect of the dual peptide micropatterning on hMSCs fate

In this third part of the project, RGD and BMP-2 peptides were simultaneously micropatterned on glass substrates in order to evaluate whether the factors reported, in study I (ligands crosstalk) and study II (geometric cues), as potent osteogenic cues can overlap to further improve osteogenesis. The differentiation of hMSCs on RGD/BMP-2 micropatterns was performed in the same cell culture conditions.
Although the interplay between RGD/BMP-2 crosstalk and geometric cues was evident, it was pattern shape dependent. In fact, osteogenic markers expression peaked on triangular and square RGD/BMP-2 micropatterns, while on rectangular micropatterns, the extent of hMSCs osteogenenic differentiation was similar to that observed on homogenous RGD/BMP-2 surfaces.

In summary, this thesis project provides valuable insights into the role of several ECM aspects in controlling stem fate decision. Such *in vitro* platforms are undoubtedly a powerful tool to benefit from a deeper understanding of how stem cells interpret and explore external signals from their microenvironment, which should pave the way towards the development of clinically relevant biomaterials.

III. Perspectives

There are still several key questions, related to this thesis project specifically, and bone tissue engineering from a general perspective, that remain unanswered and need further investigations.

From an experimental perspective

- It would be interesting to investigate the homogeneity of osteoblast cell population obtained after 4 weeks of culture on the different biomimetic materials by quantifying cells that have maintained their stemness and those exhibiting an osteoblast phenotype or other phenotypes, such as adipocyte- and chondrocyte-specific markers.
- The evaluation of hMSCs fate decision at several time intervals may also help to pursue the evolution of osteogenic markers in response to the different biochemically modified surfaces.
- Osteogenic differentiation was assessed using STRO-1 as stemness marker, Runx-2 and ALP as early osteogenic markers and OPN as late osteogenic marker. Other terminal differentiation markers such as osteocalcin, Von Kossa and Alizarin red could be used to evaluate the mineralization of deposited ECM.
- Real-time polymerase chain reaction (PCR) and western blotting are routinely employed in stem cell research and may be considered in future experiments to support the current findings.
- An additional condition that should be taken into account upon experimental design is a standard positive control for the sake of comparison with similar works from others groups.

From a fundamental perspective

In initial steps towards deciphering the mechanism by which ECM cues (RGD/BMP-2 crosstalk and the microscale distribution of single or combined ligands) guide MSCs fate determination, the following pathways should be investigated.

Given that integrins and actin-myosin machinery are systematically involved in cell-ECM interactions, it is very important to precisely evaluate the spatial distribution of integrins, the extent of focal adhesion and their size, the degree of cell spreading and cytoskeleton tension on all biomimetic material surfaces. Specifically, micropatterned surfaces containing BMP-2 peptide,

shown to positively affect hMSCs differentiation down the osteoblastic lineage are expected to elicit an adequate BMP-2 receptors (BMPR I & II) clustering, thus fostering their crosstalk and activation, which may in turn lead to an up-regulation of BMP-2 signaling pathways. It is therefore of essential importance to examine the activation of BMP-2-induced pathways, mainly Smads and MAPK signaling.

Given the reciprocal interactions between integrins and BMP-2 receptors previously highlighted, the investigation of integrin-based signaling activation, specifically the focal adhesion kinase (FAK), known as an important mediator of osteogenic differentiation, may provide further insights into the synergistic effect of RGD/BMP-2 crosstalk in regulating hMSCs osteogenic differentiation.

RhoA and its effector, ROCK, are widely recognized to play a key role during osteogenesis [241] [301]. The extent of these signals is inherently linked to the degree of actin-myosin contractility. Taking into account that geometric cues have proved in several examples to affect cytoskeleton tension, RhoA/ROCK pathways are also expected to regulate osteogenic differentiation on micropatterned surfaces developed in this work. In addition, some signaling pathways, such as MAPK and WNT have been shown to mediate osteogenesis in response to geometric cues [242], BMP-2 [31] [179] and integrin-binding ligands [244] [441], which may explain the interplay between two or more ECM cues in regulating stem cell fate, as demonstrated in the paper III. Therefore, the study of the above-mentioned pathways may help to provide an insightful interpretation of how the different artificial ECM created on glass surfaces interact with hMSCs to direct their fate towards the osteogenic lineage.

Although our group and many others are just beginning to exploit the wide range of biochemical and physical ECM properties, it is believed that the concerted efforts will lead in the future to the reconstruction stem cell niche in all its aspects. This paves the way toward the development of efficient, safe and long-term performance biomaterials capable to meet the current clinical need.

REFERENCES:

[1] R.a.B. Suzman, J., https://www.nia.nih.gov/research/publication/global-health-and-aging/living-longer, Publication Date: October 2011, Last Updated: January 22, 2015, [Access Date 2015-11-18].
[2] D.M. Cutler, A.B. Rosen, S. Vijan, The value of medical spending in the United States, 1960–2000, New England Journal of Medicine 355(9) (2006) 920-927.
[3] M. Long, H.J. Rack, Titanium alloys in total joint replacement--a materials science perspective, Biomaterials 19(18) (1998) 1621-39.
[4] E.T. Pashuck, M.M. Stevens, Designing regenerative biomaterial therapies for the clinic, Science translational medicine 4(160) (2012) 160sr4-160sr4.
[5] D. Heinegard, O. Johnell, L. Lidgren, O. Nilsson, B. Rydevik, F. Wollheim, K. Akesson, The bone and joint decade 2000-2010, Acta Orthopaedica Scandinavica 69(3) (1998) 219-220.
[6] W. Khan, E. Muntimadugu, M. Jaffe, A.J. Domb, Implantable medical devices, Focal Controlled Drug Delivery, Springer2014, pp. 33-59.
[7] P.H. Long, Medical devices in orthopedic applications, Toxicologic pathology 36(1) (2008) 85-91.
[8] M. Geetha, A. Singh, R. Asokamani, A. Gogia, Ti based biomaterials, the ultimate choice for orthopaedic implants–a review, Progress in Materials Science 54(3) (2009) 397-425.
[9] A.I. Caplan, Adult mesenchymal stem cells for tissue engineering versus regenerative medicine, Journal of Cellular Physiology 213(2) (2007) 341-347.
[10] M. Akhmanova, E. Osidak, S. Domogatsky, S. Rodin, A. Domogatskaya, Physical, Spatial, and Molecular Aspects of Extracellular Matrix of In Vivo Niches and Artificial Scaffolds Relevant to Stem Cells Research, Stem Cells International 2015 (2015) 35.
[11] M.J. Dalby, N. Gadegaard, R.O.C. Oreffo, Harnessing nanotopography and integrin-matrix interactions to influence stem cell fate, Nat Mater 13(6) (2014) 558-569.
[12] K. von der Mark, J. Park, Engineering biocompatible implant surfaces. Part II: cellular recognition of biomaterial surfaces: lessons from cell–matrix interactions, Prog Mater Sci 58 (2013) 327-381.
[13] K. Matsuo, N. Irie, Osteoclast–osteoblast communication, Archives of biochemistry and biophysics 473(2) (2008) 201-209.
[14] B. Clarke, Normal bone anatomy and physiology, Clinical journal of the American Society of Nephrology : CJASN 3 Suppl 3 (2008) S131-9.
[15] J.N. BERESFORD, Osteogenic stem cells and the stromal system of bone and marrow, Clinical orthopaedics and related research 240 (1989) 270-280.
[16] J.M. Delaissé, T.L. Andersen, M.T. Engsig, K. Henriksen, T. Troen, L. Blavier, Matrix metalloproteinases (MMP) and cathepsin K contribute differently to osteoclastic activities, Microscopy research and technique 61(6) (2003) 504-513.
[17] S. Weiner, H.D. Wagner, The material bone: structure-mechanical function relations, Annual Review of Materials Science 28(1) (1998) 271-298.
[18] G. Schmidmaier, S. Herrmann, J. Green, T. Weber, A. Scharfenberger, N.P. Haas, B. Wildemann, Quantitative assessment of growth factors in reaming aspirate, iliac crest, and platelet preparation, Bone 39(5) (2006) 1156-1163.
[19] W.J. Landis, The strength of a calcified tissue depends in part on the molecular structure and organization of its constituent mineral crystals in their organic matrix, Bone 16(5) (1995) 533-44.
[20] H.C. Anderson, Matrix vesicles and calcification, Current rheumatology reports 5(3) (2003) 222-226.
[21] J.-Y. Rho, L. Kuhn-Spearing, P. Zioupos, Mechanical properties and the hierarchical structure of bone, Medical engineering & physics 20(2) (1998) 92-102.

[22] L.T. Kuhn, M.D. Grynpas, C.C. Rey, Y. Wu, J.L. Ackerman, M.J. Glimcher, A comparison of the physical and chemical differences between cancellous and cortical bovine bone mineral at two ages, Calcified tissue international 83(2) (2008) 146-154.
[23] S. Nikolov, D. Raabe, Hierarchical modeling of the elastic properties of bone at submicron scales: the role of extrafibrillar mineralization, Biophysical journal 94(11) (2008) 4220-4232.
[24] R. Nalla, J. Kruzic, J. Kinney, M. Balooch, J. Ager, R. Ritchie, Role of microstructure in the aging-related deterioration of the toughness of human cortical bone, Materials Science and Engineering: C 26(8) (2006) 1251-1260.
[25] B. Clarke, Normal bone anatomy and physiology, Clinical journal of the American Society of Nephrology 3(Supplement 3) (2008) S131-S139.
[26] U. Kini, B. Nandeesh, Physiology of bone formation, remodeling, and metabolism, Radionuclide and hybrid bone imaging, Springer2012, pp. 29-57.
[27] F. Shapiro, Bone development and its relation to fracture repair. The role of mesenchymal osteoblasts and surface osteoblasts, Eur Cell Mater 15(53) (2008) e76.
[28] V.I. Sikavitsas, J.S. Temenoff, A.G. Mikos, Biomaterials and bone mechanotransduction, Biomaterials 22(19) (2001) 2581-2593.
[29] E.J. Mackie, Y.A. Ahmed, L. Tatarczuch, K.S. Chen, M. Mirams, Endochondral ossification: how cartilage is converted into bone in the developing skeleton, The international journal of biochemistry & cell biology 40(1) (2008) 46-62.
[30] T.A. Linkhart, S. Mohan, D.J. Baylink, Growth factors for bone growth and repair: IGF, TGFβ and BMP, Bone 19(1) (1996) S1-S12.
[31] M.S. Rahman, N. Akhtar, H.M. Jamil, R.S. Banik, S.M. Asaduzzaman, TGF-β/BMP signaling and other molecular events: regulation of osteoblastogenesis and bone formation, Bone Research 3 (2015) 15005.
[32] J.D. Stroncek, W.M. Reichert, Overview of wound healing in different tissue types, Indwelling neural implants: strategies for contending with the in vivo environment (2008).
[33] T. Wenzel, C. Damiani, T. Dreesch, S. Klein, Drug release from bone implants in-vitro: An experimental setup, Biomedical Engineering/Biomedizinische Technik 57(SI-1 Track-D) (2012) 546-548.
[34] Z.S. Ai-Aql, A.S. Alagl, D.T. Graves, L.C. Gerstenfeld, T.A. Einhorn, Molecular mechanisms controlling bone formation during fracture healing and distraction osteogenesis, Journal of dental research 87(2) (2008) 107-18.
[35] M.E. Bolander, Regulation of fracture repair by growth factors, Experimental Biology and Medicine 200(2) (1992) 165-170.
[36] B.D. Boyan, T.W. Hummert, D.D. Dean, Z. Schwartz, Role of material surfaces in regulating bone and cartilage cell response, Biomaterials 17(2) (1996) 137-146.
[37] L.J. Mock C, Goosen J, et al., Guidelines for essential trauma care. Geneva: World Health Organiziation., (2004).
[38] M. Elder, Therapeutics and Biomaterials for Musculoskeletal Disease: Global Markets. , BCC Research, (2010, [Access Date 2014-01-24].).
[39] A. Woolf, The Bone and Joint Decade 2000-2010, Annals of the Rheumatic Diseases 59(2) (2000) 81-82.
[40] A.D. Woolf, B. Pfleger, Burden of major musculoskeletal conditions, Bulletin of the World Health Organization 81(9) (2003) 646-656.
[41] O. Johnell, J. Kanis, An estimate of the worldwide prevalence and disability associated with osteoporotic fractures, Osteoporosis international 17(12) (2006) 1726-1733.
[42] M.A. Miranda, M.S. Moon, Treatment strategy for nonunions and malunions, Surgical treatment of orthopaedic trauma 1 (2007) 77-100.
[43] N. Kanakaris, P.V. Giannoudis, The health economics of the treatment of long-bone non-unions, Injury 38 (2007) S77-S84.

[44] R.W. Lindsey, Z. Gugala, E. Milne, M. Sun, F.H. Gannon, L.L. Latta, The efficacy of cylindrical titanium mesh cage for the reconstruction of a critical-size canine segmental femoral diaphyseal defect, Journal of orthopaedic research : official publication of the Orthopaedic Research Society 24(7) (2006) 1438-53.
[45] S.N. Khan, F.P. Cammisa Jr, H.S. Sandhu, A.D. Diwan, F.P. Girardi, J.M. Lane, The biology of bone grafting, Journal of the American Academy of Orthopaedic Surgeons 13(1) (2005) 77-86.
[46] M. Roccuzzo, G. Ramieri, M. Bunino, S. Berrone, Autogenous bone graft alone or associated with titanium mesh for vertical alveolar ridge augmentation: a controlled clinical trial, Clinical oral implants research 18(3) (2007) 286-94.
[47] D.L. Wheeler, W.F. Enneking, Allograft bone decreases in strength in vivo over time, Clin Orthop Relat Res (435) (2005) 36-42.
[48] H. Shin, S. Jo, A.G. Mikos, Biomimetic materials for tissue engineering, Biomaterials 24(24) (2003) 4353-4364.
[49] K.S. Katti, Biomaterials in total joint replacement, Colloids and Surfaces B: Biointerfaces 39(3) (2004) 133-142.
[50] M.S. Taljanovic, M.D. Jones, T.B. Hunter, J.B. Benjamin, J.T. Ruth, A.W. Brown, J.E. Sheppard, Joint Arthroplasties and Prostheses 1, Radiographics 23(5) (2003) 1295-1314.
[51] Z. Begum, A. Poonguzhali, R. Basu, C. Sudha, H. Shaikh, R.S. Rao, A. Patil, R. Dayal, Studies of the tensile and corrosion fatigue behaviour of austenitic stainless steels, Corrosion Science 53(4) (2011) 1424-1432.
[52] L. Zhuang, E. Langer, Effects of alloy additions on the fatigue properties of cast Co-Cr-Mo alloy used for surgical implants, Journal of Materials Science 25(1) (1990) 683-689.
[53] F.F. Buechel, M.J. Pappas, Principles of Human Joint Replacement: Design and Clinical Application, Springer2015.
[54] A.H. Hosman, H.C. van der Mei, S.K. Bulstra, R. Kuijer, H.J. Busscher, D. Neut, Influence of Co-Cr particles and Co-Cr ions on the growth of staphylococcal biofilms, The International journal of artificial organs 34(9) (2011) 759-65.
[55] R. Narayan, Fundamentals of Medical Implant Materials, (2012).
[56] K. Maehara, K. Doi, T. Matsushita, Y. Sasaki, Application of Vanadium-Free Titanium Alloys to Artificial Hip Joints, Materials Transactions 43(12) (2002) 2936-2942.
[57] V. Challa, S. Mali, R. Misra, Reduced toxicity and superior cellular response of preosteoblasts to Ti-6Al-7Nb alloy and comparison with Ti-6Al-4V, Journal of Biomedical Materials Research Part A 101(7) (2013) 2083-2089.
[58] K. Bordji, J.Y. Jouzeau, D. Mainard, E. Payan, P. Netter, K.T. Rie, T. Stucky, M. Hage-Ali, Cytocompatibility of Ti-6Al-4V and Ti-5Al-2.5Fe alloys according to three surface treatments, using human fibroblasts and osteoblasts, Biomaterials 17(9) (1996) 929-40.
[59] R. Zeng, W. Dietzel, F. Witte, N. Hort, C. Blawert, Progress and challenge for magnesium alloys as biomaterials, Advanced Engineering Materials 10(8) (2008) B3-B14.
[60] R. Sarkar, G. Banerjee, Ceramic based bio-medical implants, Interceram 59(2) (2010) 98-102.
[61] L.L. Hench, Bioceramics: from concept to clinic, Journal of the American Ceramic Society 74(7) (1991) 1487-1510.
[62] W. Cao, L.L. Hench, Bioactive materials, Ceramics International 22(6) (1996) 493-507.
[63] M. Wang, Developing bioactive composite materials for tissue replacement, Biomaterials 24(13) (2003) 2133-2151.
[64] V.P. Mantripragada, B. Lecka-Czernik, N.A. Ebraheim, A.C. Jayasuriya, An overview of recent advances in designing orthopedic and craniofacial implants, Journal of biomedical materials research. Part A 101(11) (2013) 3349-64.

[65] J.F. Mano, R.A. Sousa, L.F. Boesel, N.M. Neves, R.L. Reis, Bioinert, biodegradable and injectable polymeric matrix composites for hard tissue replacement: state of the art and recent developments, Composites Science and Technology 64(6) (2004) 789-817.
[66] G.D. Winter, B.J. Simpson, Heterotopic Bone formed in a Synthetic Sponge in the Skin of Young Pigs, Nature 223(5201) (1969) 88-90.
[67] E. Jimi, S. Hirata, K. Osawa, M. Terashita, C. Kitamura, H. Fukushima, The Current and Future Therapies of Bone Regeneration to Repair Bone Defects, International Journal of Dentistry 2012 (2012) 7.
[68] M.L.K. Tate, T.F. Ritzman, E. Schneider, U.R. Knothe, Testing of a New One-Stage Bone-Transport Surgical Procedure Exploiting the Periosteum for the Repair of Long-Bone Defects, The Journal of Bone & Joint Surgery 89(2) (2007) 307-316.
[69] T.A. DeCoster, R.J. Gehlert, E.A. Mikola, M.A. Pirela-Cruz, Management of posttraumatic segmental bone defects, Journal of the American Academy of Orthopaedic Surgeons 12(1) (2004) 28-38.
[70] H.C. Fayaz, P.V. Giannoudis, M.S. Vrahas, R.M. Smith, C. Moran, H.C. Pape, C. Krettek, J.B. Jupiter, The role of stem cells in fracture healing and nonunion, International Orthopaedics 35(11) (2011) 1587-1597.
[71] P.N. Soucacos, Z. Dailiana, A.E. Beris, E.O. Johnson, Vascularised bone grafts for the management of non-union, Injury 37(1, Supplement) (2006) S41-S50.
[72] Skalak R (1988), Fox C. editors. NSF Workshop, UCLA Symposia on Molecular and Cellular Biology; Alan R. Liss, Inc.; 1988.
[73] W.M. Miller, M.V. Peshwa, Tissue engineering, bioartificial organs, and cell therapies: I, Biotechnology and bioengineering 50(4) (1996) 347-348.
[74] I. Yannas, E. Lee, D. Orgill, E. Skrabut, G. Murphy, Synthesis and characterization of a model extracellular matrix that induces partial regeneration of adult mammalian skin, Proceedings of the National Academy of Sciences 86(3) (1989) 933-937.
[75] A. Atala, S.B. Bauer, S. Soker, J.J. Yoo, A.B. Retik, Tissue-engineered autologous bladders for patients needing cystoplasty, The lancet 367(9518) (2006) 1241-1246.
[76] P. Macchiarini, P. Jungebluth, T. Go, M.A. Asnaghi, L.E. Rees, T.A. Cogan, A. Dodson, J. Martorell, S. Bellini, P.P. Parnigotto, S.C. Dickinson, A.P. Hollander, S. Mantero, M.T. Conconi, M.A. Birchall, Clinical transplantation of a tissue-engineered airway, Lancet (London, England) 372(9655) (2008) 2023-30.
[77] R. Schimming, R. Schmelzeisen, Tissue-engineered bone for maxillary sinus augmentation, Journal of Oral and Maxillofacial Surgery 62(6) (2004) 724-729.
[78] P. Warnke, I. Springer, J. Wiltfang, Y. Acil, H. Eufinger, M. Wehmöller, P. Russo, H. Bolte, E. Sherry, E. Behrens, Growth and transplantation of a custom vascularised bone graft in a man, The Lancet 364(9436) (2004) 766-770.
[79] R. Quarto , M. Mastrogiacomo , R. Cancedda , S.M. Kutepov , V. Mukhachev , A. Lavroukov , E. Kon , M. Marcacci Repair of Large Bone Defects with the Use of Autologous Bone Marrow Stromal Cells, New England Journal of Medicine 344(5) (2001) 385-386.
[80] M. Marcacci, E. Kon, V. Moukhachev, A. Lavroukov, S. Kutepov, R. Quarto, M. Mastrogiacomo, R. Cancedda, Stem cells associated with macroporous bioceramics for long bone repair: 6- to 7-year outcome of a pilot clinical study, Tissue engineering 13(5) (2007) 947-55.
[81] C.A. Vacanti , L.J. Bonassar , M.P. Vacanti , J. Shufflebarger Replacement of an Avulsed Phalanx with Tissue-Engineered Bone, New England Journal of Medicine 344(20) (2001) 1511-1514.
[82] S. Gronthos, Reconstruction of human mandible by tissue engineering, The Lancet 364(9436) (2004) 735-736.

[83] P.H. Warnke, J. Wiltfang, I. Springer, Y. Acil, H. Bolte, M. Kosmahl, P.A.J. Russo, E. Sherry, U. Lützen, S. Wolfart, H. Terheyden, Man as living bioreactor: Fate of an exogenously prepared customized tissue-engineered mandible, Biomaterials 27(17) (2006) 3163-3167.
[84] C.A. Heath, Cells for tissue engineering, Trends in Biotechnology 18(1) 17-19.
[85] M.F. Pittenger, A.M. Mackay, S.C. Beck, R.K. Jaiswal, R. Douglas, J.D. Mosca, M.A. Moorman, D.W. Simonetti, S. Craig, D.R. Marshak, Multilineage Potential of Adult Human Mesenchymal Stem Cells, Science 284(5411) (1999) 143-147.
[86] K. Le Blanc, I. Rasmusson, B. Sundberg, C. Götherström, M. Hassan, M. Uzunel, O. Ringdén, Treatment of severe acute graft-versus-host disease with third party haploidentical mesenchymal stem cells, The Lancet 363(9419) (2004) 1439-1441.
[87] P. Taupin, OTI-010 Osiris Therapeutics/JCR Pharmaceuticals, Current opinion in investigational drugs (London, England : 2000) 7(5) (2006) 473-81.
[88] N. Amariglio, A. Hirshberg, B.W. Scheithauer, Y. Cohen, R. Loewenthal, L. Trakhtenbrot, N. Paz, M. Koren-Michowitz, D. Waldman, L. Leider-Trejo, Donor-derived brain tumor following neural stem cell transplantation in an ataxia telangiectasia patient, PLoS Med 6(2) (2009) e1000029.
[89] M. Ester Bernardo, F. Locatelli, W.E. FIBBE, Mesenchymal stromal cells: a novel treatment modality for tissue repair, Annals of the New York Academy of Sciences 1176 (2009) 101-117.
[90] R.S. Tuan, G. Boland, R. Tuli, Adult mesenchymal stem cells and cell-based tissue engineering, Arthritis research & therapy 5(1) (2003) 32-45.
[91] A.J. Friedenstein, R.K. Chailakhyan, U.V. Gerasimov, Bone marrow osteogenic stem cells: in vitro cultivation and transplantation in diffusion chambers, Cell Proliferation 20(3) (1987) 263-272.
[92] I. Drosse, E. Volkmer, R. Capanna, P.D. Biase, W. Mutschler, M. Schieker, Tissue engineering for bone defect healing: An update on a multi-component approach, Injury 39, Supplement 2 (2008) S9-S20.
[93] A. Winter, S. Breit, D. Parsch, K. Benz, E. Steck, H. Hauner, R.M. Weber, V. Ewerbeck, W. Richter, Cartilage-like gene expression in differentiated human stem cell spheroids: A comparison of bone marrow–derived and adipose tissue–derived stromal cells, Arthritis & Rheumatism 48(2) (2003) 418-429.
[94] G.I. Im, Y.W. Shin, K.B. Lee, Do adipose tissue-derived mesenchymal stem cells have the same osteogenic and chondrogenic potential as bone marrow-derived cells?, Osteoarthritis and cartilage / OARS, Osteoarthritis Research Society 13(10) (2005) 845-53.
[95] A. Dicker, K. Le Blanc, G. Astrom, V. van Harmelen, C. Gotherstrom, L. Blomqvist, P. Arner, M. Ryden, Functional studies of mesenchymal stem cells derived from adult human adipose tissue, Experimental cell research 308(2) (2005) 283-90.
[96] G.Z. Eghbali-Fatourechi, J. Lamsam, D. Fraser, D. Nagel, B.L. Riggs, S. Khosla, Circulating osteoblast-lineage cells in humans, The New England journal of medicine 352(19) (2005) 1959-66.
[97] N.J. Zvaifler, L. Marinova-Mutafchieva, G. Adams, C.J. Edwards, J. Moss, J.A. Burger, R.N. Maini, Mesenchymal precursor cells in the blood of normal individuals, Arthritis research 2(6) (2000) 477-88.
[98] J.Y. Lee, Z. Qu-Petersen, B. Cao, S. Kimura, R. Jankowski, J. Cummins, A. Usas, C. Gates, P. Robbins, A. Wernig, J. Huard, Clonal Isolation of Muscle-Derived Cells Capable of Enhancing Muscle Regeneration and Bone Healing, The Journal of Cell Biology 150(5) (2000) 1085-1100.
[99] A. Asakura, M. Komaki, M. Rudnicki, Muscle satellite cells are multipotential stem cells that exhibit myogenic, osteogenic, and adipogenic differentiation, Differentiation; research in biological diversity 68(4-5) (2001) 245-53.

[100] A. Usas, J. Huard, Muscle-Derived Stem Cells for Tissue Engineering and Regenerative Therapy, Biomaterials 28(36) (2007) 5401-5406.
[101] K. Okita, S. Yamanaka, Induced pluripotent stem cells: opportunities and challenges, Philosophical Transactions of the Royal Society of London B: Biological Sciences 366(1575) (2011) 2198-2207.
[102] G.E. Friedlaender, C.R. Perry, J. Dean Cole, S.D. Cook, G. Cierny, G.F. Muschler, G.A. Zych, J.H. Calhoun, A.J. Laforte, S. Yin, Osteogenic Protein-1 (Bone Morphogenetic Protein-7) in the Treatment of Tibial Nonunions: A Prospective, Randomized Clinical Trial Comparing rhOP-1 with Fresh Bone Autograft*, The Journal of bone and joint surgery. American volume 83-A Suppl 1(Pt 2) (2001) S151-S158.
[103] A.R. Vaccaro, D.G. Anderson, T. Patel, J. Fischgrund, E. Truumees, H.N. Herkowitz, F. Phillips, A. Hilibrand, T.J. Albert, T. Wetzel, J.A. McCulloch, Comparison of OP-1 Putty (rhBMP-7) to iliac crest autograft for posterolateral lumbar arthrodesis: a minimum 2-year follow-up pilot study, Spine 30(24) (2005) 2709-16.
[104] J.K. Burkus, S.E. Heim, M.F. Gornet, T.A. Zdeblick, The effectiveness of rhBMP-2 in replacing autograft: an integrated analysis of three human spine studies, Orthopedics 27(7) (2004) 723-8.
[105] A. Jaklenec, A. Stamp, E. Deweerd, A. Sherwin, R. Langer, Progress in the tissue engineering and stem cell industry "are we there yet?", Tissue engineering. Part B, Reviews 18(3) (2012) 155-66.
[106] G. Schmidmaier, P. Schwabe, B. Wildemann, N. Haas, Use of bone morphogenetic proteins for treatment of non-unions and future perspectives, Injury 38 (2007) S35-S41.
[107] M.P.G. Bostrom, D.A. Seigerman, The Clinical Use of Allografts, Demineralized Bone Matrices, Synthetic Bone Graft Substitutes and Osteoinductive Growth Factors: A Survey Study, HSS Journal 1(1) (2005) 9-18.
[108] K.S. Cahill, J.H. Chi, A. Day, E.B. Claus, Prevalence, complications, and hospital charges associated with use of bone-morphogenetic proteins in spinal fusion procedures, Jama 302(1) (2009) 58-66.
[109] N.E. Epstein, Complications due to the use of BMP/INFUSE in spine surgery: The evidence continues to mount, Surgical neurology international 4(Suppl 5) (2013) S343-52.
[110] Q. Chen, C. Zhu, G.A. Thouas, Progress and challenges in biomaterials used for bone tissue engineering: bioactive glasses and elastomeric composites, Progress in Biomaterials 1(1) (2012) 1-22.
[111] X. Liu, P.X. Ma, Polymeric Scaffolds for Bone Tissue Engineering, Annals of Biomedical Engineering 32(3) 477-486.
[112] A.J. Salgado, O.P. Coutinho, R.L. Reis, Bone Tissue Engineering: State of the Art and Future Trends, Macromolecular Bioscience 4(8) (2004) 743-765.
[113] R.Z. LeGeros, Biodegradation and bioresorption of calcium phosphate ceramics, Clinical Materials 14(1) (1993) 65-88.
[114] M.N. Rahaman, D.E. Day, B. Sonny Bal, Q. Fu, S.B. Jung, L.F. Bonewald, A.P. Tomsia, Bioactive glass in tissue engineering, Acta Biomaterialia 7(6) (2011) 2355-2373.
[115] M. Hamadouche, L. Sedel, CERAMICS IN ORTHOPAEDICS, Bone & Joint Journal 82-B(8) (2000) 1095-1099.
[116] H. Yuan, J.D. de Bruijn, X. Zhang, C.A. van Blitterswijk, K. de Groot, Bone induction by porous glass ceramic made from Bioglass®(45S5), Journal of biomedical materials research 58(3) (2001) 270-276.
[117] L.L. Hench, J.M. Polak, Third-generation biomedical materials, Science 295(5557) (2002) 1014-1017.
[118] L. Tan, X. Yu, P. Wan, K. Yang, Biodegradable Materials for Bone Repairs: A Review, Journal of Materials Science & Technology 29(6) (2013) 503-513.

[119] M.S. Kim, H.H. Ahn, Y.N. Shin, M.H. Cho, G. Khang, H.B. Lee, An in vivo study of the host tissue response to subcutaneous implantation of PLGA- and/or porcine small intestinal submucosa-based scaffolds, Biomaterials 28(34) (2007) 5137-43.
[120] S. Yang, K.F. Leong, Z. Du, C.K. Chua, The design of scaffolds for use in tissue engineering. Part I. Traditional factors, Tissue engineering 7(6) (2001) 679-89.
[121] M.M. Stevens, Biomaterials for bone tissue engineering, Materials Today 11(5) (2008) 18-25.
[122] J.L. Drury, D.J. Mooney, Hydrogels for tissue engineering: scaffold design variables and applications, Biomaterials 24(24) (2003) 4337-4351.
[123] M.C. Cushing, K.S. Anseth, Hydrogel Cell Cultures, Science 316(5828) (2007) 1133-1134.
[124] M.M. Stevens, R.P. Marini, D. Schaefer, J. Aronson, R. Langer, V.P. Shastri, In vivo engineering of organs: The bone bioreactor, Proceedings of the National Academy of Sciences of the United States of America 102(32) (2005) 11450-11455.
[125] C. Weinand, I. Pomerantseva, C.M. Neville, R. Gupta, E. Weinberg, I. Madisch, F. Shapiro, H. Abukawa, M.J. Troulis, J.P. Vacanti, Hydrogel-beta-TCP scaffolds and stem cells for tissue engineering bone, Bone 38(4) (2006) 555-63.
[126] M. Plecko, C. Sievert, D. Andermatt, R. Frigg, P. Kronen, K. Klein, S. Stübinger, K. Nuss, A. Bürki, S. Ferguson, U. Stoeckle, B. von Rechenberg, Osseointegration and biocompatibility of different metal implants - a comparative experimental investigation in sheep, BMC Musculoskeletal Disorders 13(1) (2012) 1-12.
[127] K. Turzo, Surface Aspects of Titanium Dental Implants, 2012.
[128] S. Bauer, P. Schmuki, K. von der Mark, J. Park, Engineering biocompatible implant surfaces: Part I: Materials and surfaces, Progress in Materials Science 58(3) (2013) 261-326.
[129] G. Mendonca, D.B. Mendonca, F.J. Aragao, L.F. Cooper, Advancing dental implant surface technology--from micron- to nanotopography, Biomaterials 29(28) (2008) 3822-35.
[130] Y. Oshida, E.B. Tuna, Science and Technology Integrated Titanium Dental Implant Systems, Advanced Biomaterials, John Wiley & Sons, Inc.2010, pp. 143-177.
[131] D.A. Puleo, A. Nanci, Understanding and controlling the bone–implant interface, Biomaterials 20(23–24) (1999) 2311-2321.
[132] J.Y. Lim, H.J. Donahue, Cell sensing and response to micro- and nanostructured surfaces produced by chemical and topographic patterning, Tissue engineering 13(8) (2007) 1879-91.
[133] M. Ramazanoglu, Y.O.c.i.d.t.P.D.H. Özger, a.w.o.w.i.t.r.o. oncology., Osseointegration and Bioscience of Implant Surfaces - Current Concepts at Bone-Implant Interface, 2011.
[134] A.J. Garcia, M.D. Vega, D. Boettiger, Modulation of cell proliferation and differentiation through substrate-dependent changes in fibronectin conformation, Molecular biology of the cell 10(3) (1999) 785-98.
[135] N.P. Lang, G.E. Salvi, G. Huynh-Ba, S. Ivanovski, N. Donos, D.D. Bosshardt, Early osseointegration to hydrophilic and hydrophobic implant surfaces in humans, Clinical oral implants research 22(4) (2011) 349-56.
[136] G. Altankov, F. Grinnell, T. Groth, Studies on the biocompatibility of materials: fibroblast reorganization of substratum-bound fibronectin on surfaces varying in wettability, J Biomed Mater Res 30(3) (1996) 385-91.
[137] X. Rausch-fan, Z. Qu, M. Wieland, M. Matejka, A. Schedle, Differentiation and cytokine synthesis of human alveolar osteoblasts compared to osteoblast-like cells (MG63) in response to titanium surfaces, Dental materials : official publication of the Academy of Dental Materials 24(1) (2008) 102-10.
[138] G. Zhao, A.L. Raines, M. Wieland, Z. Schwartz, B.D. Boyan, Requirement for both micron- and submicron scale structure for synergistic responses of osteoblasts to substrate surface energy and topography, Biomaterials 28(18) (2007) 2821-9.

[139] I. Wall, N. Donos, K. Carlqvist, F. Jones, P. Brett, Modified titanium surfaces promote accelerated osteogenic differentiation of mesenchymal stromal cells in vitro, Bone 45(1) (2009) 17-26.
[140] D.S.W. Benoit, M.P. Schwartz, A.R. Durney, K.S. Anseth, Small functional groups for controlled differentiation of hydrogel-encapsulated human mesenchymal stem cells, Nat Mater 7(10) (2008) 816-823.
[141] M.M. Bornstein, P. Valderrama, A.A. Jones, T.G. Wilson, R. Seibl, D.L. Cochran, Bone apposition around two different sandblasted and acid-etched titanium implant surfaces: a histomorphometric study in canine mandibles, Clinical oral implants research 19(3) (2008) 233-41.
[142] N. Donos, S. Hamlet, N.P. Lang, G.E. Salvi, G. Huynh-Ba, D.D. Bosshardt, S. Ivanovski, Gene expression profile of osseointegration of a hydrophilic compared with a hydrophobic microrough implant surface, Clinical oral implants research 22(4) (2011) 365-72.
[143] F. Schwarz, D. Ferrari, M. Herten, I. Mihatovic, M. Wieland, M. Sager, J. Becker, Effects of surface hydrophilicity and microtopography on early stages of soft and hard tissue integration at non-submerged titanium implants: an immunohistochemical study in dogs, Journal of periodontology 78(11) (2007) 2171-84.
[144] D. Buser, N. Broggini, M. Wieland, R.K. Schenk, A.J. Denzer, D.L. Cochran, B. Hoffmann, A. Lussi, S.G. Steinemann, Enhanced bone apposition to a chemically modified SLA titanium surface, Journal of dental research 83(7) (2004) 529-33.
[145] L. Le Guehennec, M.A. Lopez-Heredia, B. Enkel, P. Weiss, Y. Amouriq, P. Layrolle, Osteoblastic cell behaviour on different titanium implant surfaces, Acta Biomater 4(3) (2008) 535-43.
[146] S. Bauer, J. Park, K. von der Mark, P. Schmuki, Improved attachment of mesenchymal stem cells on super-hydrophobic TiO2 nanotubes, Acta Biomater 4(5) (2008) 1576-82.
[147] E.A. Bonfante, M.N. Janal, R. Granato, C. Marin, M. Suzuki, N. Tovar, P.G. Coelho, Buccal and lingual bone level alterations after immediate implantation of four implant surfaces: a study in dogs, Clinical oral implants research 24(12) (2013) 1375-80.
[148] J.B. Gomes, F.E. Campos, C. Marin, H.S. Teixeira, E.A. Bonfante, M. Suzuki, L. Witek, D. Zanetta-Barbosa, P.G. Coelho, Implant biomechanical stability variation at early implantation times in vivo: an experimental study in dogs, The International journal of oral & maxillofacial implants 28(3) (2013) e128-34.
[149] S. Heberer, S. Kilic, J. Hossamo, J.D. Raguse, K. Nelson, Rehabilitation of irradiated patients with modified and conventional sandblasted acid-etched implants: preliminary results of a split-mouth study, Clinical oral implants research 22(5) (2011) 546-51.
[150] Z.C. Karabuda, J. Abdel-Haq, V. Arisan, Stability, marginal bone loss and survival of standard and modified sand-blasted, acid-etched implants in bilateral edentulous spaces: a prospective 15-month evaluation, Clinical oral implants research 22(8) (2011) 840-9.
[151] H.C. Lai, L.F. Zhuang, X. Liu, M. Wieland, Z.Y. Zhang, Z.Y. Zhang, The influence of surface energy on early adherent events of osteoblast on titanium substrates, Journal of biomedical materials research. Part A 93(1) (2010) 289-96.
[152] G. Zhao, Z. Schwartz, M. Wieland, F. Rupp, J. Geis-Gerstorfer, D.L. Cochran, B.D. Boyan, High surface energy enhances cell response to titanium substrate microstructure, Journal of biomedical materials research. Part A 74(1) (2005) 49-58.
[153] N. Hamamoto, Y. Hamamoto, T. Nakajima, H. Ozawa, Histological, histocytochemical and ultrastructural study on the effects of surface charge on bone formation in the rabbit mandible, Archives of oral biology 40(2) (1995) 97-106.
[154] M. Krukowski, R.A. Shively, P. Osdoby, B.L. Eppley, Stimulation of craniofacial and intramedullary bone formation by negatively charged beads, Journal of oral and maxillofacial surgery : official journal of the American Association of Oral and Maxillofacial Surgeons 48(5) (1990) 468-75.

[155] K.E. Healy, C.H. Thomas, A. Rezania, J.E. Kim, P.J. McKeown, B. Lom, P.E. Hockberger, Kinetics of bone cell organization and mineralization on materials with patterned surface chemistry, Biomaterials 17(2) (1996) 195-208.
[156] J.M. Curran, R. Chen, J.A. Hunt, The guidance of human mesenchymal stem cell differentiation in vitro by controlled modifications to the cell substrate, Biomaterials 27(27) (2006) 4783-4793.
[157] G.A. Hudalla, W.L. Murphy, Using "Click" Chemistry to Prepare SAM Substrates to Study Stem Cell Adhesion, Langmuir 25(10) (2009) 5737-5746.
[158] J.E. Phillips, T.A. Petrie, F.P. Creighton, A.J. Garcia, Human mesenchymal stem cell differentiation on self-assembled monolayers presenting different surface chemistries, Acta Biomater 6(1) (2010) 12-20.
[159] J.M. Curran, R. Chen, J.A. Hunt, Controlling the phenotype and function of mesenchymal stem cells in vitro by adhesion to silane-modified clean glass surfaces, Biomaterials 26(34) (2005) 7057-67.
[160] P.L. Granja, B.D. Jéso, R. Bareille, F. Rouais, C. Baquey, M.A. Barbosa, Cellulose phosphates as biomaterials. In vitro biocompatibility studies, Reactive and Functional Polymers 66(7) (2006) 728-739.
[161] R.G. Geesink, K. de Groot, C.P. Klein, Bonding of bone to apatite-coated implants, The Journal of bone and joint surgery. British volume 70(1) (1988) 17-22.
[162] P.J.D. Manders, J.G.C. Wolke, J.A. Jansen, Bone response adjacent to calcium phosphate electrostatic spray deposition coated implants: an experimental study in goats, Clinical oral implants research 17(5) (2006) 548-553.
[163] S.S. Rajaratnam, C. Jack, A. Tavakkolizadeh, M.D. George, R.J. Fletcher, M. Hankins, J.A. Shepperd, Long-term results of a hydroxyapatite-coated femoral component in total hip replacement: a 15- to 21-year follow-up study, The Journal of bone and joint surgery. British volume 90(1) (2008) 27-30.
[164] G. Daculsi, O. Laboux, O. Malard, P. Weiss, Current state of the art of biphasic calcium phosphate bioceramics, Journal of materials science. Materials in medicine 14(3) (2003) 195-200.
[165] J.E. Davies, Understanding peri-implant endosseous healing, Journal of dental education 67(8) (2003) 932-49.
[166] T. Huang, Y. Xiao, S. Wang, Y. Huang, X. Liu, F. Wu, Z. Gu, Nanostructured Si, Mg, CO_3^{2-} Substituted Hydroxyapatite Coatings Deposited by Liquid Precursor Plasma Spraying: Synthesis and Characterization, Journal of Thermal Spray Technology 20(4) (2011) 829-836.
[167] R.A. Surmenev, M.A. Surmeneva, A.A. Ivanova, Significance of calcium phosphate coatings for the enhancement of new bone osteogenesis – A review, Acta Biomaterialia 10(2) (2014) 557-579.
[168] N. Jaiswal, S.E. Haynesworth, A.I. Caplan, S.P. Bruder, Osteogenic differentiation of purified, culture-expanded human mesenchymal stem cells in vitro, Journal of cellular biochemistry 64(2) (1997) 295-312.
[169] B. Krijgsman, A.M. Seifalian, H.J. Salacinski, N.R. Tai, G. Punshon, B.J. Fuller, G. Hamilton, An assessment of covalent grafting of RGD peptides to the surface of a compliant poly(carbonate-urea)urethane vascular conduit versus conventional biological coatings: its role in enhancing cellular retention, Tissue engineering 8(4) (2002) 673-80.
[170] M. Dettin, A. Zamuner, M. Roso, G. Iucci, V. Samouillan, R. Danesin, M. Modesti, M.T. Conconi, Facile and selective covalent grafting of an RGD-peptide to electrospun scaffolds improves HUVEC adhesion, Journal of peptide science : an official publication of the European Peptide Society 21(10) (2015) 786-95.
[171] Y. Suzuki, M. Tanihara, K. Suzuki, A. Saitou, W. Sufan, Y. Nishimura, Alginate hydrogel linked with synthetic oligopeptide derived from BMP-2 allows ectopic osteoinduction in vivo, J Biomed Mater Res 50(3) (2000) 405-9.

[172] M.D. Pierschbacher, E. Ruoslahti, Cell attachment activity of fibronectin can be duplicated by small synthetic fragments of the molecule, Nature 309(5963) (1984) 30-33.
[173] J.R. Lieberman, A. Daluiski, T.A. Einhorn, The role of growth factors in the repair of bone. Biology and clinical applications, J Bone Joint Surg Am 84-a(6) (2002) 1032-44.
[174] W.J. King, P.H. Krebsbach, Growth factor delivery: How surface interactions modulate release in vitro and in vivo, Advanced Drug Delivery Reviews 64(12) (2012) 1239-1256.
[175] M.R. Urist, Bone: formation by autoinduction, Science 150(3698) (1965) 893-9.
[176] H. Cheng, W. Jiang, F.M. Phillips, R.C. Haydon, Y. Peng, L. Zhou, H.H. Luu, N. An, B. Breyer, P. Vanichakarn, J.P. Szatkowski, J.Y. Park, T.C. He, Osteogenic activity of the fourteen types of human bone morphogenetic proteins (BMPs), The Journal of bone and joint surgery. American volume 85-a(8) (2003) 1544-52.
[177] P. Ducy, R. Zhang, V. Geoffroy, A.L. Ridall, G. Karsenty, Osf2/Cbfa1: a transcriptional activator of osteoblast differentiation, Cell 89(5) (1997) 747-54.
[178] K.S. Lee, H.J. Kim, Q.L. Li, X.Z. Chi, C. Ueta, T. Komori, J.M. Wozney, E.G. Kim, J.Y. Choi, H.M. Ryoo, S.C. Bae, Runx2 is a common target of transforming growth factor beta1 and bone morphogenetic protein 2, and cooperation between Runx2 and Smad5 induces osteoblast-specific gene expression in the pluripotent mesenchymal precursor cell line C2C12, Molecular and cellular biology 20(23) (2000) 8783-92.
[179] H. Senta, H. Park, E. Bergeron, O. Drevelle, D. Fong, E. Leblanc, F. Cabana, S. Roux, G. Grenier, N. Faucheux, Cell responses to bone morphogenetic proteins and peptides derived from them: biomedical applications and limitations, Cytokine & growth factor reviews 20(3) (2009) 213-22.
[180] J.A. Hubbell, Bioactive biomaterials, Current opinion in biotechnology 10(2) (1999) 123-9.
[181] S.L. Bellis, Advantages of RGD peptides for directing cell association with biomaterials, Biomaterials 32(18) (2011) 4205-10.
[182] S.P. Massia, J.A. Hubbell, An RGD spacing of 440 nm is sufficient for integrin alpha V beta 3-mediated fibroblast spreading and 140 nm for focal contact and stress fiber formation, J Cell Biol 114(5) (1991) 1089-100.
[183] M.A. Arnaout, B. Mahalingam, J.P. Xiong, Integrin structure, allostery, and bidirectional signaling, Annual review of cell and developmental biology 21 (2005) 381-410.
[184] J.D. Humphries, A. Byron, M.J. Humphries, Integrin ligands at a glance, Journal of cell science 119(Pt 19) (2006) 3901-3.
[185] I. Bilem, P. Chevallier, L. Plawinski, E.D. Sone, M.C. Durrieu, G. Laroche, RGD and BMP-2 mimetic peptide crosstalk enhances osteogenic commitment of human bone marrow stem cells, Acta Biomater (2016).
[186] M.C. Porte-Durrieu, F. Guillemot, S. Pallu, C. Labrugere, B. Brouillaud, R. Bareille, J. Amedee, N. Barthe, M. Dard, C. Baquey, Cyclo-(DfKRG) peptide grafting onto Ti-6Al-4V: physical characterization and interest towards human osteoprogenitor cells adhesion, Biomaterials 25(19) (2004) 4837-46.
[187] O.F. Zouani, C. Chollet, B. Guillotin, M.C. Durrieu, Differentiation of pre-osteoblast cells on poly(ethylene terephthalate) grafted with RGD and/or BMPs mimetic peptides, Biomaterials 31(32) (2010) 8245-53.
[188] B. Elmengaard, J.E. Bechtold, K. Soballe, In vivo study of the effect of RGD treatment on bone ongrowth on press-fit titanium alloy implants, Biomaterials 26(17) (2005) 3521-6.
[189] H. Schliephake, A. Aref, D. Scharnweber, S. Bierbaum, A. Sewing, Effect of modifications of dual acid-etched implant surfaces on peri-implant bone formation. Part I: organic coatings, Clinical oral implants research 20(1) (2009) 31-7.
[190] Y. Ku, C.P. Chung, J.H. Jang, The effect of the surface modification of titanium using a recombinant fragment of fibronectin and vitronectin on cell behavior, Biomaterials 26(25) (2005) 5153-7.

[191] S. Aota, M. Nomizu, K.M. Yamada, The short amino acid sequence Pro-His-Ser-Arg-Asn in human fibronectin enhances cell-adhesive function, The Journal of biological chemistry 269(40) (1994) 24756-61.
[192] M.J. Humphries, S.K. Akiyama, A. Komoriya, K. Olden, K.M. Yamada, Identification of an alternatively spliced site in human plasma fibronectin that mediates cell type-specific adhesion, J Cell Biol 103(6 Pt 2) (1986) 2637-47.
[193] A. Komoriya, L.J. Green, M. Mervic, S.S. Yamada, K.M. Yamada, M.J. Humphries, The minimal essential sequence for a major cell type-specific adhesion site (CS1) within the alternatively spliced type III connecting segment domain of fibronectin is leucine-aspartic acid-valine, The Journal of biological chemistry 266(23) (1991) 15075-9.
[194] H. Zhang, S. Hollister, Comparison of bone marrow stromal cell behaviors on poly(caprolactone) with or without surface modification: studies on cell adhesion, survival and proliferation, Journal of biomaterials science. Polymer edition 20(14) (2009) 1975-93.
[195] D.M. Ferris, G.D. Moodie, P.M. Dimond, C.W.D. Giorani, M.G. Ehrlich, R.F. Valentini, RGD-coated titanium implants stimulate increased bone formation in vivo, Biomaterials 20(23–24) (1999) 2323-2331.
[196] S. Pallu, J.C. Fricain, R. Bareille, C. Bourget, M. Dard, A. Sewing, J. Amedee, Cyclo-DfKRG peptide modulates in vitro and in vivo behavior of human osteoprogenitor cells on titanium alloys, Acta Biomater 5(9) (2009) 3581-92.
[197] C.D. Reyes, T.A. Petrie, K.L. Burns, Z. Schwartz, A.J. Garcia, Biomolecular surface coating to enhance orthopaedic tissue healing and integration, Biomaterials 28(21) (2007) 3228-35.
[198] J. Emsley, C.G. Knight, R.W. Farndale, M.J. Barnes, Structure of the integrin alpha2beta1-binding collagen peptide, Journal of molecular biology 335(4) (2004) 1019-28.
[199] K.C. Dee, T.T. Andersen, R. Bizios, Design and function of novel osteoblast-adhesive peptides for chemical modification of biomaterials, J Biomed Mater Res 40(3) (1998) 371-7.
[200] P. Gentile, C. Ghione, C. Tonda-Turo, D.M. Kalaskar, Peptide functionalisation of nanocomposite polymer for bone tissue engineering using plasma surface polymerisation, RSC Advances 5(97) (2015) 80039-80047.
[201] M. Dettin, A. Bagno, R. Gambaretto, G. Iucci, M.T. Conconi, N. Tuccitto, A.M. Menti, C. Grandi, C. Di Bello, A. Licciardello, G. Polzonetti, Covalent surface modification of titanium oxide with different adhesive peptides: surface characterization and osteoblast-like cell adhesion, Journal of biomedical materials research. Part A 90(1) (2009) 35-45.
[202] O. Drevelle, E. Bergeron, H. Senta, M.A. Lauzon, S. Roux, G. Grenier, N. Faucheux, Effect of functionalized polycaprolactone on the behaviour of murine preosteoblasts, Biomaterials 31(25) (2010) 6468-76.
[203] T.A. Barber, L.J. Gamble, D.G. Castner, K.E. Healy, In vitro characterization of peptide-modified p(AAm-co-EG/AAc) IPN-coated titanium implants, Journal of orthopaedic research : official publication of the Orthopaedic Research Society 24(7) (2006) 1366-76.
[204] H. Shin, K. Zygourakis, M.C. Farach-Carson, M.J. Yaszemski, A.G. Mikos, Attachment, proliferation, and migration of marrow stromal osteoblasts cultured on biomimetic hydrogels modified with an osteopontin-derived peptide, Biomaterials 25(5) (2004) 895-906.
[205] H. Shin, K. Zygourakis, M.C. Farach-Carson, M.J. Yaszemski, A.G. Mikos, Modulation of differentiation and mineralization of marrow stromal cells cultured on biomimetic hydrogels modified with Arg-Gly-Asp containing peptides, Journal of biomedical materials research. Part A 69(3) (2004) 535-43.
[206] A. Saito, Y. Suzuki, S. Ogata, C. Ohtsuki, M. Tanihara, Activation of osteo-progenitor cells by a novel synthetic peptide derived from the bone morphogenetic protein-2 knuckle epitope, Biochimica et biophysica acta 1651(1-2) (2003) 60-7.

[207] A. Saito, Y. Suzuki, S. Ogata, C. Ohtsuki, M. Tanihara, Prolonged ectopic calcification induced by BMP-2-derived synthetic peptide, Journal of biomedical materials research. Part A 70(1) (2004) 115-21.
[208] A. Saito, Y. Suzuki, M. Kitamura, S. Ogata, Y. Yoshihara, S. Masuda, C. Ohtsuki, M. Tanihara, Repair of 20-mm long rabbit radial bone defects using BMP-derived peptide combined with an alpha-tricalcium phosphate scaffold, Journal of biomedical materials research. Part A 77(4) (2006) 700-6.
[209] Z.Y. Lin, Z.X. Duan, X.D. Guo, J.F. Li, H.W. Lu, Q.X. Zheng, D.P. Quan, S.H. Yang, Bone induction by biomimetic PLGA-(PEG-ASP)n copolymer loaded with a novel synthetic BMP-2-related peptide in vitro and in vivo, Journal of controlled release : official journal of the Controlled Release Society 144(2) (2010) 190-5.
[210] O.F. Zouani, J. Kalisky, E. Ibarboure, M.C. Durrieu, Effect of BMP-2 from matrices of different stiffnesses for the modulation of stem cell fate, Biomaterials 34(9) (2013) 2157-66.
[211] O.F. Zouani, L. Rami, Y. Lei, M.-C. Durrieu, Insights into the osteoblast precursor differentiation towards mature osteoblasts induced by continuous BMP-2 signaling, Biology open (2013) BIO20134986.
[212] J.Y. Lee, J.E. Choo, H.J. Park, J.B. Park, S.C. Lee, S.J. Lee, Y.J. Park, C.P. Chung, Synthetic peptide-coated bone mineral for enhanced osteoblastic activation in vitro and in vivo, Journal of biomedical materials research. Part A 87(3) (2008) 688-97.
[213] J.B. Park, J.Y. Lee, H.N. Park, Y.J. Seol, Y.J. Park, S.H. Rhee, S.C. Lee, K.H. Kim, T.I. Kim, Y.M. Lee, Y. Ku, I.C. Rhyu, S.B. Han, C.P. Chung, Osteopromotion with synthetic oligopeptide-coated bovine bone mineral in vivo, Journal of periodontology 78(1) (2007) 157-63.
[214] C.K. Lee, K.T. Koo, Y.J. Park, J.Y. Lee, S.H. Rhee, Y. Ku, I.C. Rhyu, C.P. Chung, Biomimetic surface modification using synthetic oligopeptides for enhanced guided bone regeneration in beagles, Journal of periodontology 83(1) (2012) 101-10.
[215] J.B. Park, J.Y. Lee, Y.J. Park, S.H. Rhee, S.C. Lee, T.I. Kim, Y.J. Seol, Y.M. Lee, Y. Ku, I.C. Rhyu, S.B. Han, C.P. Chung, Enhanced bone regeneration in beagle dogs with bovine bone mineral coated with a synthetic oligopeptide, Journal of periodontology 78(11) (2007) 2150-5.
[216] K. Kirkwood, B. Rheude, Y.J. Kim, K. White, K.C. Dee, In vitro mineralization studies with substrate-immobilized bone morphogenetic protein peptides, The Journal of oral implantology 29(2) (2003) 57-65.
[217] Y. Chen, T.J. Webster, Increased Osteoblast Functions in the Presence of BMP-7 Short Peptides for Nanostructured Biomaterial Applications, Journal of biomedical materials research. Part A 91(1) (2009) 296-304.
[218] E. Bergeron, M. Marquis, I. Chretien, N. Faucheux, Differentiation of preosteoblasts using a delivery system with BMPs and bioactive glass microspheres, Journal of Materials Science: Materials in Medicine 18(2) (2007) 255-263.
[219] A. Saito, Y. Suzuki, S. Ogata, C. Ohtsuki, M. Tanihara, Accelerated bone repair with the use of a synthetic BMP-2-derived peptide and bone-marrow stromal cells, Journal of biomedical materials research. Part A 72(1) (2005) 77-82.
[220] B. Kloesch, B. Hoering, D. Dopler, A. Banerjee, M. van Griensven, H. Redl, Synthetic peptides derived from the knuckle epitope of hBMP-2 were evaluated for inducing osteogenic differentiation in vitro and in vivo, Eur Cell Mater 14 (2007) 70.
[221] Y.J. Seol, Y.J. Park, S.C. Lee, K.H. Kim, J.Y. Lee, T.I. Kim, Y.M. Lee, Y. Ku, I.C. Rhyu, S.B. Han, C.P. Chung, Enhanced osteogenic promotion around dental implants with synthetic binding motif mimicking bone morphogenetic protein (BMP)-2, Journal of biomedical materials research. Part A 77(3) (2006) 599-607.
[222] C.K. Poh, Z. Shi, X.W. Tan, Z.C. Liang, X.M. Foo, H.C. Tan, K.G. Neoh, W. Wang, Cobalt chromium alloy with immobilized BMP peptide for enhanced bone growth, Journal of

orthopaedic research : official publication of the Orthopaedic Research Society 29(9) (2011) 1424-30.
[223] E. Migliorini, A. Valat, C. Picart, E.A. Cavalcanti-Adam, Tuning cellular responses to BMP-2 with material surfaces, Cytokine & growth factor reviews 27 (2016) 43-54.
[224] M.F. Brizzi, G. Tarone, P. Defilippi, Extracellular matrix, integrins, and growth factors as tailors of the stem cell niche, Current opinion in cell biology 24(5) (2012) 645-51.
[225] C.F. Lai, S.L. Cheng, Alphavbeta integrins play an essential role in BMP-2 induction of osteoblast differentiation, Journal of bone and mineral research : the official journal of the American Society for Bone and Mineral Research 20(2) (2005) 330-40.
[226] M.E. Marquis, E. Lord, E. Bergeron, L. Bourgoin, N. Faucheux, Short-term effects of adhesion peptides on the responses of preosteoblasts to pBMP-9, Biomaterials 29(8) (2008) 1005-16.
[227] X. He, J. Ma, E. Jabbari, Effect of grafting RGD and BMP-2 protein-derived peptides to a hydrogel substrate on osteogenic differentiation of marrow stromal cells, Langmuir 24(21) (2008) 12508-16.
[228] X. He, X. Yang, E. Jabbari, Combined effect of osteopontin and BMP-2 derived peptides grafted to an adhesive hydrogel on osteogenic and vasculogenic differentiation of marrow stromal cells, Langmuir 28(12) (2012) 5387-97.
[229] N.M. Moore, N.J. Lin, N.D. Gallant, M.L. Becker, Synergistic enhancement of human bone marrow stromal cell proliferation and osteogenic differentiation on BMP-2-derived and RGD peptide concentration gradients, Acta Biomaterialia 7(5) (2011) 2091-2100.
[230] D.A. Fletcher, R.D. Mullins, Cell mechanics and the cytoskeleton, Nature 463(7280) (2010) 485-492.
[231] D.E. Discher, P. Janmey, Y.L. Wang, Tissue cells feel and respond to the stiffness of their substrate, Science 310(5751) (2005) 1139-43.
[232] C. Webster, L. Silberstein, A.P. Hays, H.M. Blau, Fast muscle fibers are preferentially affected in Duchenne muscular dystrophy, Cell 52(4) (1988) 503-513.
[233] A. Buxboim, D.E. Discher, Stem cells feel the difference, Nat Meth 7(9) (2010) 695-697.
[234] A. Buxboim, I.L. Ivanovska, D.E. Discher, Matrix elasticity, cytoskeletal forces and physics of the nucleus: how deeply do cells 'feel' outside and in?, Journal of cell science 123(3) (2010) 297-308.
[235] J.T. Emerman, S.J. Burwen, D.R. Pitelka, Substrate properties influencing ultrastructural differentiation of mammary epithelial cells in culture, Tissue & cell 11(1) (1979) 109-19.
[236] A.J. Engler, S. Sen, H.L. Sweeney, D.E. Discher, Matrix Elasticity Directs Stem Cell Lineage Specification, Cell 126(4) (2006) 677-689.
[237] N. Huebsch, P.R. Arany, A.S. Mao, D. Shvartsman, O.A. Ali, S.A. Bencherif, J. Rivera-Feliciano, D.J. Mooney, Harnessing traction-mediated manipulation of the cell/matrix interface to control stem-cell fate, Nat Mater 9(6) (2010) 518-526.
[238] J.P. Winer, P.A. Janmey, M.E. McCormick, M. Funaki, Bone marrow-derived human mesenchymal stem cells become quiescent on soft substrates but remain responsive to chemical or mechanical stimuli, Tissue engineering. Part A 15(1) (2009) 147-54.
[239] Y.J. Li, E.H. Chung, R.T. Rodriguez, M.T. Firpo, K.E. Healy, Hydrogels as artificial matrices for human embryonic stem cell self-renewal, Journal of biomedical materials research. Part A 79(1) (2006) 1-5.
[240] K. Ye, X. Wang, L. Cao, S. Li, Z. Li, L. Yu, J. Ding, Matrix Stiffness and Nanoscale Spatial Organization of Cell-Adhesive Ligands Direct Stem Cell Fate, Nano letters 15(7) (2015) 4720-9.
[241] R. McBeath, D.M. Pirone, C.M. Nelson, K. Bhadriraju, C.S. Chen, Cell shape, cytoskeletal tension, and RhoA regulate stem cell lineage commitment, Developmental cell 6(4) (2004) 483-95.

[242] K.A. Kilian, B. Bugarija, B.T. Lahn, M. Mrksich, Geometric cues for directing the differentiation of mesenchymal stem cells, Proc Natl Acad Sci U S A 107(11) (2010) 4872-7.
[243] O. Chaudhuri, S.T. Koshy, C. Branco da Cunha, J.-W. Shin, C.S. Verbeke, K.H. Allison, D.J. Mooney, Extracellular matrix stiffness and composition jointly regulate the induction of malignant phenotypes in mammary epithelium, Nat Mater 13(10) (2014) 970-978.
[244] Y.-R.V. Shih, K.-F. Tseng, H.-Y. Lai, C.-H. Lin, O.K. Lee, Matrix stiffness regulation of integrin-mediated mechanotransduction during osteogenic differentiation of human mesenchymal stem cells, Journal of Bone and Mineral Research 26(4) (2011) 730-738.
[245] R.J. Pelham, Jr., Y. Wang, Cell locomotion and focal adhesions are regulated by substrate flexibility, Proc Natl Acad Sci U S A 94(25) (1997) 13661-5.
[246] J.R. Tse, A.J. Engler, Stiffness gradients mimicking in vivo tissue variation regulate mesenchymal stem cell fate, PloS one 6(1) (2011) e15978.
[247] P.M. Gilbert, K.L. Havenstrite, K.E. Magnusson, A. Sacco, N.A. Leonardi, P. Kraft, N.K. Nguyen, S. Thrun, M.P. Lutolf, H.M. Blau, Substrate elasticity regulates skeletal muscle stem cell self-renewal in culture, Science 329(5995) (2010) 1078-81.
[248] B. Trappmann, J.E. Gautrot, J.T. Connelly, D.G. Strange, Y. Li, M.L. Oyen, M.A. Cohen Stuart, H. Boehm, B. Li, V. Vogel, J.P. Spatz, F.M. Watt, W.T. Huck, Extracellular-matrix tethering regulates stem-cell fate, Nat Mater 11(7) (2012) 642-9.
[249] J.H. Wen, L.G. Vincent, A. Fuhrmann, Y.S. Choi, K.C. Hribar, H. Taylor-Weiner, S. Chen, A.J. Engler, Interplay of matrix stiffness and protein tethering in stem cell differentiation, Nat Mater 13(10) (2014) 979-87.
[250] R.K. Das, V. Gocheva, R. Hammink, O.F. Zouani, A.E. Rowan, Stress-stiffening-mediated stem-cell commitment switch in soft responsive hydrogels, Nat Mater 15(3) (2016) 318-325.
[251] M. Nikkhah, F. Edalat, S. Manoucheri, A. Khademhosseini, Engineering microscale topographies to control the cell-substrate interface, Biomaterials 33(21) (2012) 5230-46.
[252] A. Cunha, O.F. Zouani, L. Plawinski, A.M. Botelho do Rego, A. Almeida, R. Vilar, M.-C. Durrieu, Human mesenchymal stem cell behavior on femtosecond laser-textured Ti-6Al-4V surfaces, Nanomedicine 10(5) (2015) 725-739.
[253] L.F. Cooper, A role for surface topography in creating and maintaining bone at titanium endosseous implants, The Journal of prosthetic dentistry 84(5) (2000) 522-34.
[254] R.K. Das, O.F. Zouani, A review of the effects of the cell environment physicochemical nanoarchitecture on stem cell commitment, Biomaterials 35(20) (2014) 5278-93.
[255] R.G. Flemming, C.J. Murphy, G.A. Abrams, S.L. Goodman, P.F. Nealey, Effects of synthetic micro- and nano-structured surfaces on cell behavior, Biomaterials 20(6) (1999) 573-88.
[256] T.T. Kawabe, D.K. MacCallum, J.H. Lillie, Variation in basement membrane topography in human thick skin, The Anatomical record 211(2) (1985) 142-8.
[257] S. Brody, T. Anilkumar, S. Liliensiek, J.A. Last, C.J. Murphy, A. Pandit, Characterizing Nanoscale Topography of the Aortic Heart Valve Basement Membrane for Tissue Engineering Heart Valve Scaffold Design, Tissue engineering 12(2) (2006) 413-421.
[258] T. Takeuchi, T. Gonda, Distribution of the pores of epithelial basement membrane in the rat small intestine, The Journal of veterinary medical science / the Japanese Society of Veterinary Science 66(6) (2004) 695-700.
[259] G.A. Abrams, E. Bentley, P.F. Nealey, C.J. Murphy, Electron microscopy of the canine corneal basement membranes, Cells, tissues, organs 170(4) (2002) 251-7.
[260] G.A. Abrams, C.J. Murphy, Z.Y. Wang, P.F. Nealey, D.E. Bjorling, Ultrastructural basement membrane topography of the bladder epithelium, Urological research 31(5) (2003) 341-6.

[261] T. Albrektsson, A. Wennerberg, Oral implant surfaces: Part 1--review focusing on topographic and chemical properties of different surfaces and in vivo responses to them, The International journal of prosthodontics 17(5) (2004) 536-43.
[262] D.M. Dohan Ehrenfest, P.G. Coelho, B.S. Kang, Y.T. Sul, T. Albrektsson, Classification of osseointegrated implant surfaces: materials, chemistry and topography, Trends Biotechnol 28(4) (2010) 198-206.
[263] B. Al-Nawas, K.A. Groetz, H. Goetz, H. Duschner, W. Wagner, Comparative histomorphometry and resonance frequency analysis of implants with moderately rough surfaces in a loaded animal model, Clinical oral implants research 19(1) (2008) 1-8.
[264] R.A. Gittens, T. McLachlan, R. Olivares-Navarrete, Y. Cai, S. Berner, R. Tannenbaum, Z. Schwartz, K.H. Sandhage, B.D. Boyan, The effects of combined micron-/submicron-scale surface roughness and nanoscale features on cell proliferation and differentiation, Biomaterials 32(13) (2011) 3395-403.
[265] S. Lossdörfer, Z. Schwartz, L. Wang, C.H. Lohmann, J.D. Turner, M. Wieland, D.L. Cochran, B.D. Boyan, Microrough implant surface topographies increase osteogenesis by reducing osteoclast formation and activity, Journal of Biomedical Materials Research Part A 70A(3) (2004) 361-369.
[266] A. Wennerberg, T. Albrektsson, Effects of titanium surface topography on bone integration: a systematic review, Clinical oral implants research 20 Suppl 4 (2009) 172-84.
[267] A. Wennerberg, T. Albrektsson, Suggested guidelines for the topographic evaluation of implant surfaces, The International journal of oral & maxillofacial implants 15(3) (2000) 331-44.
[268] R. Castellani, A. de Ruijter, H. Renggli, J. Jansen, Response of rat bone marrow cells to differently roughened titanium discs, Clinical oral implants research 10(5) (1999) 369-78.
[269] M. Esposito, Y. Ardebili, H.V. Worthington, Interventions for replacing missing teeth: different types of dental implants, The Cochrane database of systematic reviews 7 (2014) Cd003815.
[270] C.A. Pfluger, D.D. Burkey, L. Wang, B. Sun, K.S. Ziemer, R.L. Carrier, Biocompatibility of Plasma Enhanced Chemical Vapor Deposited Poly(2-hydroxyethyl methacrylate) Films for Biomimetic Replication of the Intestinal Basement Membrane, Biomacromolecules 11(6) (2010) 1579-1584.
[271] C.J. Bettinger, R. Langer, J.T. Borenstein, Engineering substrate topography at the micro- and nanoscale to control cell function, Angewandte Chemie (International ed. in English) 48(30) (2009) 5406-15.
[272] Y. Wan, Y. Wang, Z. Liu, X. Qu, B. Han, J. Bei, S. Wang, Adhesion and proliferation of OCT-1 osteoblast-like cells on micro- and nano-scale topography structured poly(l-lactide), Biomaterials 26(21) (2005) 4453-4459.
[273] O. Zinger, K. Anselme, A. Denzer, P. Habersetzer, M. Wieland, J. Jeanfils, P. Hardouin, D. Landolt, Time-dependent morphology and adhesion of osteoblastic cells on titanium model surfaces featuring scale-resolved topography, Biomaterials 25(14) (2004) 2695-711.
[274] D.W. Hamilton, B. Chehroudi, D.M. Brunette, Comparative response of epithelial cells and osteoblasts to microfabricated tapered pit topographies in vitro and in vivo, Biomaterials 28(14) (2007) 2281-93.
[275] D.W. Hamilton, K.S. Wong, D.M. Brunette, Microfabricated discontinuous-edge surface topographies influence osteoblast adhesion, migration, cytoskeletal organization, and proliferation and enhance matrix and mineral deposition in vitro, Calcif Tissue Int 78(5) (2006) 314-25.
[276] M. Ghibaudo, L. Trichet, J. Le Digabel, A. Richert, P. Hersen, B. Ladoux, Substrate topography induces a crossover from 2D to 3D behavior in fibroblast migration, Biophys J 97(1) (2009) 357-68.

[277] A.I. Teixeira, G.A. Abrams, P.J. Bertics, C.J. Murphy, P.F. Nealey, Epithelial contact guidance on well-defined micro- and nanostructured substrates, Journal of cell science 116(Pt 10) (2003) 1881-92.
[278] X. Lu, Y. Leng, Comparison of the osteoblast and myoblast behavior on hydroxyapatite microgrooves, Journal of biomedical materials research. Part B, Applied biomaterials 90(1) (2009) 438-45.
[279] M.J. Lopez-Bosque, E. Tejeda-Montes, M. Cazorla, J. Linacero, Y. Atienza, K.H. Smith, A. Llado, J. Colombelli, E. Engel, A. Mata, Fabrication of hierarchical micro-nanotopographies for cell attachment studies, Nanotechnology 24(25) (2013) 255305.
[280] H.V. Unadkat, M. Hulsman, K. Cornelissen, B.J. Papenburg, R.K. Truckenmüller, A.E. Carpenter, M. Wessling, G.F. Post, M. Uetz, M.J.T. Reinders, D. Stamatialis, C.A. van Blitterswijk, J. de Boer, An algorithm-based topographical biomaterials library to instruct cell fate, Proceedings of the National Academy of Sciences 108(40) (2011) 16565-16570.
[281] J. Fu, Y.K. Wang, M.T. Yang, R.A. Desai, X. Yu, Z. Liu, C.S. Chen, Mechanical regulation of cell function with geometrically modulated elastomeric substrates, Nature methods 7(9) (2010) 733-6.
[282] M. Guvendiren, J.A. Burdick, The control of stem cell morphology and differentiation by hydrogel surface wrinkles, Biomaterials 31(25) (2010) 6511-6518.
[283] W. Song, N. Kawazoe, G. Chen, Dependence of spreading and differentiation of mesenchymal stem cells on micropatterned surface area, J. Nanomaterials 2011 (2011) 1-9.
[284] C.H. Seo, K. Furukawa, Y. Suzuki, N. Kasagi, T. Ichiki, T. Ushida, A topographically optimized substrate with well-ordered lattice micropatterns for enhancing the osteogenic differentiation of murine mesenchymal stem cells, Macromol Biosci 11(7) (2011) 938-45.
[285] C.H. Seo, K. Furukawa, K. Montagne, H. Jeong, T. Ushida, The effect of substrate microtopography on focal adhesion maturation and actin organization via the RhoA/ROCK pathway, Biomaterials 32(36) (2011) 9568-75.
[286] Z. Schwartz, C.H. Lohmann, A.K. Vocke, V.L. Sylvia, D.L. Cochran, D.D. Dean, B.D. Boyan, Osteoblast response to titanium surface roughness and 1alpha,25-(OH)(2)D(3) is mediated through the mitogen-activated protein kinase (MAPK) pathway, J Biomed Mater Res 56(3) (2001) 417-26.
[287] D.L. Jones, A.J. Wagers, No place like home: anatomy and function of the stem cell niche, Nature reviews. Molecular cell biology 9(1) (2008) 11-21.
[288] M. Thery, Micropatterning as a tool to decipher cell morphogenesis and functions, Journal of cell science 123(Pt 24) (2010) 4201-13.
[289] J. Sun, S.V. Graeter, L. Yu, S. Duan, J.P. Spatz, J. Ding, Technique of surface modification of a cell-adhesion-resistant hydrogel by a cell-adhesion-available inorganic microarray, Biomacromolecules 9(10) (2008) 2569-72.
[290] C. Chollet, S. Lazare, C. Labrugère, F. Guillemot, R. Bareille, M.-C. Durrieu, RGD peptides micro-patterning on poly (ethylene terephthalate) surfaces, IRBM 28(1) (2007) 2-12.
[291] T. Okamoto, T. Suzuki, N. Yamamoto, Microarray fabrication with covalent attachment of DNA using bubble jet technology, Nature biotechnology 18(4) (2000) 438-41.
[292] A. Khademhosseini, G. Eng, J. Yeh, P.A. Kucharczyk, R. Langer, G. Vunjak-Novakovic, M. Radisic, Microfluidic patterning for fabrication of contractile cardiac organoids, Biomedical microdevices 9(2) (2007) 149-57.
[293] D.B. Weibel, W.R. DiLuzio, G.M. Whitesides, Microfabrication meets microbiology, Nat Rev Micro 5(3) (2007) 209-218.
[294] R. Peng, X. Yao, J. Ding, Effect of cell anisotropy on differentiation of stem cells on micropatterned surfaces through the controlled single cell adhesion, Biomaterials 32(32) (2011) 8048-8057.
[295] S.B. Carter, Principles of cell motility: the direction of cell movement and cancer invasion, Nature 208(5016) (1965) 1183-7.

[296] S.B. Carter, Haptotactic islands, Experimental cell research 48(1) (1967) 189-193.
[297] C.S. Chen, M. Mrksich, S. Huang, G.M. Whitesides, D.E. Ingber, Geometric control of cell life and death, Science 276(5317) (1997) 1425-8.
[298] A. Kumar, H.A. Biebuyck, G.M. Whitesides, Patterning Self-Assembled Monolayers: Applications in Materials Science, Langmuir 10(5) (1994) 1498-1511.
[299] D. Lehnert, B. Wehrle-Haller, C. David, U. Weiland, C. Ballestrem, B.A. Imhof, M. Bastmeyer, Cell behaviour on micropatterned substrata: limits of extracellular matrix geometry for spreading and adhesion, Journal of cell science 117(1) (2004) 41-52.
[300] R. Peng, X. Yao, B. Cao, J. Tang, J. Ding, The effect of culture conditions on the adipogenic and osteogenic inductions of mesenchymal stem cells on micropatterned surfaces, Biomaterials 33(26) (2012) 6008-19.
[301] X. Yao, R. Peng, J. Ding, Effects of aspect ratios of stem cells on lineage commitments with and without induction media, Biomaterials 34(4) (2013) 930-9.
[302] M.K. Vartiainen, S. Guettler, B. Larijani, R. Treisman, Nuclear Actin Regulates Dynamic Subcellular Localization and Activity of the SRF Cofactor MAL, Science 316(5832) (2007) 1749-1752.
[303] J.T. Connelly, J.E. Gautrot, B. Trappmann, D.W. Tan, G. Donati, W.T. Huck, F.M. Watt, Actin and serum response factor transduce physical cues from the microenvironment to regulate epidermal stem cell fate decisions, Nature cell biology 12(7) (2010) 711-8.
[304] J.D. Baranski, R.R. Chaturvedi, K.R. Stevens, J. Eyckmans, B. Carvalho, R.D. Solorzano, M.T. Yang, J.S. Miller, S.N. Bhatia, C.S. Chen, Geometric control of vascular networks to enhance engineered tissue integration and function, Proceedings of the National Academy of Sciences of the United States of America 110(19) (2013) 7586-7591.
[305] R.R. Chaturvedi, K.R. Stevens, R.D. Solorzano, R.E. Schwartz, J. Eyckmans, J.D. Baranski, S.C. Stapleton, S.N. Bhatia, C.S. Chen, Patterning vascular networks in vivo for tissue engineering applications, Tissue engineering. Part C, Methods 21(5) (2015) 509-17.
[306] A. Ohler, J. Weisser-Thomas, V. Piacentino, S.R. Houser, G.F. Tomaselli, B. O'Rourke, Two-photon laser scanning microscopy of the transverse-axial tubule system in ventricular cardiomyocytes from failing and non-failing human hearts, Cardiology research and practice 2009 (2010).
[307] https://cytoo.com/assay-development-and-screening/cellular-models/human-cardiomyocytes-derived-ips-icardio-cdi-inc [Access date: February 12, 2016].
[308] D.J. Mooney, H. Vandenburgh, Cell Delivery Mechanisms for Tissue Repair, Cell Stem Cell 2(3) (2008) 205-213.
[309] K.-F.L. Soufeng Yang, Zhaohui Du, and Chee-Kai Chua, Tissue Engineering, (December 2001, 7(6): 679-689. doi:10.1089/107632701753337645.).
[310] K.J.L. Burg, S. Porter, J.F. Kellam, Biomaterial developments for bone tissue engineering, Biomaterials 21(23) (2000) 2347-2359.
[311] A.R. Amini, C.T. Laurencin, S.P. Nukavarapu, Bone Tissue Engineering: Recent Advances and Challenges, Crit Rev Biomed Eng 40(5) (2012) 363-408.
[312] F.J. O'Brien, Biomaterials & scaffolds for tissue engineering, Mater Today 14(3) (2011) 88-95.
[313] L. Lu, S.J. Peter, M. D. Lyman, H.-L. Lai, S.M. Leite, J.A. Tamada, S. Uyama, J.P. Vacanti, L. Robert, A.G. Mikos, In vitro and in vivo degradation of porous poly(dl-lactic-co-glycolic acid) foams, Biomaterials 21(18) (2000) 1837-1845.
[314] G. Sabbatier, A. Larrañaga, A.-A. Guay-Bégin, J. Fernandez, F. Diéval, B. Durand, J.-R. Sarasua, G. Laroche, Design, Degradation Mechanism and Long-Term Cytotoxicity of Poly(l-lactide) and Poly(Lactide-co-ϵ-Caprolactone) Terpolymer Film and Air-Spun Nanofiber Scaffold, Macromol Biosci (2015) n/a-n/a.
[315] M.P. Lutolf, J.A. Hubbell, Synthetic biomaterials as instructive extracellular microenvironments for morphogenesis in tissue engineering, Nat Biotech 23(1) (2005) 47-55.

[316] J.H. Collier, T. Segura, Evolving the use of peptides as components of biomaterials, Biomaterials 32(18) (2011) 4198-4204.
[317] J.P. Jung, A.K. Nagaraj, E.K. Fox, J.S. Rudra, J.M. Devgun, J.H. Collier, Co-assembling peptides as defined matrices for endothelial cells, Biomaterials 30(12) (2009) 2400-2410.
[318] A. Horii, X. Wang, F. Gelain, S. Zhang, Biological Designer Self-Assembling Peptide Nanofiber Scaffolds Significantly Enhance Osteoblast Proliferation, Differentiation and 3-D Migration, PloS one 2(2) (2007) e190.
[319] J.D. Hartgerink, E. Beniash, S.I. Stupp, Self-assembly and mineralization of peptide-amphiphile nanofibers, Science 294(5547) (2001) 1684-1688.
[320] E.F. Banwell, E.S. Abelardo, D.J. Adams, M.A. Birchall, A. Corrigan, A.M. Donald, M. Kirkland, L.C. Serpell, M.F. Butler, D.N. Woolfson, Rational design and application of responsive [alpha]-helical peptide hydrogels, Nat Mater 8(7) (2009) 596-600.
[321] M. Zhou, A.M. Smith, A.K. Das, N.W. Hodson, R.F. Collins, R.V. Ulijn, J.E. Gough, Self-assembled peptide-based hydrogels as scaffolds for anchorage-dependent cells, Biomaterials 30(13) (2009) 2523-2530.
[322] H. Cui, M.J. Webber, S.I. Stupp, Self-assembly of peptide amphiphiles: From molecules to nanostructures to biomaterials, Peptide Science 94(1) (2010) 1-18.
[323] A. Mata, Y. Geng, K.J. Henrikson, C. Aparicio, S.R. Stock, R.L. Satcher, S.I. Stupp, Bone regeneration mediated by biomimetic mineralization of a nanofiber matrix, Biomaterials 31(23) (2010) 6004-6012.
[324] A. Rezania, K.E. Healy, The effect of peptide surface density on mineralization of a matrix deposited by osteogenic cells, J Biomed Mater Res 52(4) (2000) 595-600.
[325] H. Zhang, C.-Y. Lin, S.J. Hollister, The interaction between bone marrow stromal cells and RGD modified three dimensional porous polycaprolactone scaffolds, Biomaterials 30(25) (2009) 4063-4069.
[326] C.A. Hoesli, A. Garnier, P.-M. Juneau, P. Chevallier, C. Duchesne, G. Laroche, A fluorophore-tagged RGD peptide to control endothelial cell adhesion to micropatterned surfaces, Biomaterials 35(3) (2014) 879-890.
[327] F.K. Mante, K. Little, M.O. Mante, C. Rawle, G.R. Baran, Oxidation of Titanium, RGD Peptide Attachment, and Matrix Mineralization of Rat Bone Marrow Stromal Cells, The Journal of oral implantology 30(6) (2004) 343-349.
[328] S. Pallu, R. Bareille, M. Dard, H. Kessler, A. Jonczyk, M. Vernizeau, J. Amédée-Vilamitjana, A cyclo peptide activates signaling events and promotes growth and the production of the bone matrix, Peptides 24(9) (2003) 1349-1357.
[329] M. Schuldiner, O. Yanuka, J. Itskovitz-Eldor, D.A. Melton, N. Benvenisty, Effects of eight growth factors on the differentiation of cells derived from human embryonic stem cells, Proc Natl Acad Sci U S A 97(21) (2000) 11307-11312.
[330] D.J. Baylink, R.D. Finkelman, S. Mohan, Growth factors to stimulate bone formation, Journal of bone and mineral research : the official journal of the American Society for Bone and Mineral Research 8(S2) (1993) S565-S572.
[331] H. Uludag, D. D'Augusta, J. Golden, J. Li, G. Timony, R. Riedel, J.M. Wozney, Implantation of recombinant human bone morphogenetic proteins with biomaterial carriers: A correlation between protein pharmacokinetics and osteoinduction in the rat ectopic model, J Biomed Mater Res 50(2) (2000) 227-238.
[332] M. Wan, X. Cao, BMP signaling in skeletal development, Biochem Biophys Res Commun 328(3) (2005) 651-657.
[333] D. Weber, A. Kotzsch, J. Nickel, S. Harth, A. Seher, U. Mueller, W. Sebald, T.D. Mueller, A silent H-bond can be mutationally activated for high-affinity interaction of BMP-2 and activin type IIB receptor, BMC Struct Biol 7 (2007) 6-6.
[334] K. Miyazono, Signal transduction by bone morphogenetic protein receptors: functional roles of Smad proteins, Bone 25(1) (1999) 91-93.

[335] T. Matsubara, K. Kida, A. Yamaguchi, K. Hata, F. Ichida, H. Meguro, H. Aburatani, R. Nishimura, T. Yoneda, BMP2 Regulates Osterix through Msx2 and Runx2 during Osteoblast Differentiation, The Journal of biological chemistry 283(43) (2008) 29119-29125.
[336] J.H. Jun, W.-J. Yoon, S.-B. Seo, K.-M. Woo, G.-S. Kim, H.-M. Ryoo, J.-H. Baek, BMP2-activated Erk/MAP Kinase Stabilizes Runx2 by Increasing p300 Levels and Histone Acetyltransferase Activity, The Journal of biological chemistry 285(47) (2010) 36410-36419.
[337] J. Guicheux, J. Lemonnier, C. Ghayor, A. Suzuki, G. Palmer, J. Caverzasio, Activation of p38 Mitogen-Activated Protein Kinase and c-Jun-NH2-Terminal Kinase by BMP-2 and Their Implication in the Stimulation of Osteoblastic Cell Differentiation, Journal of bone and mineral research : the official journal of the American Society for Bone and Mineral Research 18(11) (2003) 2060-2068.
[338] N. Tang, W.-X. Song, J. Luo, X. Luo, J. Chen, K.A. Sharff, Y. Bi, B.-C. He, J.-Y. Huang, G.-H. Zhu, Y.-X. Su, W. Jiang, M. Tang, Y. He, Y. Wang, L. Chen, G.-W. Zuo, J. Shen, X. Pan, R.R. Reid, H.H. Luu, R.C. Haydon, T.-C. He, BMP-9-induced osteogenic differentiation of mesenchymal progenitors requires functional canonical Wnt/β-catenin signalling, J Cell Mol Med 13(8b) (2009) 2448-2464.
[339] R. van Amerongen, R. Nusse, Towards an integrated view of Wnt signaling in development, Development 136(19) (2009) 3205-3214.
[340] I. Papathanasiou, K.N. Malizos, A. Tsezou, Bone morphogenetic protein-2-induced Wnt/β-catenin signaling pathway activation through enhanced low-density-lipoprotein receptor-related protein 5 catabolic activity contributes to hypertrophy in osteoarthritic chondrocytes, Arthritis research & therapy 14(2) (2012) R82-R82.
[341] K. Narayanan, R. Srinivas, M.C. Peterson, A. Ramachandran, J. Hao, B. Thimmapaya, P.E. Scherer, A. George, Transcriptional Regulation of Dentin Matrix Protein 1 by JunB and p300 during Osteoblast Differentiation, The Journal of biological chemistry 279(43) (2004) 44294-44302.
[342] M. Knippenberg, M.N. Helder, B. Zandieh Doulabi, P.I.J.M. Wuisman, J. Klein-Nulend, Osteogenesis versus chondrogenesis by BMP-2 and BMP-7 in adipose stem cells, Biochem Biophys Res Commun 342(3) (2006) 902-908.
[343] J.S. Park, H.N. Yang, S.Y. Jeon, D.G. Woo, K. Na, K.-H. Park, Osteogenic differentiation of human mesenchymal stem cells using RGD-modified BMP-2 coated microspheres, Biomaterials 31(24) (2010) 6239-6248.
[344] K. Vallières, P. Chevallier, C. Sarra-Bournet, S. Turgeon, G. Laroche, AFM Imaging of Immobilized Fibronectin: Does the Surface Conjugation Scheme Affect the Protein Orientation/Conformation?, Langmuir 23(19) (2007) 9745-9751.
[345] J.H. Moon, J.W. Shin, S.Y. Kim, J.W. Park, Formation of Uniform Aminosilane Thin Layers: An Imine Formation To Measure Relative Surface Density of the Amine Group, Langmuir 12(20) (1996) 4621-4624.
[346] P. Chevallier, M. Castonguay, S. Turgeon, N. Dubrulle, D. Mantovani, P.H. McBreen, J.C. Wittmann, G. Laroche, Ammonia RF−Plasma on PTFE Surfaces: Chemical Characterization of the Species Created on the Surface by Vapor−Phase Chemical Derivatization, J Phys Chem B 105(50) (2001) 12490-12497.
[347] E.C. Jensen, Quantitative Analysis of Histological Staining and Fluorescence Using ImageJ, The Anatomical record 296(3) (2013) 378-381.
[348] V. Gauvreau, P. Chevallier, K. Vallières, É. Petitclerc, R.C. Gaudreault, G. Laroche, Engineering Surfaces for Bioconjugation: Developing Strategies and Quantifying the Extent of the Reactions, Bioconjugate Chem 15(5) (2004) 1146-1156.
[349] A.G. Secchi, V. Grigoriou, I.M. Shapiro, E.A. Cavalcanti-Adam, R.J. Composto, P. Ducheyne, C.S. Adams, RGDS peptides immobilized on titanium alloy stimulate bone cell attachment, differentiation and confer resistance to apoptosis, Journal of biomedical materials research. Part A 83A(3) (2007) 577-584.

[350] W. Chen, L.G. Villa-Diaz, Y. Sun, S. Weng, J.K. Kim, R.H.W. Lam, L. Han, R. Fan, P.H. Krebsbach, J. Fu, Nanotopography Influences Adhesion, Spreading, and Self-Renewal of Human Embryonic Stem Cells, ACS Nano 6(5) (2012) 4094-4103.
[351] V. Bucci-Sabattini, C. Cassinelli, P.G. Coelho, A. Minnici, A. Trani, D.M. Dohan Ehrenfest, Effect of titanium implant surface nanoroughness and calcium phosphate low impregnation on bone cell activity in vitro, Oral surgery, oral medicine, oral pathology, oral radiology, and endodontics 109(2) (2010) 217-24.
[352] C. Chollet, R. Bareille, M. Rémy, A. Guignandon, L. Bordenave, G. Laroche, M.-C. Durrieu, Impact of Peptide Micropatterning on Endothelial Cell Actin Remodeling for Cell Alignment under Shear Stress, Macromol Biosci 12(12) (2012) 1648-1659.
[353] M.-C. Boivin, P. Chevallier, C.A. Hoesli, J. Lagueux, R. Bareille, M. Rémy, L. Bordenave, M.-C. Durrieu, G. Laroche, Human saphenous vein endothelial cell adhesion and expansion on micropatterned polytetrafluoroethylene, Journal of biomedical materials research. Part A 101A(3) (2013) 694-703.
[354] Y. Kim, J.N. Renner, J.C. Liu, Incorporating the BMP-2 peptide in genetically-engineered biomaterials accelerates osteogenic differentiation, J Biomater Sci 2(8) (2014) 1110-1119.
[355] O.F. Zouani, C. Chollet, B. Guillotin, M.-C. Durrieu, Differentiation of pre-osteoblast cells on poly(ethylene terephthalate) grafted with RGD and/or BMPs mimetic peptides, Biomaterials 31(32) (2010) 8245-8253.
[356] Y. Takeuchi, M. Suzawa, T. Kikuchi, E. Nishida, T. Fujita, T. Matsumoto, Differentiation and Transforming Growth Factor-β Receptor Down-regulation by Collagen-α2β1 Integrin Interaction Is Mediated by Focal Adhesion Kinase and Its Downstream Signals in Murine Osteoblastic Cells, The Journal of biological chemistry 272(46) (1997) 29309-29316.
[357] S.X. Hsiong, T. Boontheekul, N. Huebsch, D.J. Mooney, Cyclic Arginine-Glycine-Aspartate Peptides Enhance Three-Dimensional Stem Cell Osteogenic Differentiation, Tissue engineering. Part A 15(2) (2009) 263-272.
[358] K. Blyth, E.R. Cameron, J.C. Neil, The runx genes: gain or loss of function in cancer, Nat Rev Cancer 5(5) (2005) 376-387.
[359] K. Miyazono, S. Maeda, T. Imamura, BMP receptor signaling: Transcriptional targets, regulation of signals, and signaling cross-talk, Cytokine & growth factor reviews 16(3) (2005) 251-263.
[360] J.-L. Su, J. Chiou, C.-H. Tang, M. Zhao, C.-H. Tsai, P.-S. Chen, Y.-W. Chang, M.-H. Chien, C.-Y. Peng, M. Hsiao, M.-L. Kuo, M.-L. Yen, CYR61 Regulates BMP-2-dependent Osteoblast Differentiation through the α(v)β(3) Integrin/Integrin-linked Kinase/ERK Pathway, The Journal of biological chemistry 285(41) (2010) 31325-31336.
[361] J.T. Koepsel, P.T. Brown, S.G. Loveland, W.-J. Li, W.L. Murphy, Combinatorial screening of chemically defined human mesenchymal stem cell culture substrates, J Mater Chem 22(37) (2012) 19474-19481.
[362] M. Suzawa, Y. Tamura, S. Fukumoto, K. Miyazono, T. Fujita, S. Kato, Y. Takeuchi, Stimulation of Smad1 Transcriptional Activity by Ras-Extracellular Signal-Regulated Kinase Pathway: A Possible Mechanism for Collagen-Dependent Osteoblastic Differentiation, Journal of bone and mineral research : the official journal of the American Society for Bone and Mineral Research 17(2) (2002) 240-248.
[363] D.T. Scadden, The stem-cell niche as an entity of action, Nature 441(7097) (2006) 1075-1079.
[364] F. Gattazzo, A. Urciuolo, P. Bonaldo, Extracellular matrix: a dynamic microenvironment for stem cell niche, Biochimica et Biophysica Acta (BBA)-General Subjects 1840(8) (2014) 2506-2519.
[365] C. Bonnans, J. Chou, Z. Werb, Remodelling the extracellular matrix in development and disease, Nat. Rev. Mol. Cell Biol 15(12) (2014) 786-801.

[366] F.M. Watt, W.T.S. Huck, Role of the extracellular matrix in regulating stem cell fate, Nature reviews. Molecular cell biology 14(8) (2013) 467-473.
[367] D. Zhang, K.A. Kilian, Peptide microarrays for the discovery of bioactive surfaces that guide cellular processes: a single step azide-alkyne "click" chemistry approach, J. Mater. Chem. B 2(27) (2014) 4280-4288.
[368] K.A. Kilian, M. Mrksich, Directing Stem Cell Fate by Controlling the Affinity and Density of Ligand–Receptor Interactions at the Biomaterials Interface, Angew. Chem., Int. Ed. Engl 51(20) (2012) 4891-4895.
[369] C.M. Metallo, J.C. Mohr, C.J. Detzel, J.J. de Pablo, B.J. Van Wie, S.P. Palecek, Engineering the stem cell microenvironment, Biotechnology progress 23(1) (2007) 18-23.
[370] J. Kim, T. Ma, Autocrine fibroblast growth factor 2-mediated interactions between human mesenchymal stem cells and the extracellular matrix under varying oxygen tension, J. Cell. Biochem 114(3) (2013) 716-727.
[371] Z. Huang, E.R. Nelson, R.L. Smith, S.B. Goodman, The sequential expression profiles of growth factors from osteoprogenitors [correction of osteroprogenitors] to osteoblasts in vitro, Tissue engineering 13(9) (2007) 2311-20.
[372] J.S. Lee, J.S. Lee, A. Wagoner-Johnson, W.L. Murphy, Modular peptide growth factors for substrate-mediated stem cell differentiation, Angewandte Chemie (International ed. in English) 48(34) (2009) 6266-9.
[373] R.A. Boomsma, D.L. Geenen, Mesenchymal Stem Cells Secrete Multiple Cytokines That Promote Angiogenesis and Have Contrasting Effects on Chemotaxis and Apoptosis, PloS one 7(4) (2012) e35685.
[374] F. Yang, S.-W. Cho, S.M. Son, S.P. Hudson, S. Bogatyrev, L. Keung, D.S. Kohane, R. Langer, D.G. Anderson, Combinatorial Extracellular Matrices for Human Embryonic Stem Cell Differentiation in 3D, Biomacromolecules 11(8) (2010) 1909-1914.
[375] Q. Wei, T.L. Pohl, A. Seckinger, J.P. Spatz, E.A. Cavalcanti-Adam, Regulation of integrin and growth factor signaling in biomaterials for osteodifferentiation, Beilstein J. Org. Chem 11(1) (2015) 773-783.
[376] C.J. Flaim, S. Chien, S.N. Bhatia, An extracellular matrix microarray for probing cellular differentiation, Nature methods 2(2) (2005) 119-25.
[377] M.J.P. Biggs, R.G. Richards, M.J. Dalby, Nanotopographical modification: a regulator of cellular function through focal adhesions, Nanomedicine: Nanotechnology, Biology and Medicine 6(5) (2010) 619-633.
[378] S.J. Liliensiek, P. Nealey, C.J. Murphy, Characterization of endothelial basement membrane nanotopography in rhesus macaque as a guide for vessel tissue engineering, Tissue Eng., Part A 15(9) (2009) 2643-2651.
[379] E. Palin, H. Liu, T.J. Webster, Mimicking the nanofeatures of bone increases bone-forming cell adhesion and proliferation, Nanotechnology 16(9) (2005) 1828.
[380] Z. Nie, E. Kumacheva, Patterning surfaces with functional polymers, Nat. Mater 7(4) (2008) 277-290.
[381] X. Wang, T. Nakamoto, I. Dulińska-Molak, N. Kawazoe, G. Chen, Regulating the stemness of mesenchymal stem cells by tuning micropattern features, J. Mater. Chem. B (2016).
[382] O. Jeon, E. Alsberg, Regulation of Stem Cell Fate in a Three-Dimensional Micropatterned Dual-Crosslinked Hydrogel System, Adv. Funct. Mater 23(38) (2013) 4765-4775.
[383] W. Song, H. Lu, N. Kawazoe, G. Chen, Adipogenic differentiation of individual mesenchymal stem cell on different geometric micropatterns, Langmuir 27(10) (2011) 6155-6162.
[384] X. Wang, C. Yan, K. Ye, Y. He, Z. Li, J. Ding, Effect of RGD nanospacing on differentiation of stem cells, Biomaterials 34(12) (2013) 2865-74.

[385] B.L. Ekerdt, R.A. Segalman, D.V. Schaffer, Spatial organization of cell-adhesive ligands for advanced cell culture, Biotechnol. J 8(12) (2013) 1411-1423.
[386] R.K. Das, O.F. Zouani, C. Labrugère, R. Oda, M.-C. Durrieu, Influence of Nanohelical Shape and Periodicity on Stem Cell Fate, ACS Nano 7(4) (2013) 3351-3361.
[387] Z.A. Cheng, O.F. Zouani, K. Glinel, A.M. Jonas, M.-C. Durrieu, Bioactive chemical nanopatterns impact human mesenchymal stem cell fate, Nano letters 13(8) (2013) 3923-3929.
[388] E. Olson, Particle Shape Factors and Their Use in Image Analysis-Part 1: Theory, Journal of GXP Compliance 15(3) (2011) 85.
[389] M. Mrksich, L.E. Dike, J. Tien, D.E. Ingber, G.M. Whitesides, Using microcontact printing to pattern the attachment of mammalian cells to self-assembled monolayers of alkanethiolates on transparent films of gold and silver, Experimental cell research 235(2) (1997) 305-13.
[390] C.S. Chen, M. Mrksich, S. Huang, G.M. Whitesides, D.E. Ingber, Micropatterned surfaces for control of cell shape, position, and function, Biotechnology progress 14(3) (1998) 356-63.
[391] S.N. Bhatia, M.L. Yarmush, M. Toner, Controlling cell interactions by micropatterning in co-cultures: hepatocytes and 3T3 fibroblasts, J Biomed Mater Res 34(2) (1997) 189-99.
[392] J. Tang, R. Peng, J. Ding, The regulation of stem cell differentiation by cell-cell contact on micropatterned material surfaces, Biomaterials 31(9) (2010) 2470-2476.
[393] G. Chen, C. Deng, Y.-P. Li, TGF-beta and BMP signaling in osteoblast differentiation and bone formation, Int J Biol Sci 8(2) (2012) 272-288.
[394] E.L. Fong, C.K. Chan, S.B. Goodman, Stem cell homing in musculoskeletal injury, Biomaterials 32(2) (2011) 395-409.
[395] R.O. Hynes, Extracellular matrix: not just pretty fibrils, Science (New York, N.Y.) 326(5957) (2009) 1216-1219.
[396] A.J. Keung, S. Kumar, D.V. Schaffer, Presentation Counts: Microenvironmental Regulation of Stem Cells by Biophysical and Material Cues, Annual review of cell and developmental biology 26(1) (2010) 533-556.
[397] C.S.D. Lee, E. Watkins, O.A. Burnsed, Z. Schwartz, B.D. Boyan, Tailoring Adipose Stem Cell Trophic Factor Production with Differentiation Medium Components to Regenerate Chondral Defects, Tissue Engineering Part A 19(11-12) (2013) 1451-1464.
[398] M.P. Lutolf, H.M. Blau, Artificial Stem Cell Niches, Advanced Materials 21(32-33) (2009) 3255-3268.
[399] T. Crouzier, L. Fourel, T. Boudou, C. Albigès-Rizo, C. Picart, Presentation of BMP-2 from a Soft Biopolymeric Film Unveils its Activity on Cell Adhesion and Migration, Advanced Materials 23(12) (2011) H111-H118.
[400] P. Bashkin, S. Doctrow, M. Klagsbrun, C.M. Svahn, J. Folkman, I. Vlodavsky, Basic fibroblast growth factor binds to subendothelial extracellular matrix and is released by heparitinase and heparin-like molecules, Biochemistry 28(4) (1989) 1737-1743.
[401] X. Wang, R.E. Harris, L.J. Bayston, H.L. Ashe, Type IV collagens regulate BMP signalling in Drosophila, Nature 455(7209) (2008) 72-77.
[402] J.D. Boerckel, Y.M. Kolambkar, K.M. Dupont, B.A. Uhrig, E.A. Phelps, H.Y. Stevens, A.J. García, R.E. Guldberg, Effects of protein dose and delivery system on BMP-mediated bone regeneration, Biomaterials 32(22) (2011) 5241-5251.
[403] R.A. Ignotz, J. Massagué, Cell adhesion protein receptors as targets for transforming growth factor-β action, Cell 51(2) (1987) 189-197.
[404] R.A. Ignotz, J. Heino, J. Massagué, Regulation of cell adhesion receptors by transforming growth factor-beta. Regulation of vitronectin receptor and LFA-1, Journal of Biological Chemistry 264(1) (1989) 389-392.
[405] E.S. Wijelath, S. Rahman, M. Namekata, J. Murray, T. Nishimura, Z. Mostafavi-Pour, Y. Patel, Y. Suda, M.J. Humphries, M. Sobel, Heparin-II Domain of Fibronectin Is a Vascular

Endothelial Growth Factor–Binding Domain: Enhancement of VEGF Biological Activity by a Singular Growth Factor/Matrix Protein Synergism, Circulation research 99(8) (2006) 853-860.
[406] M. Schneller, K. Vuori, E. Ruoslahti, Alphavbeta3 integrin associates with activated insulin and PDGFbeta receptors and potentiates the biological activity of PDGF, The EMBO Journal 16(18) (1997) 5600-5607.
[407] F.G. Giancotti, E. Ruoslahti, Integrin Signaling, Science 285(5430) (1999) 1028-1033.
[408] K.M. Yamada, S. Even-Ram, Integrin regulation of growth factor receptors, Nature cell biology 4(4) (2002) E75-E76.
[409] E. Clark, J. Brugge, Integrins and signal transduction pathways: the road taken, Science 268(5208) (1995) 233-239.
[410] S. Miyamoto, H. Teramoto, J.S. Gutkind, K.M. Yamada, Integrins can collaborate with growth factors for phosphorylation of receptor tyrosine kinases and MAP kinase activation: roles of integrin aggregation and occupancy of receptors, J Cell Biol 135(6 Pt 1) (1996) 1633-42.
[411] L. Moro, M. Venturino, C. Bozzo, L. Silengo, F. Altruda, L. Beguinot, G. Tarone, P. Defilippi, Integrins induce activation of EGF receptor: role in MAP kinase induction and adhesion-dependent cell survival, The EMBO journal 17(22) (1998) 6622-6632.
[412] S.R. Ghaemi, B. Delalat, X. Cetó, F.J. Harding, J. Tuke, N.H. Voelcker, Synergistic influence of collagen I and BMP 2 drives osteogenic differentiation of mesenchymal stem cells: A cell microarray analysis, Acta biomaterialia (2015).
[413] L. Fourel, A. Valat, E. Faurobert, R. Guillot, I. Bourrin-Reynard, K. Ren, L. Lafanechere, E. Planus, C. Picart, C. Albiges-Rizo, beta3 integrin-mediated spreading induced by matrix-bound BMP-2 controls Smad signaling in a stiffness-independent manner, J Cell Biol 212(6) (2016) 693-706.
[414] A. Shekaran, J.R. Garcia, A.Y. Clark, T.E. Kavanaugh, A.S. Lin, R.E. Guldberg, A.J. Garcia, Bone regeneration using an alpha 2 beta 1 integrin-specific hydrogel as a BMP-2 delivery vehicle, Biomaterials 35(21) (2014) 5453-61.
[415] M.P. Lutolf, P.M. Gilbert, H.M. Blau, Designing materials to direct stem-cell fate, Nature 462(7272) (2009) 433-441.
[416] M.C. Ramel, C.S. Hill, Spatial regulation of BMP activity, FEBS letters 586(14) (2012) 1929-41.
[417] L. Li, T. Xie, STEM CELL NICHE: Structure and Function, Annual review of cell and developmental biology 21(1) (2005) 605-631.
[418] T.A. Mitsiadis, O. Barrandon, A. Rochat, Y. Barrandon, C. De Bari, Stem cell niches in mammals, Experimental cell research 313(16) (2007) 3377-85.
[419] A.I. Caplan, Mesenchymal stem cells, Journal of orthopaedic research : official publication of the Orthopaedic Research Society 9(5) (1991) 641-50.
[420] M. Crisan, S. Yap, L. Casteilla, C.W. Chen, M. Corselli, T.S. Park, G. Andriolo, B. Sun, B. Zheng, L. Zhang, C. Norotte, P.N. Teng, J. Traas, R. Schugar, B.M. Deasy, S. Badylak, H.J. Buhring, J.P. Giacobino, L. Lazzari, J. Huard, B. Peault, A perivascular origin for mesenchymal stem cells in multiple human organs, Cell Stem Cell 3(3) (2008) 301-13.
[421] S. Oberhansl, A.G. Castano, A. Lagunas, E. Prats-Alfonso, M. Hirtz, F. Albericio, H. Fuchs, J. Samitier, E. Martinez, Mesopattern of immobilised bone morphogenetic protein-2 created by microcontact printing and dip-pen nanolithography influence C2C12 cell fate, RSC Advances 4(100) (2014) 56809-56815.
[422] A. Lagunas, J. Comelles, S. Oberhansl, V. Hortigüela, E. Martínez, J. Samitier, Continuous bone morphogenetic protein-2 gradients for concentration effect studies on C2C12 osteogenic fate, Nanomedicine: Nanotechnology, Biology and Medicine 9(5) 694-701.
[423] M. Yoneda, H. Terai, Y. Imai, T. Okada, K. Nozaki, H. Inoue, S. Miyamoto, K. Takaoka, Repair of an intercalated long bone defect with a synthetic biodegradable bone-inducing implant, Biomaterials 26(25) (2005) 5145-5152.

[424] O.P. Gautschi, S.P. Frey, R. Zellweger, Bone morphogenetic proteins in clinical applications, ANZ journal of surgery 77(8) (2007) 626-31.
[425] C.-C. Liang, H.-C. Chen, Sustained Activation of Extracellular Signal-regulated Kinase Stimulated by Hepatocyte Growth Factor Leads to Integrin α2 Expression That Is Involved in Cell Scattering, Journal of Biological Chemistry 276(24) (2001) 21146-21152.
[426] J.G. Meinhart, J.C. Schense, H. Schima, M. Gorlitzer, J.A. Hubbell, M. Deutsch, P. Zilla, Enhanced endothelial cell retention on shear-stressed synthetic vascular grafts precoated with RGD-cross-linked fibrin, Tissue engineering 11(5-6) (2005) 887-895.
[427] J. Ivaska, J. Heino, Cooperation between integrins and growth factor receptors in signaling and endocytosis, Annual review of cell and developmental biology 27(1) (2011) 291.
[428] J.M. Wozney, V. Rosen, A.J. Celeste, L.M. Mitsock, M.J. Whitters, R.W. Kriz, R.M. Hewick, E.A. Wang, Novel regulators of bone formation: molecular clones and activities, Science 242(4885) (1988) 1528-1534.
[429] K. Hauff, C. Zambarda, M. Dietrich, M. Halbig, A.L. Grab, R. Medda, E.A. Cavalcanti-Adam, Matrix-Immobilized BMP-2 on Microcontact Printed Fibronectin as an in vitro Tool to Study BMP-Mediated Signaling and Cell Migration, Frontiers in bioengineering and biotechnology 3 (2015) 62.
[430] C.M. Kolodziej, S.H. Kim, R.M. Broyer, S.S. Saxer, C.G. Decker, H.D. Maynard, Combination of Integrin-Binding Peptide and Growth Factor Promotes Cell Adhesion on Electron-Beam-Fabricated Patterns, Journal of the American Chemical Society 134(1) (2012) 247-255.
[431] N. Vyas, D. Goswami, A. Manonmani, P. Sharma, H.A. Ranganath, K. VijayRaghavan, L.S. Shashidhara, R. Sowdhamini, S. Mayor, Nanoscale organization of hedgehog is essential for long-range signaling, Cell 133(7) (2008) 1214-27.
[432] M.C. Ramel, C.S. Hill, The ventral to dorsal BMP activity gradient in the early zebrafish embryo is determined by graded expression of BMP ligands, Developmental biology 378(2) (2013) 170-82.
[433] M. Arnold, E.A. Cavalcanti-Adam, R. Glass, J. Blümmel, W. Eck, M. Kantlehner, H. Kessler, J.P. Spatz, Activation of Integrin Function by Nanopatterned Adhesive Interfaces, ChemPhysChem 5(3) (2004) 383-388.
[434] J.A. Deeg, I. Louban, D. Aydin, C. Selhuber-Unkel, H. Kessler, J.P. Spatz, Impact of Local versus Global Ligand Density on Cellular Adhesion, Nano letters 11(4) (2011) 1469-1476.
[435] J. Park, S. Bauer, A. Pittrof, M.S. Killian, P. Schmuki, K. von der Mark, Synergistic control of mesenchymal stem cell differentiation by nanoscale surface geometry and immobilized growth factors on TiO2 nanotubes, Small (Weinheim an der Bergstrasse, Germany) 8(1) (2012) 98-107.
[436] M.J. Kim, B. Lee, K. Yang, J. Park, S. Jeon, S.H. Um, D.I. Kim, S.G. Im, S.W. Cho, BMP-2 peptide-functionalized nanopatterned substrates for enhanced osteogenic differentiation of human mesenchymal stem cells, Biomaterials 34(30) (2013) 7236-46.
[437] M.J. López-Bosque, E. Tejeda-Montes, M. Cazorla, J. Linacero, Y. Atienza, K.H. Smith, A. Lladó, J. Colombelli, E. Engel, A. Mata, Fabrication of hierarchical micro–nanotopographies for cell attachment studies, Nanotechnology 24(25) (2013) 255305.
[438] X. Wang, S. Li, C. Yan, P. Liu, J. Ding, Fabrication of RGD Micro/Nanopattern and Corresponding Study of Stem Cell Differentiation, Nano letters 15(3) (2015) 1457-1467.
[439] G.M. Harris, M.E. Piroli, E. Jabbarzadeh, Deconstructing the Effects of Matrix Elasticity and Geometry in Mesenchymal Stem Cell Lineage Commitment, Advanced functional materials 24(16) (2014) 2396-2403.
[440] Z. Li, Y. Gong, S. Sun, Y. Du, D. Lü, X. Liu, M. Long, Differential regulation of stiffness, topography, and dimension of substrates in rat mesenchymal stem cells, Biomaterials 34(31) (2013) 7616-7625.

[441] Z. Saidak, C. Le Henaff, S. Azzi, C. Marty, S. Da Nascimento, P. Sonnet, P.J. Marie, Wnt/β-Catenin Signaling Mediates Osteoblast Differentiation Triggered by Peptide-induced α5β1 Integrin Priming in Mesenchymal Skeletal Cells, The Journal of biological chemistry 290(11) (2015) 6903-6912.